Photonic Crystal Waveguides and Devices

A thesis submitted to
Faculty of Technology, University of Delhi
for the award of the degree of

DOCTOR OF PHILOSOPHY
in
APPLIED PHYSICS

by

Swati Rawal

Under the supervision of

Dr. R. K. SINHA
Professor and Head, Department of Applied Physics
Delhi College of Engineering
Faculty of Technology
University of Delhi
Delhi-110 042, India

CERTIFICATE

This is to certify that this thesis entitled "PHOTONIC CRYSTAL WAVEGUIDES AND DEVICES", being submitted by Ms. Swati Rawal, for the award of degree of Doctor of Philosophy to the Faculty of Technology, University of Delhi, India, is a record of bonafide research work carried out by her. She has worked under my guidance and supervision and has fulfilled the requirements, which to my knowledge have reached the requisite standard for the submission of this thesis. The results obtained in this thesis have not been submitted in part or full to any other University or Institute for the award of any degree or diploma.

(Prof. R. K. Sinha)

Supervisor & Head

Department of Applied Physics,

Delhi College of Engineering,

Faculty of Technology, University of Delhi

Bawana Road, Delhi-110042, India

CERTIFICATE

This is to certify that this thesis entitled "PHOTONIC CRYSTAL WAVEGUIDES AND DEVICES", being submitted for the award of degree of Doctor of Philosophy to the Faculty of Technology, University of Delhi, India, is based on the research work carried out by me under the guidance and supervision of Prof. R. K. Sinha, Department of Applied Physics, Delhi College of Engineering, Faculty of Technology, University of Delhi, India. The results obtained in this thesis have not been submitted in part or full to any other University or Institute for the award of any degree or diploma.

(**Swati Rawal)** **Place:** Delhi

Candidate Date:

(Prof. R. K. Sinha)

Supervisor & Head

Department of Applied Physics,

Delhi College of Engineering,

Faculty of Technology,

University of Delhi

Delhi-110042, India.

(Prof. A. K. Trivedi)

Head, Applied Sciences and

Humanities &

Dean, **Faculty of**

Technology, University of

Delhi

Delhi-110042, India.

To Almighty God,
Satguru Sewa Ram Sahib Ji

and
My parents,
who have been my source of Inspiration

Acknowledgement

It would be impossible to express my thanks on this page to all those who have supported me, without whose help I could never have come so far.

As a teacher and advisor, I am greatly indebted to my Ph.D supervisor, ***Prof. R. K. Sinha*** *for his invaluable suggestions, guidance and active encouragement throughout the progress of this work. I thank almighty to give me the opportunity, and consider myself most fortunate to work under the guidance of Prof. Sinha. I sincerely thank him for his guidance and for the research freedom I have enjoyed. Sir, I am grateful to you for your understanding and support. Thanks, Sir.*

It is my privilege to express my thankfulness to ***Prof. Richard M. De La Rue****, Department of Electronics and Electrical Engineering, University of Glasgow G128QQ Scotland, U. K. to help me perform work in the exciting field of Slow light in Photonic Crystals through his stimulated discussions on research problems. I thank you Sir for your active support.*

I would like to thank ***Prof. P. B. Sharma****, Vice Chancellor, Delhi Technological University (Formerly Delhi College of Engineering, Faculty of Technology, University of Delhi) for providing ample research infrastructure to carry out the research work. I would like to thank the support of entire faculty and staff of Department of Applied Physics for their consistent support.*

I express my thanks to Delhi College of Engineering, Faculty of Technology, University of Delhi for providing financial support to carry out the research work.

No words are sufficient to express the unceasing love, unconditional support and blessings of my parents, ***Mr. Manohar Lal Rawal*** *and* ***Mrs. Geeta Bali****, who stood behind me through all the difficult moments of my life. I am grateful to my parents, for their love and support that has carried me through difficult times and helped me reach my dreams. This thesis is for them.*

I would also like to express my sincere appreciation for ***my Grand Parents,*** *my brother* ***Jatin*** *and my cousin* ***Samita*** *for their love and support from time to time.*

*I would like to thank my friends (****Monika, Bhawana*** *and* ***Ruchika****), people that have touched my life in many different ways, for their friendship, support and love.*

Finally I would like to thank all those who have helped me and supported me throughout this period. Thank You!

Swati Rawal *Place: Delhi*

Candidate *Date:*

Abstract

The extra ordinary improvement in the progress of information data processing in the past few decades is associated with the generation of high performance and considerable miniaturization of integrated circuits in semiconductor technology. However it results in increase in resistance and power dissipation in circuits. To overcome these problems, devices using photons rather than electrons as an information carrier were developed. The simple analogy between an electron in a semiconductor and a photon in a periodically varying dielectric medium, known as photonic crystal, can reveal novel electromagnetic phenomenon. These new types of structures (photonic crystals) are able to control electromagnetic waves in three dimensions since they can give rise to bandgaps for photons, analogous to bandgap in semiconductors known as forbidden energy bandgap. Furthermore, devices based on photonic crystals benefit from high speed of optical signals which provide larger bandwidth and reduced cross talks between the channels because of the absence of interaction between the photons.

The existence of unique and interesting properties such as -photonic bandgap (PBG) i.e. in the range of frequencies at which optical propagation is completely prohibited in any direction, as well as the existence of defect modes, that may appear within the photonic bandgaps when a defect is introduced into an otherwise perfect photonic crystal, has resulted in fast growth of photonic technology. The possibility of molding the flow of light through these structures has led to the design and development of efficient optoelectronic devices and systems. The high refractive index contrast provided by silicon has led to silicon based micro-photonics. In the

present thesis, first the photonic bandgap (PBG) induced wave guiding applications of photonic crystals is exploited to design 2D dual band wavelength demultiplexer (DBWD) for separating the two telecommunication wavelengths, 1.31 μm and 1.55 μm. Initially, two designs were presented based on air bridge type photonic crystal structures in which both the upper and lower cladding is made up of air. However, these types of structures are mechanically unstable from practical perspective as well as not suitable for large scale integration. On the contrary, structures with solid support are more realistic. To overcome this instability, silicon-on-insulator (SOI) based PhC DBWD is designed. In these structures, mechanical robustness is improved by the supporting dielectric material under the slab. Enhancement in spectral response is further obtained by optimizing the Y junction of de-multiplexer giving rise to high transmission and extinction ratios for the two wavelengths, 1.31 μm and 1.55 μm. Tolerance analysis was also performed to study the effect of the variation of air hole radius, etch depth and refractive index on the transmission characteristics of the proposed design of SOI based photonic crystal DBWD.

In addition the strong light matter interaction observed in silicon photonic crystals results in slowing down the group velocity of light within such photonic crystals. By carefully engineering the photonic dispersion relationship, one may obtain unique opportunities for realization of devices that exploit the impact of slow light effects within such photonic crystals. These devices serve as key sources for processing, storing and buffering, required in future all-optical communication networks and information processing systems. PhC channel waveguides can be used as defect-mode slow light structure which enables increased time-delay for optical signals. Therefore, the design of a silicon-on-insulator photonic crystal channel waveguide for slow light

propagation, with group velocity in the range of 0.0028c to 0.044c and ultra-flattened group velocity dispersion (GVD), is proposed. The proposed structure is also investigated for its application as an optical buffer with a large value of normalized delay bandwidth product (DBP), equal to 0.778. Furthermore it is also shown that the proposed structure can also be used for time or wavelength-division de-multiplexing. The tunability of PhC lattices can further be extended and controlled by filling their segments with certain types of liquid crystal (LC) material. This combination offers the possibility of shifting the frequency of the defect modes and tuning the dispersion curves, in order to obtain flat slow modes with low group velocity dispersion. Since dynamically tuned devices are essential components in optical systems, PhC waveguide configurations with infiltration of LC material offer a strong potential for realizing integrated micro-photonic devices. An SOI based LC infiltrated slow light PhC channel waveguide having rectangular air holes in silicon core is thus proposed which yields an average group index of 43 over a bandwidth of 1.02 THz and vanishing group velocity dispersion. Propagation losses and their dependence on group velocity are another matter of concern. There is little justification in exploring the slow light regime if any advantage obtained is immediately counteracted by excessive losses. Such issues of concern are tackled directly in the present thesis - in order to obtain a highly efficient slow light PhC waveguide, with a simple design, that is suitable for fabrication.

The response of a given material to an incident electromagnetic wave is characterized by the study of induced polarization of the medium. The linear response of the medium is valid only if the incident radiation is weak. However, if the intensity of incident light increases, polarization of the medium is no longer linear and becomes

nonlinear. Therefore in such media, light propagation is controlled by the intensity of the incident light. The concept of nonlinear photonic crystals can be employed by taking the advantage of slow group velocity of light achievable in such structures. In this frame of work, we next, report the effect of slow light on two photon absorption (TPA), free carrier absorption (FCA) and self phase-modulation (SPM) processes in silicon-on-insulator (SOI) photonic crystal (PhC) channel waveguides. It is important to mention here that, as optical pulses propagate through photonic crystal waveguide; their evolution in both the time and frequency domains is governed by the interplay of linear dispersion and nonlinearity. It is observed that, in the slow light regime, these nonlinear effects are enhanced and the resulting increase in the induced phase shift can be used to decrease the size and power requirements needed to operate devices such as optical switches, logic gates, etc. However, soliton dynamics will dominate the propagation of femtosecond pulses in PhC waveguides when group velocity dispersion (GVD) is strongly anomalous because of large waveguide dispersion. Keeping above facts in view, I have investigated the propagation of light in a nonlinear slow light medium formed by a channel SOI PhC structure having elliptical holes in silicon core - and it is observed that, while beginning with almost the same spectral width as that of an input pulse, the pulse spectrum broadens as the input power level increases. The rate at which the spectrum broadens with power is larger for slower waveguides. However it is found that the SPM-induced phase shift decreases as the TPA coefficient increases, which in turn depends on the slow down factor, *S*. The spectral broadening factor calculated for the waveguide shows that a higher input power level of the order of 10^2 W is required to obtain the same level of spectral broadening in fast waveguides as compared to the power level on the order of

10^0 W required in the case of slow waveguides. This type of slow light structure has considerable potential for use in photonic device applications such as optical switches, logic gates etc. - as demonstrated in chapter 6 of the present thesis.

Contents

List of Figures

List of Abbreviations

PhC	Photonic Crystal
1D	One Dimension
2D	Two Dimension
3D	Three Dimension
CWDM	Coarse Wavelength Demultiplexing
DBP	Delay Bandwidth Product
DBWD	Dual Band Wavelength Demultiplexer
ER	Extinction Ratio
FCA	Free Carrier Absorption
FCD	Free Carrier Dispersion
FDTD	Finite Difference Time Domain Method
FOD	Fourth Order Dispersion
FTTH	Fiber-to-the-home
FWHM	Full Width at Half Maximum
GVD	Group Velocity Dispersion
LC	Liquid Crystal
OEIC	Optoelectronic Integrated Circuits
PBG	Photonic Bandgap
PhC	Photonic Crystal, Plane Wave Expansion, Slow Down Factor

PWE	Plane Wave Expansion
S	Slow Down Factor
SOI	Silicon-on-Insulator
SPM	Self Phase Modulation
T_d	Delay Time
TDM	Time Division Multiplexing
TE	Transverse Electric
TM	Transverse Magnetic
TOD	Third Order Dispersion
TPA	Two Photon Absorption
WDM	Wavelength Division Multiplexing
Wg	Waveguide

Chapter 1

Introduction

1.1 Introduction

Photonics involve the research and application of light to perform tasks that could previously be carried out only by electronics. This includes transmission, manipulation and storage of data using photons. Devices based on photonic crystals benefit from the high speed of optical signals which provide larger bandwidth and reduced cross talks between the channels and open the way to faster signal processing. The high refractive index contrast provided by silicon, GaAs, etc can be used in highly integrated all optical communication systems. Since silicon is transparent above 1200 nm, therefore it is convenient to use it around telecommunication wavelength of 1310 nm and 1550 nm. In addition, photonics also offers a platform for the investigation of fundamental laws of physics that govern the behaviour of photons. Strong light matter interaction resulting in slowing down the velocity of light and the corresponding impact of slow group velocity on the nonlinear effects are some of the interesting phenomenon that can be observed when coupling between light and matter occurs at the nano-scale.

1.2 Photonic Crystals

Since their proposal by Yablonovitch and John [Yablonovitch (1987), John (1987)] in 1987, photonic crystals (PhC) have emerged as one of the most significant topics in the

field of optical communication. These are defined as materials with refractive index periodically varying along one, two or three dimensions. Thus according to the degree of refractive index periodicity, they are classified into three categories; one dimensional (1D) PhCs, two dimensional (2D) PhCs and three dimensional (3D) PhCs. It also refers to the degree of light confinement in photonic crystals. One dimensional photonic crystal is the dielectric stack where periodicity varies in one dimension. 2D photonic crystal exists when the periodicity of the dielectric stack is two dimensional. These crystals are assumed to be infinitely long in a direction perpendicular to the plane of periodicity. 3D photonic crystals, having periodicity in three dimensions, can control the propagation of light in all directions (Figure1.1). Since the fabrication of 3D PhC is still a difficult process, the use of lower dimensional PhCs is a more appealing approach.

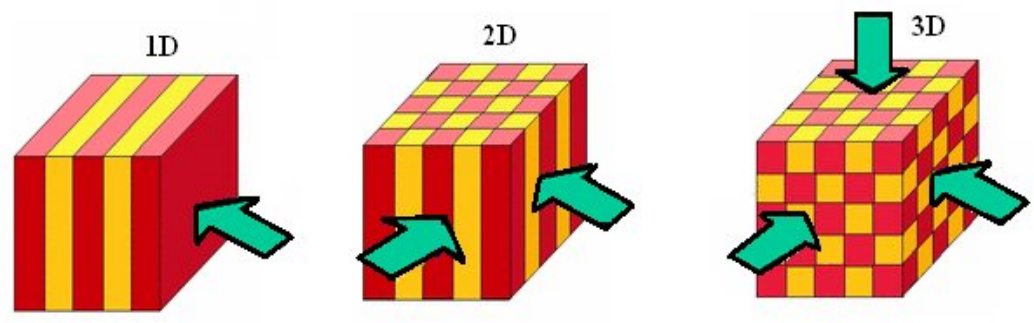

Figure 1.1 Model of 1D, 2D and 3D Photonic Crystals.

(Source: *http://ab-initio.mit.edu/photons/tutorial*)

The most important feature of photonic crystals is the existence of photonic bandgap. It corresponds to a band of frequencies within which, light is prohibited from propagating through the structures. Thus photonic bandgap materials can realize the localization and trapping of light over a band of frequencies [Joannopolous *et al.*

(1995)]. By locally breaking the periodicity of photonic crystals, by creating vacancies or by changing the radius of rods/holes, a region within the photonic crystal can be created which has optical properties different from that of the surrounding bulk photonic crystal. This is referred to as PBG optical waveguide [Sakoda (2001)] or simply PhC line defect waveguide. The deliberate creation of defects in the periodic structures gives rise to localized electromagnetic field modes in which light is trapped in the defect region of PBG. These waveguides actually support true guided modes in the frequency range lying within the photonic bandgap of the photonic crystal [Notomi *et al.* (2001), Johnson *et al.* (1999)]. The guided modes are horizontally confined by PBG and vertically by total internal reflection because of the high refractive index contrast between the slab and the cladding.

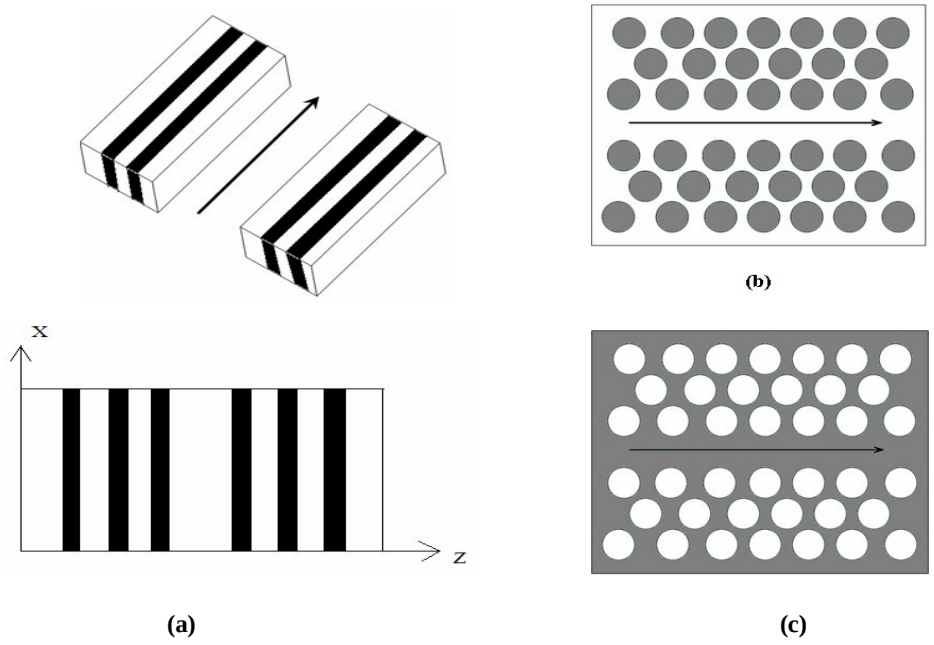

Figure 1.2 Schematic of photonic crystal line defect waveguides. (a) 1D PBG waveguide, (b) 2D PBG waveguide with low index guidance and (c) 2D PBG waveguide with high index guidance.

Different types of PBG waveguides are shown in Figure 1.2. The simplest 1D PBG waveguide consisting of a guiding layer sandwiched between 1D PBG structures is shown in Figure 1.2(a). These types of photonic crystal waveguide were first observed by Yeh and Yariv in 1970's [Yeh and Yariv (1976)]. Another type of PhC waveguides are the 2D PBG based waveguides shown in figure 1.2(b) and 1.2(c). These waveguides can further be classified as- low index guidance waveguide consisting of photonic crystal lattice arrangement of dielectric rods in air [Notomi *et al.* (2001), Sinha and Kalra (2006)] and high index guidance waveguides consisting of embedded air holes in the dielectric medium [Johnson *et al.* (1999), Vlasov *et al.* (2003)]. These symmetric structures are known as air bridge structures because they have air cladding both above and below the dielectric core. However, asymmetric structures like silicon-on-insulator (SOI) structures are more realistic and act as a good substrate for optical integration. These are made up of a silicon core with air cladding above and silica cladding below.

For symmetric structures in vertical direction, like air bridge structures, light can be classified into transverse electric (TE) and transverse magnetic (TM) modes and as even and odd modes. However for asymmetrical structures, such as SOI structures, the modes cannot be classified selectively- and each mode has an even as well as odd component. In a PhC lattice, having periodicity in xz plane, modes with H_y as predominant component are referred to as TE like modes and those with E_y as predominant component are referred to as TM-like modes (Figure 1.3). Thus in asymmetrical structures, TE like modes have both TE and TM components and the bandgap for pure TE modes cannot be calculated. However, if the amount of TM component is negligible in TE like modes, the photonic crystal supports bandgap for such modes, known as quasi bandgap. So the propagation of TE like modes can be

stopped completely within the desired frequency range. Thickness of the PhC waveguide core layer should then satisfy the single mode condition, in order to exploit the quasi PBG effectively [Shinya *et al.* (2002)].

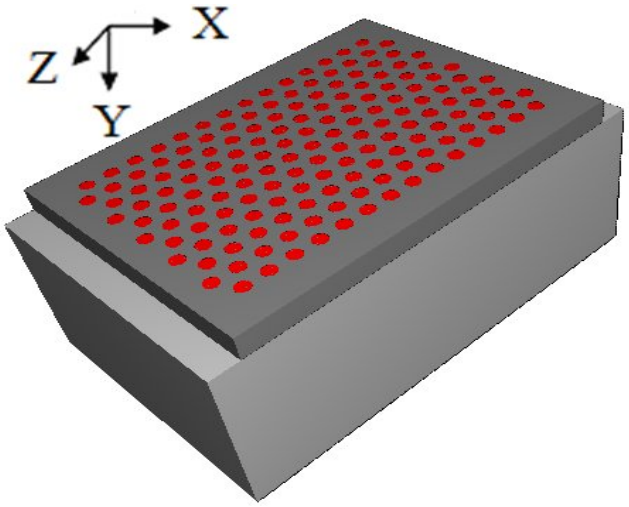

Figure 1.3. Schematic of photonic crystal structure defining the coordinate system (SOI structure).

In the present thesis, the devices based on both symmetric and asymmetric structures are studied. Chapter 2 discusses about de-multiplexers based on symmetric structures like air bridge structures having silicon slab with air cladding both above and below the slab. While in rest of the chapters, asymmetric structures based on SOI substrates are used for the study of various optical phenomenon. These structures are made up of silicon core layer sandwiched between silica (SiO_2) cladding layer below and air cladding above. Figures 1.4(a) and 1.4(b) shows the pillar type and embedded air hole type air bridge structures having air cladding both above and below the silicon core. Figures 1.4(c) shows the SOI based PhC structure with silica cladding below and air cladding above the silicon core. A photonic crystal line defect is created in the ΓK

direction which supports guided modes through them. Here *a* is the lattice constant and *r* is the radius of air holes/rods. However, photons which are incident on the interface between the semiconductor slab and air at small angles (angles smaller than critical angle for total internal reflection) escapes from the slab and convert into the radiation modes. In order to take into account these losses, we introduce a light line or a light cone in the analysis of PhC waveguides.

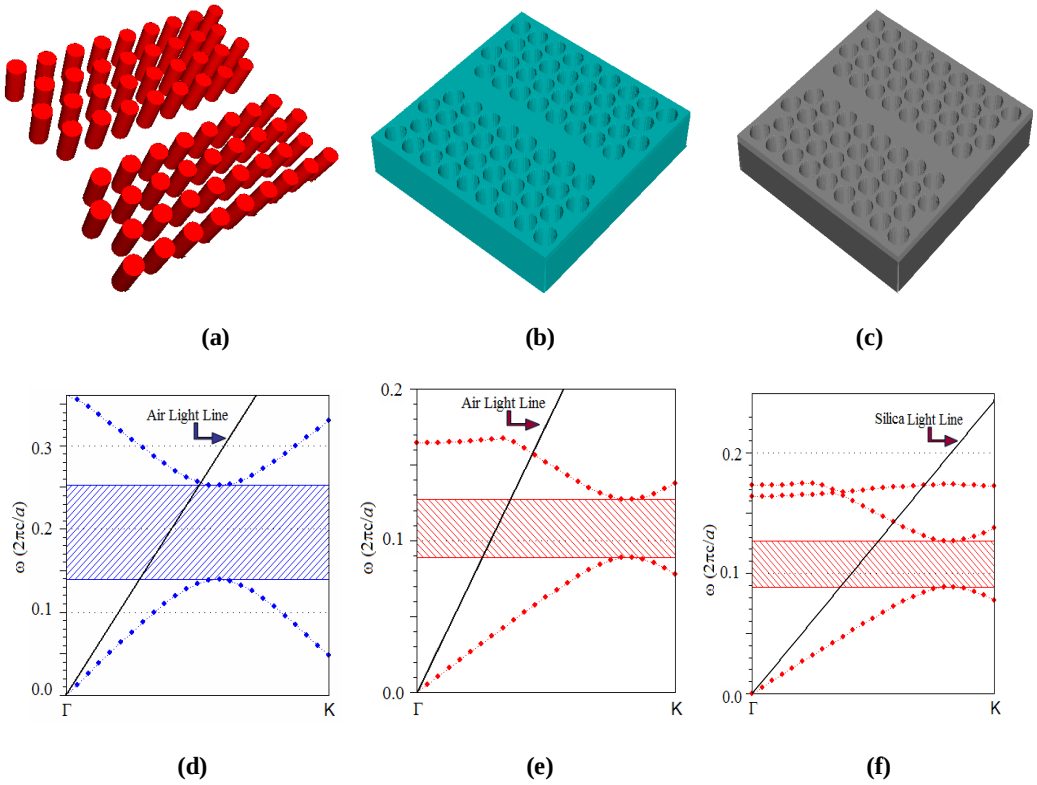

Figure 1.4. PhC line defect waveguides in (a) Pillar type and (b) slab type air bridge structures. (c) SOI based PhC line defect waveguide. Corresponding dispersion curves for (d) pillar type (TM polarization), (e) slab type (TE polarization) and (f) SOI type (TE polarization) PhC waveguides, respectively.

Figures 1.4(d), 1.4(e) and 1.4(f) shows the dispersion curves for structures in figures 1.4(a), 1.4(b) and 1.4(c), respectively. Region above the light line consist of the leaky

modes or the radiation modes. These modes travel into the waveguide but are lossy in the vertical direction. The light-line is known as air light line in air bridge structures whereas it is known as silica light line in SOI based PhC structures. However, modes which lie below the light line are the actual guided modes of the slab. Photonic bandgap in this case is the range of frequencies in which no guided modes exist. It is not a true bandgap because there are still radiation modes existing at those frequencies [Johnson and Joannopoulos *et al.* (2004)].

The controlled propagation of light in PhC waveguides has led to a variety of novel optical phenomenon including superprism effects [Kosaka *et al.* (1998)], negative refraction [Dowling and Bowen (1994), Luo *et al.* (2002), Rajput and Sinha (2010)], slow light generation [Vlasov *et al*. (2003)], and nonlinear effects [Soljacic and Joannopoulos (2004)] etc giving rise to realization of a new generation of photonic components with application in optical communication, optical signal processing and optical sensing [Joannopoulos *et al*. (1995), Sakoda (2001), Johnson and Joannopoulos *et al.* (2004)]. It has led to the design and development of novel devices such as polarizers, splitters, multiplexers and de-multiplexers, couplers, resonators, lasers, modulators, etc. [Sinha and Kalra (2006), Settle *et al*. (2006), Li (2007), Quan *et al.* (2008), Schonburn *et al.* (2006), Camarago *et al.* (2004), Chung and Lee (2007), Chien *et al.* (2006), Fan *et al.* (1999), Meier *et al.* ((1999)]. Photonic Crystals are also used for achieving slow light in the flat band regions of guided modes supported by the line defect waveguides [Gersen *et al*. (2005), Baba and Mori (2007), Fandsen *et al*. (2006)].

Slow light refers to the reduction of group velocity of light - and is a promising technology for future all-optical communication networks. It can be used for the enhancement of light-matter interaction and for the miniaturization of optoelectronic

integrated circuits (OEICs) [Krauss (2008), De La Rue (2008), Vlasov *et al*. (2005), Almieda et al. (2004), Jacobsen *et al* (2006)]. Photonic crystal (PhC) line-defect waveguides that are created within the photonic band gap (PBG) are extensively used for achieving slow light in the flat band regions of guided modes supported by these waveguides [Soljacic *et al.* (2002), Gersen *et al.* (2005), Baba and Mori (2007), Frandsen *et al.* (2006)]. Therefore they have strong application possibilities in optical buffers and other optical storage devices [Tucker *et al.* (2005)].

Recently, nonlinear effects such as the Raman effect, soliton propagation, two photon absorption (TPA), etc. have been observed by different authors [Oda *et al*. (2008), Astrov *et al*. (2000), Tsang *et al.* (2002), Ding *et al.* (2008)]. Self phase modulation (SPM), which leads to chirping and spectral broadening of ultra short pulses, has also been reported earlier [Tsang *et al.* (2002)]. However TPA limits the extent of SPM through nonlinear absorption [Nicolae et *al.* (2006)]. TPA typically involves transitions from the ground state of a system to a higher state by absorption of two photons from an incident radiation field having identical or, more generally, two different frequencies. TPA further creates free carriers that lead to additional losses through free carrier absorption (FCA) and refractive index changes through free carrier dispersion (FCD) [Yin and Agrawal (2007), Oda *et al.* (2007), Inoue *et al.* (2009)]. Thus TPA, FCA, FCD and SPM are important effects that influence the behavior of short laser pulses in silicon waveguides. However soliton dynamics will dominate the propagation of femtosecond pulses in PhC waveguides when group velocity dispersion (GVD) is strongly anomalous because of large waveguide dispersion [Ding *et al.* (2008)]. The spatial compression experienced by light when it enters from fast light to slow light waveguide and the more time it spends in the waveguide because of the slow

group velocity, leads to the increase in light matter interaction and enhancement of nonlinear effects [Soljacic *et al.* (2002)]. Slow light PhC waveguides may thus cause the reduction in input power and physical length of the waveguide needed to see same linear and nonlinear effects in fast light regime [Soljacic *et al.* (2002), Soljacic and Joannopolous (2004)].

1.3 Master Equation

Maxwell's Equations are given as-

$$\nabla . D = \rho \tag{1.1}$$

$$\nabla . B = 0 \tag{1.2}$$

$$\nabla \times E = -\frac{\partial B}{\partial t} \tag{1.3}$$

$$\nabla \times H = \frac{\partial D}{\partial t} + \sigma E \tag{1.4}$$

$$D = \varepsilon E \tag{1.5}$$

$$B = \mu H \tag{1.6}$$

where E is the electric field, H is the magnetic field and ρ is the charge density. In an isotropic medium, the permittivity is written as $\varepsilon = \varepsilon_0 \varepsilon_r$ where ε_0 is the permittivity of vacuum and ε_r is the relative permittivity. The materials used in this work are considered as non-magnetic insulators i.e. $\mu = \mu_0$ and $\sigma = 0$, therefore equation (1.3) and (1.4) are written as:

$$\nabla \times E(r,t) = -\frac{\partial}{\partial t}\left[\mu_0 H(r,t)\right] \tag{1.7}$$

$$\nabla \times H(r,t) = \frac{\partial}{\partial t}\left[\varepsilon_0 \varepsilon_r(r) E(r,t)\right] \tag{1.8}$$

Solving equation (1.8) for *E* and inserting it into time derivative of equation (1.7) gives:

$$\nabla \times \left(\frac{1}{\varepsilon_0 \varepsilon_r(r)} \nabla \times H(r,t) \right) = -\frac{\partial^2}{\partial t^2} \mu_0 H(r,t) \tag{1.9}$$

Time dependence of magnetic field allows us to write:

$$H(r,t) = H(r) e^{-i\omega t}$$

Therefore equation (1.9) becomes:

$$\nabla \times \left(\frac{1}{\varepsilon_0 \varepsilon_r(r)} \nabla \times H(r) \right) = \left(\frac{\omega}{c} \right)^2 H(r) \tag{1.10}$$

where $c = \frac{1}{\sqrt{\mu_0 \varepsilon_0}}$ is the speed of light in vacuum. Equation (1.10) is known as the master equation for the magnetic field. In homogeneous medium, equation (1.10) becomes:

$$\nabla^2 H(r) = -n^2 \left(\frac{\omega}{c} \right)^2 H(r) \tag{1.11}$$

where $n = \sqrt{\varepsilon_r}$ is the refractive index of the medium. Solution of equation (1.11) gives the superposition of plane waves of the form:

$$H(r,t) = H_0 e^{i(k.r - \omega t)} \tag{1.12}$$

$k = \left|\vec{k}\right| = \frac{n\omega}{c} = n\frac{2\pi}{\lambda}$ and λ is the wavelength in vacuum. Therefore, the plane wave is traveling in a direction defined by *k* with phase velocity v_p given by

$$v_p = \frac{\omega}{k} = \frac{c}{n} \tag{1.13}$$

However, for group index n_g, group velocity is given by

$$v_g = \frac{\partial \omega}{\partial k} = \frac{c}{n_g} \tag{1.14}$$

Since n depends on ω, therefore dispersion relation ω (k) is not linear. $\Rightarrow v_p \neq v_g$.

1.4 Computational Methods

1.4.1 Plane Wave Expansion (PWE) Method

Plane wave expansion method remains a reference method for calculation of bandgap in photonic crystals based on Fourier expansion of electromagnetic field and dielectric function [Johnson and Joannopoulous (2001), Joannopoulous *et al.* (1995)]. This method gives rise to a set of eigen values $\frac{\omega a}{2\pi c}$ for each value of k; the optical modes are solved in the vector space i.e. in the reciprocal space. The PWE method utilizes the periodicity of PhCs for expansion of electromagnetic fields and refractive index distribution. However, some structures without periodicity, such as cavities and straight waveguides, can be simulated by implementing a supercell. Dispersion relations in this work have been calculated using RSOFT's Bandsolve package.

1.4.2 Finite Difference Time Domain (FDTD) method

FDTD method calculates time evolution of the electromagnetic waves by direct discretization of Maxwell's Equations. In this method, the differentials in Maxwell's Equation are replaced by finite differences to connect the electromagnetic fields in one time interval to the ones in the next interval [Taflov (1998), Qiu and He (2000)]. FDTD method is therefore best suited for modeling time dependent problems like simulating

pulse propagation through a photonic device. Since this method solves Maxwell's equations without any assumptions, therefore it is flexible in terms of geometry of the device under study. FDTD simulations in this work are carried out by RSOFT's Fullwave package.

1.5 Fabrication Techniques

Photonic crystals are generally not found in nature and have to be designed and fabricated. Therefore a number of methods of fabrication of photonic crystals have been developed [Busch *et al.* (2004)]. Two photon lithography and e beam lithography were the first methods for fabrication of photonic crystal. Two photon lithography utilizes the fact that certain materials, such as polymers are sensitive enough for two photon excitation to trigger chemical or physical changes in the material structure with nanoscale resolution in three dimensions [Cunpston *et al.* (1999)]. In e beam lithography, sample is covered with an electron sensitive material called resist which undergoes a substantial change in its chemical and physical properties, when exposed to an electron beam [Subramania and Lin (2004)]. Another technique which has been developed recently is the holographic lithography which utilizes the interference between two or more coherent light waves to produce a periodic intensity pattern to produce a periodic photonic structure in a photo resist [Campbell *et al.* (2000)]. Self assembly is another most popular approach to fabricate 3D photonic crystals. It is based on the natural tendency of the mono dispersive colloidal particles to self assemble into ordered arrays called artificial opals [Park and Xia (1999), Vlasov *et al.* (2001)]. Auto cloning technique is another fabrication technique which includes three processes occurring simultaneously; the sputtering deposition of dielectric layers, their physical

etching by ions accelerated perpendicularly to the surface and the redeposition of the neutral particles torn from the deposited layer by accelerated ions. The subtle balance achieved between these processes result in repetition of the topology of a prestructured growth substrate from one deposited layer to other [Kawakami (2002)].

1.6 Outline of the thesis

The main focus of this thesis is the design and characterization of devices based on photonic crystal line defect waveguides. These devices include dual band wavelength de-multiplexers, optical buffers and delay lines, soliton propagator, optical switches and logic gates. The research work carried out in the thesis also demonstrates the generation of slow light in elliptical and rectangular hole photonic crystal waveguides and the extension of their tunability, by filling its segments with certain types of liquid crystal (LC) materials. The impact of slow light on the third order nonlinearities have also been investigated in such photonic crystal channel waveguides. This chapter, i.e. Chapter 1, defines the introduction and outline of the proposed thesis.

In Chapter 2, photonic bandgap (PBG) induced wave guiding application of photonic crystals is exploited to design 2D dual band wavelength demultiplexer (DBWD) for separating two telecommunication wavelengths, 1.31 μm and 1.55 μm. Two designs that use silicon rods in air and embedded air holes in silicon material are realized for this purpose. 2D plane wave expansion (PWE) method and 2D finite difference time domain (FDTD) methods are used to design and analyze the DBWD in Y type photonic crystal structures.

In Chapter 3, a highly efficient 3D photonic crystal DBWD using Silicon-on-Insulator (SOI) substrates is proposed for de-multiplexing the two optical

communication wavelengths, 1.31 μm and 1.55 μm. De-multiplexing of the two wavelength channels is obtained by modifying the propagation properties of guided modes, in two arms of Y-type photonic crystal structure. Propagation characteristics of proposed DBWD are analyzed utilizing 3D FDTD method. Enhancement in spectral response is further obtained by optimizing the Y junction of de-multiplexer giving rise to high transmission and extinction ratio for the wavelengths, 1.31 μm and 1.55 μm. Hence it validates the efficiency of proposed optimized DBWD design for separating two optical communication wavelengths, 1.31 μm & 1.55 μm. Tolerance analyses was also performed to check the effect of variation of air hole radius, etch depth and refractive index on the transmission characteristics of the proposed design of SOI based photonic crystal DBWD.

In Chapter 4, a silicon-on-insulator photonic crystal waveguide with hexagonal arrangement of elliptical air holes is reported for slow light propagation with group velocity in the range, 0.0028c to 0.044c and ultra-flattened group velocity dispersion (GVD). The proposed structure is also investigated for its application as an optical buffer with a large value of normalized delay bandwidth product (DBP), equal to 0.778. Furthermore it has been shown that the proposed structure can also be used for time or wavelength-division demultiplexing to separate the two telecom wavelengths, 1.31 μm and 1.55 μm, on a useful time-scale and with minimal distortion.

In Chapter 5, an SOI-based liquid-crystal (LC)-infiltrated photonic-crystal channel waveguide having rectangular air holes in a Silicon core is proposed - that has an average group index of 43 over a bandwidth of 1.02 THz, with vanishing group velocity dispersion, as well as reduced higher-order dispersion. The possible propagation losses due to coupling inefficiency are also investigated for the proposed structure. It is found

that high transmission is obtained for a broad bandwidth from the output of the heterogeneous waveguide finally designed, which consists of an LC-infiltrated PhC slow waveguide surrounded by fast PhC regions on either side. The LC-infiltrated W0.7 PhC waveguide that has been designed for slow light propagation should be highly tolerant to fabrication errors - and has enhanced sensitivity in comparison with conventional PhC waveguides.

In Chapter 6, the effect of slow light on two photon absorption (TPA), free carrier absorption (FCA) and self phase-modulation (SPM) processes in silicon-on-insulator (SOI) photonic crystal (PhC) channel waveguides has been reported. It is found that, in the slow light regime, these nonlinear effects are enhanced, but that the enhancement produced depends on the input peak power level. The increase in the induced phase shift produced by lower group velocities can be used to decrease the size and power requirements needed to operate devices such as optical switches, logic gates and wavelength translators. Simulations also indicate the possibility of soliton-like propagation of 111 fs pulses at 1.55 μm inside such a photonic crystal waveguide.

Finally, the conclusions from the proposed thesis are presented with discussion about the avenues of further research. The future scope of the thesis include the design and development of devices based on slow light in 3D photonic crystals as well as the impact of the enhanced nonlinear effects on different processes such as soliton formation and Raman effect.

Chapter 2

2D Photonic Crystal Air Bridge Dual Band Wavelength Demultiplexer[1]

2.1 Introduction

As discussed in Chapter 1, Photonic crystals (PhCs) have the potential of realizing nanoscale optical components and devices. Radiation losses exhibited by the PhC sharp bend waveguides are far lesser than the conventional waveguides [Valsov and McNab (2004)]. Therefore, two dimension PBG waveguides can be used to design a variety of structures such as directional couplers [Nagpal and Sinha (2004)], beam splitters [Chen *et al.* (2004)], multiplexers and demultiplexers [Centeno *et al.* (1999); Tekeste and Yarrison-Rice (2006)], resonators [Fan *et. al.* (1999)], polarizers [Sinha and Kalra (2006)], polarization beam splitter [Zabelin *et al.* (2007**)]** and so on.

In the recent past, interest has grown in the design and development of Dual Band Wavelength Demultiplexer (DBWD) because of their wide applications in bidirectional communication networks (Chien *et al.* 2004; Chien *et al.* 2006; Chung and Lee 2007). For example, 1.31/1.55 μm duplex devices are commonly used in fiber-to-the-home (FTTH) transmission systems as well as in Coarse Wavelength Division Multiplexed (CWDM) systems [Fiberdyne Labs (2007)]. PhCs have opened

[1] Parts of the results reported in this chapter has been published in the paper, "Modeling and design of 2D photonic crystal based Y type dual band wavelength demultiplexer," ***Optical and Quantum Electronics,*** 40,603-613, July, 2008 .

new possibilities for ultra compact wavelength selective optical devices owing to their PBG induced wave guiding properties. Hence, in the proposed chapter, wave guiding phenomenon due to PBG property of PhC is exploited for the formation of DBWD in Y type air bridge PhC structures, as shown in Figure 2.1(b) and Figure 2.5(b). This design of DBWD separates the two telecommunication wavelengths 1.31 μm and 1.55 μm with a very high extinction ratio and superior quality factor and transmission characteristics. Since the PBG structures strongly control the flow of light, therefore defect created in periodic lattice of PhC results in the confinement of light along specified one arm of the Y type crystal.

Here, the designs of two types of air bridge structures are reported, -one is the hexagonal lattice arrangement of silicon rods in air and the other is the hexagonal lattice arrangement of embedded air holes in silicon material. Both Y type PhC heterostructures were analyzed using 2D Plane Wave Expansion (PWE) method and the performance characteristics in terms of extinction ratio, quality factor and transmittance was obtained by applying 2D Finite Difference Time Domain (FDTD) method.

2.2 Design Characteristics

PhC based DBWD was designed having hexagonal arrangement of silicon rods in air or embedded air holes in silicon material. The lattice constant and radius of rods/holes were chosen so as to provide a wide wavelength span (1.25-1.60 μm) at the band edge of input waveguide of DBWD. Selection of lattice constant and radius of rods/holes of the structure is based on the fact that the bandgap exist for both the wavelengths, 1.31

μm and 1.55 μm so that when line defects are created in photonic crystals, they produce guided modes in photonic crystals corresponding to these wavelengths. Defect radius is chosen such that band gap exist for 1.55 μm in one arm of the Y type DBWD and not for 1.31 μm and vice versa for other arm. Structures having silicon rods in air provide large PBG at technologically convenient geometrical parameters with r/a<0.5, as described in reference [Suknoivanov *et al.* (2006)]. Propagation of light is simulated by 2D FDTD method for wavelengths, 1.31 μm and 1.55 μm and it indicates that 1.31/1.55 μm mixed light will be separated into two lights and guided into two output ports of Y type PhC structure.

2.2.1. 2D PhC DBWD having silicon rods in air

First, the design of a 2D PhC with hexagonal arrangement of Si (n=3.42) rods in air is presented. PWE method was used to study the photonic bandgap variation for transverse magnetic modes (TM polarization) of the incident light where the electric field component of electromagnetic waves is oriented perpendicular to the plane of propagation.

To obtain PBG for the desired range of wavelengths, covering both 1.31 μm and 1.55 μm, we have chosen the lattice constant, a=0.68 μm and rod radius r = 0.2 μm. With these parameters, PhC provides a large bandgap in range of normalized frequency, 0.42318 to 0.54325, for TM polarization (Figure 2.1(a)). Figure 2.1(b) shows the schematic of the finally designed DBWD with silicon rods in air.

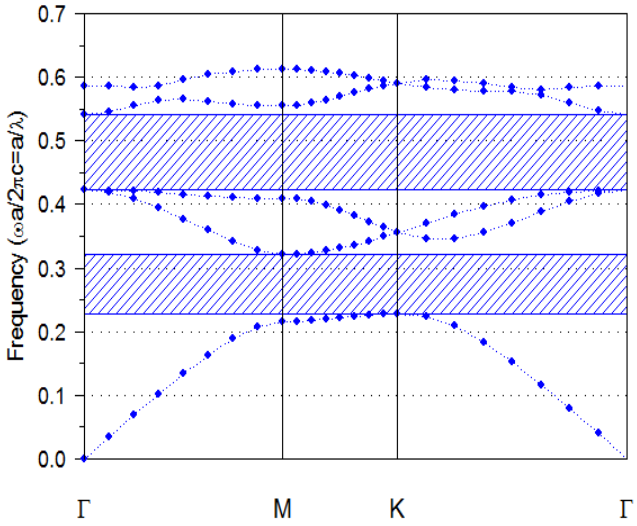

(a)

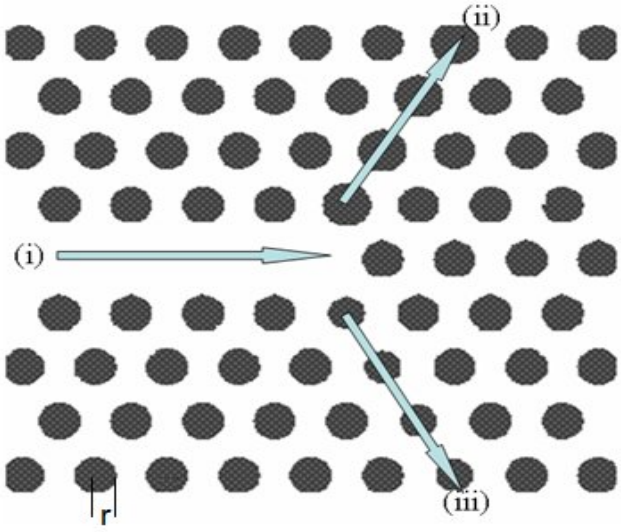

(b)

Figure 2.1 (a) TM band structure of bulk photonic crystal having silicon rods in air, for r = 0.2 μm. (b) Schematic of proposed DBWD having silicon rods in air with (i) Input Wg, (ii) Output Wg1 and (iii) Output Wg2.

A linear defect waveguide is then formed by removing few rods from the direction of propagation of incident light i.e. from ΓK direction. Since the designed structure

possesses bandgap for TM polarization of light, in the wavelength range 1.25 μm ≤ λ ≤ 1.60 μm, both wavelengths, 1.31 μm and 1.55 μm, are guided through the region of input waveguide (Input Wg). Presence of guided mode for both the wavelengths in the input waveguide is confirmed in the figure 2.2(a).

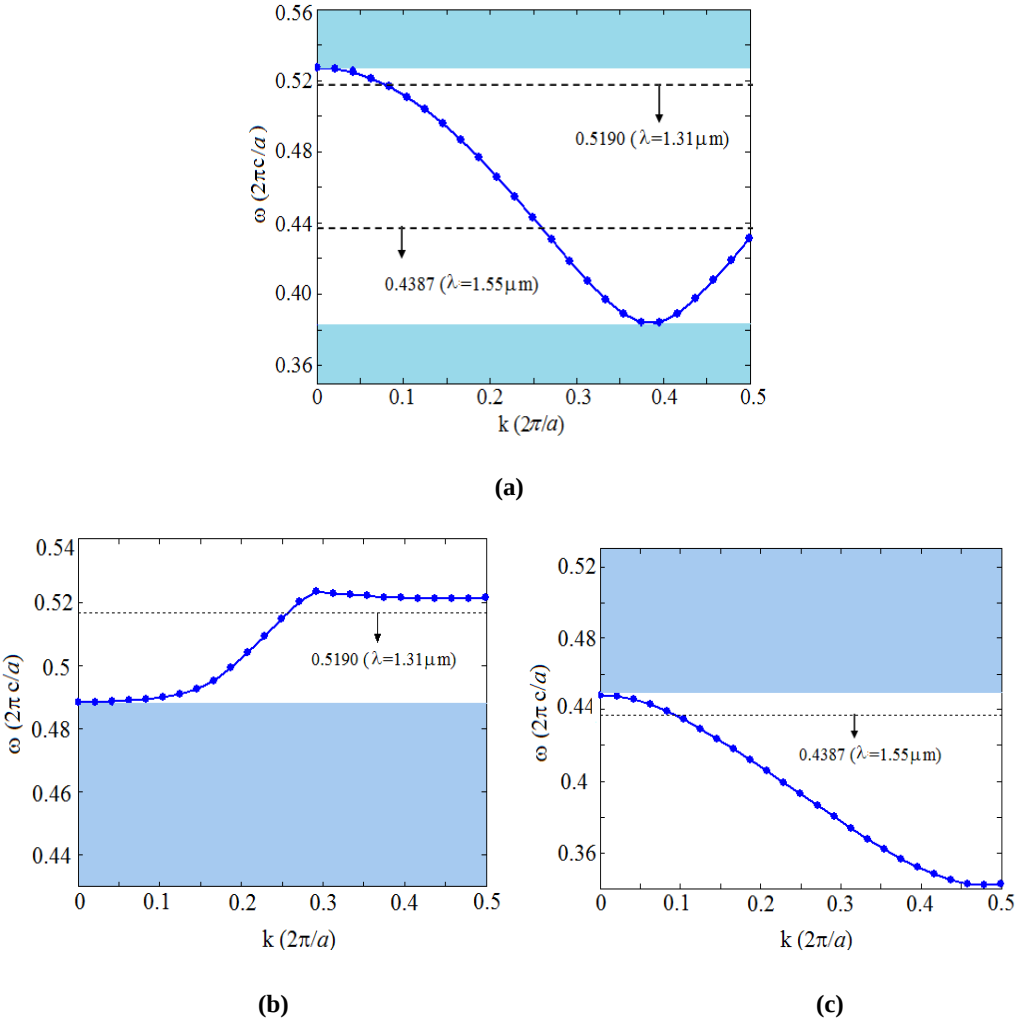

Figure 2.2. Dispersion relations of the three involved PhC waveguides. The blue line (pointed line) corresponds to the respective guided modes for TM polarization in (a) Input Wg, (b) Output Wg1 and (c) Output Wg2.

Further, DBWD was designed by changing the geometrical parameters of Si rods in two arms of Y type photonic bandgap induced waveguides (Figure 2.1(b)). Radii of Si rods in one arm of the structure, named Output Wg1, is changed such that signal of 1.55 μm experiences bandgap and 1.31 μm passes through while radii of Si rods in other arm of the structure, named Output Wg2, is changed such that signal of 1.31 μm experiences bandgap and 1.55 μm passes through. Figures 2.2(b) and 2.2(c) shows the existence of guided modes for 1.31 μm in Output Wg1 and 1.55 μm in Output Wg2.

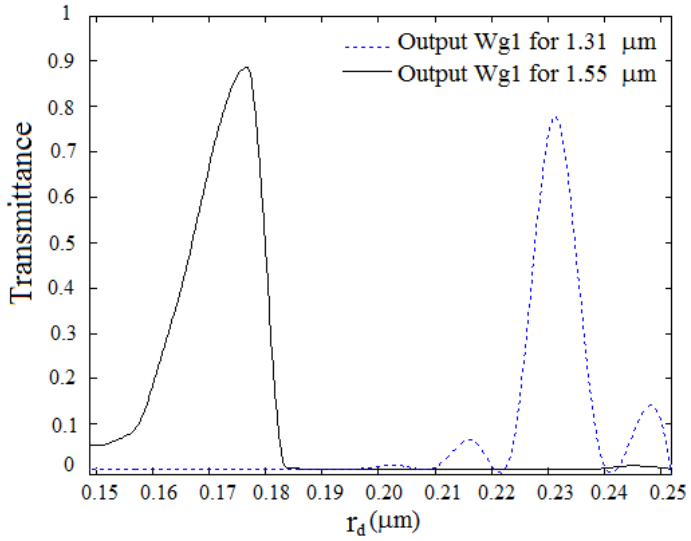

Figure 2.3. Variation of transmittance with defect radius r_d in two output waveguides, Output Wg1 and Output Wg2 for TM polarization of 1.31 μm and 1.55 μm.

While selecting the radii having above specifications for the two output waveguides, it was observed that, a range of radii exists for which the desired range of bandgap appears. Hence the defect radius r_d is investigated by studying the variation of transmittance from the output ports. (Figure 2.3). 2D FDTD method for TM polarization was utilized to generate data for these plots and that radius was chosen, for which transmitted power was maximum. Note that the maximum efficiency of the

device is obtained when defect radius in output Wg1 is r_d=0.2318 μm so that wavelength of 1.31 μm can pass through and 1.55 μm suffers bandgap. In similar line, the maximum transmission efficiency for wavelength of 1.55 μm from the device is obtained when defect radius in output Wg2 is r_d=0.1768 μm. The field pattern for TM polarization for the two telecom wavelengths, 1.31 μm and 1.55 μm in Y type DBWD having silicon rods in air is shown in Figure 2.4.

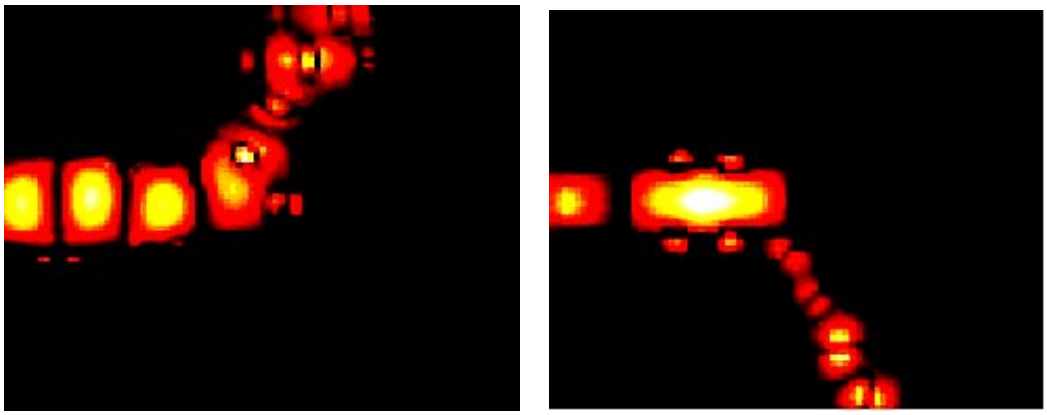

(a) **(b)**

Figure 2.4. Field pattern for TM polarization at (a) λ=1.31 μm and (b) λ=1.55 μm for the designed Y type DBWD having silicon rods in air.

The type of launch field used was Gaussian continuous wave (CW) and beam width and step size was taken to be 0.1 μm and 0.005 μm. Boundary conditions for 2D FDTD simulation of designed structure were taken as X (min): X (max) = -5.6525 μm: 5.6525 μm & Z (min): Z (max) = -2.9996 μm: 2.9996 μm. Output power was determined by the time monitors at output end of the two output waveguides. It is observed that 1.31 μm was obtained from Output Wg1 having defect radius r_d=0.2318 μm and 1.55 μm was obtained from Output Wg2 having defect radius r_d=0.1768 μm.

2.2.2. 2D PhC DBWD having embedded air holes in silicon:

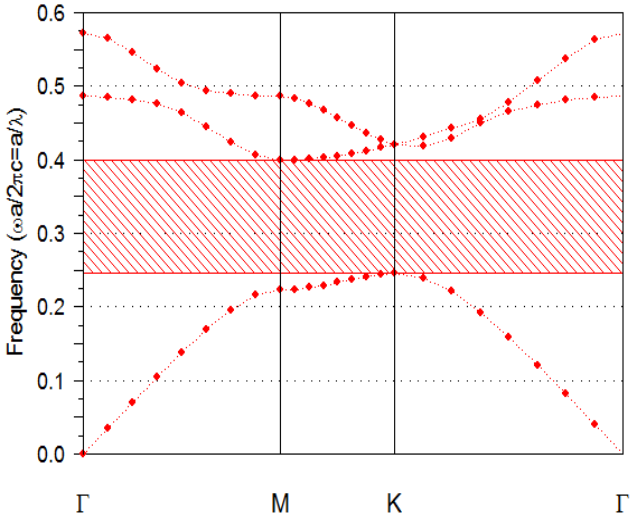

(a)

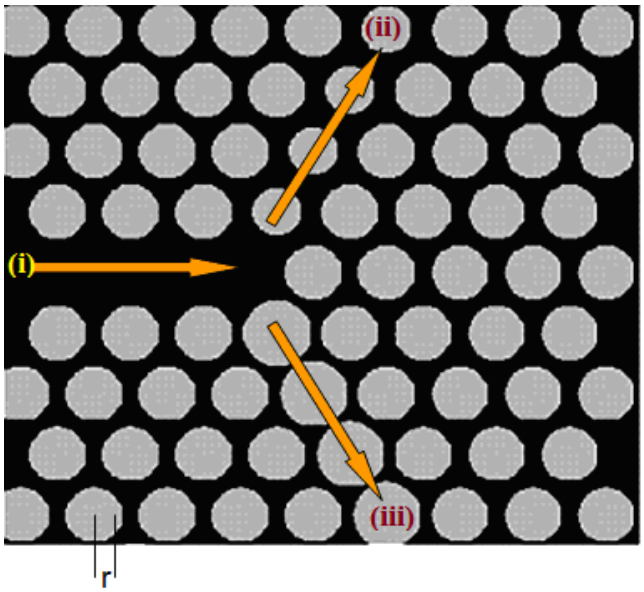

(b)

Figure 2.5. (a) TE band diagram of PhC structure having embedded air holes in silicon for r=0.1896μm. (b) Schematic of proposed DBWD having embedded air holes in silicon material with (i) Input Wg, (ii) Output Wg1 and (iii) Output Wg2.

The second type of DBWD was designed using silicon material (n = 3.42) with embedded hexagonal lattice arrangement of air holes. The lattice constant was chosen to be, a = 0.48 μm. While studying the photonic bandgap variation using PWE method, it was found that large photonic bandgap in the range 1.25 μm ≤ λ ≤ 1.60 μm can be obtained for the transverse electric modes (TE polarization) in the hexagonal arrangement of embedded air holes in silicon material. These air holes have radius r = 0.1896 μm (Figure 2.5). A linear waveguide in the crystal was then created, by removing a few holes from the periodic structure so that TE polarization of wavelengths from 1.25 μm to 1.60 μm can be guided into the input waveguide, shown as Input Wg in Figure 2.5. The PBG based Y type DBWD was created by changing the geometrical parameters of the air holes in the two arms of Y type photonic bandgap induced waveguides such that the wavelength of 1.31 μm was obtained at the output end of one of the arms and wavelength of 1.55 μm was obtained at the output end of the other arm.

Thus radius of the air holes in the two output waveguides are varied such that wavelength of 1.55 μm experiences bandgap in one arm (output Wg1) of Y type demultiplexer and 1.31 μm is guided through, while wavelength of 1.31 μm experiences bandgap in the other arm (output Wg2) of Y type demultiplexer and 1.55 μm passes through it. Figure 2.6 shows the guided modes for the three involved photonic crystal waveguides.

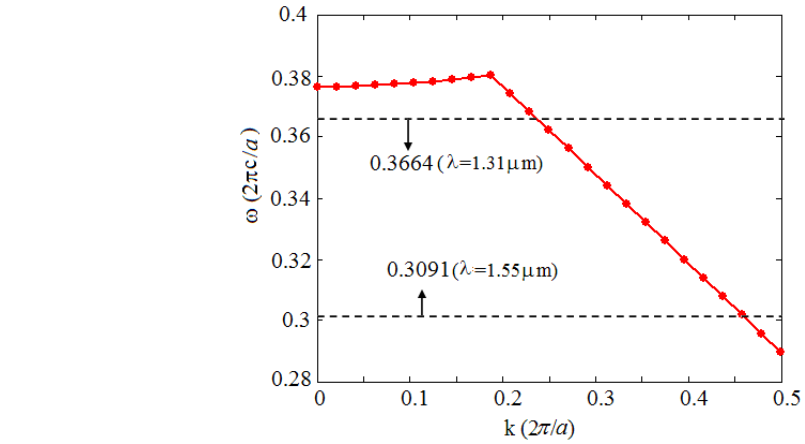

(a)

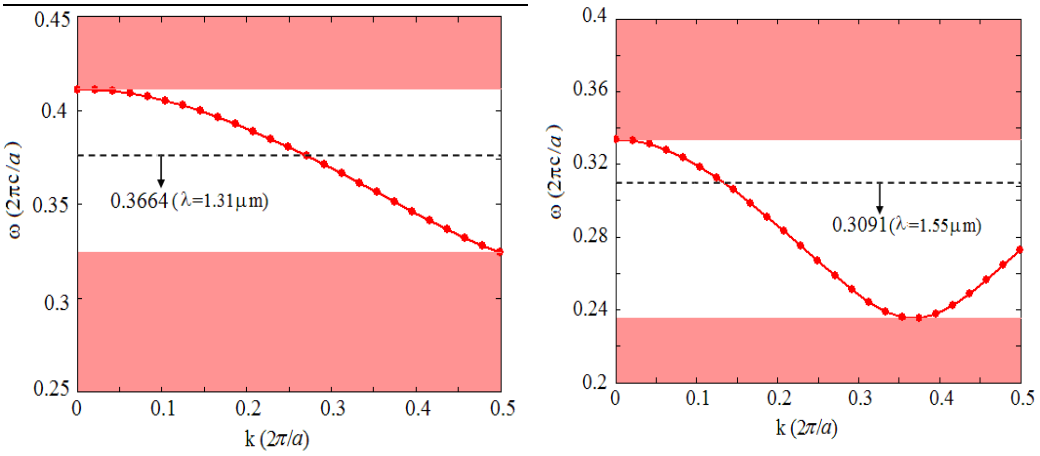

(b) **(c)**

Figure 2.6. Dispersion relation of the three involved PhC waveguides. The red line (pointed line) corresponds to the respective guided modes for TE polarization in (a) Input Wg, (b) Output Wg1 and (c) Output Wg2

It's observed, while varying the radii to obtain the desired bandgap, a range of radii exists for which the given bandgap appears. However, that radii was chosen, for which the transmitted power is maximum. This was investigated by studying its variation with the transmittance from two output ports at 1.31 μm and 1.55 μm, for TE polarization (Figure 2.7). It was found that the maximum efficiency for 1.31 μm

guidance can be obtained when defect radius is r_d=0.1646 µm, in output Wg1, while maximum efficiency of 1.55 µm can be obtained when defect radius is r_d=0.228 µm, in Output Wg2.

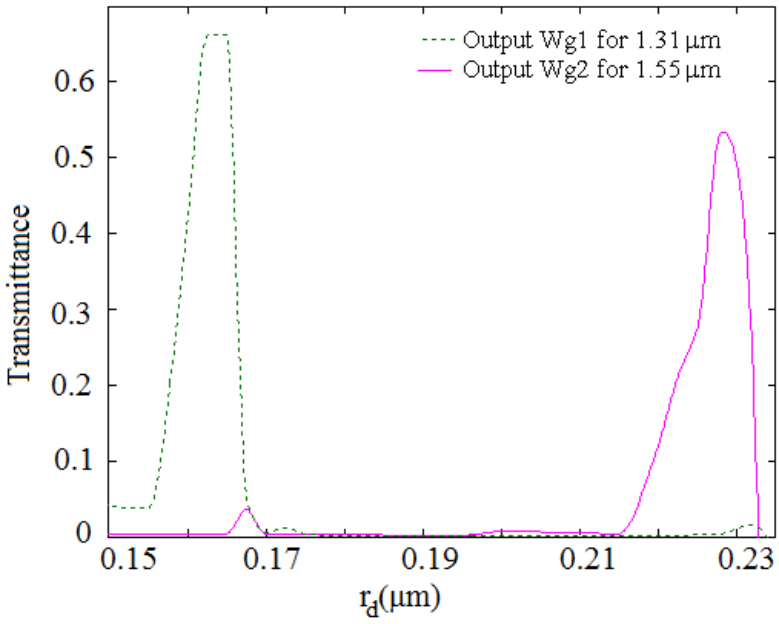

Figure 2.7 Variation of transmittance with defect radius r_d in two output waveguides, Output Wg1 and Output Wg2 for TE polarization of 1.31 µm and 1.55 µm.

The field pattern for TE polarization of the two telecom wavelengths, 1.31 µm and 1.55 µm, in Y type DBWD having embedded air holes in silicon material is shown in Figure 2.7. The type of launch field is Gaussian Continuous Wave (CW). Beam width and step size is taken to be 0.1 µm and 0.00025 µm. Boundary conditions for 2D FDTD simulation of embedded air hole type DBWD is taken as X (min): X (max) = -2.6775 µm: 2.6775 µm & Z (min): Z (max) = -2.9894 µm: 2.9894 µm. Output power is determined by the time monitors at output end of two output waveguides. It was observed that 1.31µm is obtained from Output Wg1 having defect radius r_d=0.1646 µm and 1.55 µm is obtained from Output Wg2 having defect radius r_d=0.228 µm.

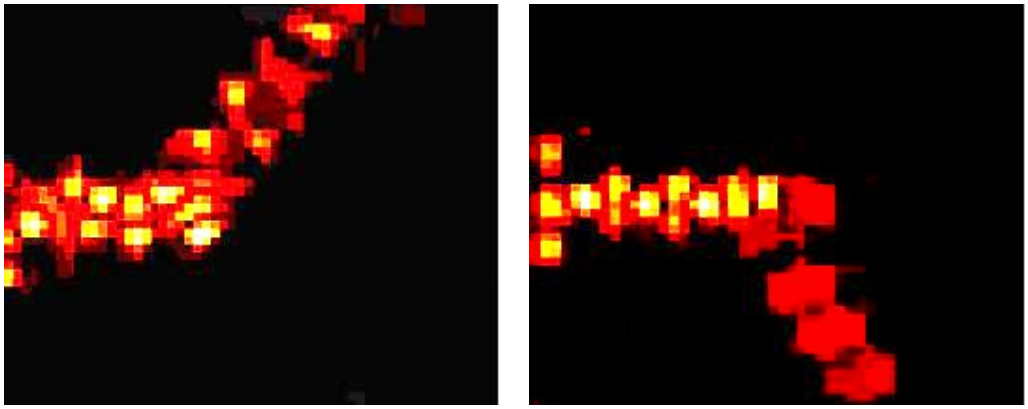

(a) **(b)**

Figure 2.8 Field pattern for TM polarization at (a) λ=1.31 μm and (b) λ=1.55 μm for the designed Y type DBWD having embedded air holes in silicon material

2.3. Numerical Analysis

The proposed Y type DBWD was simulated using 2D FDTD method. Output Wg1 reflects the radiation of wavelength 1.55 μm and allows 1.31 μm while and Output Wg2 reflects the radiation of wavelength 1.31 μm and allows 1.55μm. Efficiency of the device was then investigated by calculating different parameters like transmittance, extinction ratio and quality factor.

2.3.1 Transmittance:

Transmittance of the designed DBWD is defined as the ratio of output intensity [I_{out}] from either of the two output waveguides to the incident intensity [I_{in}] at the entrance of the Y type waveguide: $T = \frac{I_{out}}{I_{in}}$

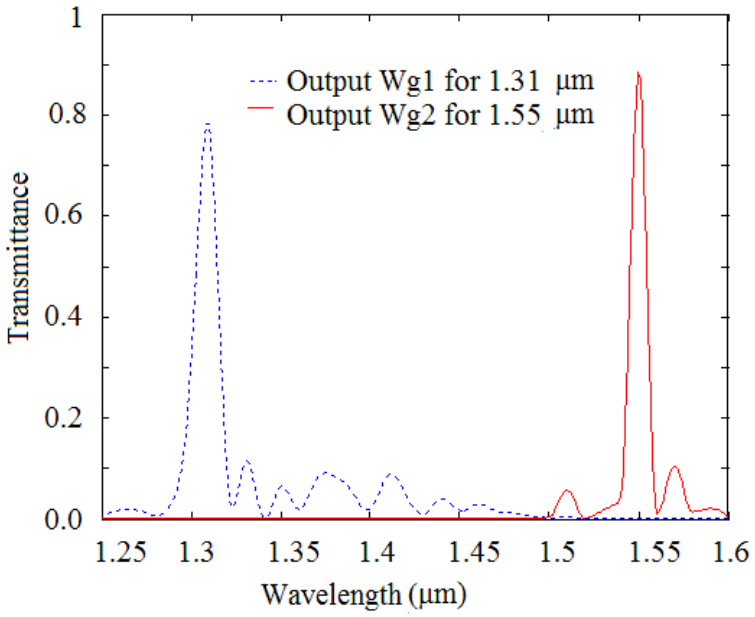

(a)

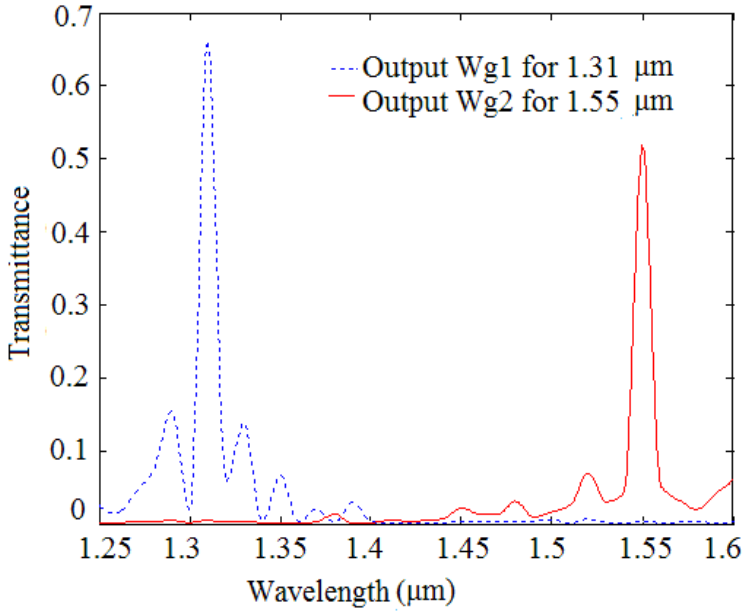

(b)

Figure 2.9. Variation of Transmittance with wavelength at the output end of each output waveguide for (a) the silicon rods in air-based DBWD and (b) embedded air holes in silicon-based DBWD

Variation of transmittance from the two output waveguides of Y type PhC structure consisting of silicon rods in air-based DBWD is shown in Figure 2.9(a) and for embedded air holes in silicon-based DBWD is shown in Figure 2.9(b). It is noted from the two graphs, that maximum efficiency in output Wg1 is shown for the wavelength of 1.31 μm whereas in output Wg2, maximum transmission is shown for the wavelength of 1.55 μm. Hence, the two telecommunication wavelengths 1.31 μm and 1.55 μm can be separated out easily using these two designs of DBWD.

2.3.2 Extinction Ratio:

Further, the extinction ratios ER1 and ER2 of the DBWD were calculated, which explains that the separation of two wavelengths, 1.31 μm and 1.55 μm can be respectively, achieved in such structures. The extinction ratios ER1 and ER2 are defined as:

$$ER1 = 10\log_{10}\frac{\text{fractional output power for 1.31 μm wavelength in waveguide1}}{\text{fractional output power for 1.31 μm wavelength in waveguide2}}$$

$$ER2 = 10\log_{10}\frac{\text{fractional output power of 1.55 μm wavelength in waveguide2}}{\text{fractional output power of 1.55 μm wavelength in waveguide1}}$$

Simulation by 2D FDTD method indicates that in case of silicon rods in air-based DBWD, extinction ratios were calculated to be; ER1 = 36.30 dB and ER2 = 30.40 dB while in case of embedded air holes in silicon-based DBWD, extinction ratios were calculated to be 22.05dB and 22.70 dB for the two wavelengths, 1.31 μm and 1.55 μm, respectively. The PBG induced DBWDs thus have high extinction ratio for

filtering two telecom wavelengths, 1.31μm and 1.55μm, efficiently [Wang *et.al.,* (2005), Chung and Lee (2007)].

2.3.3 Quality Factor:

Quality factor is defined as the ratio of wavelength at peak transmission λ_0, to the full width at half maximum intensity (FWHM) or $\Delta\lambda$.

$$Q = \frac{\lambda_0}{\Delta\lambda}$$

Quality factor for wavelength 1.31 μm and 1.55 μm, in case of silicon rods in air-based DBWD was calculated to be 109.16 and 172.22 respectively, while in case of embedded air holes in silicon-based DBWD, it was found to be 131.0 and 155.0, respectively, at the output end of the two output waveguides. It is mentioned here that these values of quality factors are significantly higher at two widely used telecommunication wavelength windows and hence these designs of PhC based DBWD are having superior filter characteristics.

2.4. Conclusions

In this chapter, the design of Y type DBWDs for separating two telecommunication wavelengths, 1.31 μm and 1.55 μm, in PhC employing (i) silicon rods in air and (ii) embedded air holes in silicon material, is presented. Designs of the appropriate structures were obtained using PWE method, while transmission and other filter characteristics were investigated using 2D FDTD method. It has been demonstrated that the PhC consisting of silicon rods in air -based DBWD reported in this chapter

exhibit high extinction ratio of 36.30 dB for the wavelength of 1.31 μm and 30.40 dB for a wavelength of 1.55 μm. Similarly the other PhC DBWD having embedded air holes in silicon, exhibit extinction ratios as 22.05 dB and 22.70 dB for the wavelength of 1.31 μm and 1.55 μm, respectively. The proposed designs also exhibit superior transmittance and high quality factor values at these widely used telecommunication wavelengths. Thus the proposed DBWD PhC structure can be effectively used in bidirectional optical transmission systems and networks covering broad spectrum of optical communication windows.

Chapter 3

3D Silicon-on-Insulator Photonic Crystal Dual Band Wavelength Demultiplexer[1]

3.1 Introduction

In chapter 2, it has been studied that various types of line defect waveguides can be formed in the PhC's by changing the radius of rods/holes or by removing them completely. These waveguides support true guided modes in the frequency range lying within the PBG of photonic crystal [Johnson *et al.* (1999), Notomi *et al.* (2001)]. These guided modes are horizontally confined by PBG of the photonic crystal and vertically by total internal reflection because of high refractive index contrast between the slab and the cladding. For symmetric structures in vertical direction, like air bridge structures, light can be classified into transverse electric (TE) and transverse magnetic (TM) modes and as even and odd modes. However, for asymmetrical structures, such as SOI structures, the modes cannot be classified selectively- and each mode has an even as well as odd component. In a PhC lattice, having periodicity in xz plane, modes with H_y as predominant component are referred to as TE like modes and those with E_y as predominant component are referred to as TM-like modes

[1] Part of the results reported in this chapter has been published in the paper: "Design, Analysis and Optimization of Silicon-on-Insulator Photonic Crystal Dual Band Wavelength Demultiplexer", **Optics Communication**, 282, 3889-3894, Oct 2009.

(Figure 1.3). Thus in asymmetrical structures, TE like modes have both TE and TM components and the bandgap for pure TE modes cannot be calculated. However, if the amount of TM component is negligible in TE like modes, the photonic crystal supports bandgap for such modes, known as quasi bandgap. So the propagation of TE like modes can be stopped completely within the desired frequency range. Thickness of the PhC waveguide core layer should then satisfy the single mode condition, in order to exploit the quasi PBG effectively [Shinya *et al.* (2002)]. However, from practical perspective, air bridge type structures having air cladding on both sides are mechanically unstable and cannot be used as a platform for future integrated circuits [Kawai *et al*. (2001), Sinha and Kalra (2006), Sinha and Rawal (2008)]. A PhC slab on oxide cladding is more of a promising candidate for large scale integration than air bridge structures. A frequently used material for realizing such PhC slabs is Silicon-on-Insulator (SOI) substrates having silicon layer between silicon-dioxide (SiO_2) cladding on one side and air cladding on the other side. Various PhC components like waveguides, directional couplers, polarizers and polarization splitters have already been realized [Settle *et al.* (2006), Quan *et al.* (2008), Schonbrun *et al.* (2006), Cui *et al.* (2008), Camargo *et al.* (2004), Camargo and De La Rue (2004)] using photonic crystal architecture on SOI substrates. DBWD's are the key components for transmitter receiver devices in bidirectional communication in local area optical networks. 1.31/1.55μm duplex de-multiplexers are also used in fiber-to-home (FTTH) transmission systems and in Coarse Wavelength Division Multiplexing (CWDM) systems [Fyberdyne Labs (2007), Chung and Lee (2007), Chien *et al* (2006)]. In the recent past, various photonic crystal dual band demultiplexers have been realized for demultiplexing signals of wavelength 1.31μm and 1.55μm which are important in the

field of optical communication [Chung and Lee (2007), Chien *et al*. (2006), Sukhoivanov *et al*. (2006), Huang *et al.* (2008), Sinha and Rawal (2008)]. However, these designs are based on air bridge structures with air cladding on both sides i.e. the PhC structures are freely suspended in air and hence are mechanically unstable from practical perspective as well as not suitable for large scale integration. Structures with solid support are more realistic. To overcome this instability, SOI based PhC DBWDs are required to be designed and developed. In these structures, mechanical robustness is improved by the existence of supporting dielectric material under the slab [Notomi *et al.* (2002), Qui (2002), Tanaka *et al*. (2004), Tanaka *et al.* (2004)]. Further such Y type structures are also required to be optimized for high transmission from both the output waveguides [Dekkiche and Naoum (2006)].

In this chapter, earlier approach is extended to design a 3D silicon-on-insulator photonic crystal dual band wavelength demultiplexer (DBWD) for de-multiplexing the two telecom wavelengths, 1.31 μm and 1.55 μm. The structure designed is purely 3D with a silicon (core) thickness of 0.35μm and silica (cladding) thickness of 3 μm. Dispersion curves were obtained using 3D Plane Wave Expansion (PWE) method to explain the guidance in three concerned waveguides; Input Waveguide, Output Waveguide1 and Output Waveguide2. Modes in these waveguides, which lie below the silica light line, are guided in the plane along the defect. However, modes which lie above the light line are lossy in the vertical direction and are called the radiation modes. 3D guidance of the light is thus confirmed in the proposed structure.

Optimization of Y bend is also carried out by adding a air hole near the Y junction of proposed SOI based DBWD. This reduces the multimode effect and backward scattering in the input waveguide from Y junction. Increased transmission of the

resulting structure is also calculated using 3D FDTD method. Tolerance of the device to fabrication is also investigated by varying the radius of air holes; etch depth and refractive index of Si core. Demultiplexing function is demonstrated using 3D Finite Difference Time Domain (FDTD) method. Numerical analysis indicates that the proposed structure demultiplexes the TE like polarization of 1.31µm and 1.55µm, effectively. It is expected that such designs will help in realizing devices and components for broad band optical communication systems and networks.

3.2. Structure Design

The Y type DBWD was designed; consisting of hexagonal arrangement of embedded air holes in Si (n=3.42) PhC slab having thickness 0.35µm on silica (SiO_2) cladding of thickness, 3µm.

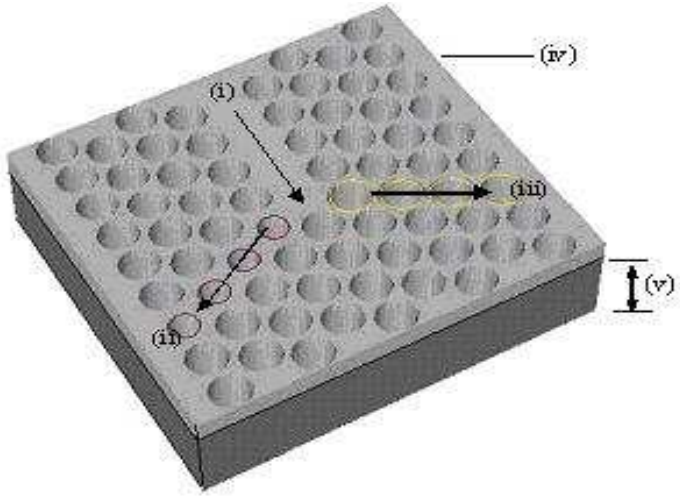

Figure 3.1 Schematic view of proposed non optimized DBWD having embedded air holes in silicon material with (i) Input Wg (ii) Output Wg1 with r_1=0.129 µm (iii) Output Wg2 with r_2=0.187 µm (iv) Silicon material and (v) Silica. Radius of holes in the bulk structure is chosen to be 0.175µm.

Selection of radius of the holes of the entire structure is based upon the fact that bandgap exist for the telecom wavelengths, 1.31 µm and 1.55 µm, so that when line defect is created in such structures, they produce guided modes corresponding to both these wavelengths. Defect radius in the two arms of Y type structure is chosen so that bandgap exist for 1.55 µm in one arm and not for 1.31 µm in the same arm and vice versa for the other arm (Figure 3.1). To obtain PBG for desired range of wavelengths covering both 1.31µm and 1.55µm, we have chosen lattice constant, a to be 0.42 µm and hole radius r =0.175µm. 3D PWE method is utilized for calculating guided modes below silica light-line. With these parameters, the structure supports a large photonic band gap for TE like modes in the range of normalized frequency varying from 0.2558 to 0.4367 i.e. wavelength λ ranging from 1.64 µm to 0.96 µm (Figure 3.2).

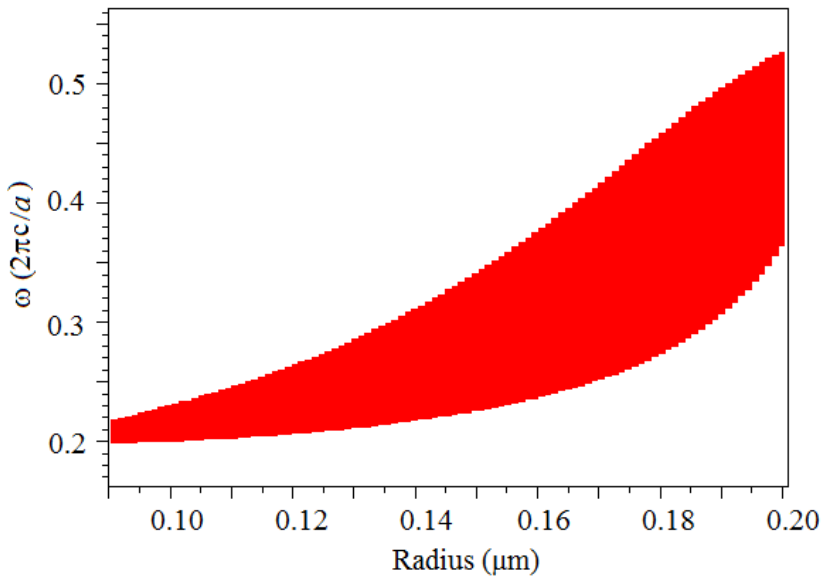

Figure 3.2 Band structure for TE like modes for hexagonal lattice having hole radius r=0.175 µm, r_1=0.129 µm, r_2=0.187 µm and lattice constant a=0.42 µm.

The input waveguide (Input Wg) is formed by removing a few holes in a row from the direction of propagation. Since the designed structure possess PBG for TE like modes of telecom wavelengths, 1.31μm and 1.55μm, the line defect, input waveguide, created supports the guided modes for both these wavelengths. Figure 3.3(a) shows the dispersion curve for Input Wg, which supports the light propagation for normalized frequency, 0.3206 and 0.2709, in the proposed design of PhC. The black solid line is the SiO_2 light line. The waveguide modes which lie below the light line are guided modes while those which lie above the light line become resonant i.e. they are still guided in the plane along the line defect but they are lossy in the vertical direction. Thus wavelengths, 1.31 μm and 1.55 μm are guided in the input waveguide. The PBG based DBWD is then created by changing the geometrical parameters in two arms of the Y type structure. The radii in the two arms of the structure are chosen such that signal for wavelength of 1.31 μm is obtained from output end of one arm and signal for wavelength of 1.55 μm is obtained from output end of the other arm. For this we need to have a bandgap for 1.55 μm in first arm and for 1.31 μm in second arm. Figure 3.2 explains that for defect radius r_1= 0.129 μm, PBG exist for normalized frequency 0.2709 (λ=1.55μm) and not for 0.3206 (λ=1.31 μm). While for defect radius r_2=0.187 μm, PBG exist for normalized frequency of 0.3206 and not for 0.2709. Thus we change the radii of holes in one arm of the Y type structure to r_1 and named it as Output Wg1 and radii of holes in other arm of the Y type structure are changed to r_2 and named as Output Wg2. Thus Output Wg1 is a reduced index region because it is obtained by increasing the radii of embedded air holes in silicon slab while Output Wg2 is an increased index region because it is obtained by decreasing the radii of air holes.

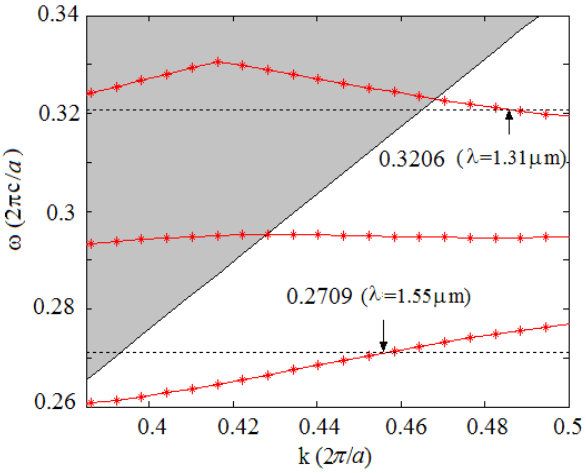

(a)

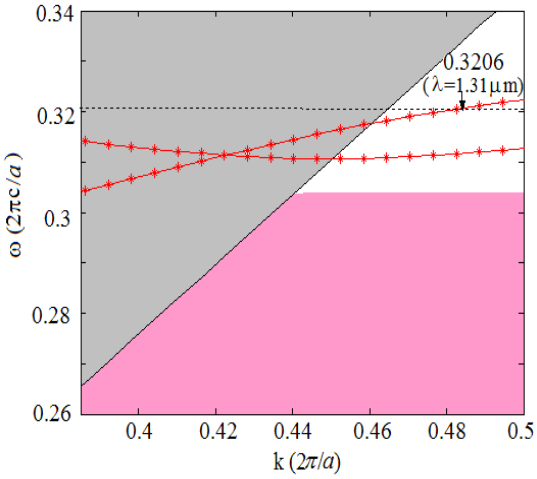

(b)

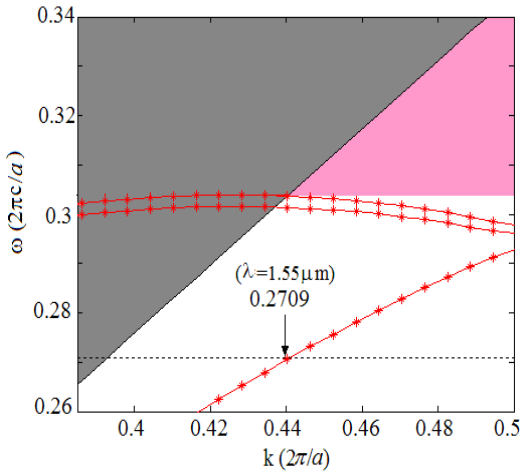

(c)

Figure 3.3 Dispersion relations of the three involved PhC waveguides. The black (solid) line corresponds to SiO_2 light line and the red lines corresponds to the respective single guided modes in (a) Input Wg, (b) Output Wg1 and (c) Output Wg2.

Dispersion curve in Figure 3.3(b) shows that the guided modes exist for normalized frequency 0.3206 corresponding to optical wavelength of 1.31 μm while normalized frequency of 0.2709 i.e. wavelength of 1.55 μm is clearly not supported by Output Wg1. Hence if incident light is 1.31 μm, it will be well confined within the

waveguide having defect radius r_1 i.e. Output Wg1. However if the incident light is 1.55 µm, it will be completely radiated out from Output Wg1. In the same way dispersion curve in Fig. 3.3(c) shows that guided mode exist for normalized frequency of 0.2709 corresponding to optical wavelength of 1.55 µm in Output Wg2 while no guided mode exist for 1.31 µm in the same waveguide having defect radius r_2. Thus the incident light of 1.55µm is propagated in Output Wg2 and 1.31 µm is radiated out. Hence in the proposed design of DBWD, we obtain wavelength of 1.31µm from Output Wg1 and 1.55 µm from Output Wg2.

3.3. FDTD Simulation Results and Discussion

3D FDTD simulation was performed to determine the de-multiplexing efficiency of the designed DBWD for separating two telecom wavelengths, 1.31 µm and 1.55 µm.

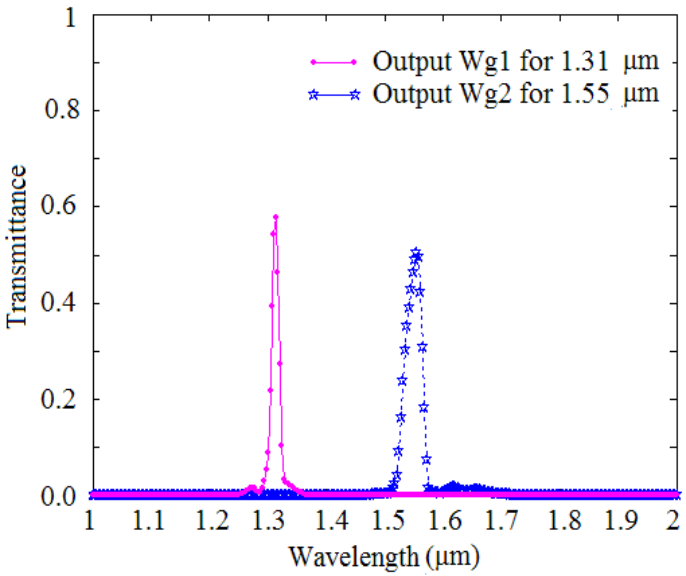

Figure 3.4 Variation of transmittance with wavelength from two output waveguides for TE like polarization of incident light for non optimized SOI based DBWD.

3D FDTD simulations were carried out by PhotonD (Crystal Wave) package where mesh size is taken to be Period/3 and device dimensions are taken to be 3.31μmx5.86μm in XZ plane. Here Transmittance (T) is defined as the ratio of output power obtained from either of the output waveguides to the input power i.e. $T = P_{out}/P_{in}$. Figure 3.4 shows the spectral response of proposed DBWD for TE like polarization of incident light. From this figure, it is clear that the proposed structure successfully split the two telecom wavelengths but the maximum peaks obtained from two output waveguides is 50% of input signal for 1.55 μm and 58% of input signal for 1.31 μm. This weak transmission is due to the backward scattering, in the input waveguide, from Y junction as well as excitation of higher order modes which cannot correctly propagate in the output waveguides. In order to improve transmission, junction region has to be modified by adding a smaller hole near the junction in the input waveguide. This reduces multimode effect and backward scattering by varying the optical width of the waveguide.

3.4. Optimized Structure

In order to enter the proper optimization for increasing the transmission at the two output ports, one has to define the position and radius of the hole which is inserted near the Y junction of proposed SOI based DBWD. This caused gentle perturbation of the incoming wave while changing its direction from input waveguide to either of the output waveguides. By tailoring the radius of induced air hole, transmittance peaks from two output waveguides can be increased. Figure 3.5 shows the variation of radius (*R*) of the additional air hole placed at different positions (*L* as shown in Figure

3.6) with transmittance from two output waveguides corresponding to two telecom wavelengths, 1.31 µm and 1.55 µm.

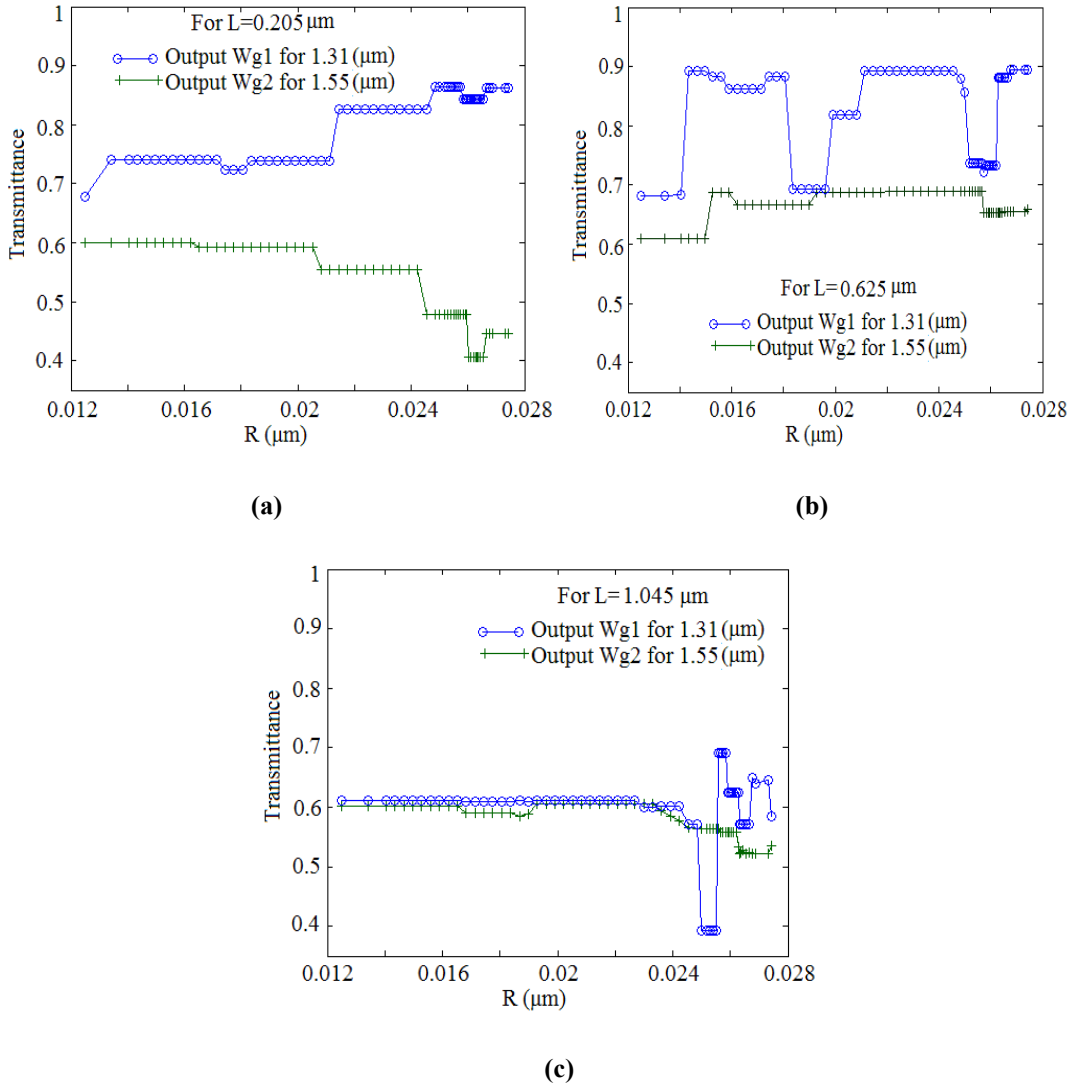

Figure 3.5 Variation of Transmittance with radius *R* of additional air hole added at different positions (a) *L*=0.205 µm , (b) *L*=0.625 µm and (c) *L*=1.045 µm.

It is observed that, for *R*=0.0245 µm and *L*=0.625 µm, transmittance from two output waveguides increases significantly which corresponds to decrease in backward scattering from the junction. The resulting optimized SOI based DBWD is shown in

Figure 3.6. Placing the additional air hole near the junction clearly increases the power transmission as observed in 3D FDTD simulation of optimized structure.

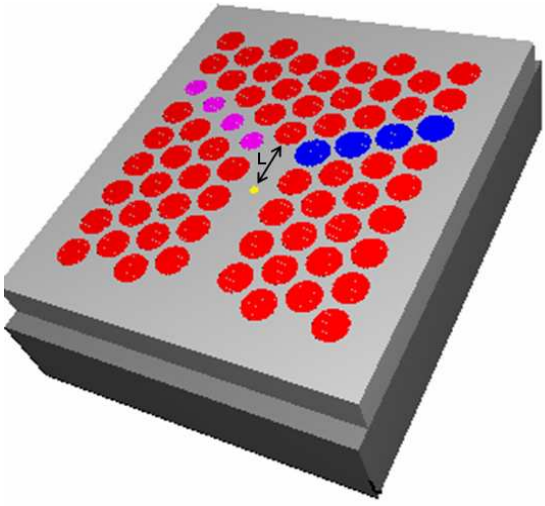

(a)

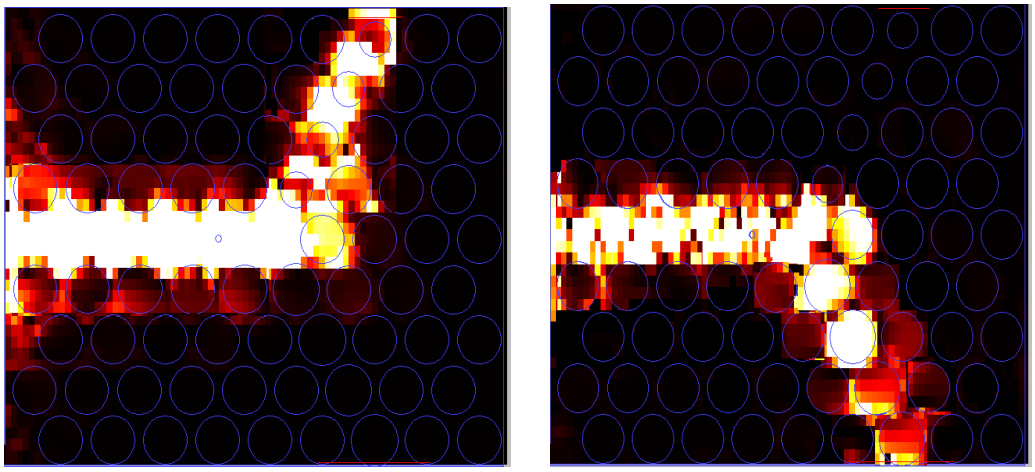

(b) **(c)**

Figure 3.6 (a) Optimized structure of SOI based DBWD with *R*=0.0245 µm and *L*=0.625 µm. Field pattern for TE like polarization at (b) λ=1.31 µm and (b) λ=1.55 µm for the proposed SOI based DBWD.

Spectral response of transmittance for proposed optimized SOI based photonic crystal DBWD is shown in Figure 3.7. It explains that the two wavelengths 1.31 µm

and 1.55 μm separate out efficiently and are received from the two output waveguides, respectively. Power transmittance efficiency for 1.31 μm obtained from Output Wg1 is calculated to be 89% and transmission efficiency of 1.55 μm obtained from Output Wg2 is found to be 69%.

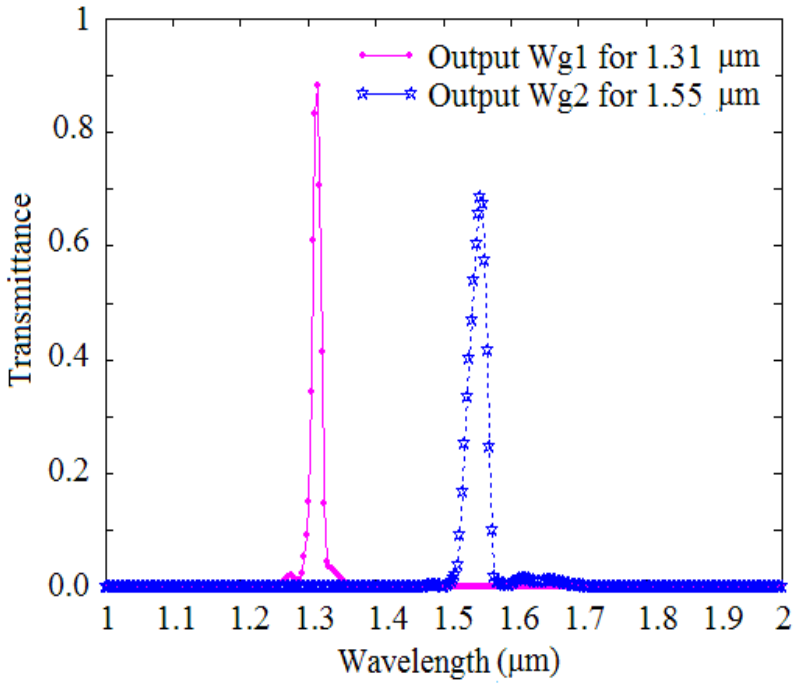

Figure 3.7. Variation of transmittance with wavelength from two output waveguides for TE like polarization of incident light for optimized SOI based DBWD.

Efficiency of the device is further confirmed by calculating its extinction ratio which is defined as:

$$ER1 = 10\log_{10}\frac{\text{Transmittance for 1.31 μm obtained from Output Waveguide1}}{\text{Transmittance for 1.31 μm obtained from Output Waveguide2}}$$

and

$$ER2 = 10\log_{10}\frac{\text{Transmittance of 1.55 μm obtained from Output Waveguide2}}{\text{Transmittance of 1.55 μm obtained from Output Waveguide1}}$$

The values are calculated to be; ER1=26.10 dB for 1.31 μm and ER2=27.50 dB for 1.55 μm. It is mentioned here that these values of extinction ratio are sufficiently high for SOI based PhCs.

3.5. Tolerance Analysis

In this section, the effect of change in air hole radius, variation of angle from vertical of the optimizing air hole near Y junction and variation of refractive index of silicon core by 0.01 to 0.001 on the transmission characteristics of optimized SOI based DBWD in PhC is studied. First, it is shown, how the transmission changes for ±3% variation in r_1 and r_2 because for these variations in the radius, desired frequencies lie well within the desired bandgap. Figure 3.8 shows the variation of transmittance plotted on both left and right hand y-axis of graph with tolerance on x-axis. The solid curve corresponds to the tolerance in Output Wg1 i.e. in defect radius r_1 while the dash-dot curve corresponds to the tolerance in Output Wg2 i.e. in defect radius r_2. It can be seen from the tolerance analysis that although increase or decrease in defect radii by ±3% do not cause significant change in photonic band gap, the wavelength region of the guided mode remains unaffected in the proposed DBWD.

Hence, simulation results in figure 3.8 explains (i) the change in intensity of the transmitted light of wavelength 1.55 μm falls to 52% from 69% with -3% change in defect radius r_2 in Output Wg2 while it rises to 83% when r_2 increases by 3% and (ii) the intensity of the transmitted light of wavelength 1.31 μm with ±3% change in defect radius r_1 in Output Wg1 varies approximately from 89% to 72%.

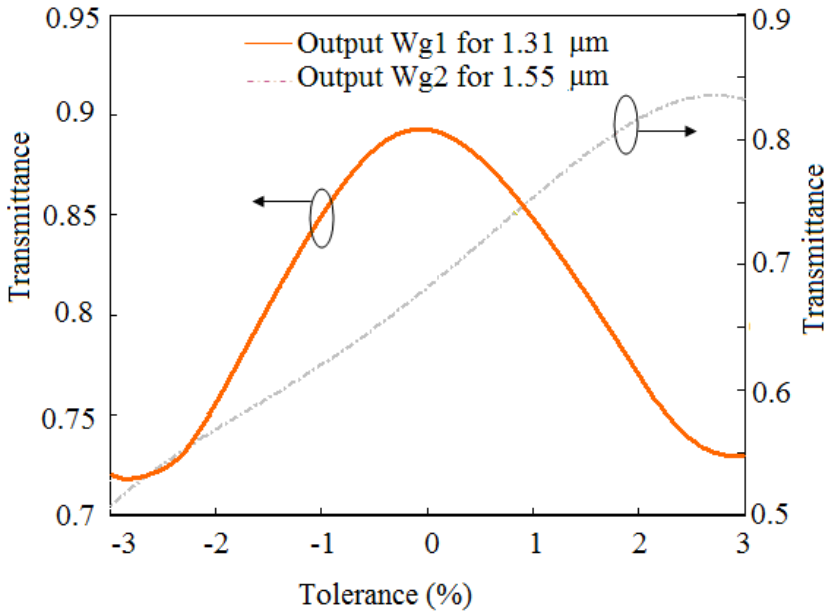

Figure 3.8 Effect of tolerances in defect radius r_1 and r_2 on the transmission characteristics of proposed optimized DBWD.

Further, the tolerance analysis of the device was carried out for variation in etch depth of optimizing air hole having radius *R*=24.5nm inserted near the Y junction of the structure. During fabrication, air holes with small radius usually etch at a slower rate and hence tend to be shallower. Also the shape of the hole would be conic since the defect is quiet small with regard to lattice holes. Therefore impact of conic angle from vertical, with a corresponding change in etch depth, on transmittance is shown in Figure 3.9(a).

The variation in refractive index of silicon core and its impact on transmission characteristics of proposed SOI based DBWD (Figure 3.9(b)) is also studied and it is observed that transmittance changes by less than ±0.02% from either of the output waveguides. Tolerance analysis of above factors leads us to conclude that the

proposed DBWD on SOI based photonic crystal has a reasonable fabrication tolerance.

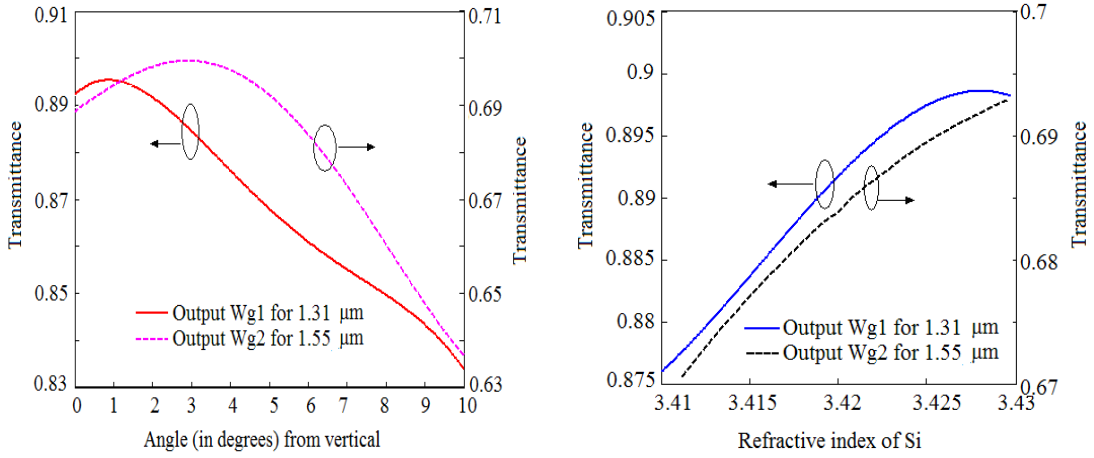

(a) **(b)**

Figure 3.9 Effect of tolerances in (a) angle from vertical of optimizing defect radius *R* having conic shape and (b) variation of refractive index of Si core on the transmission characteristics of proposed optimized DBWD.

3.6. Conclusion

In this chapter, the design of SOI based DBWD to split the TE like polarization of two telecommunication wavelengths, 1.31 μm and 1.55 μm is presented. The principle of the design of DBWD is based on the phenomenon of light wave guidance due to photonic bandgap in horizontal direction and refractive index contrast in vertical direction and thereby the existence of guided modes in defect waveguides. The filtering characteristics were computed using 3D FDTD method and it was found that the two telecom wavelengths can be de-multiplexed efficiently. Transmission characteristics are enhanced by optimizing the structure by adding smaller air hole near the Y junction. Transmittance peaks obtained from two output waveguides is 89% for 1.31 μm and 69% for 1.55 μm. Extinction ratio of the optimized structure is

calculated to be 26.10 dB for 1.31 μm and 27.50 dB for 1.55 μm. Tolerance analysis of the device was also carried out for ±3% change in defect radius in the two output waveguides and it is found that wavelength region of the guided mode remains unaffected in the proposed optimized SOI based DBWD with increase or decrease in defect radii by 3%. Effects of variation in etch depth of the optimizing air hole and variation of refractive index of slab on transmittance is also studied.

Chapter 4

Slow Light with Ultra-Flattened Dispersion in SOI Photonic Crystal[1]

4.1 Introduction

Slow light refers to reduction of the group velocity of light - and is a promising technology for future all-optical communication networks. As discussed in Chapter 1, photonic crystal (PhC) line-defect waveguides that are created within the photonic band gap (PBG), are extensively used for achieving slow light in the flat band regions of guided modes supported by these waveguides [Soljacic *et al.* (2002), Gersen *et al.* (2005), Baba and Mori (2007), Frandsen *et al.* (2006)]. Therefore they have strong application possibilities in optical buffers and other optical storage devices [Tucker *et al.* (2005)]. The high refractive index contrast achievable in SOI structures provides strong confinement of light in the vertical direction, while the PBG of the PhC lattice provides confinement of light in the horizontal direction. Slow light in PhCs has already been observed by several authors [Povinelli *et al.* (2005), Baba *et al*. (2004), Krauss (2007)] near the edge of the Brillouin zone. Recently Mori and Baba have experimentally demonstrated a slow light device based on a chirped PhC coupled waveguide [Mori and Baba (2005), Mori and Baba (2004)] and have achieved the low

[1] Part of the results reported in this chapter has been published in the paper: "Slow Light Miniature Devices with Ultra-Flattened Dispersion in Silicon-on-Insulator Photonic Crystal", **Optics Express,** 17, 13315-13325, August 2009.

group velocity of 0.017c. However fabrication of such complex devices is challenging and may limit their practical utilization in large scale integration.

In this chapter, the design of an SOI based PhC structure having elliptical air holes within a silicon core is reported. However, for asymmetrical structures, such as SOI structures, the modes cannot be classified selectively- and each mode has even as well as odd components. Modes with H_y as the predominant component are referred to as TE-like modes - and those with E_y as the predominant component is referred to as TM-like modes. (See Figure 1) The thickness of the PhC waveguide core layer should then satisfy the single-mode condition, in order to exploit the quasi PBG effectively [Shinya *et al.* (2002)]. The SOI waveguide structure is made up of a silicon core layer sandwiched between a silica cladding layer below and an air cladding above. The major and minor axes of the elliptical air holes are tuned to obtain a flat section of dispersion curve below the silica light-line for slow light propagation.

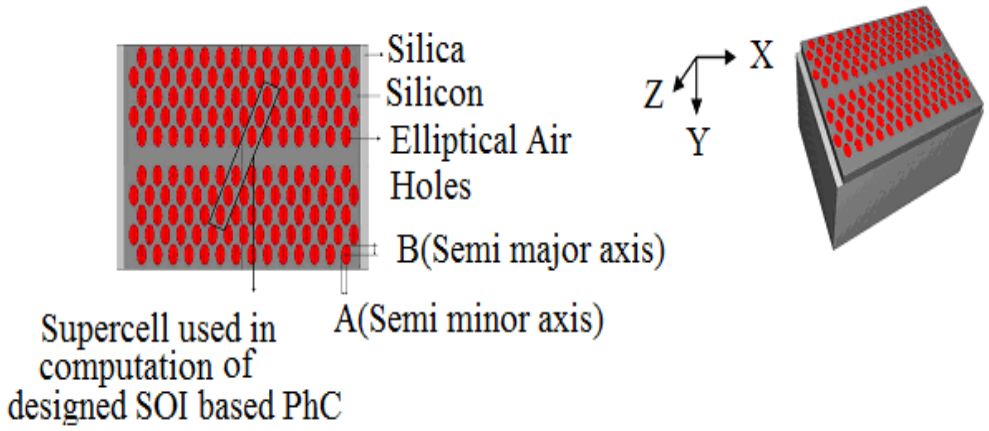

(a) **(b)**

Figure 4.1. (a) Schematic of the proposed design for the W1 line defect channel waveguide configuration with length equal to 15*a*. (b) Diagram defining the coordinate system.

Figure 4.1 shows a schematic of the proposed design that has elliptical holes in a hexagonal arrangement - with a W1 line-defect channel waveguide configuration. The inset in Figure 4.1 shows the super-cell used in computational modelling of the designed structure. For the device applications of such waveguides, the group velocity dispersion (GVD) and other higher-order dispersion parameters should be very low [Di-Falco *et al.* (2008), Wang *et al.* (2008)] thereby enabling the optical signal to propagate with reduced distortion - as would be demonstrated using FDTD simulations. The band structure was obtained using a 3D PWE method. Using these simulation tools we have been able to design an SOI based PhC channel waveguide with slow light behaviour - having a group velocity in the range from 0.0028c to 0.044c – and with vanishing GVD, third order dispersion (TOD) and fourth order dispersion (FOD) parameters. The structure designed has also been investigated for its possible application in the design of (i) an optical buffer with a value of normalized DBP that is equal to 0.778 - a value that is higher than previously reported values [Mori and Baba (2005), Settle et al. (2007), Ma and Jiang (2008)] - and (ii) a time and wavelength division de-multiplexing device. The proposed device is designed to de-multiplex the two telecommunication wavelengths, 1.31 μm and 1.55 μm as well as other wavelengths around 1.55 μm, using time discrimination and with minimal distortion, while exhibiting an ultra-flattened dispersion curve for both wavelengths.

4.2. Design Aspects and Device Description

For the design, a hexagonal arrangement of air holes in an SOI based PhC structure was first assumed. The refractive index of silicon has been taken to be 3.50 and its

thickness has been taken to be 450 nm. Computed results for the band-structure of a W1 channel waveguide aligned along the Γ-K direction are shown in figure 4.2. They indicate that only a single guided mode exists below the silica light-line - and the calculated value of the effective index of the guided mode for the fundamental TE-like guided mode is calculated to be 3.25. This core guiding layer of silicon is typically bonded on to a silica (SiO_2) lower cladding layer that may be as much as 3 μm thick, in practice.

The lattice constant for the air holes has been chosen to be a =0.42 μm, with a basic air hole radius of 0.33a. As shown in Figure 4.2(a), the band gap of the designed structure lies in the frequency range 0.2130($2\pi c/a$) to 0.3058($2\pi c/a$), for the TE like polarization. A W1 PhC channel waveguide was then obtained by creating a single line defect in the photonic crystal. By examining the dispersion diagram in Figure 4.2(b), it is possible to identify a flat section for the even-symmetry transverse mode of the W1 waveguide located at frequencies around 0.24($2\pi c/a$). The inset in the figure shows the super-cell used in the 3D PWE calculation.

It is observed that the group velocity becomes very low because of the flat (i.e. near horizontal) dispersion curve, but the waveform of the optical signal is likely to be severely distorted by the large GVD parameter, on the order of 10^8 ps^2/km for this situation, thus limiting the achievable bandwidth for slow light transmission.

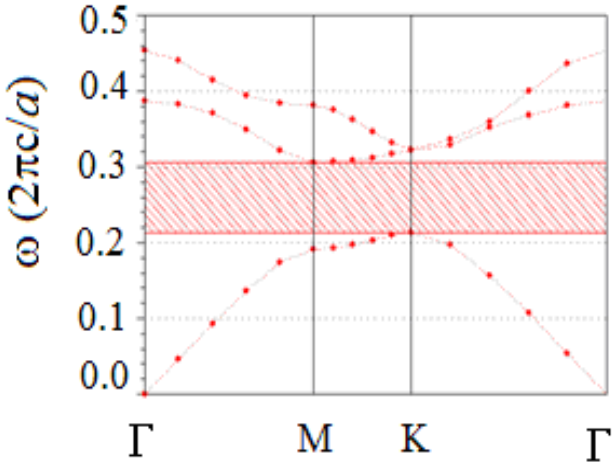

(a)

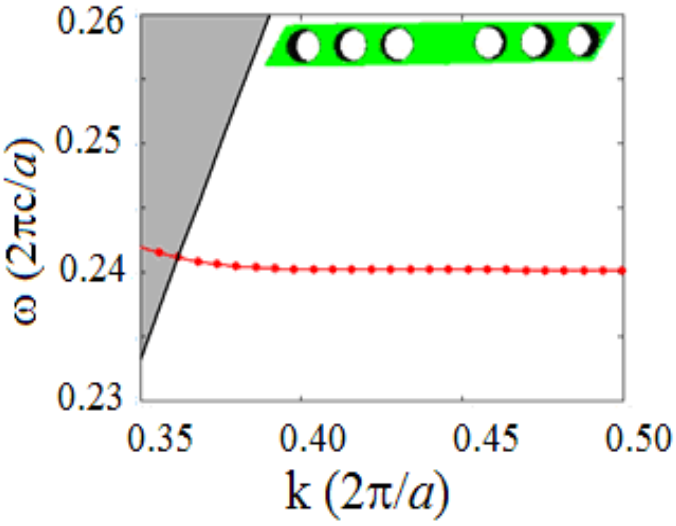

(b)

Figure 4.2. (a) TE bandgap map and (b) dispersion diagram having flat section of guided modes in the hexagonal lattice with lattice constant *a* = 0.35 μm and basic air hole radius r=0.33*a*. The inset in the figure shows the super-cell used in the 3D PWE method. The black solid line is the silica light line, while the red line is the dispersion curve.

Our main goal in this work was to obtain slow guided-light modes that feature the combination of low group velocity and vanishing GVD parameter. The main

requirements for such modes to be achieved are: (a) operation below the silica light-line, because the modes which lie above the light-line are intrinsically lossy (i.e. leaky) in the vertical direction - and (b) a flat section of dispersion curve should be obtained i.e. the slope of the dispersion curve should not only be small but it should also be close to constant for a given range. Otherwise the higher order derivatives of the dispersion curve will lead to GVD, third-order dispersion (TOD) and fourth-order dispersion (FOD).

To satisfy the above requirements we change the embedded circular air holes into an array of identical elliptical air holes with semi minor axis (A) and semi major axis (B), while retaining a hexagonal lattice arrangement. The dependence of the dispersion diagram on the semi-minor axis (A) and semi-major axis (B) of the air holes is shown in Figure 4.3(a) and 4.3(b). As indicated earlier, these are the normalized dispersion curves for propagation for a W1 channel waveguide oriented along the ΓK axis of the PhC lattice, for different values of A and B. Figure 4.3(a) shows that the dispersion curves move up in frequency in the slow light regime when the magnitude of the semi-minor axis A of the elliptical air holes is varied progressively from 0.20a to 0.32a -and the effective indices of the modes of the structure increase. In obtaining these curves, the value of the semi-major axis B has been fixed at 0.45a. In the same way, when the semi-major axis B is varied progressively from 0.39a to 0.48a, the dispersion curve again moves up in frequency, as shown in Figure 4.3(b) - where A is fixed at 0.28a. The tuning of the two structural parameters, A and B has been performed in order to tailor the dispersion properties of the waveguide in the slow light regime below the silica light line and for the desired frequency range.

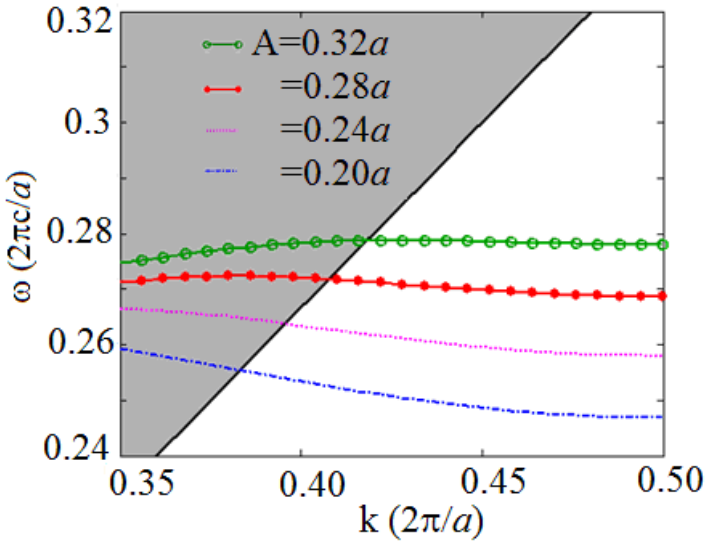

(a)

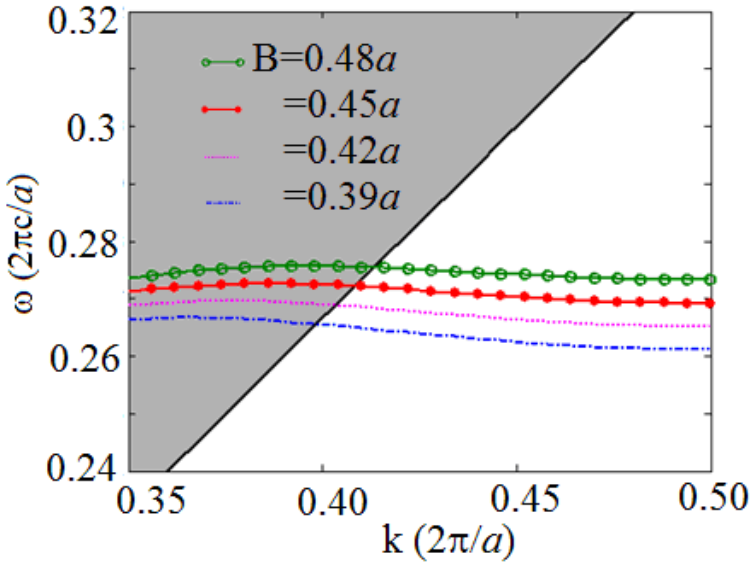

(b)

Figure 4.3. Movement of the dispersion curves when (a) the semi-minor axis A and (b) the semi-major axis B changes gradually.

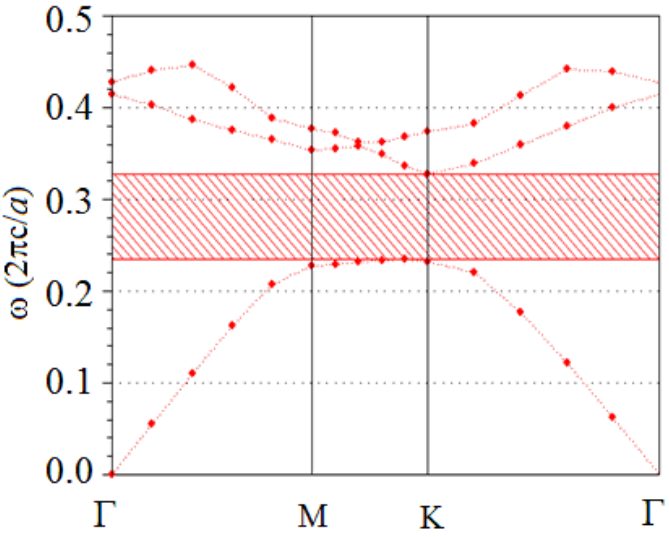

(a)

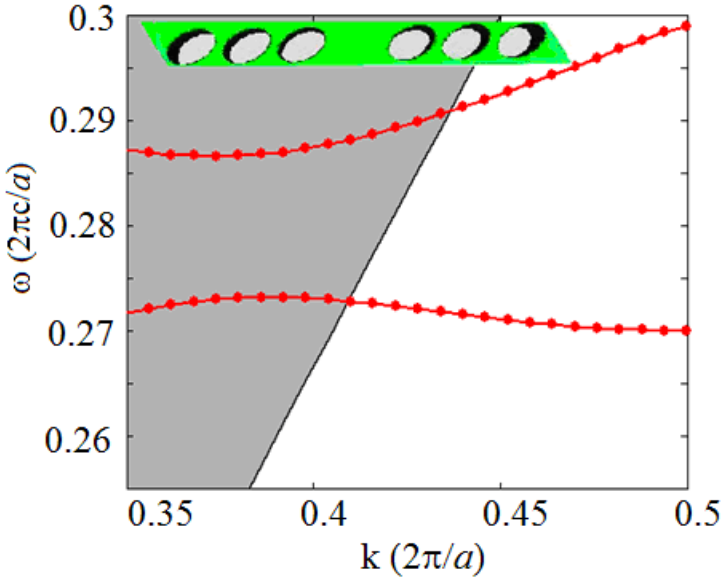

(b)

Figure 4.4. (a) TE band diagram of finally designed structure. (b) Dispersion diagram for the proposed SOI based single line defect photonic crystal having elliptical air holes with semi-minor axis A=0.286*a* and semi-major axis B=0.457*a*. Flat section of dispersion curve corresponds to slow light region.

Finally, an optimal waveguide was obtained with elliptical air holes that have a semi-minor axis A = 0.286*a* and semi-major axis B = 0.457*a*. Figure 4.4(a) shows the band structure for TE-like modes of the designed structure with lattice constant *a* = 0.42 μm, semi-minor axis A = 0.286*a* and semi-major axis B = 0.457*a*. For these parameter values, the bandgap ranges from 0.2352(2πc/*a*) to 0.3277(2πc/*a*). The dispersion curve obtained for the fundamental mode of the W1 waveguide is shown in Figure 4.4(b), together with the super-cell used in the 3D PWE method. The region $0.41 < (2\pi/a) < 0.5$ is chosen for slow light transmission - because in this region the flattest section of the dispersion curve is obtained that lies below silica light-line and is within the PBG region. i.e. the slow modes are confined vertically by total internal reflection and horizontally by the photonic bandgap of the PhC regions.

4.3. Numerical Results and Discussion

4.3.1. Group velocity:

In the previous section a W1 channel waveguide in an SOI based photonic crystal structure with a hexagonal lattice of elliptical air holes in silicon is presented. The structure shows a flat dispersion curve below the silica light line. The key velocity of such modes is their group velocity, defined as the velocity with which the envelope of a short pulse propagates through space. The standard definition for group velocity is [Agarwal (1997)]:

$$v_g = \frac{d\omega}{dk} \qquad (4.1)$$

where ω is the angular frequency and *k* is the wave-vector along the waveguide.

4.3.2. Group Velocity Dispersion (GVD):

The GVD is defined as the derivative of the inverse group velocity w.r.t. angular frequency.

$$\begin{aligned} \beta &= \frac{d^2k}{d\omega^2} \\ &= \frac{d}{d\omega}\left(\frac{1}{d\omega/dk}\right) \\ &= -\frac{1}{\left(d\omega/dk\right)^3}\frac{d^2\omega}{dk^2} \\ \beta &= -\frac{1}{v_g^3}\frac{d^2\omega}{dk^2} \end{aligned} \qquad (4.2)$$

From Equation (4.2), it can be observed that if the group velocity converges to zero, the GVD parameter goes to infinity - which causes the spreading of an optical pulse in time and as a result of different frequency components of the pulse travelling at different velocities may merge together.

Keeping the above fact in view, we have designed our structure to obtain a flat-band situation that is characterized by small and nearly constant slope, with relatively low group velocity and GVD parameter. In Figure 4.5 the frequency dependence of the group velocity - and the GVD parameter - on normalized frequency are plotted for the slow wave region shown in Figure 4.4(b). The flat band of the dispersion curve lying below silica lightline i.e. the frequency range between 0.2700($2\pi c/a$) and 0.2733($2\pi c/a$) was considered. It was observed that, for this range of frequencies, the group velocity remains in the range 0.0028c to 0.044c - and the GVD parameter lies in the range of 10^2 ps^2/km.

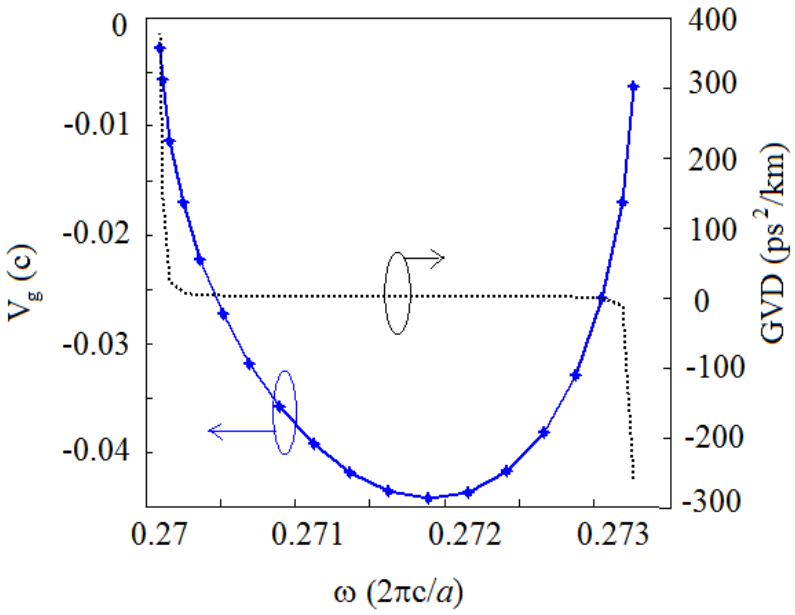

Figure 4.5. Variation of group velocity and Group Velocity Dispersion (GVD) parameter for flat section of dispersion curve plotted in Figure 4.4.

The GVD has positive as well as negative values and, for a particular spectral region, it becomes flat - i.e., for a bandwidth of $\Delta\upsilon = \frac{\Delta\omega}{2\pi} = 2.1\ \mathrm{THz}$, the GVD parameter lies below 10 ps^2/km.The low group velocity obtained at the extreme points (~0.005c) is at the cost of large GVD, on the order of 10^2 ps^2/km - while near the mid point, around $\omega = 0.2718$ $(2\pi c/a)$, $vg \sim 0.044c$ and the GVD parameter vanishes. Hence a very low GVD value is obtained over the wide spectral bandwidth of 2.1 THz.

4.3.3 Third Order Dispersion (TOD) and Fourth Order Dispersion (FOD):

The TOD parameter was deduced by calculating:

$$TOD = \frac{1}{v_g}\frac{\partial(GVD)}{\partial k} \qquad (4.3)$$

i.e. the first derivative of the GVD.

and the FOD parameter was deduced by calculating:

$$FOD = \frac{1}{v_g}\frac{\partial(TOD)}{\partial k} \qquad (4.4)$$

i.e. first derivative of the TOD.

Figure 4.6(a) shows that the upper limit of the TOD is on the order of 10^4 ps^3/km for the slow light regime below the silica light-line i.e. in the frequency range from 0.2700 ($2\pi c/a$) to 0.2733 ($2\pi c/a$) However a flat curve near the centre of frequency range was obtained, over a bandwidth of 2.1 THz, where TOD varies from 10^1 to 10^2 ps^3/km. Figure 4.6(b) shows that the upper limit of the FOD is on the order of 10^6 ps^4/km for the slow light regime, but again a flat curve is obtained for a bandwidth of 2.1 THz near the centre. These values of TOD and FOD are less than those reported in previous work [Di Falco *et al*. (2008), Assefa and Vlasov (2007)]. Thus both TOD and FOD vanish for a particular frequency range in the proposed SOI based structure having elliptical air holes PhC.

The results obtained for the TOD and FOD are important for evaluating the pulse broadening that is due to higher order dispersion, as well as for evaluating nonlinear effects that are dependent on high order dispersion in the slow light regime. Their low values, tending to zero in a bandwidth of 2.1 THz, show that the proposed waveguide can be used for device applications such as multiplexing and de-multiplexing, as well as in realizing delay lines for optical buffers.

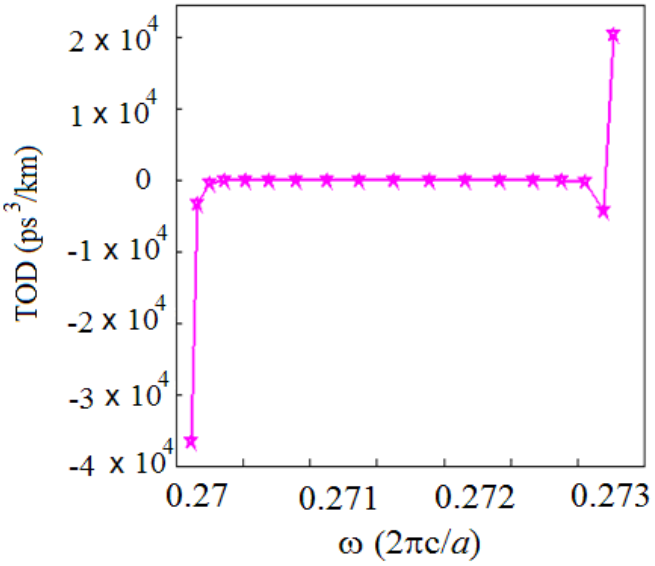

(a)

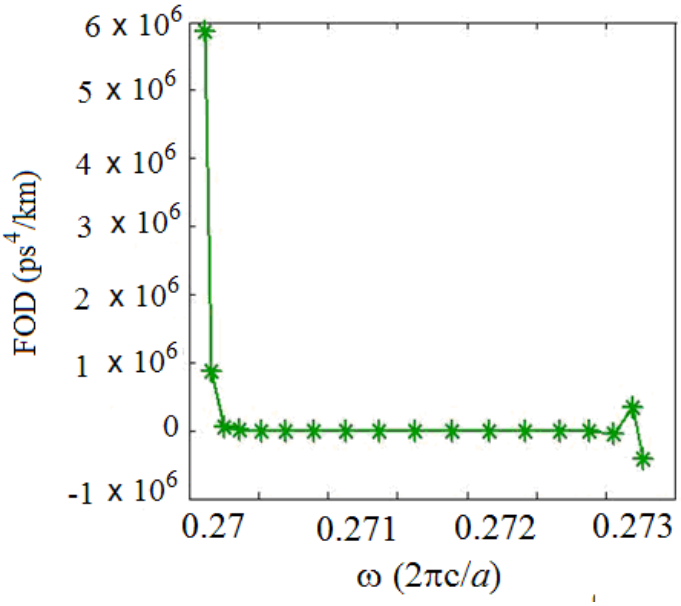

(b)

Figure 4.6. Variation of higher order dispersion parameters (a) TOD and (b) FOD with frequency.

4.4. Photonic Crystal Waveguide as an Optical Buffer

The optical buffer is a device that temporarily stores and adjusts the timing of optical packets. Application of PhC waveguides with slow light in optical buffers has recently been attracting wide attention [Tucker *et al*. (2005)]. We then investigated the properties of the SOI-based elliptical air hole W1 channel waveguide for use as an optical buffer - and determine the limitations of slow light propagation in the proposed structure. The number of bits that can be stored in a slow light device is given by its Delay Bandwidth Product (DBP). The expression for the DBP is:

$$DBP = T_d \,.\, B \tag{4.5}$$

where T_d is the time of propagation of a pulse in the waveguide and B is the bandwidth. If L is the length of the structure and the pulse is propagating with minimum distortion, the upper limitation on the DBP is given by [Ma and Jiang (2008b)]:

$$\begin{aligned} DBP &= T_d \,.\, B \le \frac{L}{\tilde{v}_g}\left(\frac{1}{4\pi L\,|\beta|}\right)^{1/2} \\ \Rightarrow\ DBP &\le \left(\frac{L}{4\pi}\right)^{1/2} \frac{1}{\tilde{v}_g\,|\beta|^{1/2}} \end{aligned} \tag{4.7}$$

Thus the DBP depends upon the length of the structure, the average group velocity and the GVD parameter. If the length of the structure is fixed, the DBP is inversely proportional to $\tilde{v}_g\,|\beta|^{1/2}$. i.e., in order to increase the value of DBP, we need to decrease the value of the average group velocity $\tilde{v}_g$ and the GVD parameter, β. Next, the upper limit of the DBP was calculated in the proposed SOI-based PhC having a hexagonal arrangement of elliptical air holes, in the slow light regime below the silica light-line.

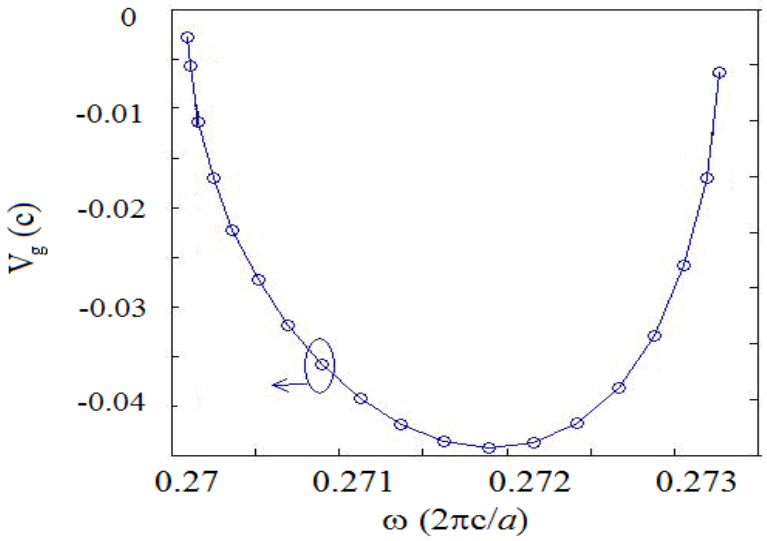

Figure 4.7. Variation of group velocity with frequency in the slow light region below the silica light-line.

At frequencies $\omega_0 = 0.2709$ ($2\pi c/a$), i.e. for an incoming wave at $\lambda_0 = 1.55$ μm, the average group velocity is calculated to be 0.035c - and the average GVD parameter is $\beta = 0.5$ ps^2/km (from Figure 4.5). Therefore, $\tilde{v}_g|\beta|^{1/2} \approx 0.0247c.\text{ps km}^{1/2}$. This value is highly reduced as compared to the value of 4.4c ps.km$^{1/2}$ in reference [Ma and Jiang (2008b)]. Even for the slowest velocity achieved at a frequency of 0.27009($2\pi c/a$) i.e. $\lambda_0 = 1.555$ μm, the average group velocity is 0.0028c and $\beta = 376$ ps^2/km - and therefore, $\tilde{v}_g|\beta|^{1/2} \approx 0.0543c.\text{ps km}^{1/2}$. Hence the upper limitation on the delay bandwidth product is strongly enhanced in our structure.

The DBP, defined by T_d.B, provides a measure of the buffering capacity that a slow light device potentially provides. However its normalized form can become more useful if devices that have different lengths and different frequencies are compared. The value of the normalized DBP was also calculated for the proposed SOI

based photonic-crystal channel-waveguide. Figure 4.7 shows the variation of the group velocity with frequency. The average group index in the frequency range Δω is calculated as:

$$\tilde{n}_g = \int_{\omega_0 - \Delta\omega/2}^{\omega_0 + \Delta\omega/2} n_g(\omega) \frac{d\omega}{\Delta\omega} \tag{4.8}$$

From Figure 4.7, the average value of group index is- $\tilde{n}_g = 66.60$, in the normalized frequency bandwidth of $\frac{\Delta\omega}{\omega} = 0.0117$. The normalized DBP is calculated to be- $\tilde{n}_g \frac{\Delta\omega}{\omega} = 0.778$, which is substantially greater than that reported in references [Mori and Baba (2005), Ma and Jiang (2008a)]. The normalized DBP calculated in [Settle *et al.* (2007)] is equal to 0.359, which is also less than the value of 0.778 that we have calculated for the proposed structure. The proposed structure can therefore be used as an optical buffer with a high DBP value.

4.5. FDTD Simulation

In this section an investigation is described for the broadening of pulses propagating through the waveguide of the proposed structure, using FDTD simulations. FDTD simulations were carried out using the RSOFT FULLWAVE package with the mesh size taken to be Period/3 and device dimensions- taken to be 6.72μm x 5.04μm in XZ plane. If the central frequency is fixed at $\omega_0 = 0.2709(2\pi c/a)$ i.e. at $\lambda_0 = 1.55$ μm, the group velocity and GVD parameter at this wavelength are 0.035c and 0.5 ps^2/km, respectively.

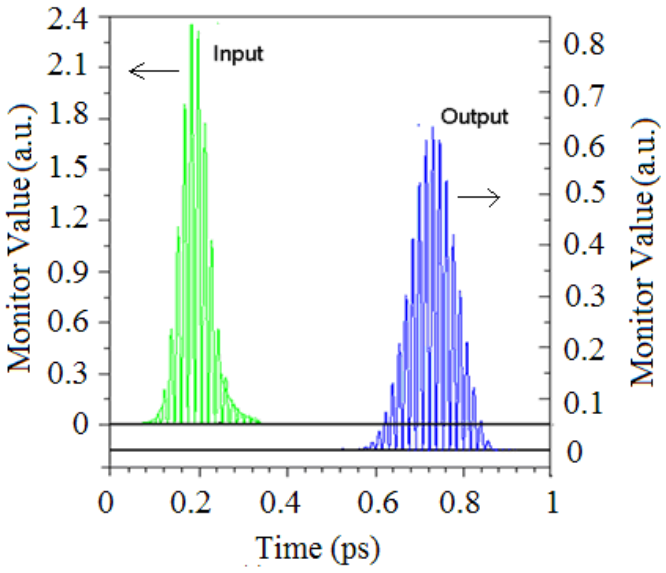

(a)

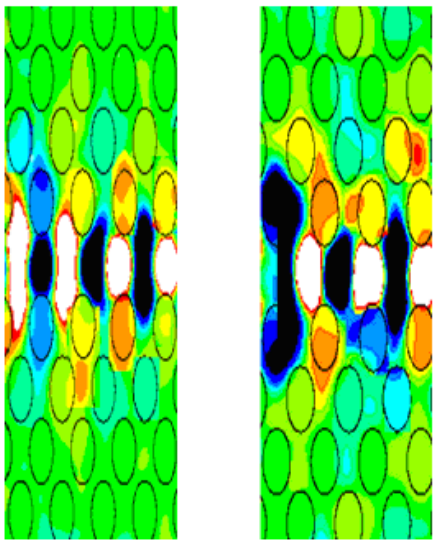

(b) **(c)**

Figure 4.8(a): Field amplitude of the Gaussian pulse recorded at the input end and output end of the waveguide as a function of time for λ_0=1.55 μm. Modal field distribution in the PhC waveguide for (b) 1.550 μm and (c) 1.555 μm.

As shown in Figure 4.8(a), for wavelength of 1.55 μm, time delay between the input peak and output peak is nearly 0.57 ps for a waveguide length of 15*a*. Hence the

corresponding group velocity is 0.036c which is slightly larger than that observed using PWE method (i.e. 0.035c). The slowdown factor, which is defined as the ratio of the phase velocity to the group velocity ($S=v_p/v_g$) is calculated to be 17 at $\lambda_0 = 1.55$ μm. Thus the width of the Gaussian pulse at the output end is approximately equal to that of the pulse at the input end, with very little pulse expansion, as shown in Figure 4.8(a). Here, the length of waveguide is taken to be 15*a*, as shown in Figure 4.1. The incident pulse with a full width at half-maximum (FWHM) of 0.07 ps expands to 0.11 ps at the output. The modal field distribution for an incident wave at a wavelength of 1.55 μm was observed in Figure 4.8(b) - which shows that the light spreads substantially into the first and second nearest rows of elliptical air holes of the PhC, due to the slow light propagation in the waveguide. Figure 4.8(c) shows the spreading of the wave for $\lambda_0 = 1.555$ μm - for which the slowest group velocity value of 0.0028c is achieved in the proposed SOI based photonic crystal waveguide.

4.6. Time and Wavelength Division Demultiplexing (TDM and WDM)

The proposed SOI based PhC, with elliptical air holes, is next investigated for use in time and wavelength division demultiplexing (TDM and WDM). It is found that the proposed structure has a bandgap in the frequency range of 0.2352 ($2\pi c/a$) to 0.3277 ($2\pi c/a$) as shown in Figure 4.4(a). Hence the bandgap exist for both the wavelengths, 1.31 μm, which corresponds to a frequency of 0.3206 ($2\pi c/a$) and 1.55μm, which corresponds to a frequency of 0.2709 ($2\pi c/a$).

Figure 4.9(a) shows the frequency dependence of the group velocity and GVD parameter for a section of dispersion curve below the silica light-line. For an incoming pulse of light at a wavelength of 1.31 µm, the group velocity is calculated to be 0.178c and the GVD parameter is 0.0083 ps^2/km, which implies low signal distortion for a wavelength of 1.31 µm. Thus a signal at a wavelength of 1.31 µm is more than five times faster than one at 1.55 µm, where the velocity is equal to 0.035c. Therefore the channel guides a signal at a wavelength of 1.31µm at faster velocity - and hence it reaches the output end of the W1 waveguide earlier than a signal at the wavelength of 1.55 µm.

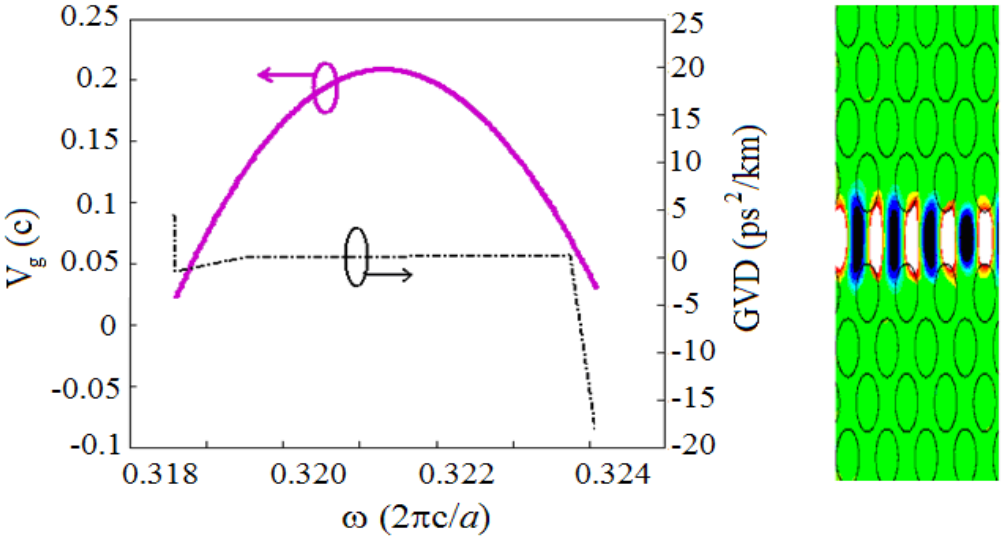

(a) **(b)**

Figure 4.9. (a)Variation of group velocity and Group Velocity Dispersion (GVD) parameter for region having central wavelength near 1.31µm (b) Modal field distribution in PhC channel waveguide for a wavelength of 1.31µm.

The FDTD simulation for 1.31 µm is shown in Figure 4.9(b), indicating that the spread of light wave in theW1 waveguide at 1.31 µm is less than that for 1.55 µm, as observed in Figure 4.8(b). If the device length is assumed to be 600 µm, the delay time for a wavelength of 1.55 µm is calculated to be 57 ps - and for a wavelength of 1.5534 µm it is calculated to be 89 ps. For a wavelength of 1.5550 µm, it is calculated to be 704 ps, while for a wavelength of 1.31 µm; it is calculated to be 11 ps (Figure 4.10). Here, it is observed that even for the slowest velocity achieved i.e. 0.0028c, the GVD parameter is relatively small (on the order of 10^2 ps^2/km) and hence this waveguide PhC structure can be used in both time and wavelength division de-multiplexing.

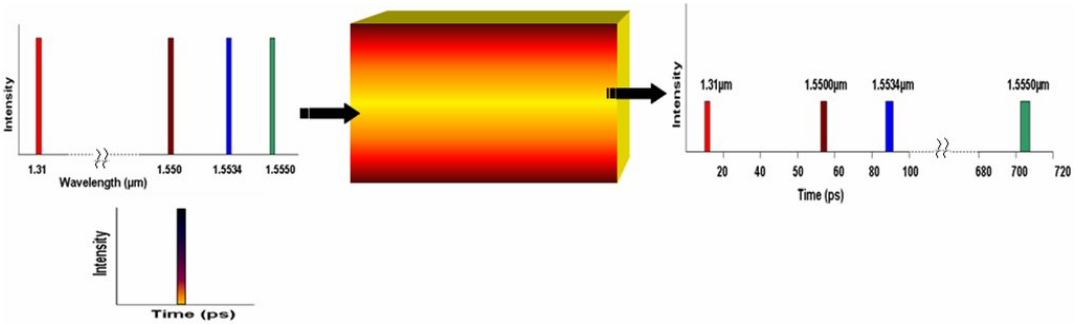

Figure 4.10. Schematic for separation of pulses of light at telecom wavelength 1.31 µm, 1.5500 µm, 1.5534 µm and 1.5550 µm for time and wavelength division de-multiplexing.

4.7. Conclusions

In this chapter, the design of an SOI based PhC channel waveguide with elliptical air holes is reported for use in slow light propagation, with group velocities in the range from 0.0028c to 0.044c – and with extremely low GVD, TOD and FOD parameters. This combination of small values for key parameters causes an input signal to pass

through the PhC waveguide with much less distortion. The proposed structure has considerable potential for use in photonic device applications such as optical buffers, TDM and WDM processing -as we have demonstrated.

Chapter 5

Slow Light Propagation in Liquid-Crystal Infiltrated SOI Photonic Crystal Channel Waveguides[1]

5.1 Introduction

Photonic crystals with photonic bandgap properties have attracted much attention as a possible platform for densely integrated photonic circuits and novel photonic functionality. Results obtained in chapter 4 explains that, by carefully engineering the photonic dispersion relationship, one may obtain unique opportunities for realization of devices that exploit slow light effects [Soljacic *et al.* (2002), Gersen *et al.* (2005), Baba and Mori (2007), Frandsen *et al.* (2006)]. PhC channel waveguides can be used as defect-mode slow light structures. However, slow light is typically accompanied by large amounts of dispersion, which can remove much of the advantage of operation in the slow light regime - because it limits the bandwidth that can be utilized [Engelen *et al.* (2006)]. This bandwidth-dispersion issue can be overcome by tuning the structure towards dispersion-free behaviour [Yanik and Fan (2004)]. This approach has resulted

---

[1] Part of the results reported in this chapter has been published in the paper: "Low-loss slow light transmission in photonic crystal waveguides comprising of liquid crystal infiltration", Journal of Electronic Science and Technology (JEST), 8, 2010.

Updated part of the results reported in this chapter has been published in the paper: "Slow Light Propagation in Liquid-Crystal Infiltrated Silicon-on-Insulator Photonic Crystal Channel Waveguides" **IEEE/OSA Journal of Lightwave Technology,** 28, 2560-2571, 2010.

in more complex devices, fabrication of which is challenging and hence potentially limits their practical utilization. In Chapter 4, we have demonstrated the feasibility and benefits of using an elliptical air-hole based photonic crystal structure to obtain slow light behaviour [Rawal *et al.* (2009)]. However, it has been shown by a number of authors that square hole photonic crystal structures present better performance in comparison with circular hole PhC structures in terms of transmittivity, loss characteristics and maximization of the transmission bit rate of the signal in optical networks. Even the group index obtained in the low GVD regime of PhC channel waveguides is higher in square hole waveguides than in circular hole waveguides [Bavat *et al.* (2009), Koerkamp *et al*. (2004), Zhang *et al.* (2010)]. The tunability of PhC lattices can further be extended and controlled by filling their segments with certain types of liquid crystal (LC) material [Alagappan *et al*. (2006), Kosmidou *et al*. (2005)]. This combination offers the possibility of shifting the frequency of the defect modes and tuning the dispersion curves, in order to obtain flat slow modes with low group velocity dispersion (GVD) [Ebnali-Heidari *et al.* (2009)]. Liquid Crystal (LC) material has been simulated using an anisotropic form of the finite-difference time-domain (FDTD) method [Kriezis and Elston (2000)]. Since dynamically tuned devices are essential components in optical systems, PhC waveguide configurations with microfluidic infiltration of LC material offer a strong potential for realizing integrated micro-photonic devices. C.L.C. Smith and co-workers [Smith *et al.* (2008)] have described how the required LC infiltration in a PhC can be achieved by using a tapered glass micro-tip. The droplets that are attached to the length of capillary tube due to adhesive forces between glass and liquid are deposited on a device chip besides the PhC structure. A microscope objective is used - which resolves properly the air

holes in the PhC and provides sufficient working distance for the tapered microtip to draw the chosen droplet along the air hole, perpendicular to the PhC waveguide, during infiltration. Propagation losses and their dependence on group velocity are another matter of concern. There is little justification in exploring the slow light regime if any advantage obtained is immediately counteracted by excessive losses. These losses include losses due to backscattering (into the guided Bloch modes), with propagation in the opposite direction - and losses due to inefficient coupling. Backscattering is mainly disorder-induced and increases with the inverse group velocity squared [Petrov *et al* (2009), Kuramochi *et al.* (2005), Gerace and Andreani (2007)]. Hence it is dominant in the case of slow group velocities, while inefficient coupling occurs due to the large mismatch at the interface between the slow light PhC waveguide that results from large changes in group index. This mismatch can be considered, in a general sense, as a form of impedance mismatch that involves conservation of power flow and the possibility of energy storage in evanescent modes. One way of overcoming the problem of impedance mismatch is the use of adiabatic tapers [Pottier *et al.* (2007)], but these tend to be relatively long and the construction of systematic design procedures is challenging. An alternative way is to introduce a finite region that firstly couples the light from a ridge or stripe waveguide into a fast mode PhC waveguide and then into the slow mode PhC waveguide [Ozaki *et al.* (2007),Velha *et al*. (2007), Martijn de Sterke *et al* (2007), Hugonin *et al.* (2007)]. Such issues of concern are tackled directly in the present chapter - in order to obtain a highly efficient slow light PhC waveguide with a simple design that is suitable for fabrication.

In this chapter, the design of an SOI based PhC structure is reported that has a silicon core sandwiched between a silica cladding layer below the core and an air cladding region above. A hexagonal lattice arrangement of rectangular air holes is introduced into the silicon waveguide core. Since it is an asymmetric structure vertically, the Bloch modes of the waveguide cannot be strictly classified into purely transverse electric (TE) and transverse magnetic (TM) modes, since each Bloch mode has an even as well as an odd distribution component. For the even modal components, the magnetic field should lie in the direction perpendicular to the plane of the structure, i.e. along the y-direction - and, for odd components, the electric field should lie along the y-direction. In general a mixture of all six field components is obtained for the modal distributions when periodic structuring is added. This periodic structuring leads to Bloch modes having only quasi-TE or quasi-TM characteristics. Modes with H_y as the predominant component are referred to as TE-like modes and those with E_y as the predominant component are referred to as TM-like modes [Shinya *et al.* (2002)].

The PhC structure is designed to exhibit a full PBG for TE-like modes. Therefore these modes are horizontally confined by PBG effects and vertically by total internal reflection. The rectangular holes are then filled with LC material, which provides an extra free parameter for achieving very small dispersion slow light waveguides. The infilling LC material is assumed to occupy only the exact depth of the holes in the silicon waveguide core - and only in one row of holes on either side of the waveguide.

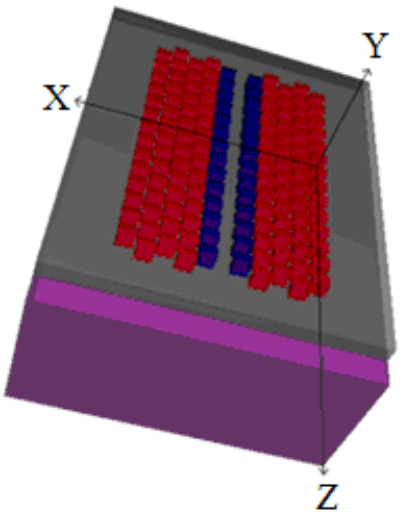

(a)

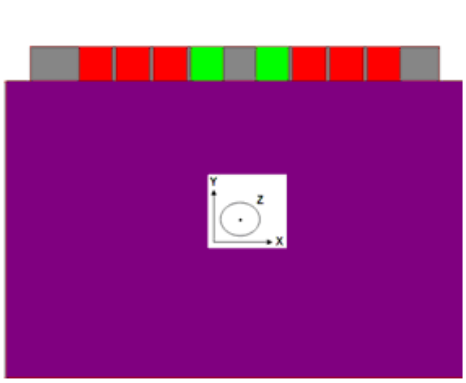

(b)

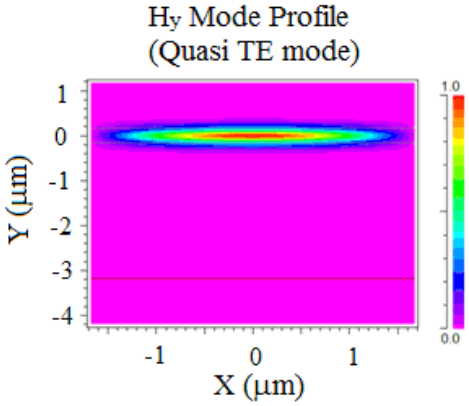

(c)

Figure 5.1. (a) Schematic of the proposed design with the first neighbouring holes on either sides of the W0.7 waveguide having Liquid Crystal infiltration. (b) XY view of slow light photonic crystal channel waveguide with (c) field component of the quasi TE guided mode.

Figure 5.1 gives a schematic of the proposed design, with the first neighbouring holes on either side of the W0.7 waveguide having liquid crystal infiltration. The minimum values for the losses and defect mode dispersion below the silica light-line are found for the W0.7 waveguide. For this reason, a typical structure employed in the

experiments is a W0.7 PhC waveguide [Kuramochi *et al.* (2005), Pottier *et al.* (2007), Petrov and Eich (2004), Notomi *et al.* (2001)]. For the device application of such waveguides, the group velocity dispersion (GVD) and other higher order dispersion parameters should be very low, thereby enabling the optical signal to propagate with least distortion, as demonstrated previously in Chapter 4 - and will be demonstrated again in the present chapter. We shall also describe the tolerance analysis of the proposed structure with respect to variations in the waveguide geometry and variations in the refractive index of the liquid crystal and silicon core. The sensitivity of the proposed LC-infiltrated PhC channel waveguide is also compared with that of conventional waveguides. The structure designed has also been investigated for possible propagation losses, which include losses due to coupling inefficiency. It is found that high transmission is obtained over a broad bandwidth for the hetero-waveguide finally designed, which consists of a locally LC infiltrated slow PhC channel waveguide terminated at either end by fast PhC waveguide sections.

5.2 Slow light photonic crystal waveguide

Line defect PhC waveguides can lead to guided mode bands that can either be index-guided or bandgap guided - or a combination of both. Anti-crossing between these two types of mode can determine the local shape of dispersion curves, the slope of which determines the group velocity of the mode [Khayam and Benisty (2009), Petrov and Eich (2004), Notomi *et al.* (2001), Li *et al*. (2008)]. These guided mode bands can be made as flat as desired by appropriate design for the achievement of slow group velocity, together with low group velocity dispersion (GVD), over a broad bandwidth. In order to obtain slow guided modes with low group velocity and a

vanishing GVD parameter, two basic requirements have to be fulfilled. The first one is structure oriented, i.e. the geometrical properties (waveguide width, hole size or position) are modified to obtain a flat section of dispersion curve, with not only small but constant slope - over a given range of frequencies - because, otherwise, higher order derivatives of the dispersion curve will lead to GVD, third-order dispersion (TOD) and fourth-order dispersion (FOD). The second requirement is loss oriented, i.e. the possibility of operation of the waveguide below the silica light-line is considered - because modes that lie above the light-line are intrinsically lossy (i.e. leaky) out-of-plane. The FDTD method and the PWE method [Plihal and Maradudin (1991)] are two powerful numerical tools that can be used to simulate Maxwell's Equations with minimal approximation. They are known to be able to reproduce experimental results very closely. RSOFT's version 8.1 is used for carrying out PWE and FDTD analysis. Some useful parameters for characterization of PhC waveguides are:

(i) *Group Velocity*: which is defined as the velocity at which the envelope of a short pulse propagates through space - and is expressed as [Agarwal (1997)]

$$v_g = \frac{d\omega}{dk} \tag{5.1}$$

Group index $$n_g = \frac{c}{v_g} \tag{5.2}$$

The average values of group velocity and group index in frequency range $\Delta\omega$ are given as:

$$\tilde{v}_g = \int_{\omega_0 - \Delta\omega/2}^{\omega_0 + \Delta\omega/2} v_g(\omega) \frac{d\omega}{\Delta\omega} \tag{5.3}$$

$$\text{and} \quad \tilde{n}_g = \int_{\omega_0 - \Delta\omega/2}^{\omega_0 + \Delta\omega/2} n_g(\omega) \frac{d\omega}{\Delta\omega} \tag{5.4}$$

(ii) *Group Velocity Dispersion (GVD):* is defined as the derivative of the inverse group velocity and is given as (refer Chapter 4):

$$\beta = \frac{d^2k}{d\omega^2} = -\frac{1}{v_g^3}\frac{d^2\omega}{dk^2} \tag{5.5}$$

It is observed that to obtain a distortion-less slow light pulse, i.e. low GVD parameter, the value of group velocity should be small - and with nearly constant slope.

(iii) *Third order Dispersion (TOD) and Fourth order Dispersion (FOD):* TOD and FOD are expressed as:

$$TOD = \frac{1}{v_g}\frac{\partial(GVD)}{\partial k} \tag{5.6}$$

$$\text{and} \quad FOD = \frac{1}{v_g}\frac{\partial(TOD)}{\partial k} \tag{5.7}$$

(iv) *Delay-Bandwidth-Product (DBP):* which defines the number of bits stored in a slow light device - and is expressed as:

$$\text{DBP} = T_d \,.\, \text{B} \tag{5.8}$$

where T_d is the delay time of the propagating pulse and B is the bandwidth. For a given length L of the structure, the upper limit on the DBP is given by [Ma and Jiang (2008)]:

$$DBP \le \left(\frac{L}{4\pi}\right)^{1/2} \frac{1}{\tilde{v}_g |\beta|^{1/2}} \tag{5.9}$$

Therefore, in order to increase the value of the DBP, one has to decrease the value of the product $\tilde{v}_g |\beta|^{1/2}$ for a fixed length L of the device. For comparison of

devices having varying lengths, the normalized form of DBP can be useful - and is defined as: $DBP = \tilde{n}_g \frac{\Delta\omega}{\omega}$.

5.2.1 Design Aspects

For the design, the possibilities for slow light propagation in an SOI based waveguide PhC structure realized in a 335 nm thick silicon layer supported by a 3000 nm thick silica (n=1.45) layer, with air above the silicon waveguide core, were considered. The hexagonal periodic arrangement of square holes having width = 300 nm and lattice constant a = 420 nm is embedded in silicon (n=3.50). Figure 5.2(a) shows the plane view schematic of the square hole SOI structure designed to obtain a flat dispersion curve. The PhC structure that has been designed exhibits a band-gap for TE-like modes between $\omega_{min} = 0.2573(2\pi c/a)$ and $\omega_{max} = 0.4311(2\pi c/a)$, as shown in Figure 5.2(b). In order to guide Bloch modes in the structure, a line defect W0.7 PhC waveguide is conceptually created by removing a row of square holes along the ΓK direction and shifting the two PhC regions closer to one another - resulting in a PhC waveguide width 0.7 times that of W1, i.e. a W0.7 PhC waveguide.

The dispersion diagram shown in Figure 5.2(c), which was obtained using the 3D PWE method, indicates the existence of only a single guided mode below the silica light-line. By examining the dispersion diagram in Figure 5.2(c), we have found that only a modestly enhanced group index (~ 15) with high GVD (~ 10^5 ps^2/km) is achieved for this situation, limiting its possible use in slow light based PhC devices.

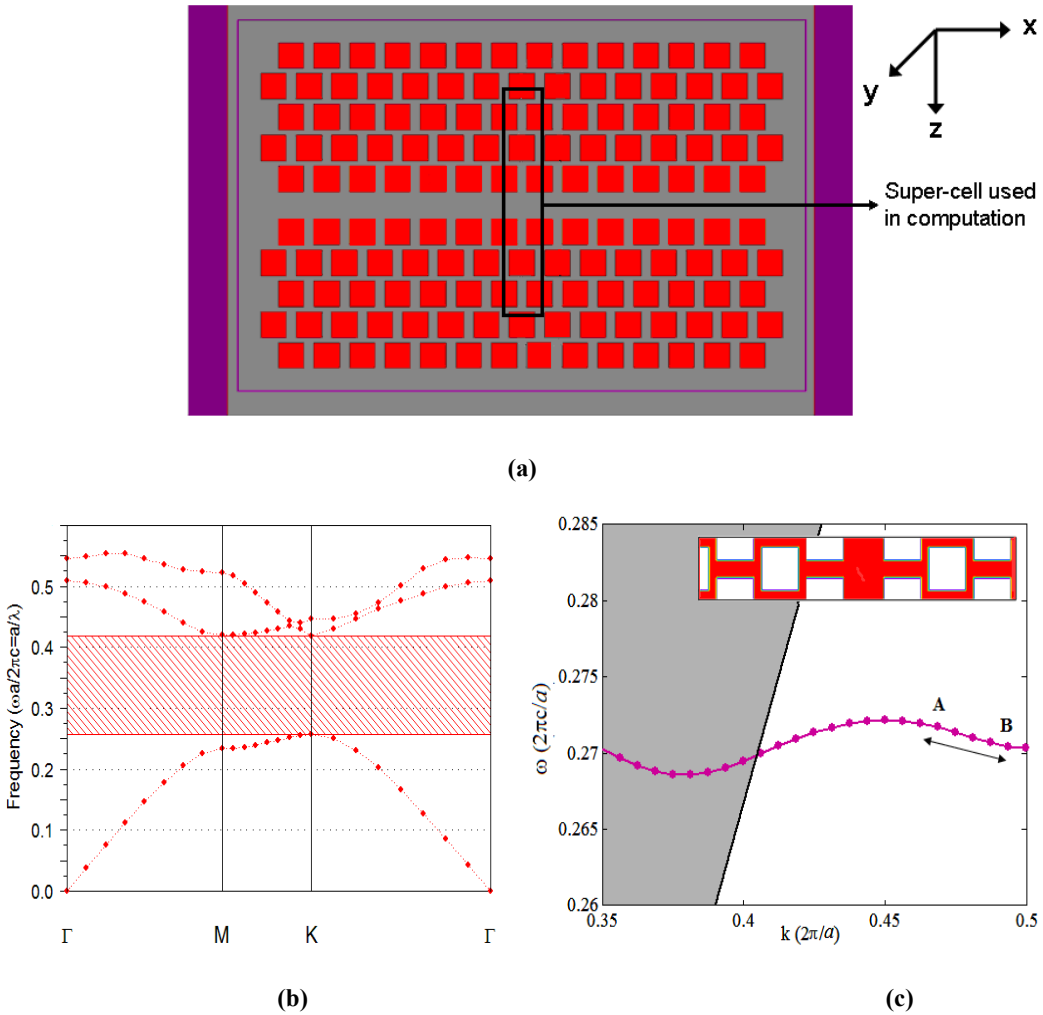

Figure 5.2. (a) Plane view schematic of square hole SOI structure showing the super-cell used in the computation, (b) TE band-gap map and (c) dispersion diagram having flat section AB of guided mode with lattice constant a = 420 nm and square hole width as 300 nm. The black solid line is the silica light-line, while the red line is the dispersion curve. The inset in the figure (c) shows the super-cell used in 3D PWE calculation.

In order to satisfy the two requirements, (structure-oriented and loss-oriented) for achieving slow light systems, it was chosen to change the embedded square air holes into an array of rectangular air holes by varying the width of the X axis (X1) and Z axis (Z1) of each square, while retaining the hexagonal lattice arrangement. A

parameter scan was performed in order to tailor the dispersion properties of the waveguide and is shown in Figures 5.3(a) and 5.3(b). As mentioned earlier, these are dispersion curves for W0.7 PhC waveguides oriented along the ΓK direction, with different values of X1 and Z1 for the square air holes. In Figure 5.3(a), the value of Z1 is fixed at 330nm, while in Figure 5.3(b) the value of X1 is fixed at 220nm.

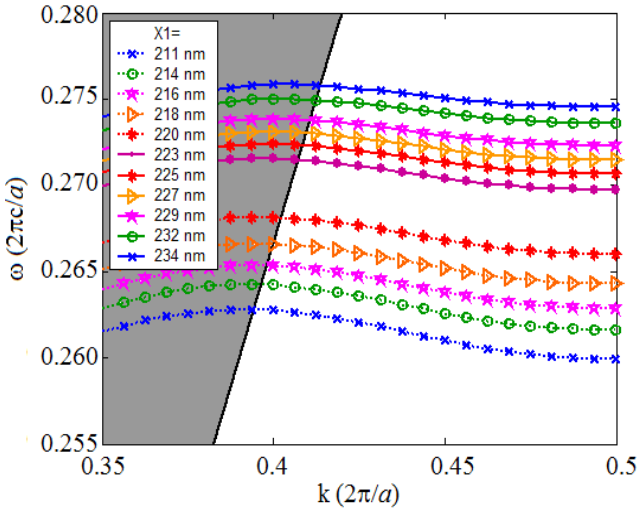

(a)

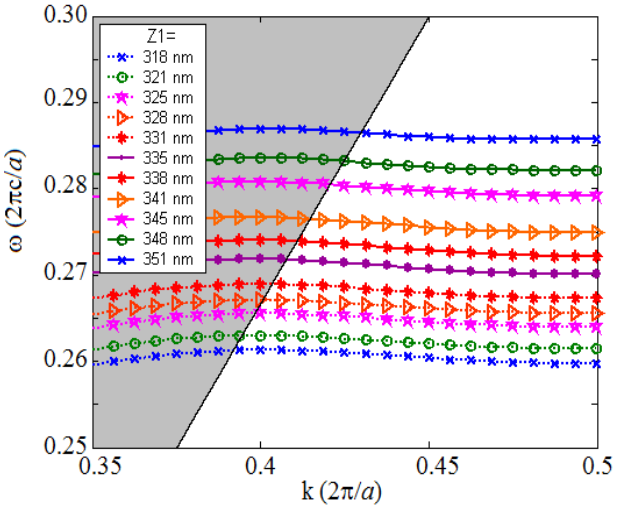

(b)

Figure 5.3. Movement of the dispersion curves when (a) X1 and (b) Z1 vary gradually. The black solid line is the silica light-line.

A parameter scan was then performed to achieve a flat section of dispersion curve below the silica light line and for the desired frequency range. Figure 5.3 makes it possible to trace a flat-band slow-light region for X1 = 223 nm and Z1 = 335 nm. Hence a slow light waveguide is achieved for triangular lattice rectangular air holes with X1 = 223 nm and Z1 = 335 nm together with a lattice constant of a = 420 nm, along the ΓK direction.

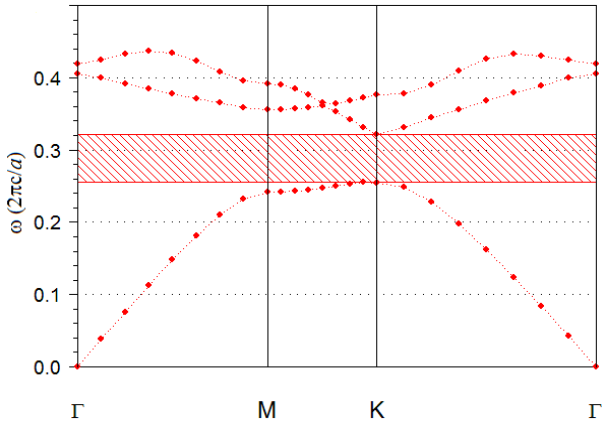

(a)

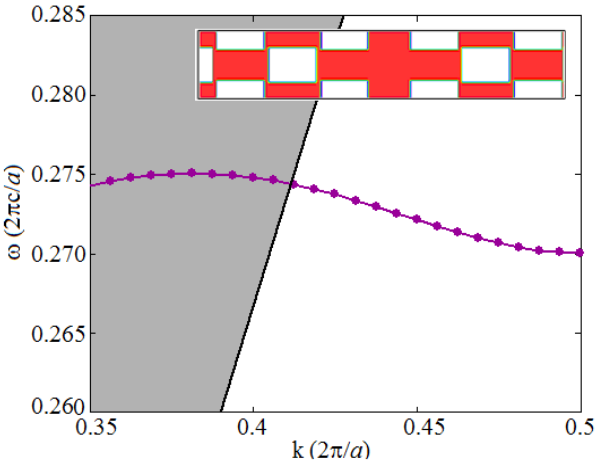

(b)

Figure 5.4. (a) TE bandgap map for the PhC having rectangular air holes with parameters X1=223 nm and Z1= 335 nm. (b) Dispersion curve with single mode guidance for the designed structure. Inset shows the super-cell used in 3D PWE method.

For these parameter values, the band-gap ranges from $\omega_{min} = 0.2579(2\pi c/a)$ to $\omega_{max} = 0.3217(2\pi c/a)$, as shown in Figure 5.4(a). The dispersion diagram for this W0.7 waveguide design is shown in Figure 5.4(b), together with the super-cell used in the 3D PWE method. However, an even slower group velocity, together with less GVD, can further be achieved by the use of liquid crystal (LC) infiltration. The combination of the rectangular hole PhC structure with such micro-fluidic regions gives an extra free parameter in the waveguide design, which allows the fine tuning of its group velocity and dispersion.

5.2.2 Vanishing dispersion slow light in photonic crystal waveguides with liquid crystal infiltration:

Liquid crystals (LCs) offer a tuning mechanism for achieving slow light waveguides with highly reduced GVD, as their refractive index can be varied with temperature change - or by applying a local electric field [Chandrashekhar (1995)]. Selective liquid crystal infiltration in the some of the rectangular air holes of the PhC channel waveguide offers the possibility of shifting the frequency of the defect mode in the desired range - and obtaining a flat section of dispersion curve with small but constant slope. In order to investigate the shape of the dispersion curve, calculations on the LC infiltrated photonic crystal were carried out using the PWE method. The refractive index of TE polarized light or TM polarized light depends upon the alignment of the optic axis of the liquid crystal inside the rectangular holes. If it is now assumed, that the extraordinary axis lies along the *y*-axis parallel to the main axis of the holes, then the TM-like polarization, with the electric field aligned along the *y*-axis, samples only the extraordinary index of refraction, and TE-like polarization, with the electric field

lying in the *x*-*z* plane, samples only the ordinary index of refraction. Hence the calculation for TE polarized light was carried out using the ordinary refractive index of liquid crystal [Leonard *et al.* (2000)].

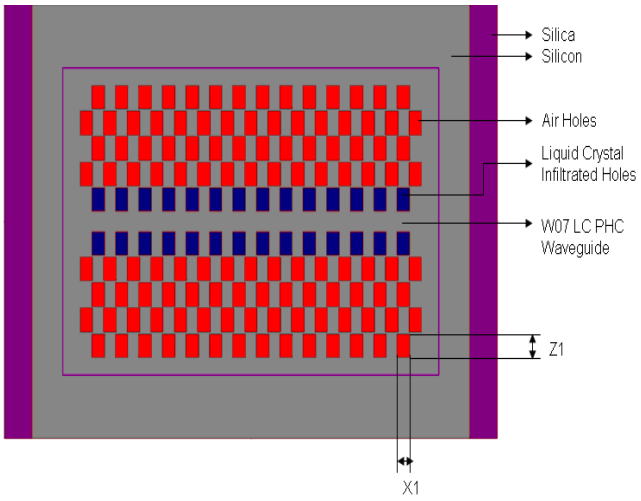

(a)

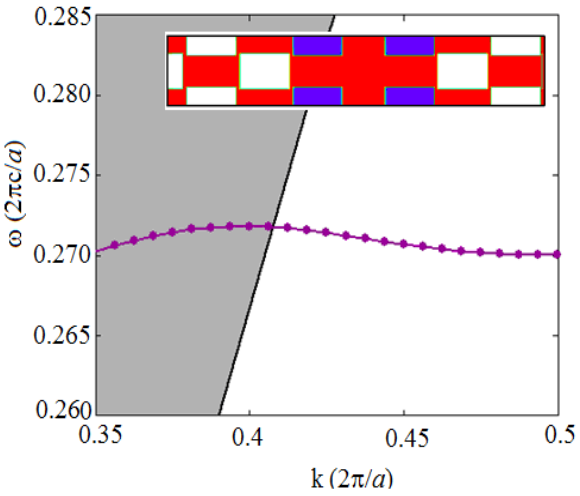

(b)

Figure 5.5. (a) Schematic of the final design for the slow light PhC waveguide with rectangular air holes. The first row closest to the waveguide on either side is infiltrated with liquid crystal. (b) Single guided dispersion curve with a flat section of dispersion curve for achieving slow light.

The LC material used to generate refractive index values for our calculations, is a phenyl acetylene derivative (nematic LC), that has an ordinary refractive index n_o equal to 1.6 and an extraordinary refractive index n_e equal to 2.2. [Alagappan et al. (2006),Takeda and Yohino (2002)]. The first row of rectangular air holes closest to the W0.7 waveguide on either side is infiltrated with the LC, in order to obtain a flat dispersion curve with vanishing GVD, as displayed in Figure 5.5(b). The region chosen for slow light transmission varies over the range $0.4 < k\ (2\pi/a) < 0.5$ because, in this region, the dispersion curve satisfies the single mode guidance condition below the silica light-line and has a flat section with small but constant slope. Figure 5.5(a) shows a schematic of the SOI-based LC W0.7 PhC waveguide with liquid crystal infiltration. We have then compared the group index n_g and the GVD for the flat band obtained from the W0.7 PhC waveguide shown in figure 5.4(b) and the one obtained from the LC W0.7 PhC waveguide shown in figure 5.5(b). The results obtained are shown in figure 5.6(a) and 5.6(b).

As can be observed, the average group index $\tilde{n}_g$ increases from 8 in the W0.7 PhC waveguide to 54.7 in the partially LC-infilled W0.7 PhC waveguide, because of the increased effective index of the waveguide produced by liquid crystal infiltration. However, the variation in β is comparatively small, since it reduces from 1 ps^2/km in the W0.7 PhC waveguide to $0.2ps^2/km$ in the partially LC-infilled W0.7 PhC waveguide, for frequencies near the centre of the slow group velocity band. The high value of the group index (~347) obtained at the extreme points is at the cost of high GVD, on the order of 10^3 ps^2/km. As a result, it is possible to identify a region of very low GVD over the wide spectral width of 1.02 THz, with an average group index of 43.05.

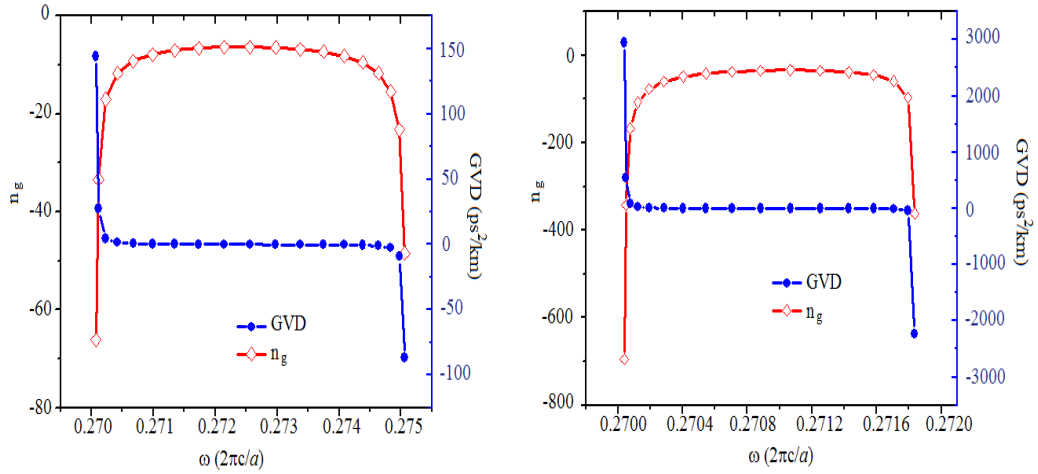

(a)

(b)

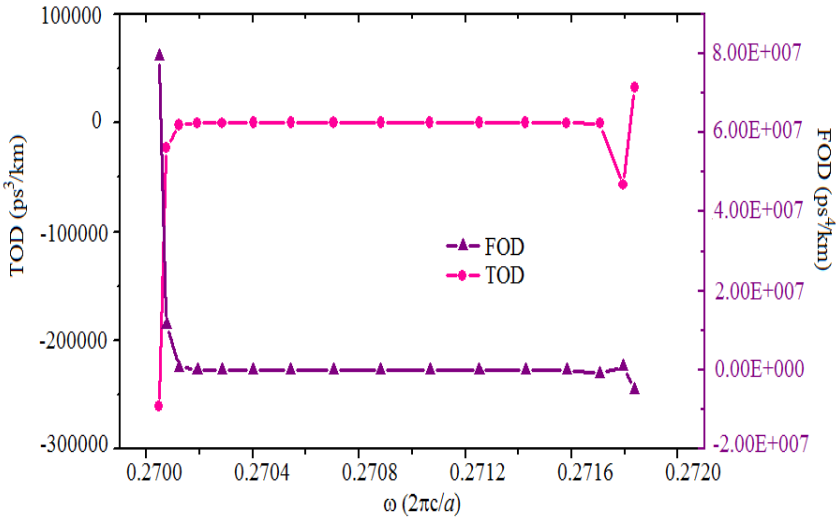

(c)

Figure 5.6. Variation of group velocity and GVD parameter for the flat section of dispersion curve, for: (a) a W0.7 PhC waveguide and (b) the partially in-filled LC W0.7 PhC waveguide. (c) Variation of higher order dispersion parameters TOD and FOD for LC W0.7 PhC waveguide with frequency in slow light region.

Since the value of the GVD parameter β is nearly constant in a region near the centre of the range, the values of the TOD and FOD are also low, as observed in Figure 5.6(c). The upper limit of the TOD is on the order of 10^4 ps^3/km, for the slow

light regime, below the silica light-line. However near the centre it varies from 10^1 to 10^2 ps^3/km. Similarly the upper limit of the FOD is on the order of 10^6 ps^4/km, but near the centre it varies from 10^2 to 10^3 ps^4/km. These results indicate that the higher order dispersion is strongly suppressed in the proposed partially LC-in-filled W0.7 PhC waveguide for a bandwidth of 1.02 THz, with average group index of 43.05, which further suppresses the pulse broadening and non-linear effects that are dependent on the higher-order dispersion parameters. As a result, the proposed partially infiltrated PhC waveguide has considerable potential for device applications such as multiplexers and de-multiplexers, delay lines and optical buffers. We shall now estimate the quantitative performance of the proposed SOI based partially LC-infilled W0.7 PhC waveguide.

From equation (5.9), the high value for the upper limit of the delay-bandwidth product (DBP) can be evaluated by reducing the value of $\tilde{v}_g \left|\beta\right|^{1/2}$. At the operating wavelength, $\lambda = 1.55$ μm, i.e. for a frequency of 0.2709 ($2\pi c/a$), the average group velocity is calculated to be 0.029c and the GVD parameter is $\beta = 0.0243$ ps^2/km. Therefore $\tilde{v}_g \left|\beta\right|^{1/2}$ =0.0007c ps.km$^{1/2}$. This value is highly reduced as compared to the value of 4.4c ps.km$^{1/2}$ in reference [Ma and Jiang (2008)]. We therefore observe that, for a given length of waveguide, the upper limitation on the DBP is greatly enhanced in our structure. The normalized DBP ($=\tilde{n}_g \frac{\Delta\omega}{\omega}$) is calculated to be 0.226, which is sufficiently large for the possible use of tunable slow light PhC waveguides in optical buffers.

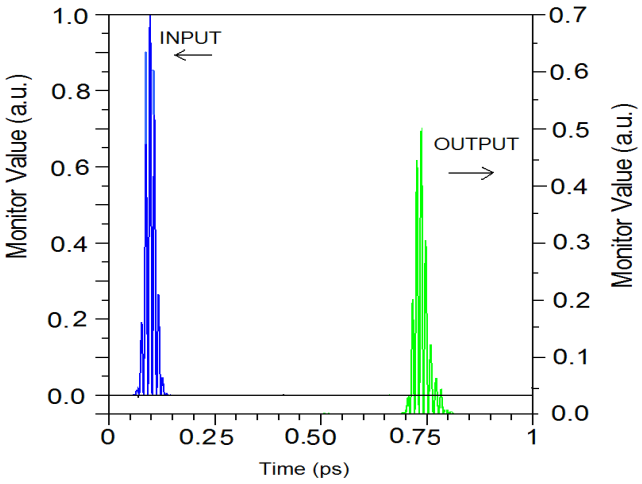

(a)

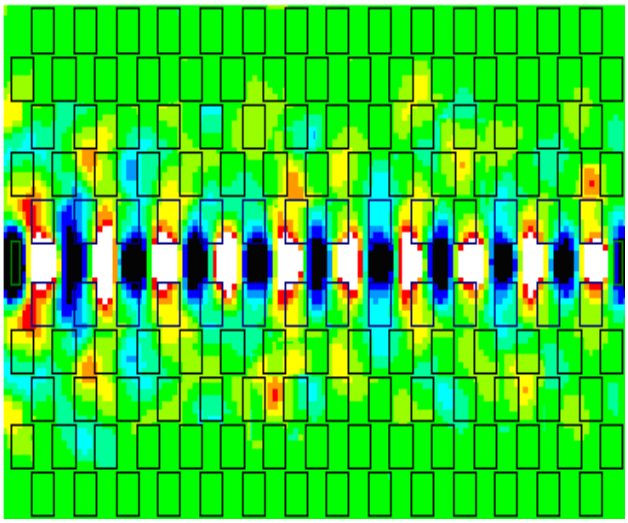

(b)

Figure 5.7. (a) Field amplitude of the pulse recorded at the input and output ends of the partially LC-infiltrated W0.7 PhC waveguide. (b) Modal field distribution at λ=1.55μm.

Further, the slow-down factor achieved in the partially LC-infilled W0.7 PhC channel waveguide was also calculated. It is defined as the ratio of phase-velocity to group-velocity ($S = V_p/V_g$) - and was calculated to be 20.91 at $\lambda = 1.55$ μm, for the designed rectangular-hole PhC-infiltrated channel waveguide. Assuming that the optical axis of the LC in-fill is perpendicular to the periodic plane, i.e. it lies parallel

to the y-axis, then we obtain the dielectric tensor $\varepsilon = \text{diag}\ (n_0, n_e, n_e)$ [Kao and Yu (2009)].

Applying 2D FDTD method, TE polarized analysis of PhC waveguide along ΓK direction is obtained in Figure 5.7. For a Gaussian pulse at a centre frequency of $\omega_0 = 0.2709\ (2\pi c/a)$, i.e. at $\lambda_0 = 1.55\ \mu m$, $v_g = 0.029c$ and the GVD = 0.0243 ps^2/km. Due to this vanishing dispersion, the width of the pulse at the input end is nearly equal to that at the output end, as shown in Fig. 5.7(a). The length of waveguide is nearly 16*a*, where *a* is the lattice constant. The modal field distribution for the input wave is shown in Figure 5.7(b). It can be seen that the incident pulse spreads substantially into the neighbouring rows of partially LC-infilled W0.7 PhC waveguide, due to the slow light propagation.

5.3. Tolerance Analysis

In this section, a study of the tolerances associated with the infiltration based approach for variations in the parameters of the rectangular air holes - and for variation in the refractive index of the Si core and infiltrated liquid crystal regions is presented.

5.3.1 Parameter Tolerances for rectangular air holes

Firstly it was shown, how the group index of the designed, SOI-based, partially LC-infiltrated W0.7 PhC waveguide varies with a ±4% variation in either X1 or Z1 - and Figures 5.8(a) and 5.8(b) show this variation. Figures 5.8(c) and 5.8(d) show the corresponding change in the group index of the partially LC-infiltrated W0.7 PhC waveguide. It can be seen that changes in the parameters of the rectangular air holes,

by ±4%, shift the dispersion curve up in frequency - but that there is less than 2.5 dB change in the group index for this particular frequency range, i.e. it still remains constant near the centre - and hence much less variation can be seen in the DBP (Delay Bandwidth Product).

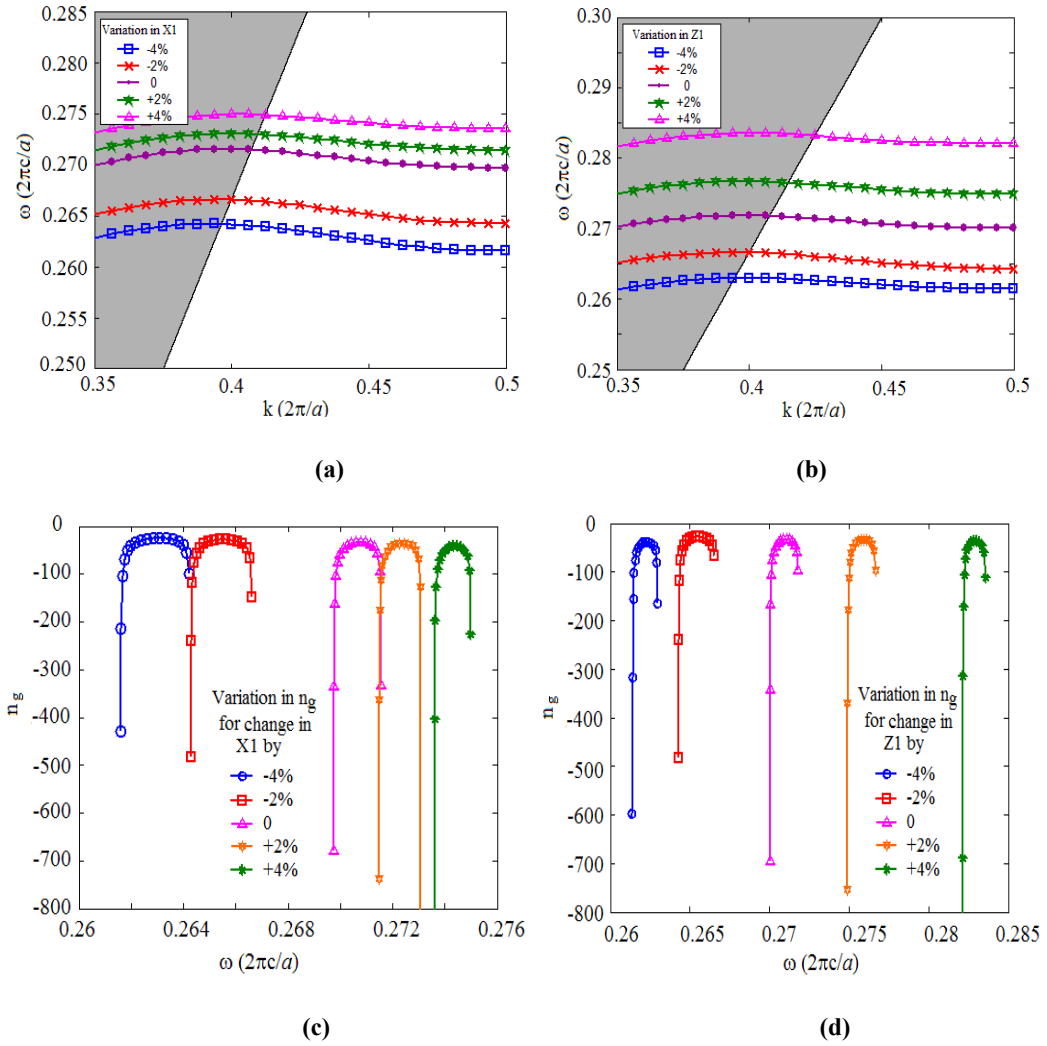

Figure 5.8: (a) and (b) show the shift in the dispersion curve with ±4% variation in X1 or Z1. (c) and (d) show the corresponding change in the group index of the partially LC-infilled W07 PhC waveguide.

5.3.2 Tolerance in refractive index

Tolerance analysis of the device will be carried out for variations in the refractive index of the silicon core and of the liquid crystal used.

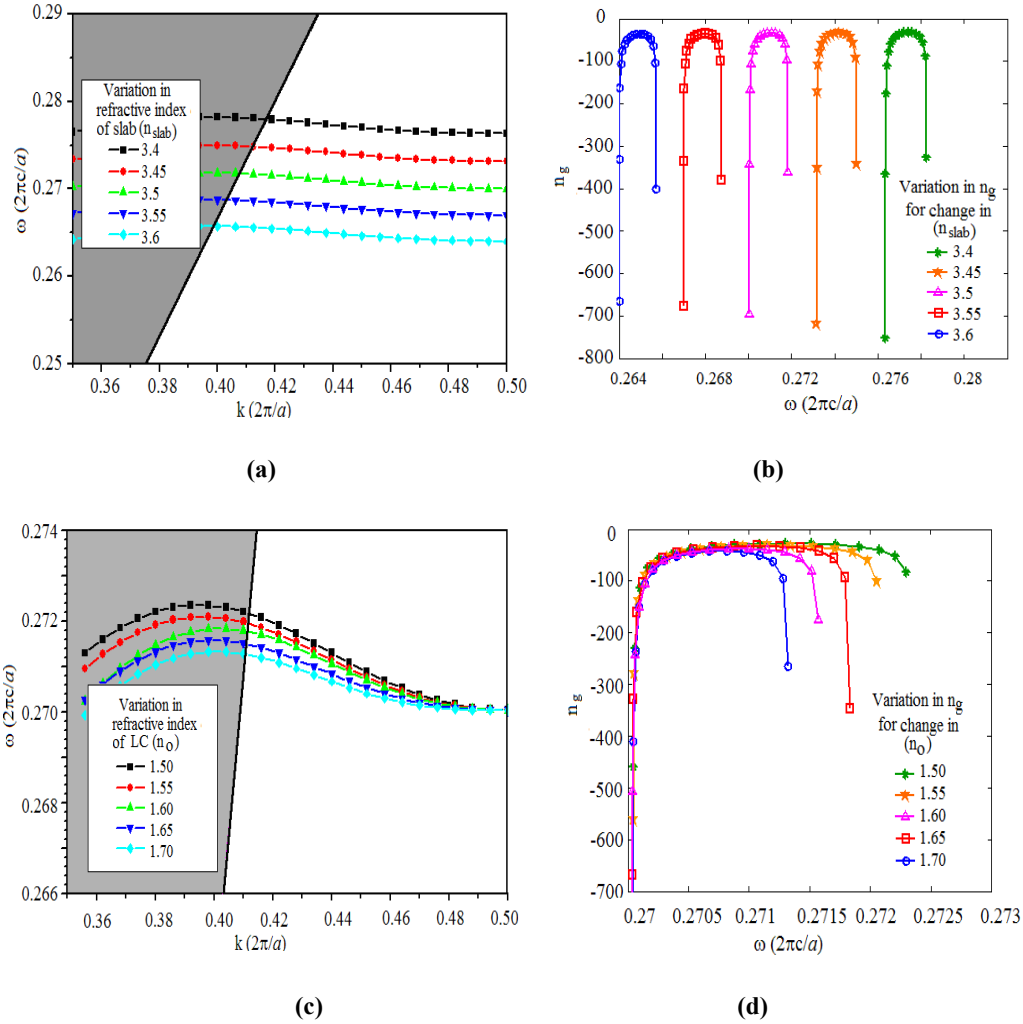

Figure 5.9. Movement of dispersion curve with variation in (a) refractive index of slab, n_{slab} and (c) ordinary refractive index of liquid crystal, n_{LC}. (b) and (d) represents the corresponding change in group index with variation in refractive index of slab and liquid crystal respectively.

Figure 5.9(a) shows the shift in the dispersion curve when the refractive index of Si changes by ±0.05. Corresponding variations in the group index are shown in Figure

5.9(b). Similarly, Figure 5.9(c) shows the shift in the dispersion curve for $\Delta n = \pm 0.05$ variation in the ordinary refractive index of the liquid crystal in-fill - and the corresponding variation in the group index is shown in Figure 5.9(d).

It can be seen that the small variations in refractive index (less than 20 %) incurred during PhC fabrication or changes in temperature still allow us to achieve the flat-band situation corresponding to the slow light regime with nearly constant group velocity - and near the centre. In the above, we have shown that the proposed SOI based partially LC-infilled W0.7 PhC waveguide is highly tolerant for small variations in refractive index - and there is no significant change in the group index of the partially LC-infilled W0.7 waveguide produced by such fabrication errors. The average group index in the respective ranges of frequency remains approximately the same - with a variation of less than 25 %.

5.3.3 Material Dispersion Consideration

Material dispersion, which corresponds to the dependence of refractive index on the optical frequency, is now considered in the PWE method. We first calculate the guided modes in LC-infilled PhC waveguides for different refractive indices of Si, as shown in Figure 5.9(a). Reference data of refractive index for material dispersion of Si is calculated by using the Sellmeier-type formula [Handbook of Optics (1994), Guryev and Sukhoivanov (2007)]:

$$n^2 - 1 = \frac{C_1 \lambda^2}{(\lambda^2 - C_2^2)} + \frac{C_3 \lambda^2}{(\lambda^2 - C_4^2)} + \frac{C_5 \lambda^2}{(\lambda^2 - C_5^2)}$$

where

$C_1 = 10.6684293$, $C_2 = 0.301516485$, $C_3 = 0.003043475$, $C_4 = 1.13475115$, $C_5 = 1.54133408$, $C_6 = 1104.0$

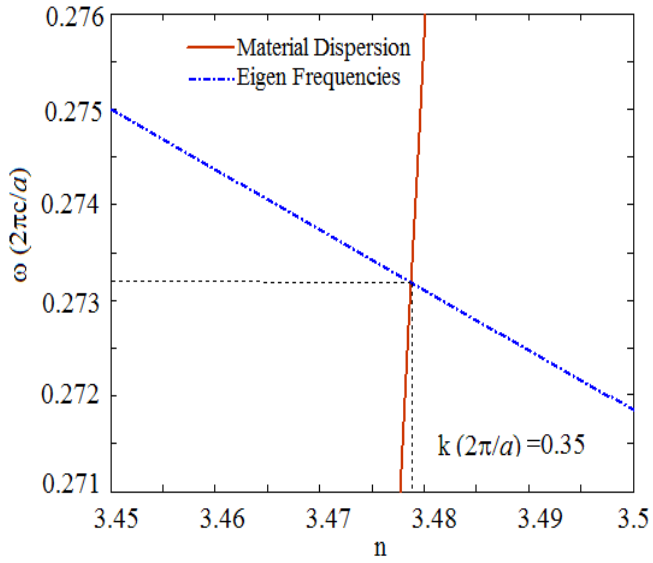

Figure 5.10 Variation of eigen frequencies at k ($2\pi/a$) = 0.35 (dash dot line) with refractive index and material dispersion of (solid line) silicon.

The intersection between the material dispersion curve and the line formed by different eigen frequencies taken at a specific k point, for different refractive index values, gives the eigen frequency of the structure with material dispersion taken into account, as shown in Figure 5.10.

If all k-points of the guided mode are now considered, the intersection with the material dispersion curve takes the form of points that give rise to a new guided mode with material dispersion taken into account. The variation in group index for the new guided mode in a partially LC-infilled PhC waveguide (figure 5.11) was then calculated. It shows that not only there is a slight decrease in average group index to

~41.00, but also that the bandwidth increases, raising the normalized value of the DBP to 0.245.

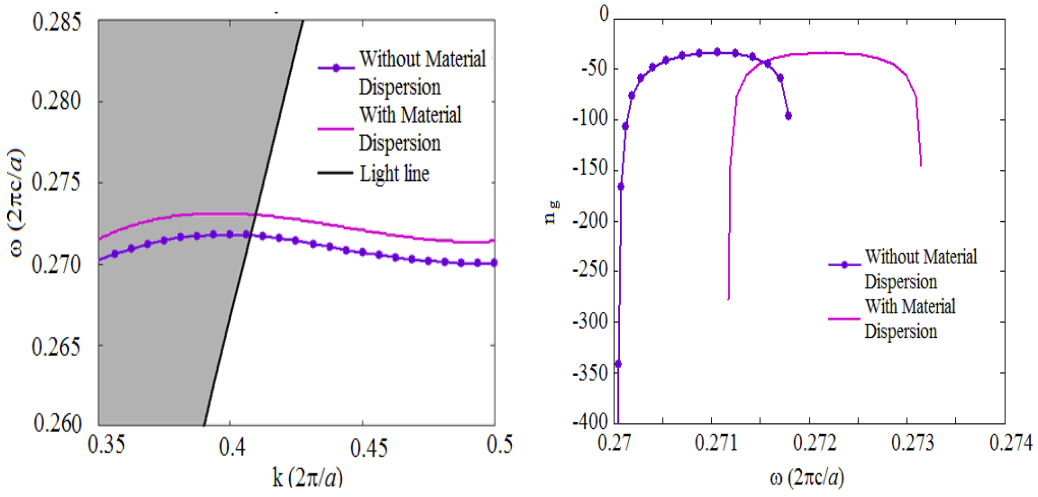

(a) **(b)**

Figure 5.11 (a) Band structure and (b) variation in group index with (solid line) and without (dotted marked line) material dispersion consideration.

5.4. Sensitivity

Sensitivity can be evaluated by determining the magnitude of the change in the cut-off frequency of the even guided mode with variation in the refractive index of the medium. In this section we have compared the sensitivity of the cut-off frequency for a liquid-infiltrated photonic crystal waveguide (LC W0.7 PhC waveguide) with conventional PhC waveguide (W0.7 PhC waveguide), both composed of a hexagonal arrangement of rectangular air holes in an SOI-based PhC. Here we consider a situation where the volume above the conventional stripe waveguide, the W0.7 PhC waveguide - and inside the holes is filled with air of refractive index n_a. Figure 5.12(a) shows the cut-off wavelength as a function of refractive index n_o (the ordinary refractive index of the liquid crystal) for LC infiltrated W0.7 PhC waveguide and n_a

(refractive index of gas in-filled holes) for the 'conventional' W0.7 PhC waveguide. The change in wavelength is nearly linear with variation in refractive index.

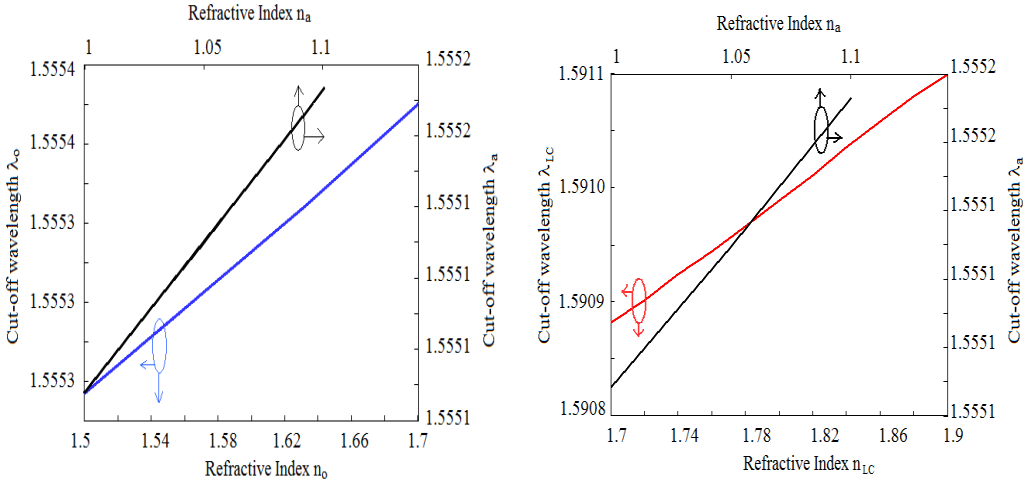

(a) **(b)**

Figure 5.12. Variation of cut-off wavelength as a function of refractive index of air n_a and (a) n_o and (b) n_{LC} , respectively.

If sensitivity is defined as $\frac{\Delta\lambda}{\lambda_0}$ expressed as a percentage, then the sensitivity is 0.0012% for infiltrated LC W0.7 PhC waveguides and 0.0005% for the conventional waveguide. Therefore a PhC waveguide infiltrated with LC that has its optical axis perpendicular to the x-z plane is more than twice as sensitive as a conventional W0.7 PhC waveguide to variations in the refractive index of the holes.

Now consider that the photonic crystal is locally filled with a liquid crystal for which the optic axis orientation changes randomly and becomes parallel to the periodic plane, i.e. the x-z plane, then it acts as an isotropic material with refractive index given by $n_{LC} = (n_e + 2\ n_o)/3$ [Takeda and Yoshino (2002)]. Here the liquid crystal used has extra-ordinary and ordinary refractive index values of 2.20 and 1.60,

respectively. Therefore n_{LC} = 1.8. Fig. 5.12(b) shows the variation of cut-off wavelength as a function of n_{LC} , since now the optic axis of the liquid crystal is parallel to the periodic plane. The sensitivity is calculated to be 0.00147%, which is nearly three times as sensitive as for conventional waveguides. These results show that the tunability of photonic crystal waveguides can be significantly increased by field enhancement and slow light effects.

5.5. Pulse Transmittance Measurements

An immediate problem arising from the design of the slow-light waveguide is its capability for input and output coupling of slow modes efficiently, in the slow light regime. This problem arises from the large mismatch at the boundaries of the PhC waveguide that arises from large differences in the group index.

To solve this complex problem, short intermediate sections of fast PhC channel waveguide that act as coupler sections are added at both ends, in addition to the slow light PhC waveguide obtained through partial liquid crystal infiltration. The model of the proposed heterogeneous waveguide is shown schematically in Figure 5.13(a). The calculated photonic band structure of the fast PhC waveguide with a stretched period (*a*'=450nm) obtained using the 3D PWE method is shown in Figure 5.13(b). From the slope of the dispersion curve of the fast waveguide, it is observed that the velocity of a signal at 1.55 μm is 0.169c, which is much higher than that obtained in slow-light partially LC-infilled W0.7 PhC waveguide (~ 0.029c) - or homogeneous waveguide. The 3D FDTD method was used for calculating the transmittance through the proposed heterogeneous PhC waveguide.

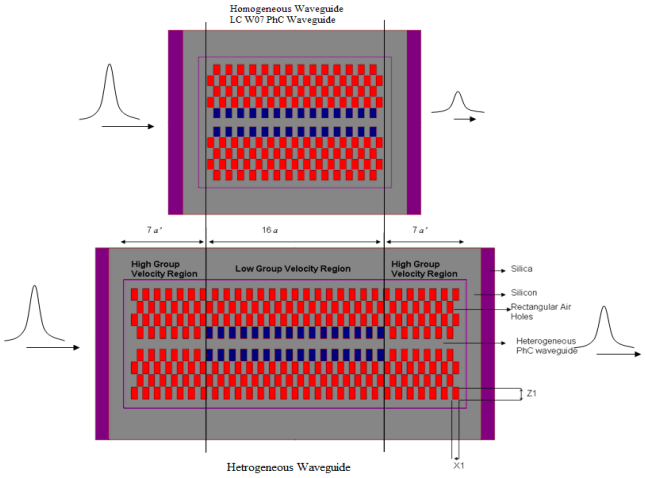

(a)

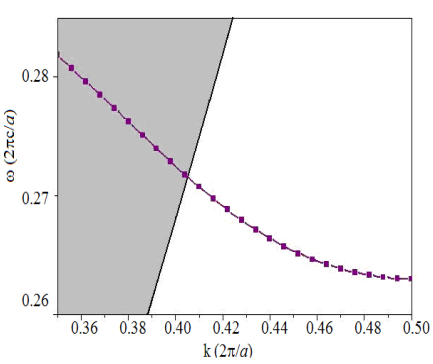

(b)

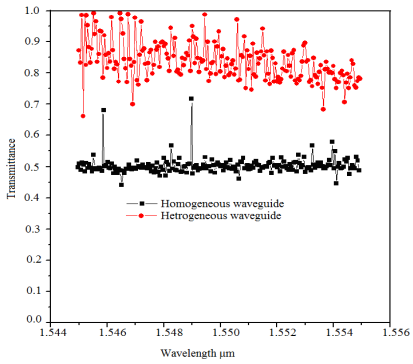

(c)

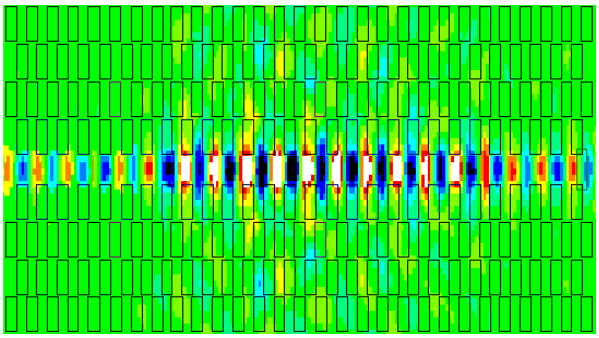

(d)

Figure 5.13. (a) Schematic of the proposed heterogeneous PhC waveguide. (b) The dispersion curve of the fast PhC waveguide with a stretched period *a*'=450nm obtained using the 3D PWE method. (c) Transmittance obtained from the homogeneous and heterogeneous liquid infilled PhC waveguide. (d) Modal distribution with a continuous wave at λ_0=1.55 µm.

As observed in reference [Hugonin *et al.* (2007)], efficient coupling of light is obtained between the fast and slow photonic crystal waveguides having large group index mismatch, (of the order of 20) at the interface. This optimization of injection efficiency is carried out by adding a taper between the two waveguides in a region which forms a transition zone**.** However in our case, the group index mismatch between the fast and the slow waveguides is only (35/6) 5.83, so such modification for efficient coupling is not required. Figure 5.13(d) shows the modal field distribution with a continuous wave at λ_0=1.55μm going from a fast PhC waveguide into a slow PhC waveguide. It shows the existence of a transition zone at the interface where the field varies smoothly as it penetrates the slow waveguide.

Figure 5.13(c) summarizes the transmittance of the propagating pulse through a heterogeneous PhC waveguide consisting of a 16*a* long partially LC-infiltrated W0.7 slow light waveguide surrounded by two sections of fast PhC channel waveguide made up of high group velocity regions. The coupler length is chosen so that maximum coupling efficiency is obtained along the coupler and through the transition zone i.e. evanescent modes excited at each end of the coupler do not overlap and interfere destructively [Sa¨yna¨tjoki *et al*. (2008)]. This results in maximum transmission. As shown in Figure 5.13(c), the transmittance of the heterogeneous PhC waveguide for the slow-light flat-band window ranging from 1.545 μm to 1.555 μm is higher than 80% while the transmittance obtained for a homogeneously LC-infilled W0.7 PhC waveguide alone is nearly 50%. This higher (lower) transmittance in a heterogeneous (homogeneous) waveguide is due to better (poorer) coupling into the slow mode.

5.6. Conclusions

In the present chapter, an SOI-based partially liquid-infiltrated photonic crystal W0.7 channel waveguide having rectangular air holes in a silicon core is proposed. It has been demonstrated that the proposed structure has an average group index of 43 over a bandwidth of 1.02 THz, with vanishing group velocity dispersion and likewise small values of the other higher-order dispersion terms. The designed partially LC-infiltrated W0.7 PhC waveguide for slow light propagation is highly tolerant of fabrication errors and has nearly twice higher sensitivity than conventional PhC waveguides. The structure designed has also been investigated for possible propagation losses, which include losses due to coupling inefficiency. It is found that high transmission can be obtained over a broad bandwidth in the heterogeneous waveguide that was finally designed - and consists of a partially LC-infiltrated PhC slow waveguide, surrounded by fast PhC waveguide on either side.

Chapter 6

The Impact of Slow Light on Third Order Non-linearities in SOI Photonic Crystal Channel Waveguides[1]

6.1 Introduction

As discussed in Chapters 4 and 5, high refractive index contrast structures such as photonic crystals (PhCs) have been demonstrated to be a promising approach to the achievement of slow light behavior [Gersen *et al*. (2005), Vlasov *et al*. (2005), De La Rue (2008), Krauss (2008), Rawal *et al*. (2009), Rawal *et. al*. (2010)]. However, linear effects such as gain, the thermo-optic effect - and some types of electro-optic interaction - scale linearly with the slow-down factor, while non-linear effects such as two photon absorption (TPA) and Kerr nonlinearity scale with the square of the slow-down factor [Krauss (2007), Soljacic and Joannopolous (2004)]. The spatial compression experienced by light when it goes from a fast light situation to a slow light situation - and the greater time that light spends in the waveguide, because of the

[1] Part of the results reported in this chapter is submitted in the paper: "Slow light enhanced third order non-linearities with device application in silicon-on-insulator photonic crystal channel waveguides"

slow group velocity, increase the strength of the light-matter interaction and imply the enhancement of nonlinear effects. Thus slow light behaviour causes a reduction in the input power level and the physical length of waveguide needed to produce a given magnitude of linear and nonlinear effects in the fast light regime [Krauss (2007), Soljacic *et al.* (2002), Setlle *et al.* (2007)]. By carefully engineering the photonic dispersion relationship, one may obtain unique opportunities for the realization of devices that exploit slow light effects [Baba and Mori (2007), Frandsen *et al.* (2006)]. Recently, nonlinear effects such as the Raman effect, soliton propagation, two-photon absorption (TPA), etc. have been observed by different authors [Oda *et al*. (2008), Astrov *et al.* (2000), Tsang *et al.* (2002), Ding *et al.* (2008), Miller *et al.* (1999)]. Self phase-modulation (SPM), which leads to chirping and spectral broadening of ultra-short pulses, has also been reported earlier [Tsang *et al.* (2002)]. However TPA limits the extent of SPM through nonlinear absorption [Nicole *et al.* (2006)]. TPA typically involves transitions from the ground state of a system to a higher state by absorption of two photons from an incident radiation field having identical or, more generally, two different frequencies. TPA further creates free carriers that lead to additional losses through free-carrier absorption (FCA) and refractive index changes through free-carrier dispersion (FCD) [Yin and Agrawal (2007), Oda *et al.* (2007), Inoue *et al.* (2009)]. Thus TPA, FCA, FCD and SPM are important effects that influence the behavior of short laser pulses in silicon waveguides. However soliton dynamics will dominate the propagation of femtosecond pulses in PhC waveguides when the group velocity dispersion (GVD) is strongly anomalous because of large waveguide dispersion [Ding *et al.* (2008)]. It is important to mention here that, as optical pulses propagate through photonic crystal waveguides; their evolution in both the time and

frequency domains is governed by the interplay of linear dispersion and nonlinearity. These effects are characterized by the characteristic lengths, namely the GVD length, L_D, and the nonlinear length L_{NL} [Agrawal (2001)]. Depending on the relative magnitudes of L_D, L_{NL} and the waveguide length, L, pulses evolve in various different ways. Here:

$$L_D = \frac{T_0^2}{|\beta_2|},\ L_{NL} = \frac{1}{\gamma P_0}$$

where T_0 is the initial width, in time, of the pulse, P_0 is the incident power, β_2 is the GVD parameter and γ is the nonlinear parameter defined in subsequent sections. As a consequence, the propagation behaviour of the pulse is classified as follows:

(i) For the first case, $L << L_{NL}$ and $L << L_D$

Here neither dispersive nor nonlinear effects come into play during pulse propagation and the waveguide acts merely as a transporter of the optical pulses.

(ii) In the second case, $L << L_{NL}$ and $L > L_D$

In this case, pulse evolution is governed by GVD and nonlinear effects play a relatively minor role.

(iii) A third case is defined by $L << L_D$ and $L > L_{NL}$

Here the pulse evolution is governed by SPM and leads to spectral broadening of the pulse.

(iv) If $L >> L_D$ and $L >> L_{NL}$

Here GVD and nonlinearity act together during pulse propagation. Interplay between GVD and SPM can lead to soliton generation in the anomalous dispersion regime ($\beta_2 < 0$).

In reference [Monat *et al.* (2010)], Monat and co-workers describe how slow light with a group velocity on the order of c/50 can be obtained in silicon based PhC waveguides having an air-bridge, or membrane, structure. Such structures are inherently mechanically vulnerable. It has been shown that dispersion engineered slow light PhC waveguides provide a suitable platform for enhancing nonlinear effects, making it possible to realize compact, low power, all-optical signal processing devices.

For Gaussian pulses, an important criterion for comparing the relative magnitudes of the effects FCA, FCD and TPA comes from the dimensionless parameter [Lin *et al*. (2007)]: $r_a = \frac{S\sigma P_{in} T_0 \sqrt{\pi}}{2\sqrt{2} h\upsilon_o A_{eff}}$. The free carrier density near the input end of the waveguide is negligible when r_a<<1 - i.e. the pulse peak power level is relatively low (e.g. a value of 100 mW in the context of the present paper). In this situation, only TPA comes into play to a significant extent - and the observed reduction in output power is almost solely due to TPA.

In the present chapter, propagation of light is investigated in a nonlinear slow light medium, formed by a channel waveguide, in a silicon-on-insulator (SOI) photonic crystal structure having elliptical holes in a silicon core – and mechanically supported by the silica cladding, which remains in place. Our SOI PhC structure also uses a substantially thicker core layer that is compatible with the smaller index contrast implied by retaining the silica lower cladding layer. The supported structure configuration is inherently more robust and practically suitable. This choice of device architecture is demonstrably an effective and flexible way of controlling the speed of

light (down to the order of c/99) and its associated group velocity dispersion (GVD), as described in reference [Rawal *et al.* (2009b)].

A detailed study of the effect of the input peak power level and the impact of varying the slow-down factor on the nonlinear effects achievable in the proposed configuration for a photonic crystal channel waveguide is further carried out - and have also shown the effect of the slow-down factor on the induced phase-shift at the optical frequency of the photonic bandgap. The transmitted spectrum becomes broader with increasing P_{in} - and develops multiple peaks when P_{in} is further increased - which is due to the magnitude of the induced nonlinear refractive index. This leads to a marked evolution of the optical frequency spectrum as the peak power level, P_{in}, is increased. The impact of the slow-down factor and the corresponding increase in nonlinear effects also defines the amount of input power required to achieve a particular level of spectral broadening in such waveguides. The present paper provides a comprehensive study of the effect of the slow-down factor and peak input power level on TPA, FCA and the SPM produced in PhC channel waveguides. The large SPM response achieved in the structure is vital for applications such as optical switching, as shown in the present paper. It has been reported that femtosecond pulse propagation in SOI photonic wire waveguides can give rise to solitonic behaviour [Ding *et al.* (2008)]. With appropriate re-scaling, it becomes clear that the length of the PhC channel waveguide required to produce solitonic behaviour will be greatly reduced.

6.2 Slow Light Generation: Design Aspects

An SOI based photonic crystal having a hexagonal arrangement of elliptical air holes in a silicon core layer is used for the design. The thickness of the underlying silica layer was chosen to be 3 μm, on top of which the silicon core layer was chosen to have a thickness equal to 0.443 μm. The refractive index of silicon and silica are taken to be 3.49 and 1.45, respectively. A W0.7 waveguide was then created conceptually by omitting a row of air holes along the ΓK direction - and shifting the two photonic crystal regions closer to each other so that the channel waveguide width becomes 0.7 times that of W1. The minimum values for the losses and defect mode dispersion below the silica light-line are found for a W0.7 waveguide. For this reason, one typical structure employed in experiments has been a W0.7 PhC waveguide [Notomi *et al.* (2001)].

The two neighbouring rows of holes on either side of the waveguide are filled with silica rods. The lattice constant a, semi-major radius r_1 and semi-minor radius r_2 of the elliptical air holes were 0.42 μm, 0.16 μm and 0.118 μm, respectively. These parameters were obtained by properly optimizing the proposed structure to obtain a flat section of dispersion curve below the silica light-line - because modes that lie above the light line are lossy in the vertical direction - i.e. into the substrate. Figure 6.1(a) shows a schematic of the proposed structure and Figure 6.1(b) shows the calculated dispersion curves for transverse electric polarization in the defect mode. The flat section of the dispersion curve displays a slow group velocity over a substantial bandwidth.

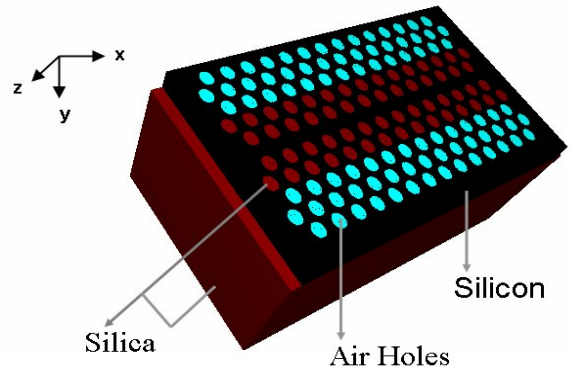

(a)

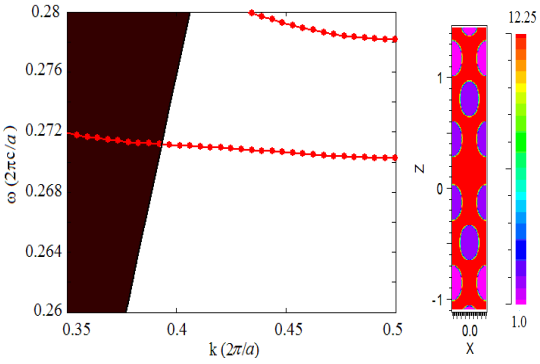

(b) **(c)**

Figure 6.1. (a) Schematic of the proposed structure with elliptical holes in a hexagonal arrangement. The two neighbouring holes on either side of the waveguide are filled with silica rods. (b) The calculated dispersion curve for transverse electric polarization in the defect mode. The black solid line is the silica light line and the lower pointed red dispersion curve is used for calculating the group velocity. (c) Super-cell used in computation of the band structure.

The low velocity range is now defined to be those values that give a ±10 % variation in the group index n_g [Hamachi *et al.* (2009)], therefore group index obtained for our structure is $n_g = 99$, over a frequency range of 344 GHz. Therefore the normalized value of the Delay-Bandwidth Product (DBP), which is defined as $n_g*(\Delta\omega/\omega)$, is calculated to be 0.20. It is further investigated, the delay for pulses propagating through the waveguide using FDTD simulations. Figure 6.2 shows the

field amplitude of the Gaussian pulse recorded at the input end and output end of the waveguide as a function of time, for λ_0=1.55μm. Length of the waveguide is 15*a*.

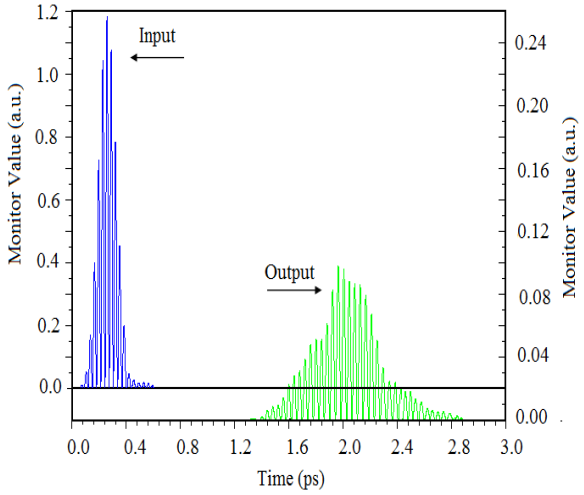

Figure 6.2. Field amplitude of Gaussian pulse at the input and output end of the waveguide, at λ_0=1.55 μm.

The group velocity dispersion (GVD) parameter β_2 is related to the second order derivative of the dispersion curve by the following expression:

$$\beta_2 = \frac{d^2k}{d\omega^2} = \frac{d}{d\omega}\left(\frac{1}{d\omega/dk}\right)$$
$$\Rightarrow \beta_2 = -\frac{1}{v_g^3}\frac{d^2\omega}{dk^2} \qquad (6.1)$$

The group velocity n_g and the GVD parameter in the flat regime below the silica light line are shown, in Figure 6.3, as a function of frequency. The figure shows that the GVD parameter is on the order of 10^4 ps^2/m and that the average group index is 99.

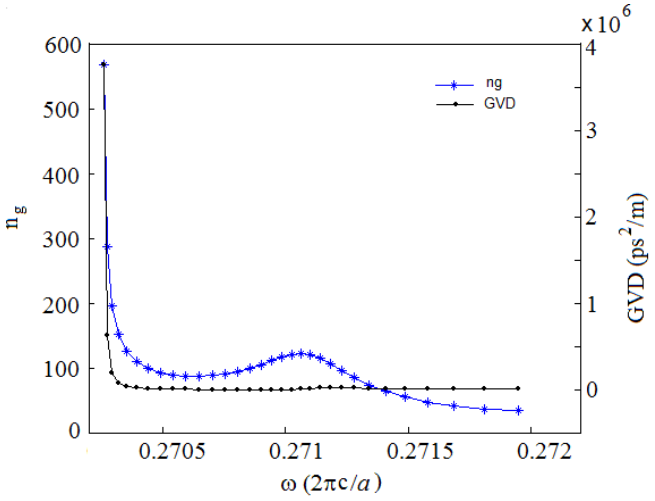

Figure 6.3. Variation of group index and group velocity dispersion with frequency.

We further define the slow-down factor (S) as the ratio of group index n_g to the refractive index, n_{si}, of bulk silicon. It is calculated to be 28.28 at $\lambda_o = 1.55\ \mu m$ for the designed elliptical hole PhC waveguide.

6.3 Nonlinear Modeling of Pulse Propagation

Next we evaluate the nonlinearity of an SOI-based photonic crystal waveguide. The propagation of the optical pulse having amplitude *A(z,t)* is given, for sufficiently strong confinement, by the following nonlinear Schrödinger Equation [Monat et al. (2009), Rukhlenko et al. (2009), Yin and Agrawal (2007)] in one space dimension and time:

$$\frac{\partial A}{\partial z}+\frac{\alpha}{2}A+\frac{i\beta_2}{2}\frac{\partial^2 A}{\partial t^2}-\frac{\beta_3}{6}\frac{\partial^3 A}{\partial t^3}=i\kappa|A|^2A-N_c\left(\frac{\sigma}{2}+ik_ck_0\right)A \qquad (6.2)$$

where α accounts for the linear component of the propagation losses, β_2 is the dispersion parameter at wavelength λ_o, n_2 is the Kerr coefficient of silicon, κ defines

the nonlinearity in the waveguide and is given by $\kappa = \gamma + i\frac{\zeta}{2}$, where $\gamma = \frac{2\pi n_2}{\lambda_o A_{eff}}$ is the nonlinear parameter and ζ is related to the two photon absorption (TPA) coefficient, β_{TPA}, defined as $\zeta = \frac{\beta_{TPA}}{2A_{eff}}$. A_{eff} is the cross-sectional area of the PhC channel waveguide mode. The second term on the right-hand side of equation (6.2) gives the free carrier absorption (FCA) defined by the parameter σ and the free carrier dispersion (FCD), accounted for by k_c - and N_c is the carrier density produced by TPA. In silicon, the free carriers generated by TPA are governed by the following rate equation:

$$\frac{\partial N_c(t)}{\partial t} = \frac{\beta_{TPA}}{2\hbar\omega_o}|A|^4 - \frac{N_c}{\tau_c} \tag{6.3}$$

where τ_c is the carrier lifetime in silicon and is taken to be approximately equal to 1 ns [Yin and Agrawal (2007)]. At $\lambda_o = 1.55\ \mu m$, the parameters identified in equations (6.2) and (6.3) have the following values [Monat et al. (2009), Yin and Agrawal (2007)]:

$n_2 = 6\times10^{-18}\ m^2/W$, $\beta_{TPA} = 5\times10^{-12}\ m/W$, $\sigma = 1.45\times10^{-21}\ \mathrm{m}^2$, $k_c = 1.35\times10^{-27} m^3$, $\alpha = 20\ dB/cm = 230.41\ Neper/m$

For $T_0 = 1$ ps and $A_{eff} = 0.12\ \mu m^2$, the GVD and TOD are found to be -8291 ps^2/m and -78 ps^3/m, respectively at $\lambda_o = 1.55\ \mu m$. As described in the introductory section, the linear dispersion and nonlinearity in SOI-based PhC waveguides are characterized by their characteristic lengths, given by dispersion lengths L_D and L_D'' - and the nonlinear length L_{NL}, where:

$$L_D = \frac{T_0^2}{|\beta_2|} = 1.22\times10^4\,\mu m\,,\quad L_D^{"} = \frac{T_0^3}{|\beta_3|} = 1.28\times10^7\,\mu m \text{ and } L_{NL} = \frac{1}{S^2\gamma P_{in}} \approx 3\mu m$$

For a 30 μm waveguide length, S = 28.28, $\gamma = 202\ m^{-1}W^{-1}$ and $P_{in} = 2\ W$. Since $L_{NL} < L < L_D$, the dispersion effects in the waveguide have been ignored and the pulse evolution is thus dominated by self phase modulation and two-photon absorption, which is accompanied by free-carrier effects [Agrawal (2001)]. Hence the GVD and TOD parameters are now neglected from equation (6.2). It can be written as:

$$\frac{\partial A}{\partial z} + \frac{\alpha}{2}A = i\kappa|A|^2 A - N_c\left(\frac{\sigma}{2} + ik_c k_0\right)A \tag{6.4}$$

$$\frac{\partial A}{\partial z} + \frac{\alpha}{2}A = i\gamma|A|^2 A - \frac{\beta_{TPA}}{2A_{eff}}|A|^2 A - N_c\left(\frac{\sigma}{2} + ik_c k_0\right)A \tag{6.5}$$

The reduction in the group velocity of the mode inside the waveguide causes optical localization and field enhancement in the waveguide. The slow-down factor, S, may therefore be introduced into equation (6.5) by replacing α, γ and β_{TPA} - by $\alpha \times S$, $\gamma \times S^2$ and $\beta_{TPA}\times S^2$, respectively. Equation (6.5) therefore becomes:

$$\frac{\partial A}{\partial z} + \frac{S\alpha}{2}A = iS^2\gamma|A|^2 A - \frac{S^2\beta_{TPA}}{2A_{eff}}|A|^2 A - SN_c\left(\frac{\sigma}{2} + ik_c k_0\right)A \tag{6.6}$$

When $T_0 << \tau_c$ - and the pulse repetition rate is very low - the second term on the right-hand side of equation (6.3), corresponding to carrier recombination, can be ignored - because the recombination time, τ_c, is much larger than the pulse duration. Therefore the carrier density profile of $N_c(t)$ near the input end of the waveguide for a Gaussian pulse, with the temporal power profile written as:

$$|A(0,t)|^2 = P(0,t) = P_{in}\exp\,(-t^2/T_0^2)$$

is found to be:

$$N_c(t) = \frac{\beta_{TPA} P_{in}^2 T_0}{2\hbar\omega_o A_{eff}^2} \sqrt{\frac{\pi}{8}} \left(1 + erf\left(\frac{\sqrt{2}t}{T_0}\right)\right) \tag{6.7}$$

where P_{in} is the input peak power. For Gaussian pulses, the criterion for testing the relative magnitudes of FCA, FCD and TPA is given by the dimensionless parameter [Lin *et al.* (2007)]: $r_a = \frac{S\sigma P_{in} T_0 \sqrt{\pi}}{2\sqrt{2}\hbar\omega_o A_{eff}}$. For N_c to be negligible, r_a<<1 - i.e. the peak power should not be very high. If we consider P_{in} = 0.2 W and T_0 = 1 ps, we obtain r_a = *0.329 <<1*. For such low power levels, we can neglect the free-carrier density, N_c. Equation (6.6) can now be written as:

$$\frac{\partial A}{\partial z} + \frac{\alpha S}{2} A = iS^2\gamma |A|^2 A - \frac{S^2 \beta_{TPA}}{2A_{eff}} |A|^2 A \tag{6.8}$$

Setting $A = \sqrt{\frac{P}{A_{eff}}} \exp(i\phi - \alpha S z/2)$ and solving equation (6.8), we find the following relationship:

$$\frac{P0,t)}{P(L,t)} = e^{S\alpha L} + S^2 \frac{\beta_{TPA}}{\alpha S}\left(\frac{e^{S\alpha L} - 1}{A_{eff}}\right) P(0,t) \tag{6.9}$$

If $L_{eff} = \frac{1 - e^{-\alpha SL}}{\alpha S}$ is the effective length of waveguide, then equation (6.9) becomes:

$$\frac{P(0,t)}{P(L,t)} = e^{\alpha SL} + \frac{S^2 \beta_{TPA}}{e^{-S\alpha L}} \frac{L_{eff}}{A_{eff}} P(0,t) \tag{6.10}$$

Similarly the phase induced in the output waveform is given by:

$$\phi(L,t) = \frac{\gamma A_{eff}}{\beta_{TPA}} ln\left[1 + S^2 \frac{\beta_{TPA}}{A_{eff}} P(0,t) L_{eff}\right] \tag{6.11}$$

Since $2\zeta = \frac{\beta_{TPA}}{A_{eff}}$, equation (6.10) and equation (6.11) can be re-written as:

$$\frac{P(0,t)}{P(L,t)} = e^{\alpha SL} + \left(2\zeta S^2 \frac{L_{eff}}{e^{-\alpha SL}} \right) P(0,t) \tag{6.12}$$

and

$$\phi(L,t) = \frac{\gamma}{2\zeta} ln \left[1 + 2\zeta S^2 P(0,t) L_{eff} \right] \tag{6.13}$$

Figure 6.4 gives the power-dependent transmission curves for $\lambda_0 = 1.55\ \mu m$ - and shows that the slow-down factor significantly affects the output power. The S^2 dependence of β_{TPA} and γ enhances the nonlinear absorption in the PhC channel waveguides. For nearly the same input peak (P_{in}) power level of 0.5 W (so that $r_a < 1$), the output power obtained from a slow light waveguide ($S = 28.28$) is around 7 times less than that obtained from a fast light waveguide ($S = 1$). This result demonstrates that the group velocity plays an important role in determining the magnitude of the nonlinear interaction.

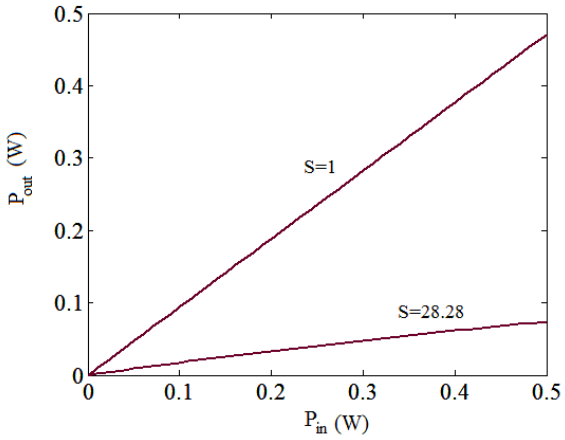

Figure 6.4. Power-dependent transmission curves for different slow down factors.

When TPA is negligible, i.e the TPA coefficient $\beta_{TPA} \rightarrow 0$ or $\zeta \rightarrow 0$, the maximum nonlinear phase shift ϕ_{max} occurs at the pulse centre and is given by:

$$\phi_{max} = S^2 \gamma L_{eff} P_{in} \tag{6.14}$$

However, in the presence of TPA, the nonlinear phase shift at the pulse centre is:

$$\phi_o = \phi(L,t) = \frac{ln\left(1+\frac{2\zeta}{\gamma}\phi_{\max}\right)}{\frac{2\zeta}{\gamma}} \tag{6.15}$$

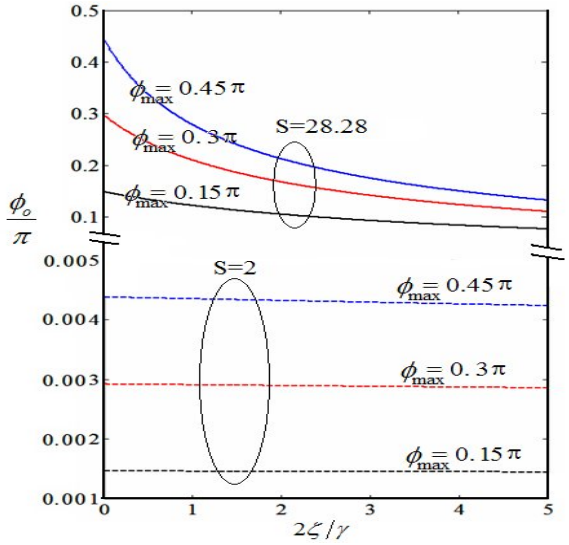

(a)

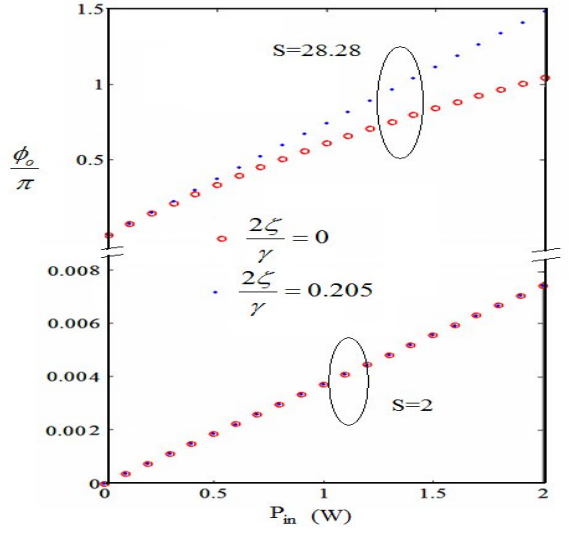

(b)

Figure 6.5 (a) Variation of SPM induced phase shift with 2ζ/γ for different values of maximum nonlinear phase shift ϕ_{max} . (b) Variation of ϕ_o with input power P_{in} in the presence (dotted line)

and in the absence (solid line) of TPA coefficient. These variations are shown for both slower and faster waveguides.

Figure 6.5(a) shows the variation of the SPM-induced phase-shift (normalized with respect to a phase-shift of π) as a function of the dimensionless ratio $\frac{2\zeta}{\gamma}$ for different values of the maximum phase-shift, $\phi_{\max}$ and for different slow down factors. The ratio $\frac{2\zeta}{\gamma}$ is wavelength dependent and may be considered as a normalized TPA coefficient. It can be seen that in case of slow waveguides, (S=28.28), the SPM-induced phase-shift decreases with increasing normalized TPA coefficient - and that the reduction becomes more severe at higher input powers (but r_a is still less than 1), i.e. for higher values of $\phi_{\max}$. However in case of fast waveguides (S=2), the phase angle remains nearly constant throughout the increase in TPA coefficient.

Figure 6.5(b) shows ϕ_0 as a function of input power $P_{in,}$ for $\frac{2\zeta}{\gamma} = 0.205$ and $\frac{2\zeta}{\gamma} = 0$,for different slow down factors, S=28.28 and S= 2. Comparison of the two sketches in figure 6.5(b) shows that for $\frac{2\zeta}{\gamma} = 0.205$, i.e. in the presence of two-photon absorption coefficient, β_{TPA} , ϕ_o increases logarithmically for S=28.28 and for $\frac{2\zeta}{\gamma} = 0$, i.e. in the absence of β_{TPA}, an increase in P_{in} produces a linear increase in ϕ_o. Thus TPA is mainly responsible for this depletion of the incident power and, as P_{in} becomes larger, the influence of TPA becomes stronger - and the phase shift is no longer proportional to the input power. However for fast waveguides, S=2, the

influence of TPA vanishes and hence the increase in Pin produces linear increase in ϕ_0 both in the presence as well as in the absence of $\beta_{TPA.}$

Figure 6.6 shows the calculated optical power distribution along the waveguide at P_{in} = 0.6 W, 0.4 W and 0.2 W, respectively. The presence of TPA in slower waveguides (S=28.28) causes the rapid attenuation of light near the input end of the waveguide. This is due to the high dependence of nonlinear behaviour on the velocity of light inside the waveguide. However in faster waveguides (S=2), the light is attenuated very slowly throughout the 30 μm long PhC waveguide.

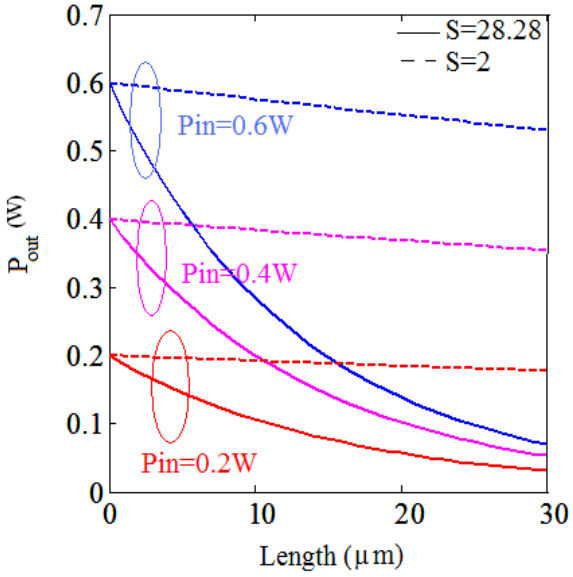

Figure 6.6. Variation of the output power along the length of the PhC waveguide, for different input power levels and for different slow down factors.

We now consider the effect of FCA and FCD, for the situation where the dimensionless parameter [Lin *et al.* (2007)], $r_a = \dfrac{S\sigma P_0 T_0 \sqrt{\pi}}{2\sqrt{2}\hbar\upsilon_o A_{eff}} >> 1$, for higher input

power levels - and N_c is not negligible. These types of effects are also observed by Monat *et al* in 2010. Equations (6.6) and (6.7) given below:

$$\frac{\partial A}{\partial z}+\frac{S\alpha}{2}A=iS^2\gamma\left|A\right|^2A-\frac{S^2\beta_{TPA}}{2A_{eff}}\left|A\right|^2A-SN_c\left(\frac{\sigma}{2}+ik_ck_0\right)A$$

$$N_c(t)=\frac{\beta_{TPA}P_{in}^2T_0}{2h\upsilon_oA_{eff}^2}\sqrt{\frac{\pi}{8}}\left(1+erf\left(\frac{\sqrt{2}t}{T_0}\right)\right)$$

are then solved using the split-step Fourier method and available values for the parameters of silicon.

Figure 6.7 shows the output spectra observed for an input spectrum centered at 1.55 μm, for different P_{in} values and values of the slow down factor S. It is observed that self phase-modulation (SPM) induced spectral broadening and splitting of short Gaussian pulses (with a characteristic pulse length of T_0 = 1 ps) occurs when they are transmitted through a PhC waveguide of length L = 30 μm. However, the free carriers produced by TPA cause a decrease in the refractive index, which further causes the generation of increased frequency components in the pulse spectrum. Hence an overall blue shift of the pulse is observed in figures 6.7(a) and at higher slow-down factor values. The figure also displays the major role played by group velocity reduction in the nonlinear interaction. It can be seen that the output pulse spectrum broadens as the input power level increases. Figure 6.7(b) is the time domain variation in the PhC waveguide. It shows that the input curve and the output curve for S=2 overlaps whereas the output curve for S=28.28 contracts w.r.t. input curve. This indicates that the temporal curve obtained at the output end depends on the slowdown factor of the waveguide. These results show that the output power and SPM are affected by the slow-down factor S - and hence by the other nonlinear parameters,

such as the TPA parameter, ζ , and the Kerr nonlinear parameter, γ - which scales with the square of the slow-down factor - and the FCA parameter, σ, and the FCD parameter, k_c - which scales directly with the slow-down factor, S.

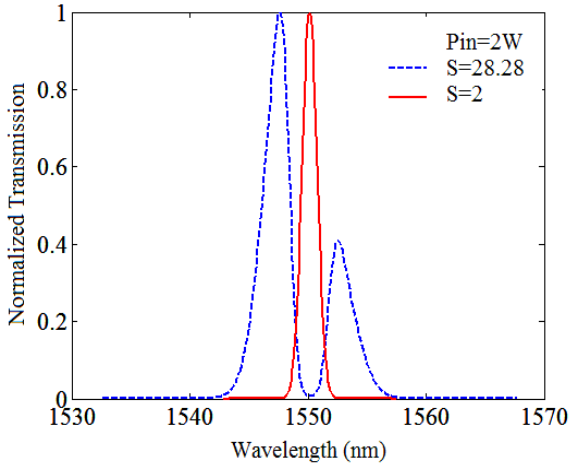

(a)

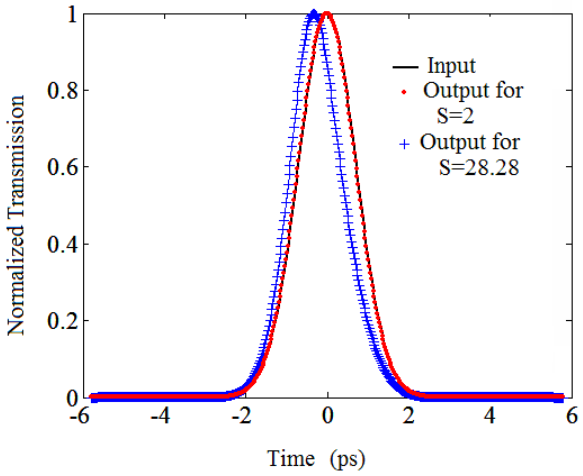

(b)

Figure 6.7 (a) SPM broadened pulse spectra at the output end of a 30μm long SOI PhC waveguide at P_{in} = 2 W for different slow-down factors S. (b) Temporal pulse shape for different slowdown factors.

The nonlinear phase shift, ϕ_{NL}, introduced into the incident wave due to these factors is shown in Figures 6.8(a) and 6.8(b). It is observed that the phase profile is symmetric for the case where only TPA is significant. However it becomes asymmetric and attains negative values when both FCA and FCD are included. The wavelength blue shift observed is due to the negative values observed in the nonlinear phase-shift. Figures 6.8(a) and 6.8(b) show that the phase-shift due to these nonlinear parameters is enhanced linearly for slower waveguides (S=28.28) in comparison with faster waveguides (S=2).

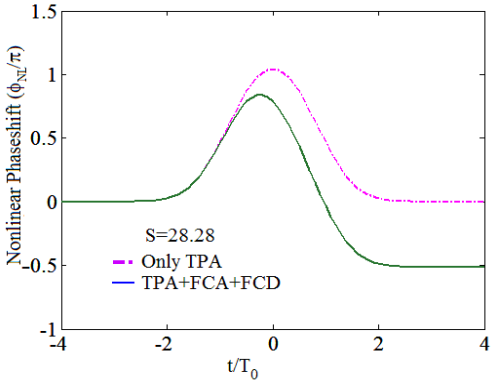

(a)

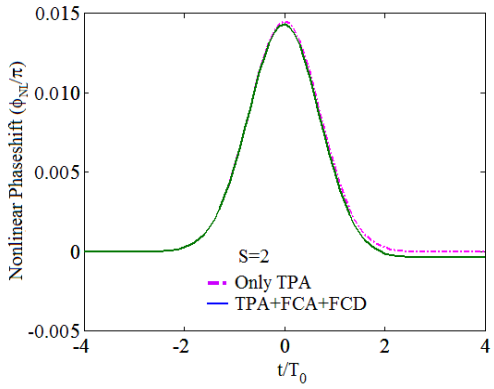

(b)

Figure 6.8. Nonlinear phase shift showing the impact of TPA, FCA and FCD for (a) *S*=28.28 and (b) *S*=2.

6.4 The Spectral Broadening Factor

We now introduce the spectral broadening factor, *f*. The spectral broadening factor for a Gaussian pulse is given by [Agrawal (2001), Lin *et al.* (2007)]:

$$f = \left(1 + \frac{4}{3\sqrt{3}}\phi_{NL}^2\right)^{1/2}$$

where $\phi_{NL}(L,0)$ is the nonlinear phase shift induced in the PhC waveguide due to the effects of TPA, FCA and FCD.

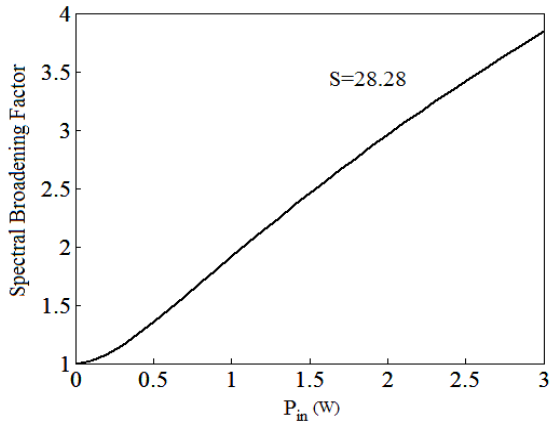

(a)

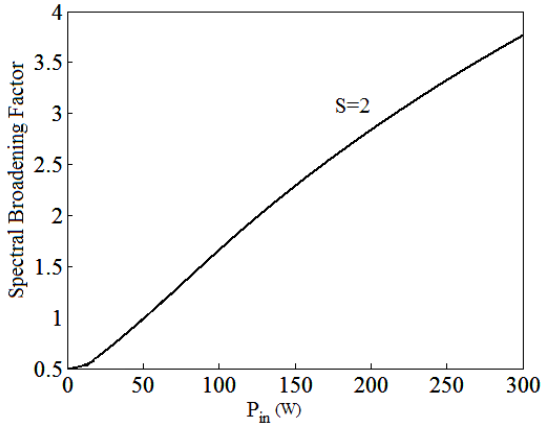

(b)

Figure 6.9. Variation of spectral broadening factor f with input power density for (a) *S* = 28.28 and (b) *S* = 2.

The results in Figures 6.9(a) and 6.9(b) show the spectral broadening as a function of the input power density level, at different slow down factor values, $S = 28.28$ and $S = 2$, respectively. For a particular slow-down factor, at high input power levels, TPA limits the maximum broadening and is responsible for the saturation behaviour. It is also demonstrated that spectral broadening is greater in slow waveguides than in fast waveguides. A much higher input power level is required to obtain the same level of spectral broadening in fast waveguides as in slow waveguides.

6.5 The Photonic Crystal Waveguide as an All-Optical Switch

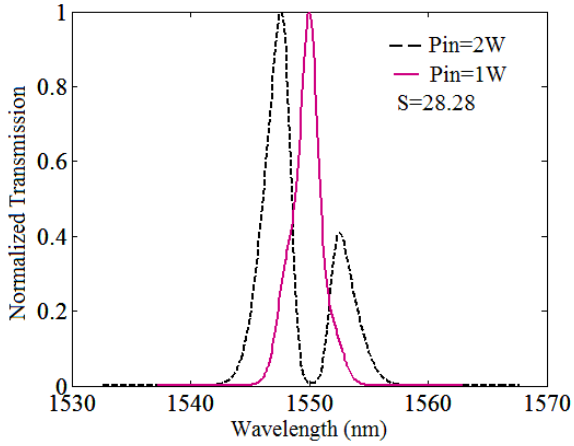

Figure 6.10. Switching in the transmission spectrum of the SOI based PhC channel waveguide at different input power levels.

The input wavelength is chosen as 1.55 μm, which lies within the photonic bandgap. Figure 6.10 shows the signal that is transmitted through the waveguide when the peak incident power level is 1 W - which corresponds to the ON state at the output. When the incident peak power level is increased to 2 W, the transmission resonance at 1.55 μm is replaced by a transmission minimum. This low level of output

signal can be considered as the OFF state. The reason for this dramatic variation in the transmission spectrum is the changes in the refractive index induced by the nonlinear optical effects that includes the Kerr effect and the free carrier dispersion (FCD) effect produced by TPA.

The Kerr effect is mainly responsible for the symmetric spectral broadening of the pulse. However FCD also contributes to the spectral broadening - and is also responsible for an additional overall blue-shift of the pulse spectrum. This blue-shift is due to the density of free carriers generated by the pulse as it propagates through the medium, which results in a decrease in the refractive index of the silicon. This decrease creates an asymmetric and positive frequency chirp across the pulse that causes the generation of a blue-shifted spectrum. A phase change of π induced in the proposed structure made from Si therefore switches the signal between its ON and OFF states at the wavelength of 1.55 μm - and hence the photonic crystal channel waveguide acts as a form of all-optical switch.

These results are consistent with those obtained experimentally by A. Baron *et al.* in GaAs PhC channel waveguides [Baron *et al.* (2009)]. However, since it is primarily the Kerr effect that is sought for the non-linear optical manipulation, TPA may be regarded as a hindrance. With the values of Kerr coefficient being n_2 equal to 1.6 x 10^{-17} m^2/W in GaAs and 0.5 x 10^{-17} m^2/W in Si, but the much larger TPA coefficient for GaAs, as compared with silicon - in the relevant wavelength range, larger values for the Kerr phase-shift are obtainable in Si than GaAs. In contrast, the larger total magnitude of the non-linearity in GaAs has been successfully exploited to modify the resonant behaviour of high Q-factor PhC micro-cavities [Combrie et al. (2008)].

6.6 The Photonic Crystal Waveguide as a Soliton Propagator

A soliton can be formed in a waveguide when the input pulse width is in the femtosecond regime, i.e. short compared with the width of the resulting soliton - and also $\beta_2 < 0$.

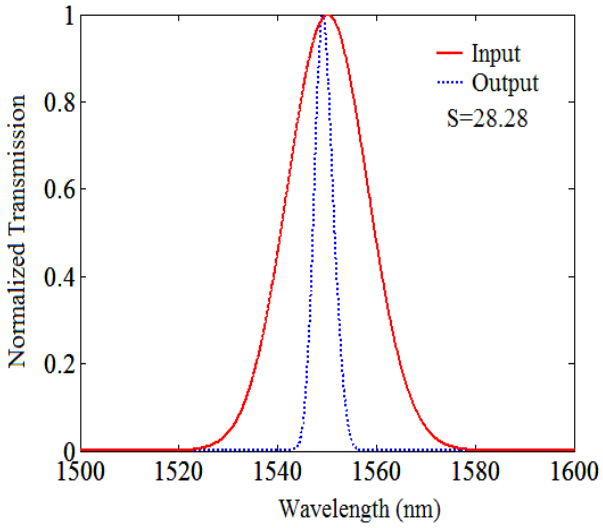

(a)

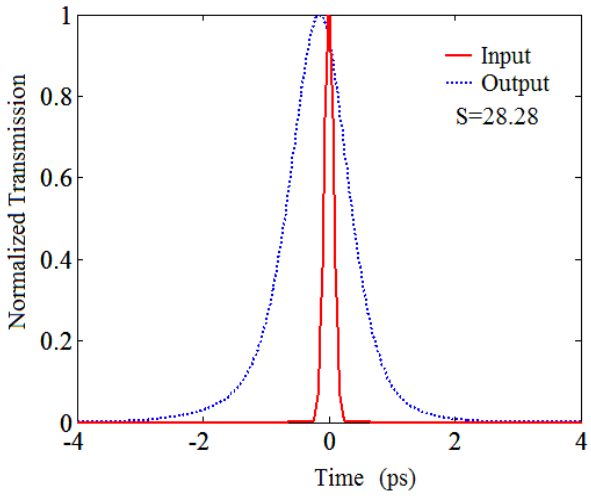

(b)

Figure 6.11. Propagation of 111 fs pulse through a SOI PhC waveguide; (a) Spectrum and (b) temporal pulse shape.

According to standard soliton propagation theory [Agrawal (2001)], a fundamental soliton can be excited if $\gamma P_0 L_D$=1. Also the time domain expansion is simultaneously accompanied by spectral narrowing. This criterion acts as a test for soliton formation in silicon photonic waveguides [Ding *et al.* (2008)]. We now consider T_0 = 0.111 ps, L_D = 1.5 μm and L_{NL} = 1.5 μm, with γ = 202 mW^{-1} and P_{in} = 4W at λ_0 = 1.55 μm.

Hence the condition for the propagation of a fundamental soliton is satisfied. Figure 6.11(a) and Figure 6.11(b) show the input and output pulse profiles and corresponding spectra. The presence of β_{TPA} and α deforms the shape of the output pulse and leads to spectral contraction and time-domain expansion of the output pulse with respect to the spectrum and length of the input pulse.

6.7 Conclusions

In this chapter, the design of an SOI-based PhC channel waveguide with elliptical holes is reported. Two neighbouring rows on either side of the channel waveguide are filled with silica rods to obtain an average group index of 99 at a wavelength of 1550 nm. Further, nonlinear modeling of the wave propagation in such a waveguide is carried out - and it is observed that, while beginning with almost the same spectral width as that of an input pulse, the pulse spectrum broadens as the input power level increases. The rate at which the spectrum broadens with power is larger for slower waveguides. A detailed study of the effect of input peak power and different slow down factors on the nonlinear effects achieved in proposed photonic crystal channel waveguide is also presented. However, it is found that the SPM-induced phase-shift decreases as the TPA coefficient increases, which in turn depends on the slow-down

factor, *S*. The impact of FCA and index changes induced by FCD on the amplitude and phase of optical pulses has also been studied in this chapter. The spectral broadening factor calculated for the waveguide shows that a higher input power level, on the order of 10^2 W, is required to obtain the same level of spectral broadening in fast waveguides as compared to the power level on the order of 1 W required in the case of slow waveguides. This type of slow light structure has considerable potential for use in photonic device applications such as optical switches - as we have already demonstrated in the present paper. If the input pulse width is in the femtosecond regime, the waveguide can generate soliton-like propagation at moderate pulse energies.

References

Agrawal, G. P., Fiber Optic Communication systems, Hoboken, NJ: Wiley-Interscience (1997).

Agrawal, G.P., Nonlinear Fiber Optics III, Academic Press, San Diego (2001).

Alagappan, G., Sun, X. W., Yu, M. B., Shum, P. and Engelsen, D. D., "Tunable dispersion properties of liquid crystal infiltrated into a two-dimensional photonic crystal", IEEE Journal of Quantum Electronics, 42, 404-407 (2006).

Almeida, V. R., Barrios, C. A., Panepucci, R. R. and Lipson, M., "All optical control of light on a silicon chip", Nature, 481, 1081-1084 (2004).

Assefa, S. and Vlasov, Y. A., "High order dispersion in photonic crystal waveguides," Optics Express, 15, 17562 (2007).

Astrov, V.N., Stevenson, R. M., Culshaw, I.S., Whittaker, D.M., Skolnick, M.S., Krauss, T.F., and De La Rue, R.M., "Heavy photon dispersions in photonic crystal waveguides", Applied Physics Letters, 77, 178-180 (2000).

Baba, T., Mori, D., Inoshita, K. and Kuroki, Y., "Light localization in line defect photonic waveguides", IEEE Journal of Quantum Electronics, 10, 484-491 (2004).

Baba, T. and Mori, D., "Slow light engineering in photonic crystals", Journal of Physics D: Applied Physics, 40, 2659-2665 (2007).

Baron, A., Ryasnyanskiy, A., Dubreuil, N., Delaye, P., Vy Tran, Q., Combrié, S., Alfredo de Rossi, Frey, R. and Roosen, G., "Light localization induced enhancement of third order nonlinearities in a GaAs photonic crystal waveguide", Optics Express, 17, 552-557 (2009).

Bayat, K., Chaudhuri, S. K., Naeini, S. S., and Baroughi, M. F., "Design and Simulation of Photonic Crystal Based Polarization Converter", IEEE Journal of Lightwave Technology, 27, 5483-5491 (2009).

Busch, K., Lolkes, S., Weherspohn, R. H. and Foll, H., "Photonic Crystals: Advances in design, fabrication and characterization", Wiley-VCH (2004).

Camargo, A., Chong, H. M. H. and De La Rue, R. M., "Four port coupled channel guide device based on2D photonic crystal structure", Photonics and Nanostructure, 2, 207-213 (2004).

Camargo, A. and De La Rue, R. M., "Photonic crystal channel guide Y-junction beam splitter based on an AlGaAs/GaAs epitaxial structure", Integrated Photonics Research, San Francisco, CA, June 30 (2004).

Campbell, M., *et.al.*, "Fabrication of photonic crystals for visible spectrum by holographic lithography", Nature, 404, 53-56 (2000).

Centeno, E., Guizal, B., and Felbacq, D., "Multiplexing and Demultiplexing with Photonic Crystals", Pure and Applied Optics, 1, 10-13 (1999).

Chandrashekhar, S., Liquid Crystals, Cambridge, U.K.: Cambridge Univ. Press, (1995).

Chen, C.C., Chien, H.D., Luan, P.G. "Photonic Crystal Beam Splitters" Applied Optics, 43, 6188-6190 (2004).

Chien, F.S.-S., Hsu, Y.J., Hsieh, W.F., and Cheng, S.-C, "Dual wavelength demultiplexing by coupling and decoupling of photonic crystal waveguides", Optics Express, 12, 1119-1125 (2004).

Chien, F. S., Cheng, S. C., Hsu, Y. J. and Hsieh, W. F., "Dual band multiplexer/ demultiplexer with photonic crystal waveguide couplers for bidirectional communications", Optics Communication, 266, 592-597 (2006).

Chung, L.W. and Lee, S. L., "Photonic crystal based dual band demultiplexers on silicon materials", Optical and Quantum Electronics, 39, 677-687 (2007).

Combrié, S., Alfredo De Rossi, S., Vy Tran, Q. and Benisty, H., "GaAs photonic crystal cavity with ultrahigh *Q*: microwatt nonlinearity at 1.55 μm", Optics Letters, 33, 1908-1910 (2008).

Cui, Y., Wu, Q., Schonbrun, E., Tinker, M., Lee, J-B. and Park, W., "Silicon based 2D slab photonic crystal TM polarizer at telecommunication wavelength", IEEE Photonics Technology Letters, 20, 641-643 (2008).

Cunpston, B. H., Ananthavel, S. P., Barlow, S., Dyer, D. L., Erheich, J. E., Erskine, L. L., Heikal, A. A., Kuebler, S. M., Lee, I. Y. S., McCord-Maughon, D., Qin, J., Rockel, H., Rumi, M., Wu, X. L., Marder, S. R. and Perry J. W., "Two photon polymerization initiators for three dimensional optical data storage and microfabrication", Nature, 398, 51-54 (1999).

Dekkiche, L. and Naoum, R., "Improved transmission for photonic crystal Y junctions", Electrical Engineering, 89, 71-77 (2006).

De La Rue, R. M., "Slower for longer", Nature Photonics, 2(12), 715-716 (2008).

Di Falco, A., L. O'Faolain and T.F. Krauss, "Dispersion control and slow light in slotted photonic crystal waveguides," Applied Physics Letters, 92, 083501 (2008).

Ding, W., Benton, C., Gorbach, A.V., Wadsworth, W.J., Knight, J.C., Skryabin, D.V., Gnan, M., Sorrel, M. and De La Rue, R.M., "Solitons and spectral

broadening in long silicon-on-insulator photonic wires", Optics Express, 16, 3310-3319 (2008).

Dowling, J. P. and Bowen, C., "Anomalous index of refraction in photonic bandgap materials", Journal of Modern Optics, 44, 345-351 (1994).

Ebnali-Heidari, M., Grillet, C., Monat, C., and Eggleton, B. J.,"Dispersion engineering of slow light photonic crystal waveguides using microfluidic infiltration", Optics Express, 17, 1628-1635 (2009).

Fan, S., Villeneuve, P. R. and Joannopolous, J. D., "Theoretical analysis of channel drop tunnelling processes", Physical Review B, 59, 15882-15892 (1999).

Frandsen, L. H., Lavrinenko, A. V., Fage-Pedersen, J. and Borel, P.I., "Photonic crystal waveguides with semi-slow light and tailored dispersion properties", Optics Express, 14, 9444-9450 (2006).

Fyberdyne Labs: http://www.fyberdyne.com/products/pdf/avdmintro.PDF, cited 11 September 2007 (2007).

Gerace, D. and Andreani, L. C., "Light-matter interaction in photonic crystal slabs," Physics Status Solid B, 244, 3528–3539 (2007).

Gersen, H., Karle, T. J., Engelen, R. J. P., Bogaert, W., Korterik, J. P., Van Hulst, N. F., Krauss, T. F. and Kuipers, L., "Real space observation of ultra slow light in photonic crystal waveguides", Physical Review Letters, 94, 073903 (2005).

Guryev, I. V. and Sukhoivanov, I. A., "Plane Wave Expansion Method with Considered Material Dispersion", CADSM'2007, February 20-24, 2007, Polyana, UKRAINE (2007).

Hamachi, Y., Kubo, S. and Baba, T., "Slow light with low dispersion and nonlinear enhancement in a lattice shifted photonic crystal waveguide", Optics Letters, 34, 1072-1074 (2009).

Handbook of Optics, vol. 2, 2nd edition, McGraw-Hill, 1994

Huang, W., Zhang, Y. and Li, B., "Ultracompact wavelength and polarization beam splitters in periodic dielectric waveguides", Optics Express, 16, 1600-1609 (2008).

Hugonin, J. P., Lalanne, P., White, T. P. and Krauss, T. F., "Coupling into slow-mode photonic crystal waveguides", Optics Letters, 32, 2638-2640 (2007).

Inoue, K., Oda, H., Ikeda, N. and Asakawa, K., "Enhanced third order nonlinear effects in slow light photonic crystal slab waveguides of line defect", Optics Express, 17, 7206-7216 (2009).

Jacobsen, R. S., Andersen, K., Borel, P. I., Pedersen, J. F., Hansen, O., Kristensen, M., Lavrinenko, A., Moulin, G., Ou, H., Peucheret, C., Zsigri, B. and Bjarklev, A., "Strained silicon as a new electro-optic material," Nature 441, 199-202 (2006).

Joannopolous, J. D., Meade, R. D. and Winn, J. N., "Photonic Crystals: Molding the flow of light", Princeton University Press, Princeton, NJ (1995).

John, S., "Strong localization of photon in certain disorder dielectric superlattices", Physical Review Letters, 58, 2486-2489 (1987).

Johnson, S. G., Fan, S., Villeneuve, P. R., Joannopolous, J. D. and Kolodziejski, L. A. "Guided modes in photonic crystal slabs", Physical Review B, 60, 5751-5758 (1999).

Johnson, S. G. and Joannopoulous, J. D., "Block iterative frequency domain methods for Maxwell's equations in plane wave basis", Optics Express, 8, 173-190 (2001a).

Johnson, S. G. and Joannopoulos, J. D., "Photonic crystals: The road from theory to practice", Kluwer Academic Publishers (2001b).

Kao, C. L. and Yu, C. P. "Band Structure Analysis of Liquid-crystal Photonic Crystal Fibers" Progress In Electromagnetics Research Symposium, Beijing, China, March 23-27, (2009).

Kawai, N., Inoue, K., Carlsson, N., Ikeda, N., Sugimoto, Y., Asakawa, K. and Takemori, T., "Confined Band Gap in an Air-Bridge Type of Two-Dimensional AlGaAs Photonic Crystal", Physical Review Letters, 86, 2289-2292 (2001).

Kawakami, M., "Photonic crystals for the visible range fabricated by autocloning technique and their applications", Optical and Quantum Electronics, 34, 63-70 (2002).

Khayam, O. and Benisty, H., "General recipe for flat bands in photonic crystal waveguides", Optics Express, 17, 14634-48 (2009).

Koerkamp, K. J. K., Enoch, S., Segerink, F. B., Van Hulst, N. F. and Kuipers, L., "Strong influence of hole shape on extraordinary transmission through Periodic arrays of sub-wavelength holes", Physical Review Letters., 92, 183901 (2004).

Kosaka, H., Kawashima, Tomita, A., Notomi, M., Tamamura, T., Sato, T., and Kawakami, S., „superprism phenomenon in photonic crystals", Physical Review B, 58, R10096 (1998).

Kosmidou, E. P., Kriezis, E. E., Tsiboukis, T. D., "Analysis of tunable photonic crystal devices comprising liquid crystal materials as defects", IEEE Journal of Quantum Electronics, 41, 657-665 (2005).

Kuramochi, E., Notomi, M., Hughes, S., Shinya, A., Watanabe, T. and Ramunno, L., "Disorder-induced scattering loss of line-defect waveguides in photonic crystal slabs," Physical Review B, 72, 161318 (2005).

Krauss, T. F., "Slow light in photonic crystal waveguides," Journal of Physics D: Applied Physics, 40, 2666-2670 (2007).

Krauss, T. F., "Why do we need slow light?," Nature Photonics, 2, 448-450 (2008).

Kriezis, E. E. and Elston, S. J., "Light wave propagation in liquid crystal displays by the 2-D finite difference time domain method", Optics Communication, 177, 69-77 (2000).

Leonard, S. W., Mondia, J. P., Van Driel, H. M., Toader, O., John, S., Busch, K., Birner, A., Go¨sele, U. and Lehmann, V., "Tunable two dimensional photonic crystals using liquid crystal infiltration", Physics Review B, 61, R2389 (2000).

Li, J., "Terahertz modulator using photonic crystals", Optics Communication, 269, 98-101 (2007).

Li, J., White, T. P., O'Faolain, L., Gomez-Iglesias, A. and Krauss, T. F., "Systematic design of flat band slow light in photonic crystal waveguides", Optics Express, 16, 6227-6232 (2008).

Lin, Q., Painter, O.J., and Agrawal, G.P., "Nonlinear optical phenomena in siliconwaveguides: Modeling and applications", Optics Express, 15, 16604-16644 (2007).

Luo, C., Johnson, S. G., Joannopoulos and Pendry, J. D., "All angle negative refraction without negative effective index", Physical Review B, 65, 201104 (2002).

Ma, J. and Jiang, C., "Demonstration of ultra slow modes in asymmetric line defect photonic crystal waveguides", IEEE Photonics Technology Letters, 20, 1237-1239 (2008a).

Ma, J. and Jiang, C., "Flat band slow light in asymmetric line defect photonic crystal waveguide featuring low group velocity and dispersion", IEEE Journal of Quantum Electronics, 44, 763-769 (2008b).

Martijn de Sterke, C., Walker, J., Dossou, K. B., and Botten, L. C., "Efficient slow light coupling into photonic crystals", Optics Express, 15, 10984-10990 (2007).

Meier, M., Mekis, A., Dobabalapur, A., Timko, A., Slusher, R. E., Joannopolos, J. D. and Nalamasu, O., "Laser action from two dimensional distributed feedback in photonic crystals", Applied Physics Letters, 74, 7-9 (1999).

Mekis, A., Chen, J. C., Kurland, I., Fan, S., Villeneuve, P. R. and J. D. Joannopolous, "High transmission through sharp bends in photonic crystal waveguides", Physical Review Letters, 77, 3787-3790 (1996).

Monat, C., Lorcoran, B., Heidari, M. E., Grillet, C., Eggleton, B.J., White, T.P., O'Faolain, L. and Krauss. T.F., "Slow light enhancement of nonlinear effects in silicon engineered photonic crystal waveguides", Optics Express, 17, 2944-2953 (2009).

Monat,C., Corcoran, B., Pudo, D., Ebnali-Heidari, M., Grillet, C., Pelusi, M.D., Moss, D. J., Eggleton, B. J., White, T. P., O'Faolain, L. and Krauss, T. F., "Slow Light Enhanced Nonlinear Optics in Silicon Photonic Crystal Waveguides", IEEE Journal of Selected Topics in Quantum Electronics, 16, 344-357 (2010).

Mori, D. and Baba, T. "Dispersion controlled optical group delay device by chirped photonic crystal waveguides," Applied Physics Letters, 85, 1101-1103 (2004).

Mori, D. and Baba, T., "Wideband and low dispersion slow light by chirped photonic crystal coupled waveguide," Opt. Express 13, 9398-9408 (2005).

Nagpal Y. and Sinha, R.K., "Modeling of photonic bandgap directional couplers", Microwave and Optical Technology Letters, 43, 47-50 (2004).

Nicolae, X. C., Panoiu, C., Hsieh, I., Dadap, J. I. and Osgood, R. M., "Third order dispersion and ultrafast pulse propagation in silicon wire waveguides", IEEE Photonics Technology Letters, 18, 2617-2619 (2006).

Notomi, M., Shinya, A., Yamda, K., Takahashi, J., Takahashi, C. and Yokohama, I., "Single mode transmission within photonic bandgap of width varied single line defect photonic crystal waveguides on SOI substrates", Electronic Letters, 37, 293-295 (2001).

Notomi, M., Yamada, K., Shinya, A., Takahashi, J., Takahashi, C. and Yokohama, I., "Extremely large group velocity dispersion of line-defect waveguides in photonic crystal slabs," Physical Review Letters, 87, 253902 (2001b).

Notomi, M., Shinya, A., Yamda, K., Takahashi, J., Takahashi, C. and Yokohama, I., "Structural tuning of guiding modes of line defect waveguides of silicon-on-insulator photonic crystal slabs", IEEE Journal of Quantum Electronics, 38, (2002).

Oda, H., Inoue, K., Tanaka, Y., Ikeda, N., Sugimoto, Y., Ishikawa, H. and Asakawa, K., "Self phase modulation in photonic crystal slab line defect waveguides", Applied Physics Letters., 90, 231102 (2007).

Oda, H., Inoue, K., Yamanaka, A., Ikeda, N., Sugimoto, Y. and Asakawa, K., "Light amplification by stimulated Raman scattering in AlGaAs based photonic crystal line defect waveguides, Applied Physics Letters., 93, 051114 (2008).

Ozaki,N., Kitagawa, Y., Takata, Y., Ikeda, N., Watanabe, Y., Mizutani, A., Sugimoto, Y. and Asakawa, K., "High transmission recovery of slow light in a photonic crystal waveguide using a hetero group velocity waveguide", Optics Express, 15, 13, 7974-7983 (2007).

Park, S. H. and Xia, Y., "Self assembly of mesoscale particles over large areas and its application in fabricating tunable optical filters", Langmuir, 15, 266-273 (1999).

Petrov, A. and Eich, M., "Zero dispersion at small group velocities in photonic crystal waveguides," Applied Physics Letters, 85, 4866-4868 (2004).

Petrov, A., Krause, M. and Eich, M., "Backscattering and disorder limits in slow light photonic crystal waveguides", Optics Express, 17, 10, 8676-8684 (2009).

Plihal, M. and Maradudin, A. A., "Photonic band structures of two dimensional systems- The Triangular lattice," Physics Review B, 44, 1865-8571 (1991).

Pottier, P., Gnan, M. and De La Rue, R. M., "Efficient coupling into slow-light photonic crystal channel guides using photonic crystal tapers", Optics Express, 15, 6569-6576 (2007).

Povinelli, M. L., Johnson, S. G. and Joannopoulous, J. D., "Slow light, band edge waveguides for tunable time delays," Optics Express 13, 7145-7159 (2005).

Qiu, M. and He, S., "A non-orthogonal finite difference time domain method for computing the band structure of a two dimensional photonic crystal with dielectric and metallic inclusions", Journal of Applied Physics, 87, 8268-8275 (2000).

Qiu, M., "Bandgap effects in asymmetric photonic crystal slabs", Physical Review B, 66, 033103 (2002).

Quan, Y. J., Han, P. D., Ran, Q. J., Zeng, F. P., Gaoand, L. P. and Zhao, C. H., "A photonic wire based directional coupler based on SOI", Optics Communication, 281, 3105-3110 (2008).

Rajput, M. and Sinha, R. K., "All Angle Negative Refraction for visible light from left handed Metallo-Dielectric Photonic Crystal: Theoretical and Numerical demonstration with nano-Photonic Device Applications", 98, 99-106 (2010).

Rawal, S. and Sinha, R. K., "Design, Analysis and Optimization of Silicon-on-Insulator Photonic Crystal Dual Band Wavelength Demultiplexer", Optics Communication, 282, 3889-3894 (2009a).

Rawal, S., Sinha, R. K. and De La Rue, R. M., "Slow Light Miniature Devices with Ultra-Flattened Dispersion in Silicon-on-Insulator Photonic Crystal" , Optics Express, 17, 13315-13325 (2009b).

Rawal, S., Sinha, R. K. and De La Rue, R. M., "Slow light propagation in liquid crystal infiltrated silicon-on-insulator photonic crystal channel waveguides", IEEE Journal of Lightwave Technology, 28, 2560-2571 (2010)

Rukhlenko, I.D., Premaratne, M., Dissanayake, C. and Agrawal, G. P., "Nonlinear Pulse Evolution in Silicon Waveguides: An Approximate Analytic Approach" IEEE Journal of Lightwave Technology, 27, 3241-3248 (2009).

Sakoda, K., "Optical properties of photonic crystals", Springer Series, New York (2001).

Sa¨yna¨tjoki, A., Vynck, K., Mulot, M., Cassagne, D., Ahopelto, J. and Lipsanen, H., "Efficient light coupling into a photonic crystal waveguide with flatband slow mode", Phot.onics and Nanostructures, 6, 1127-133 (2008).

Schonbrun, E., Wu, Q., Park, W., Yamashita, T. and Summers, C. J., "Polarization beam splitter based on photonic crystal heterostructure", Optics Letters, 31, 3104-3106 (2006).

Settle, M. D., Salib, M., Michaeli, A and Krauss, T. F., "Low loss silicon-on-insulator photonic crystal waveguides made by 193nm optical lithography", Optics Express, 14, 2440-2445 (2006).

Settle, M. D., Engelen, R. J. P., Salib, M., Michaeli, A., Kuipers, L. and Krauss, T. F., "Flatband slow light in photonic crystals featuring spatial pulse compression and terahertz bandwidth," Optics Express, 15, 219 (2007).

Shinya, A., Notomi, M., Yokohama, I., Takashashi, C. and Takahashi, J., "Two dimensional silicon photonic crystals on oxide using SOI substrates", Optical and Quantum Electronics, 34, 113-121 (2002).

Sinha, R. K., Kalra, Y., Design of optical waveguide polarizer using photonic bandgap", Optics Express, 14, 10790-10794 (2006).

Sinha, R. K., and Rawal, S., "Modeling and design of 2D photonic crystal based Y type dual band wavelength demultiplexer", Optical and Quantum Electronics, 40, 603-613 (2008).

Smith, C. L. C., Bog, U., Tomljenovic-Hanic, S., Lee, M. W., Wu, D. K. C., O'Faolain, L., Monat, C., Grillet, C., Krauss, T. F., Karnutsch, C., McPhedran, R. C. and Eggleton, B. J., "Reconfigurable microfluidic photonic crystal slab cavities", Optics Express, 16, 15887-15897 (2008).

Soljacic, M., Johnson, S. G., Fan, S., Baneseu, M. I., Ippen, E. and Joannopoulos, J. D., "Photonic crystal slow light enhancement of nonlinear phase sensitivity", Journal of Optical Society of America B, 19, 2052-2059 (2002).

Soljacic, M. and Joannopoulos, J. D., "Enhancement of nonlinear effects using photonic crystals", Nature Material, 3, 211-219 (2004).

Subramania, G. and Lin, S. Y., "Fabrication of three dimensional photonic crystal with alignment based on electron beam lithography", Applied Physics Letters, 85, 5037-5039 (2004).

Suknoivanov, I.A., Guryev, I. V., Shulika, O. V., Kublyk, A. V., Mashoshina, O. V., Alvardo-Mendez, E. and Andrado-Lucio, J. A., "Design of photonic crystal demultiplexers for ultra short optical pulses using gap map analysis", Journal of Optoelectronics and Advanced Mathematics, 8, 1626-1630 (2006).

Taflove, "Advances in computational electrodynamics-The finite difference time domain method", Artech House (1998).

Takeda, H. and Yoshino, K., "Tunable photonic band schemes of opals and inverse opals infiltrated with liquid crystals", Journal of Applied Physics, 92, (2002).

Tanaka, Y., Asano, T., Hatsuta, R. and Noda, S., "Analysis of a line defect waveguide on a silicon-on-insulator two dimensional photonic crystal slab", IEEE J. Lightwave Technology, 22, 2787-2792 (2004).

Tanaka, Y., Sugimoto, Y., Ikeda, N., Nakamura, H., Watanabe, Y., Asakawa, K., and Inoue, K., "Guided modes of a width reduced photonic crystal slab line defect waveguide with asymmetric cladding", IEEE Journal of Lightwave Technology, 23, 2749-2755 (2005).

Tekeste, M.Y., Yarrison-Rice, J.M. "High efficiency photonic crystal based wavelength demultiplexer", Optics Express, 14, 7931-7942 (2006).

Tsang, H., Tsang, H.K., Wong, C.S., Liang, T.K., Day, I.E., Roberts, S.W., Harpin, A., Drake, J. and Asghari, M., "Optical dispersion, two photon absorption and self

phase modulation in silicon waveguides at 1.5 μm wavelength", Applied Physics Letters, 80, 416 (2002).

Tucker, R. S., Ku, P. C. and Chang-Hasnain, C. J., "Slow light optical buffers: Capabilities and fundamental limitations," Journal of Lightwave Technology, 23, 4046-4066 (2005).

Vlasov, Y. A., Bo, X. Z., Sturm, J. C. and Norris, D. J., "On chip material assembly of silicon photonic bandgap crystals", Nature, 414, 289-293 (2001).

Vlasov, Y. A., O'Boyle, M., Hamann, H. F. and McNab, S. J., "Active control of slow light on a chip with photonic crystal waveguides", Optics Express, 11, 2927-2939 (2003).

Valsov, Y., McNab, S., "Losses in single mode silicon-on-insulator strip waveguides and bends", Optics Express, 12, 1622-1631 (2004).

Velha, P., Hugonin, J. P. and Lalanne, P., "Compact and efficient injection of light into band-edge slow-modes", Optics Express, 15, 6102-6112 (2007).

Wang, F., Ma, J. and Jiang, C., "Dispersionless slow wave in Novel 2-D photonic crystal line defect waveguides," IEEE Journal of Lightwave Technology, 26, 1381-1386 (2008).

Wang, W.K., Wang, S.J., Chen, C.C., Wu, Y.H., Huang, F.H., Chan, Y.J., "1.3/1.55 μm optical directional coupler by photonic crystal with a defect shifting design", Proceedings of IEEE Conference on Nanotechnology, Nagoya, Japan, July (2005).

Yablonovitch, E., "Inhibited spontaneous emission in solid state physics and electronics", Physical Review Letters, 58, 2059-2062 (1987).

Yanik, M. F. and Fan, S., "Stop Light on a Chip", Physical Review Letters, 92, 083901 (2004).

Yeh, P. and Yariv, A., “Bragg refelction waveguides”, Optics Communication, 19, 427-430 (1976).

Yin, L. and Agrawal, G.P., “Impact of two photon absorption on self phase modulation in silicon waveguides”, Optics Letters., 32, 2031-2033 (2007).

Zabelin, V., Dunbar, L.A., Thomas, N.Le, Houdre, R., “Self-collimating photonic crystal polarization beam splitter”, Optics Letters, 32, 530-532 (2007).

Zhang, X., Tian, H. and Ji, Y. “Group index and dispersion properties of photonic crystal waveguides with circular and square air holes”, Optics Communication, 283, 1768-1772 (2010).

Photonic Crystal Waveguides and Devices

A thesis submitted to
Faculty of Technology, University of Delhi
for the award of the degree of

DOCTOR OF PHILOSOPHY
in
APPLIED PHYSICS

by

Swati Rawal

Under the supervision of

Dr. R. K. SINHA
Professor and Head, Department of Applied Physics
Delhi College of Engineering
Faculty of Technology
University of Delhi
Delhi-110 042, India

Photonic Crystal Waveguides and Devices

Synopsis

Photonics involve the research and application of light to perform tasks that could previously be carried out only by electronics. This includes transmission, manipulation and storage of data using photons. Devices based on photonic crystals benefit from the high speed of optical signals which provide larger bandwidth and reduced cross talks between the channels and open the way to faster signal processing. These new types of structures (photonic crystals) are able to control electromagnetic waves in three dimensions since they can give rise to a photon bandgap analogous to forbidden electron energy bandgap in semiconductors. The existence of unique and interesting properties such as photonic bandgap (PBG) i.e. in the range of frequencies at which optical propagation is completely prohibited in any direction, as well as the existence of defect modes that may appear within the photonic bandgaps when a defect is introduced into an otherwise perfect photonic crystal, has resulted in the fast growth of photonic technology. It gives rise to realization of a new generation of photonic components with application in optical communication, optical signal processing and optical sensing and has led to the design and development of efficient optoelectronic devices and systems. The controlled propagation of light in PhC waveguides has led to a variety of novel optical phenomenon including slow light generation and enhancement of nonlinear effects because of this slow light generation in photonic crystals.

Slow light refers to reduction of the group velocity of light - and is a promising technology for future all-optical communication networks. It can be used for the enhancement of light-matter interaction and for the miniaturization of optoelectronic integrated circuits. Photonic crystal (PhC) line-defect waveguides that are created within the photonic band gap (PBG) are extensively used for achieving slow light in the flat band regions of guided modes supported by these waveguides. Therefore they have strong application possibilities in optical buffers and other optical storage devices.

Recently, nonlinear effects such as the Raman Effect, soliton propagation, two photon absorption (TPA), etc. have been observed by different authors. Self phase modulation (SPM), which leads to chirping and spectral broadening of ultra short pulses, has also been reported earlier. However TPA limits the extent of SPM through nonlinear absorption. TPA typically involves transitions from the ground state of a system to a higher state by absorption of two photons from an incident radiation field having identical or, more generally, two different frequencies. TPA further creates free carriers that lead to additional losses through free carrier absorption (FCA) and refractive index changes through free carrier dispersion (FCD). Thus TPA, FCA, FCD and SPM are important effects that influence the behavior of short laser pulses in silicon waveguides. However soliton dynamics will dominate the propagation of femtosecond pulses in PhC waveguides when group velocity dispersion (GVD) is strongly anomalous because of large waveguide dispersion. The spatial compression experienced by light when it enters from fast light to slow light waveguide and the more time it spends in the waveguide is because of the slow group velocity, leads to the increase in light matter interaction and

enhancement of nonlinear effects. Slow light PhC waveguides may thus cause the reduction in input power and physical length of the waveguide needed to see same linear and nonlinear effects in fast light regime.

The main focus of this thesis is the design and characterization of devices based on photonic crystal line defect waveguides. These devices include dual band wavelength de-multiplexers, optical buffers and delay lines, soliton propagator, optical switches and logic gates. The research work carried out in the thesis also demonstrates the generation of slow light in elliptical and rectangular hole photonic crystal waveguides and the extension of their tunability, by filling its segments with certain types of liquid crystal (LC) materials. The impact of slow light on the third order nonlinearities have also been investigated in such photonic crystal channel waveguides. This chapter, i.e. Chapter 1, defines the introduction and outline of the proposed thesis.

In Chapter 2, photonic bandgap (PBG) induced wave guiding application of photonic crystals is exploited to design 2D dual band wavelength demultiplexer (DBWD) for separating two telecommunication wavelengths, 1.31 μm and 1.55 μm. Two designs that use silicon rods in air and embedded air holes in silicon material are realized for this purpose. 2D plane wave expansion (PWE) method and 2D finite difference time domain (FDTD) methods are used to design and analyze the DBWD in Y type photonic crystal structures.

In Chapter 3, a highly efficient 3D photonic crystal DBWD using Silicon-on-Insulator (SOI) substrates is proposed for de-multiplexing the two optical communication wavelengths, 1.31 μm and 1.55 μm. De-multiplexing of the two wavelength channels is

obtained by modifying the propagation properties of guided modes, in two arms of Y-type photonic crystal structure. Propagation characteristics of proposed DBWD are analyzed utilizing 3D FDTD method. Enhancement in spectral response is further obtained by optimizing the Y junction of de-multiplexer giving rise to high transmission and extinction ratio for the wavelengths, 1.31 μm and 1.55 μm. Hence it validates the efficiency of proposed optimized DBWD design for separating two optical communication wavelengths, 1.31 μm & 1.55 μm. Tolerance analyses was also performed to check the effect of variation of air hole radius, etch depth and refractive index on the transmission characteristics of the proposed design of SOI based photonic crystal DBWD.

In Chapter 4, a silicon-on-insulator photonic crystal waveguide with hexagonal arrangement of elliptical air holes is reported for slow light propagation with group velocity in the range, 0.0028c to 0.044c and ultra-flattened group velocity dispersion (GVD). The proposed structure is also investigated for its application as an optical buffer with a large value of normalized delay bandwidth product (DBP), equal to 0.778. Furthermore it has been shown that the proposed structure can also be used for time or wavelength-division demultiplexing to separate the two telecom wavelengths, 1.31 μm and 1.55 μm, on a useful time-scale and with minimal distortion.

In Chapter 5, an SOI-based liquid-crystal (LC)-infiltrated photonic-crystal channel waveguide having rectangular air holes in a Silicon core is proposed - that has an average group index of 43 over a bandwidth of 1.02 THz, with vanishing group velocity dispersion, as well as reduced higher-order dispersion. The possible propagation losses

due to coupling inefficiency are also investigated for the proposed structure. It is found that high transmission is obtained for a broad bandwidth from the output of the heterogeneous waveguide finally designed, which consists of an LC-infiltrated PhC slow waveguide surrounded by fast PhC regions on either side. The LC-infiltrated W0.7 PhC waveguide that has been designed for slow light propagation should be highly tolerant to fabrication errors - and has enhanced sensitivity in comparison with conventional PhC waveguides.

In Chapter 6, the effect of slow light on two photon absorption (TPA), free carrier absorption (FCA) and self phase-modulation (SPM) processes in silicon-on-insulator (SOI) photonic crystal (PhC) channel waveguides has been reported. It is found that, in the slow light regime, these nonlinear effects are enhanced, but that the enhancement produced depends on the input peak power level. The increase in the induced phase shift produced by lower group velocities can be used to decrease the size and power requirements needed to operate devices such as optical switches, logic gates and wavelength translators. Simulations also indicate the possibility of soliton-like propagation of 111 fs pulses at 1.55 μm inside such a photonic crystal waveguide.

Finally, the conclusions from the proposed thesis are presented with discussion about the avenues of further research. The future scope of the thesis include the design and development of devices based on slow light in 3D photonic crystals as well as the impact of the enhanced nonlinear effects on different processes such as soliton formation and Raman effect.

List of Publications

A. Papers in International Journals

1. **Swati Rawal**, Ravindra K. Sinha and Richard M. De La Rue, "Slow Light Propagation in Liquid-Crystal Infiltrated Silicon-on-Insulator Photonic Crystal Channel Waveguides" *IEEE/OSA Journal of Lightwave Technology*, **28,** 2560-2571 (2010).
2. **Swati Rawal**, Ravindra K. Sinha and Richard M. De La Rue, "Slow Light Miniature Devices with Ultra-Flattened Dispersion in Silicon-on-Insulator Photonic Crystal", *Optics Express*, **17**, 13315-13325 (2009).
3. **Swati Rawal** and R. K. Sinha, "Design, Analysis and Optimization of Silicon-on-Insulator Photonic Crystal Dual Band Wavelength Demultiplexer", *Optics Communication*, **282**, 3889-3894, Oct 2009.
4. R. K. Sinha and **Swati Rawal**, "Modeling and design of 2D photonic crystal based Y type dual band wavelength demultiplexer," *Optical and Quantum Electronics*, **40**, 603-613 (2008).
5. **Swati Rawal** and R. K. Sinha, "Low-loss slow light transmission in photonic crystal waveguides comprising of liquid crystal infiltration", *Journal of Electronic Science and Technology (JEST)*, **8**, 2010.
6. **Swati Rawal**, R. K. Sinha and Richard M. De La Rue, "Slow light enhanced third order non-linearities with device application in silicon-on-insulator photonic crystal channel waveguides" Submitted.

B. Book Chapter

7.R. K. Sinha and **Swati Rawal**, "Slow Light in photonic crystal waveguides: Theory and Application" Accepted for publication in a book entitled "Photonic Crystals" by *NOVA Publications, USA*.

C. Papers in International Conferences

8.**Swati Rawal**, R. K. Sinha and Richard M. De La Rue, "Impact of slow light on nonlinear phase sensitivity in SOI photonic crystals" Accepted for presentation in Photonics 2010 to be held in IIT Guwahati in December 2010.

9.**Swati Rawal**, R. K. Sinha and Richard M. De La Rue, "Effect of Slow Light on Self Phase Modulation in Photonic Crystal Channel Waveguides", Proceedings of PECS – IX, held from 26-28th September 2010 at Spain.

10. **Swati Rawal** and R. K. Sinha, "Impact of slow light on nonlinear effects in silicon-on-insulator photonic crystal waveguide with device application", Accepted for presentation in Frontiers in Optics 2010 to be held from 24th to 28th October 2010 at Rochester, NY, USA.

11. **Swati Rawal** and R. K. Sinha, "Low velocity propagation in liquid in-filled photonic crystal waveguides", Published in SPIE Proceedings of Optics and Photonics 2010, held from 1st to 5th August 2010 at San Diego, CA,USA.

12. **Swati Rawal** and R. K. Sinha, "High delay bandwidth product and low dispersion slow light in silicon-on-insulator based photonic crystal waveguides", Proceedings of the *SPIE*, Optics + Photonics 2009, 7420, 742014-742014-5 (2009).

13. **Swati Rawal** and R. K. Sinha, "Dual-band wavelength demultiplexer consisting of SOI based photonic crystals: design and analysis," Proceedings of the *SPIE*, 7056, 70560T-70560T-6 (2008).
14. **Swati Rawal** and R. K. Sinha, "Liquid Crystal Tuning of Slow light Propagation in Photonic Crystal Waveguides", IEEE Xplore Digital library, pp- 580-582, ELECTRO-2009.
15. **Swati Rawal** and R. K. Sinha, "Slow light Propagation in Photonic Crystal Waveguides due to Liquid Crystal infiltration: Design and Applications" Proceedings of 12th International Symposium on Microwave and Optical Technology-2009, December 16-19, 2009, Delhi, India
16. **Swati Rawal** and R. K. Sinha, "Liquid Crystal Assisted slow light propagation in Photonic Crystal and Device Application" Proceedings of OSA Frontiers in Optics 2009, October 11-15th, 2009, San Jose, California, USA
17. **Swati Rawal**, R. K. Sinha and Richard M. De La Rue, "Slow Light Devices in Silicon-on-Insulator Photonic Crystal" Proceedings of ICOP 2009-International Conference on Optics and Photonics held at Chandigarh, India from 30th Oct.-1st Nov., 2009.
18. **Swati Rawal** and R. K. Sinha, "Modeling and design of silicon-on-insulator based 1.31/1.55μm photonic crystal de-multiplexer," PHOTONICS-2008: International Conference on Fiber Optics and Photonics, December 13-17, 2008 (Paper No. PM-34).

List of Publications

A. Papers in International Journals

1. **Swati Rawal**, Ravindra K. Sinha and Richard M. De La Rue, "Slow Light Propagation in Liquid-Crystal Infiltrated Silicon-on-Insulator Photonic Crystal Channel Waveguides" *IEEE/OSA Journal of Lightwave Technology*, **28,** 2560-2571 (2010).
2. **Swati Rawal**, Ravindra K. Sinha and Richard M. De La Rue, "Slow Light Miniature Devices with Ultra-Flattened Dispersion in Silicon-on-Insulator Photonic Crystal", *Optics Express*, **17**, 13315-13325 (2009).
3. **Swati Rawal** and R. K. Sinha, "Design, Analysis and Optimization of Silicon-on-Insulator Photonic Crystal Dual Band Wavelength Demultiplexer", *Optics Communication*, **282**, 3889-3894, Oct 2009.
4. R. K. Sinha and **Swati Rawal**, "Modeling and design of 2D photonic crystal based Y type dual band wavelength demultiplexer," *Optical and Quantum Electronics*, **40**, 603-613 (2008).
5. **Swati Rawal** and R. K. Sinha, "Low-loss slow light transmission in photonic crystal waveguides comprising of liquid crystal infiltration", *Journal of Electronic Science and Technology (JEST)*, **8**, 2010.
6. **Swati Rawal**, R. K. Sinha and Richard M. De La Rue, "Slow light enhanced third order non-linearities with device application in silicon-on-insulator photonic crystal channel waveguides" Submitted.

B. Book Chapter

7.R. K. Sinha and **Swati Rawal**, "Slow Light in photonic crystal waveguides: Theory and Application" Accepted for publication in a book entitled "Photonic Crystals" by *NOVA Publications, USA*.

C. Papers in International Conferences

8.**Swati Rawal**, R. K. Sinha and Richard M. De La Rue, "Impact of slow light on nonlinear phase sensitivity in SOI photonic crystals" Accepted for presentation in Photonics 2010 to be held in IIT Guwahati in December 2010.

9.**Swati Rawal**, R. K. Sinha and Richard M. De La Rue, "Effect of Slow Light on Self Phase Modulation in Photonic Crystal Channel Waveguides", Proceedings of PECS – IX, held from 26-28th September 2010 at Spain.

10. **Swati Rawal** and R. K. Sinha, "Impact of slow light on nonlinear effects in silicon-on-insulator photonic crystal waveguide with device application", Accepted for presentation in Frontiers in Optics 2010 to be held from 24th to 28th October 2010 at Rochester, NY, USA.

11. **Swati Rawal** and R. K. Sinha, "Low velocity propagation in liquid in-filled photonic crystal waveguides", Published in SPIE Proceedings of Optics and Photonics 2010, held from 1st to 5th August 2010 at San Diego, CA,USA.

12. **Swati Rawal** and R. K. Sinha, "High delay bandwidth product and low dispersion slow light in silicon-on-insulator based photonic crystal waveguides", Proceedings of the *SPIE*, Optics + Photonics 2009, 7420, 742014-742014-5 (2009).

13. **Swati Rawal** and R. K. Sinha, "Dual-band wavelength demultiplexer consisting of SOI based photonic crystals: design and analysis," Proceedings of the *SPIE*, 7056, 70560T-70560T-6 (2008).
14. **Swati Rawal** and R. K. Sinha, "Liquid Crystal Tuning of Slow light Propagation in Photonic Crystal Waveguides", IEEE Xplore Digital library, pp- 580-582, ELECTRO-2009.
15. **Swati Rawal** and R. K. Sinha, "Slow light Propagation in Photonic Crystal Waveguides due to Liquid Crystal infiltration: Design and Applications" Proceedings of 12th International Symposium on Microwave and Optical Technology-2009, December 16-19, 2009, Delhi, India
16. **Swati Rawal** and R. K. Sinha, "Liquid Crystal Assisted slow light propagation in Photonic Crystal and Device Application" Proceedings of OSA Frontiers in Optics 2009, October 11-15th, 2009, San Jose, California, USA
17. **Swati Rawal**, R. K. Sinha and Richard M. De La Rue, "Slow Light Devices in Silicon-on-Insulator Photonic Crystal" Proceedings of ICOP 2009-International Conference on Optics and Photonics held at Chandigarh, India from 30th Oct.-1st Nov., 2009.
18. **Swati Rawal** and R. K. Sinha, "Modeling and design of silicon-on-insulator based 1.31/1.55μm photonic crystal de-multiplexer," PHOTONICS-2008: International Conference on Fiber Optics and Photonics, December 13-17, 2008 (Paper No. PM-34).

Opt Quant Electron (2008) 40:603–613
DOI 10.1007/s11082-008-9248-z

Modeling and design of 2D photonic crystal based Y type dual band wavelength demultiplexer

R. K. Sinha · Swati Rawal

Received: 28 November 2007 / Accepted: 23 September 2008 / Published online: 6 November 2008

Abstract In this paper, photonic bandgap (PBG) induced wave guiding application of photonic crystals is exploited to design Dual Band Wavelength Demultiplexer (DBWD) for separating two telecommunication wavelengths, 1.31 and 1.55 μm. Two designs that use silicon rods in air and embedded air holes in silicon are realized for this purpose. Plane wave expansion (PWE) method and two dimension Finite Difference Time Domain (FDTD) methods are used to design and analyze the DBWD in Y type photonic crystal structure. Numerical analysis indicates that these designs enable the separation of two wavelengths with very high optical power extinction ratios. Other filter parameters like transmittance and quality factor are also calculated to confirm superior performance of the proposed design of photonic crystal based DBWD.

Keywords Photonic crystal · Photonic bandgap materials · Linear defect waveguide · Wavelength demultiplexer

1 Introduction

Photonic crystals (PhCs) introduced by Yablonovitch (1987) have emerged as one of the most significant topics in the field of optical telecommunication. These are defined as materials which have refractive index periodically varying along one, two or three dimension. If the refractive index contrast is sufficiently high, it gives rise to the formation of photonic bandgap (PBG) materials which can realize the localization and trapping of light over a band of frequencies (Joannopolous et al. 1995). By locally breaking the periodicity of

R. K. Sinha · S. Rawal (✉)
Department of Applied Physics, Centre of Relevance and Excellence in Fiber Optics and Optical Communication, Faculty of Technology, Delhi College of Engineering, University of Delhi, Bawana Road, Delhi 110042, India
e-mail: swati.rawal@yahoo.com

R. K. Sinha
e-mail: dr_rk_sinha@yahoo.com

photonic crystal, by creating vacancies or changing the radius of rods/holes, a region with optical properties different from surrounding bulk photonic crystal can be created. This is referred to as PBG optical waveguide (Sakoda 2001) or simply PhC waveguide (WG). Radiation losses exhibited by the PhC sharp bend waveguides are far lesser than conventional waveguides (Valsov and McNab 2004). Two dimension PBG waveguides can be used to design a variety of structures as directional couplers (Nagpal and Sinha 2004), beam splitters (Chen et al. 2004), multiplexers and demultiplexers (Centeno et al. 1999; Tekeste and Yarrison-Rice 2006; Haxha et al. 2005), resonators (Fan et al. 1999), polarizers (Sinha and Kalra 2006a,b), polarization beam splitter (Zabelin et al. 2007) and so on.

In the recent past, interest has been grown in the design and development of DBWD because of their wide applications in bidirectional communication networks (Chien et al. 2004, 2006; Chung and Lee 2007). For example, 1.31/1.55 µm duplex devices are commonly used in fiber-to-the-home (FTTH) transmission systems and are used in the Coarse Wavelength Division Multiplexed (CWDM) systems as well (Fyberdyne Labs 2007). PhCs have opened new possibilities for ultra compact wavelength selective optical devices owing to their PBG induced wave guiding properties. Hence, in the proposed paper wave guiding phenomenon due to PBG property of PhC is exploited for the formation of DBWD in Y type PhC structure, as shown in Figs. 2 and 7. This design of DBWD separates the two telecommunication wavelengths 1.31 and 1.55 µm with a very high extinction ratio and superior quality factor and transmission characteristics. Since the PBG structures strongly control the flow of light, therefore defect created in periodic lattice of PhC results in the confinement of light along specified one arm of the two arms of Y type crystal. Here, we report the design of two structures, one is a hexagonal lattice with silicon rods in air and other is the embedded hexagonal lattice arrangement of air holes in silicon. Both Y type PhC hetrostructures are analyzed using PWE method (Plihal and Maradudin 1991; Villeneuve and Piche 1992) and the performance characteristics in terms of extinction ratio, quality factor and transmittance is obtained by applying 2D FDTD method (Taflove 1998; Yee 1966).

2 Structure design

In the proposed paper we have designed PhC based DBWD having hexagonal lattice of silicon rods in air or embedded air holes in silicon material. The lattice constant and radius of rods or holes were chosen to provide a wide wavelength span (1,250–1,600 nm) at the band edge of input waveguide of DBWD. Selection of lattice constant and radius of rods/holes of the structure is based on the fact that the bandgap exist for both the wavelengths, 1.31 and 1.55 µm so that when line defects are created in photonic crystals, they produce guided modes in photonic crystals corresponding to these wavelengths. Defect radius is chosen such that band gap exist for 1.55 µm in one arm of the Y type DBWD and not for 1.31 µm and vice versa for other arm. Structures having silicon rods in air provide large PBG at technologically convenient geometric parameters with $r/a < 0.5$, as described in Sukanoivanov (2006). However, taking into view practical applications for fabrication, structure having embedded air holes in silicon material is more promising candidate for large scale integration than that of structure having silicon rods in air. Propagation of light is simulated by 2D FDTD method for wavelengths 1.31 and 1.55 µm and it indicates that 1.31/1.55 µm mixed light will be separated into two lights and guided into two output ports of Y type PhC.

2.1 2D PhC wavelength demultiplexer using silicon rods in air

In this section we have designed a 2D PhC slab with hexagonal lattice of Si ($n = 3.42$) rods in air. We first study the photonic bandgap variation using PWE method for Transverse magnetic modes (TM polarization) where the electric field component of electromagnetic waves is oriented perpendicular to the plane of propagation. To obtain PBG for the desired range of wavelength covering both 1.31 and 1.55 µm, we have chosen lattice constant, $a = 0.68\,\mu m$ and rod radius $r = 0.2\,\mu m$. With these parameters PhC provides a large bandgap in range of normalized frequency 0.42318–0.54325 for TM polarization (Fig. 1).

Now, a linear defect waveguide is formed by removing few rods from the direction of propagation. Since the designed structure possesses PBG for TM polarization in the wavelength range $1.25\,\mu m \leq \lambda \leq 1.6\,\mu m$, both wavelengths, 1.31 and 1.55 µm, are guided through the region of input waveguide (Input Wg) as shown in Fig. 3a. Further we design a DBWD by changing the geometrical parameters of Si rods in two arms of Y type photonic bandgap induced waveguides (Fig. 2). Radii of Si rods in one arm of the structure, named Output Wg1, is changed such that signal of 1.55 µm experiences bandgap and 1.31 µm passes through while radii of Si rods in other arm of the structure, named Output WG2, is changed such that signal of 1.31 µm experiences bandgap and 1.55 µm passes through. Figure 3b and c shows that guided modes exist for 1.31 µm in Output Wg1 and 1.55 µm in Output Wg2.

Here we observe that a range of radii exists for which the desired range of bandgap appears. Hence we investigated the defect radius by studying the variation of transmittance in the output ports with defect radius r_d (Fig. 4). 2D FDTD method for TM polarization was utilized to generate data for these plots and that radius is chosen for which transmitted power is maximum.

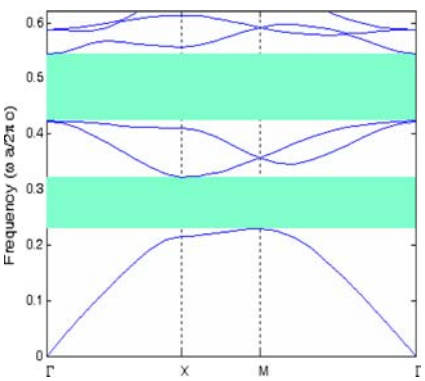

Fig. 1 TM band structure of photonic crystal structure having silicon rods in air, for $r = 0.2\,\mu m$

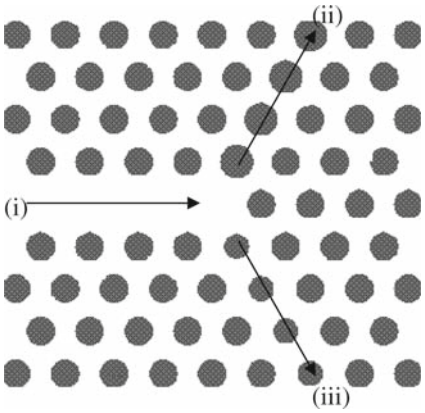

Fig. 2 Schematic diagram of proposed DBWD having silicon rods in air with (i) input Wg, (ii) output Wg1 and (iii) output Wg2

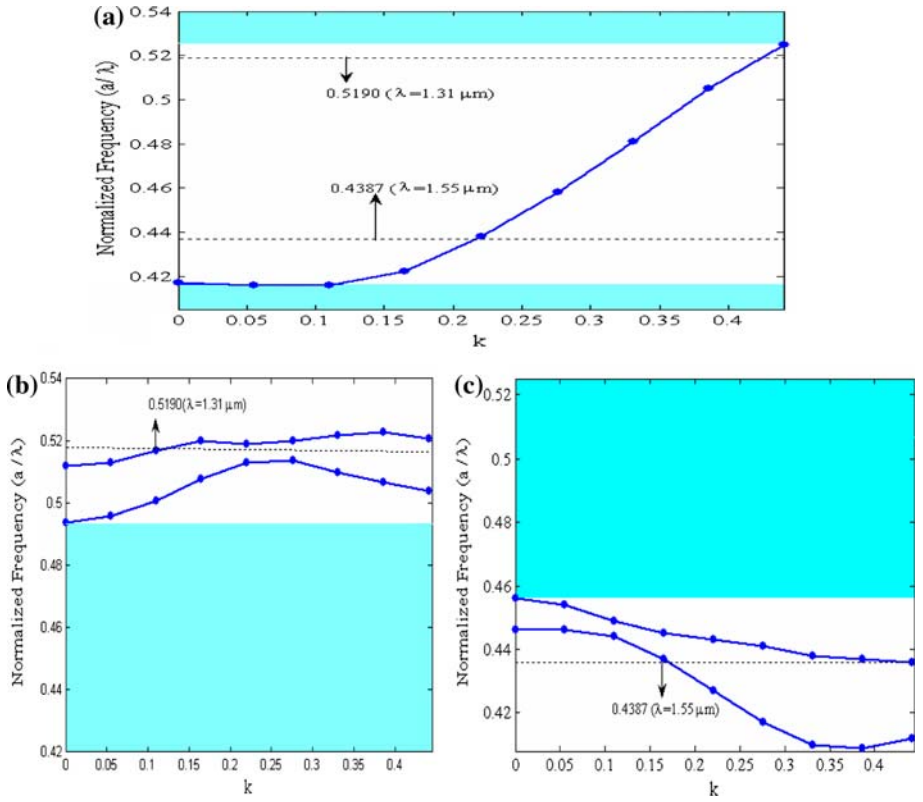

Fig. 3 Dispersion relation of the three involved PhC waveguides. The blue line corresponds to the respective guided modes for TE polarization in **a** input Wg, **b** output Wg1 and **c** output Wg2

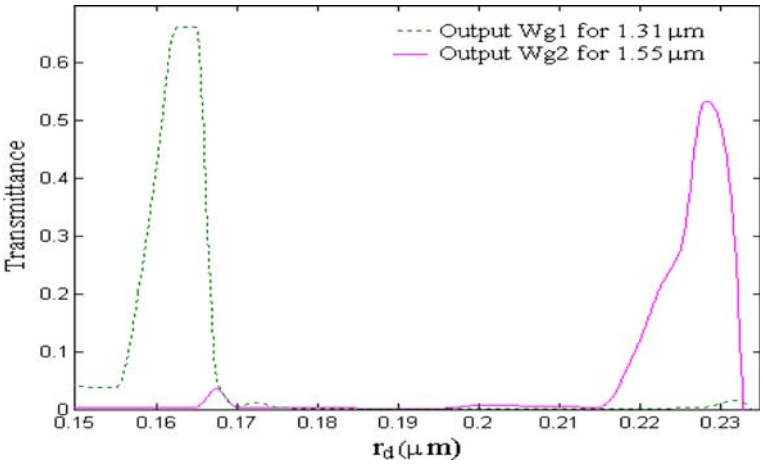

Fig. 4 Variation of transmittance with defect radius r_d in two output waveguides, output Wg1 and output Wg2 for TM polarization of 1.31 and 1.55 μm

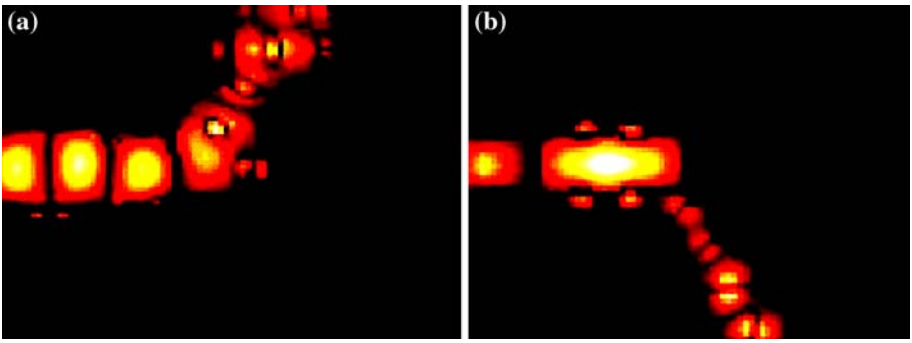

Fig. 5 Field pattern for TM polarization at **a** $\lambda = 1.31\,\mu m$ and **b** $\lambda = 1.55\,\mu m$ for the designed Y type DBWD having silicon rods in air

Note that the maximum efficiency of the device is obtained when defect radius in output Wg1 is $r_d = 0.2318\,\mu m$ for wavelength 1.31 μm to pass through and 1.55 μm to suffer bandgap. In similar line, the maximum transmission efficiency for wavelength 1.55 μm of the device is obtained when defect radius in output Wg2 is $r_d = 0.1768\,\mu m$. The field pattern for TM polarization for the two telecom wavelengths, 1.31 and 1.55 μm in Y type DBWD having silicon rods in air is shown in Fig. 5. The type of launch field is Gaussian Continuous Wave (CW). Beam width and step size is taken to be 0.1 and 0.005 μm. Boundary conditions for 2D FDTD simulation of designed structure is taken as $X(\min) : X(\max) = -5.6525\,\mu m : 5.6525\,\mu m$ & $Z(\min) : Z(\max) = -2.9996\,\mu m : 2.9996\,\mu m$. Output power is determined by the time monitors at output end of two output waveguides. It is observed that 1.31 μm is obtained from Output Wg1 having defect radius $r_d = 0.2318$ and 1.55 μm is obtained from Output Wg2 having defect radius $r_d = 0.1768\,\mu m$ (Fig. 5).

2.2 2D PhC wavelength demultiplexer using air holes in silicon

The second type of DBWD is designed using silicon material ($n = 3.42$) with embedded hexagonal lattice arrangement of air holes. Lattice constant is chosen to be $a = 0.48\,\mu m$. While studying the photonic bandgap variation using PWE we found that large photonic bandgap in the range $1.25\,\mu m \leq \lambda \leq 1.60\,\mu m$ is obtained for the transverse electric modes (TE polarization) in the hexagonal arrangement of embedded air holes in silicon material. These air holes have radius $r = 0.1896\,\mu m$ (Fig. 6).

Now, we create a linear waveguide in the crystal by removing few holes from the periodic structure so that TE polarization of wavelengths 1.25–1.60 μm can be guided into the input waveguide, shown as Input Wg in Fig. 7. The PBG based Y type DBWD is then created by changing the geometrical parameters of the air holes in the two arms of Y type photonic bandgap induced waveguides such that wavelength of 1.31 μm is obtained at the output end of one of the arms and wavelength of 1.55 μm is obtained at the output end of the other arm. Thus radius of the air holes in the two output waveguides are varied such that wavelength 1.55 μm experiences bandgap in one arm (output Wg1) of Y type demultiplexer and 1.31 μm is guided through it while wavelength 1.31 μm experiences bandgap in the other arm (output Wg2) of Y type demultiplexer and 1.55 μm passes through it. Figure 8 shows the guided modes for the three involved photonic crystal waveguides.

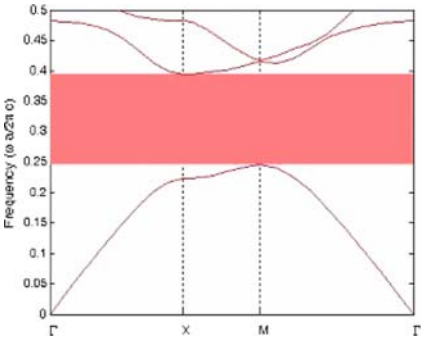

Fig. 6 TE band structure of photonic crystal structure having embedded air holes in silicon for $r = 0.1896\,\mu m$

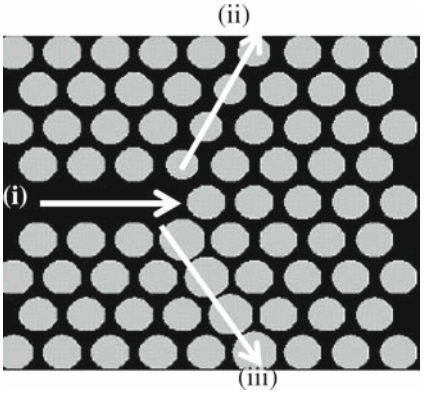

Fig. 7 Schematic diagram of proposed DBWD having embedded air holes in silicon material with (i) input Wg, (ii) output Wg1 and (iii) output Wg2

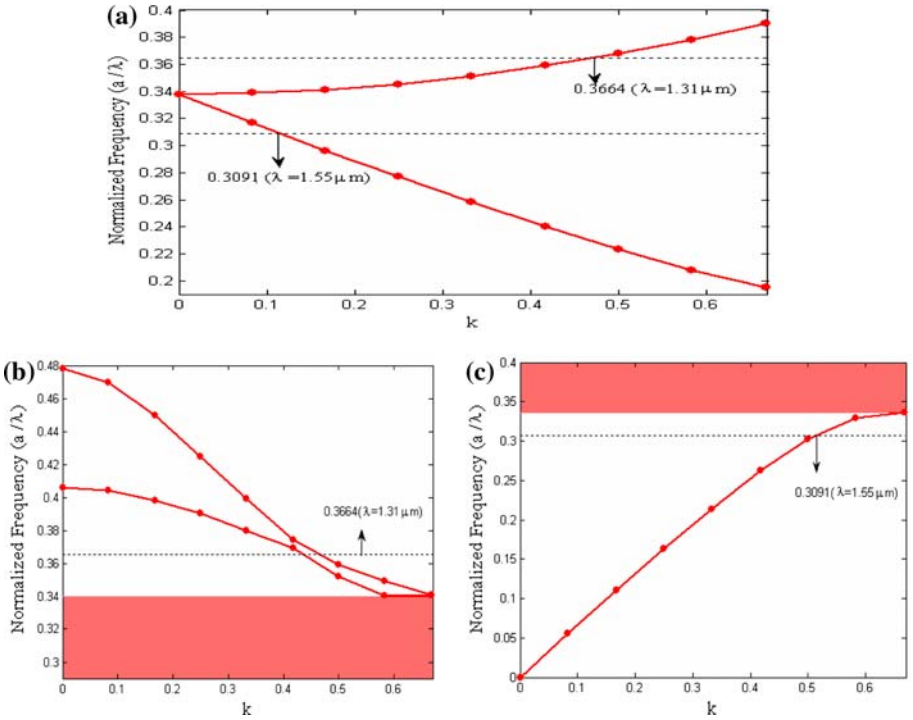

Fig. 8 Dispersion relation of the three involved PhC waveguides. The blue line corresponds to the respective guided modes for TE polarization in **a** input Wg, **b** output Wg1 and **c** output Wg2

Here we observe that while varying the radii to obtain the desired bandgap, a range of radii exists for which the given bandgap appears. We have chosen that radii for which transmitted power is maximum. Hence, we investigated the defect radius by studying its variation with transmittance in the two output ports at 1.31 and 1.55 μm for TE polarization

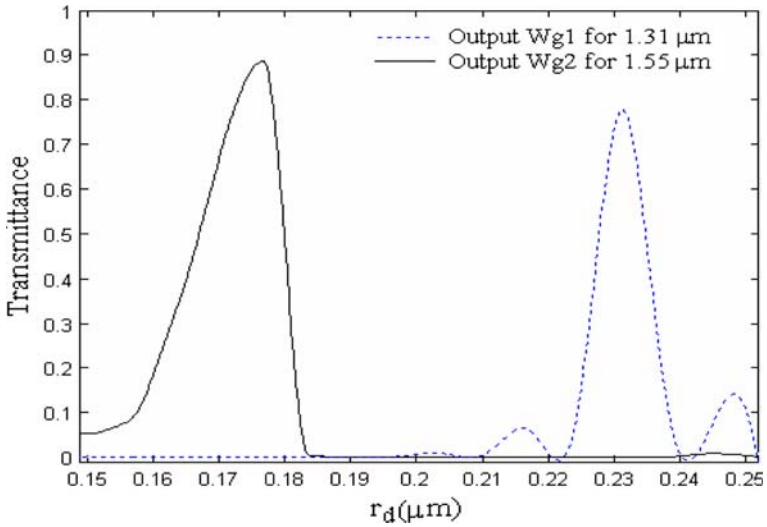

Fig. 9 Variation of transmittance with defect radius r_d in two output waveguides, output Wg1 and output Wg2 for TE polarization of 1.31 and 1.55 μm

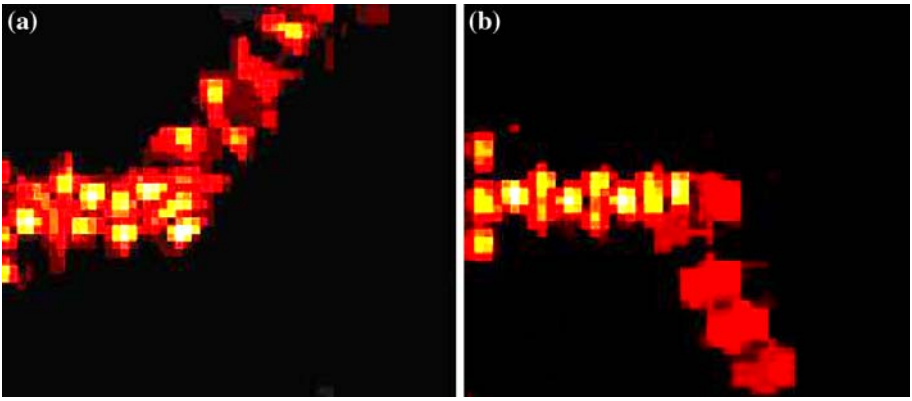

Fig. 10 Field pattern for TM polarization at **a** $\lambda = 1.31$ μm and **b** $\lambda = 1.55$ μm for the designed Y type DBWD having embedded air holes in silicon material

(Fig. 9). It is noted that maximum efficiency for 1.31 guidance is obtained when defect radius is $r_d = 0.1646$ μm in output Wg1 while maximum efficiency of 1.55 μm is obtained when defect radius is $r_d = 0.228$ μm in Output Wg2. The field pattern for TE polarization for the two telecom wavelengths, 1.31 and 1.55 μm in Y type DBWD having embedded air holes in silicon material is shown in Fig. 10. The type of launch field is Gaussian Continuous Wave (CW). Beam width and step size is taken to be 0.1 and 0.00025 μm. Boundary conditions for 2D FDTD simulation of embedded air hole type DBWD is taken as X (min): X (max) = −2.6775 μm: 2.6775 μm & Z (min): Z (max) = −2.9894 μm: 2.9894 μm. Output power is determined by the time monitors at output end of two output waveguides. It is observed that 1.31 μm is obtained from Output Wg1 having defect radius $r_d = 0.1646$ and 1.55 μm is obtained from Output Wg2 having defect radius $r_d = 0.228$ μm (Fig. 10).

3 Numerical analysis

The proposed Y type DBWD is simulated using 2D FDTD method. Output Wg1 reflects the radiation with wavelength 1.55 µm and Output Wg2 reflects the radiation with wavelength 1.31 µm. Efficiency of the device in both type of structure (i.e. for silicon rods in air and embedded air holes in silicon) was investigated by calculating different filter parameters like transmittance, extinction ratio and quality factor.

3.1 Transmittance

Transmittance of the designed DBWD is defined as the ratio of output intensity (I_{out}) from either of the two output waveguides to the incident intensity (I_{in}) at the entrance of the Y type waveguide:

$$T = \frac{I_{\text{out}}}{I_{\text{in}}}$$

Variation of transmittance from the two output waveguides of Y type PhC structure consisting of silicon rods in air-based DBWD is shown in Fig. 11a and for air holes in silicon-based DBWD is shown in Fig. 11b. It can be noted from the two graphs that maximum efficiency in output Wg1 is shown for wavelength 1.31 µm and in output Wg2 is shown for 1.55 µm. Hence the two telecommunication wavelengths 1.31 and 1.55 µm can be separated out easily using these two designs of DBWD.

3.2 Extinction ratio

Further we calculate extinction ratios ER1 and ER2 of the DBWD which explains that separation of two wavelengths, 1.31 and 1.55 µm is achieved. The extinction ratios ER1 and ER2 are defined as

$$\text{ER1} = 10\log_{10}\frac{\text{fractional output power for 1.31 µm wavelength in waveguide1}}{\text{fractional output power for 1.31 µm wavelength in waveguide2}}$$

and

$$\text{ER2} = 10\log_{10}\frac{\text{fractional output power of 1.55 µm wavelength in waveguide2}}{\text{fractional output power of 1.55 µm wavelength in waveguide1}}.$$

Simulation by 2D FDTD method indicates that in case of silicon rods in air-based DBWD extinction ratios are ER1 = 36.30 dB and ER2 = 30.40 dB while in case of air holes in silicon-based DBWD extinction ratios are 22.05 and 22.70 dB for the two wavelengths, 1.31 and 1.55 µm.

The PBG induced DBWDs thus have high extinction ratio for filtering two telecom wavelengths, 1.31 and 1.55 µm efficiently (Wang et al. 2005; Chung and Lee 2007).

3.3 Quality factor

Quality factor is defined as ratio of wavelength at peak transmission λ_0 to full width at half maximum intensity (FWHM) or $\Delta\lambda$

$$Q = \frac{\lambda_0}{\Delta\lambda}.$$

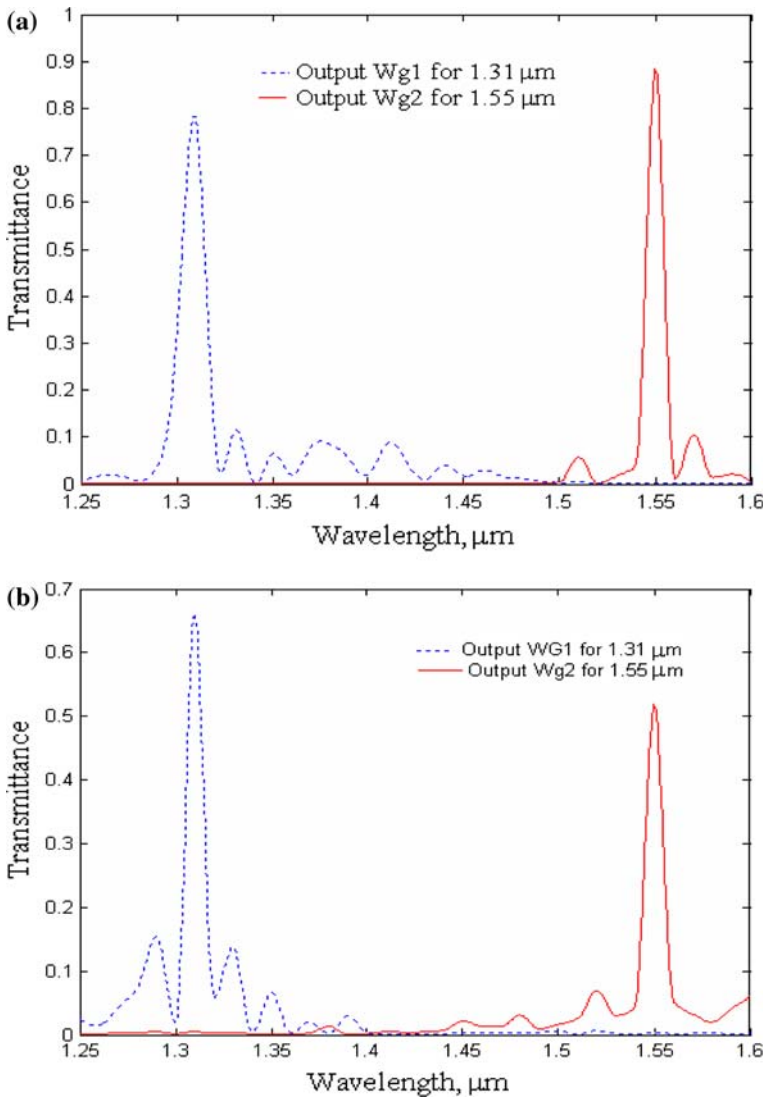

Fig. 11 Variation of transmittance with wavelength at the output end of each output waveguide for **a** the silicon rods in air-based DBWD and **b** air holes in silicon-based DBWD

Quality factor for wavelength 1.31 and 1.55 μm, in case of silicon rods in air-based DBWD is 109.16 and 172.22 while in case of air holes in silicon-based DBWD it is given as 131.0 and 155.0, at the output end of two output waveguides. It is mentioned that these values of quality factors are significantly high at two widely used telecommunication wavelength windows and hence these designs of PhC based DBWD are having superior filter characteristics.

4 Conclusion

In the proposed paper, we have designed photonic crystal based Y type DBWD for two telecommunication wavelengths, 1.31 and 1.55 μm, in PhC employing (i) silicon rods in

air and (ii) embedded air holes in silicon material. Designs of appropriate structures were obtained using PWE method while transmission and other filter characteristics were investigated using 2D FDTD method. It has been demonstrated that the PhC consisting of silicon rods in air -based DBWD reported in this paper exhibit high extinction ratio of 36.30 dB for wavelength 1.31 µm and 30.40 dB for wavelength 1.55 µm. Similarly the other PhC structure i.e. embedded air holes in silicon based DBWD exhibits 22.05 and 22.70 dB for wavelength 1.31 and 1.55 µm respectively. The proposed design also exhibit superior transmittance and high quality factor at these widely used telecommunication wavelengths. Thus the proposed DBWD consisting PhC structure can be effectively used in bidirectional optical transmission systems and networks covering broad spectrum of optical communication windows.

Acknowledgements The authors gratefully acknowledge the initiatives and support towards establishment of "TIFAC Centre of Relevance and Excellence in Fiber Optics and Optical Communication at Delhi College of Engineering, Delhi" through "Mission REACH" program of Technology Vision-2020, Government of India.

References

Centeno, E., Guizal, B., Felbacq, D.: Multiplexing and demultiplexing with photonic crystals. Pure Appl. Opt. **1**, 10–13 (1999). doi:10.1088/1464-4258/1/5/103

Chen, C.C., Chien, H.D., Luan, P.G.: Photonic crystal beam splitters. Appl. Opt. **43**, 6188–6190 (2004)

Chien, F.S.-S., Hsu, Y.J., Hsieh, W.F., Cheng, S.-C.: Dual wavelength demultiplexing by coupling and decoupling of photonic crystal waveguides. Opt. Express **12**, 1119–1125 (2004). doi:10.1364/OPEX.12.001119

Chien, F.S.-S., Cheng, S.-C., Hsu, Y.-J., Hsieh, W.-F.: Dual-band multiplexer/demultiplexer with photonic-crystal-waveguide couplers for bidirectional communications. Opt. Commun. **266**, 592–597 (2006). doi:10.1016/j.optcom.2006.05.055

Chung, L.-W., Lee, S.-L.: Photonic crystal based dual-band demultiplexers on silicon materials. Opt. Quant. Electron. **39**, 677–686 (2007). doi:10.1007/s11082-007-9118-0

Fan, S., Villeneuve, P.R., Joannopolous, J.D.: Theoretical analysis of channel drop tunneling processes. Phys. Rev. B. **59**, 15882–15892 (1999). doi:10.1103/PhysRevB.59.15882

Fyberdyne Labs. http://www.fiberdyne.com/products/pdf/cwdmintro.PDF. Cited 11 Sept 2007 (2007)

Haxha, S., Belhadj, W., AbdelMalek, F., Bouchriha, H.: Analysis of wavelength demultiplexer based on photonic crystals. Optoelectronics **152**, 193–198 (2005). doi:10.1049/ip-opt:20050003

Joannopolous, J.D., Meade, R.D., Winn, J.N.: Photonic Crystals: Molding the Flow of Light. Princeton University Press, Princeton (1995)

Nagpal, Y., Sinha, R.K.: Modeling of photonic bandgap directional couplers. Microw. Opt. Technol. Lett. **43**, 47–50 (2004). doi:10.1002/mop.20371

Plihal, M., Maradudin, A.A.: Photonic band structures of two dimensional systems—the triangular lattice. Phys. Rev. B **44**, 1865–8571 (1991). doi:10.1103/PhysRevB.44.8565

Sakoda, K.: Optical properties of photonic crystals. Springer Series, New York (2001)

Sinha, R.K., Kalra, Y.: Design of photonic bandgap polarizer. Opt. Eng. Lett. **45**, 110503–110505 (2006a)

Sinha, R.K., Kalra, Y.: Design of optical waveguide polarizer using photonic bandgap. Opt. Express **14**, 10790–10794 (2006b). doi:10.1364/OE.14.010790

Sukhoivanov, I.A., Guryev, I.V., Shulika, O.V., Kublyk, A.V., Mashoshina, O.V., Alvarado-Mendez, E., Andrade-Lucio, J.A.: Design of the photonic crystal demultiplexers for ultra-short optical pulses using the gap-maps analysis. J. Optoelectron. Adv. Mater. **8**, 1622–1626 (2006).

Taflove, A.: Advances in Computational Electrodynamics—The Finite Difference Time Domain Method. Artech House, Norwood (1998)

Tekeste, M.Y., Yarrison-Rice, J.M.: High efficiency photonic crystal based wavelength demultiplexer. Opt. Express **14**, 7931–7942 (2006). doi:10.1364/OE.14.007931

Valsov, Y., McNab, S.: Losses in single mode silicon-on-insulator strip waveguides and bends. Opt. Express **12**, 1622–1631 (2004). doi:10.1364/OPEX.12.001622

Villeneuve, P.R., Piche, M.: Photonic bandgaps in two dimensional square lattices-square and circular rods. Phys. Rev. B **46**, 4973–4975 (1992). doi:10.1103/PhysRevB.46.4973

Wang, W.K., Wang, S.J., Chen, C.C., Wu, Y.H., Huang, F.H., Chan, Y.J.: 1.3/1.55 µm optical directional coupler by photonic crystal with a defect shifting design. In: Proceedings of IEEE Conference on Nanotechnology, Nagoya, Japan, July (2005)

Yablonovitch, E.: Inhibited spontaneous emission in solid state physics and electronics. Phys. Rev. Lett. **58**, 2059–2062 (1987). doi:10.1103/PhysRevLett.58.2059

Yee, K.S.: Numerical solution of initial boundary value problems involving Maxwell's equations in isotropic media. IEEE Trans. Antenna Propag. **14**, 302–307 (1966). doi:10.1109/TAP.1966.1138693

Zabelin, V., Dunbar, L.A., Le Thomas, N., Houdre, R.: Self-collimating photonic crystal polarization beam splitter. Opt. Lett. **32**, 530–532 (2007). doi:10.1364/OL.32.000530

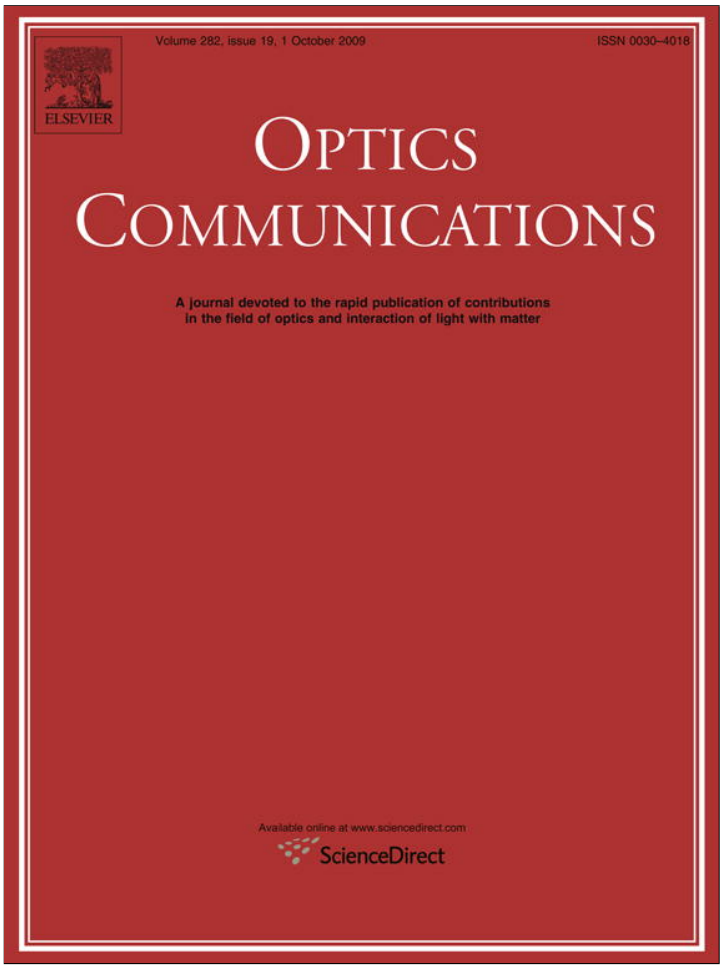

Optics Communications 282 (2009) 3889–3894

Contents lists available at ScienceDirect

Optics Communications

journal homepage: www.elsevier.com/locate/optcom

Design, analysis and optimization of silicon-on-insulator photonic crystal dual band wavelength demultiplexer

Swati Rawal, R.K. Sinha *

TIFAC-Centre of Relevance and Excellence in Fiber Optics and Optical Communication, Department of Applied Physics, Delhi College of Engineering, Faculty of Technology, University of Delhi, Bawana Road, Delhi 10042, India

ARTICLE INFO

Article history:
Received 13 April 2009
Received in revised form 16 June 2009
Accepted 18 June 2009

Keywords:
Photonic crystal bandgap
Guided waves
Silicon-on-insulator

ABSTRACT

A highly efficient photonic crystal dual band wavelength demultiplexer (DBWD) using silicon-on-insulator (SOI) substrates is proposed for demultiplexing two optical communication wavelengths, 1.31 μm and 1.55 μm. Demultiplexing of two wavelength channels is obtained by modifying the propagation properties of guided modes in two arms of *Y* type photonic crystal structure. Propagation characteristics of proposed DBWD are analyzed utilizing 3D finite difference time domain (FDTD) method. Enhancement in spectral response is further obtained by optimizing the *Y* junction of demultiplexer giving rise to high transmission and extinction ratio for the wavelengths, 1.31 μm and 1.55 μm. Hence it validates the efficiency of proposed optimized DBWD design for separating two optical communication wavelengths, 1.31 μm and 1.55 μm. Tolerance analysis was also performed to check the effect of variation of air hole radius, etch depth and refractive index on the transmission characteristics of the proposed design of SOI based photonic crystal DBWD.

1. Introduction

Photonic crystals (PhC) are attracting attention because of the existence of interesting properties such as photonic bandgap (PBG), i.e. the range of frequencies at which optical propagation is prohibited in any direction and defect mode, i.e. by introducing some defects in PhC, allowed modes appear in photonic bandgaps which are localized within the small volume around the defect [1–3]. Various types of line defect waveguides can be formed in the PhC's by changing the radius of rods/holes or by removing them completely. These waveguides support true guided modes in the frequency range lying in PBG of photonic crystal [4,5]. These guided modes are horizontally confined by PBG of the photonic crystal and vertically by total internal reflection because of high index contrast between the slab and the cladding. For symmetric structures in vertical direction, like air-bridge structures, light can be strictly classified into transverse electric (TE) and transverse magnetic (TM) modes or even and odd modes. In such structures PBG for TE mode or even mode can be used selectively. However for asymmetrical structures, like SOI structures, the modes cannot be classified selectively. Each mode has even as well as odd component. Modes having predominant component as H_y is referred to as TE like mode and those having predominant component as E_y is referred to as TM like mode. Thus in asymmetrical structures, TE like modes have both TE as well as TM components. If the ratio of TM element is negligible in TE like mode, there exist a quasi-PBG in PhC where TE like mode hardly propagates. Thickness of PhC should satisfy the single mode condition for using quasi-PBG [6]. Since from practical perspective, air-bridge type structures having air cladding on both sides are mechanically unstable and cannot be used as a platform for future integrated circuits [7,8]. Thus, a PhC slab on oxide cladding is more of a promising candidate for large scale integration than air-bridge structures. A frequently used material for realizing such PhC slabs is silicon-on-insulator (SOI) substrates having silicon layer between silicon-dioxide (SiO_2) cladding on one side and air cladding on other side. Various PhC components like waveguides, directional couplers, polarizers and polarization splitters have already been realized [9–14] using photonic crystal architecture on SOI substrates. DBWD's are the key components for transmitter receiver devices in bidirectional communication in local area optical networks. 1.31/1.55 μm duplex demultiplexers are also used in fiber-to-home (FTTH) transmission systems and in coarse wavelength division multiplexing (CWDM) systems [15–17]. In the recent past, various photonic crystal dual band demultiplexers have been realized for demultiplexing signals of wavelength 1.31 μm and 1.55 μm which is important in the field of optical communication [16–20]. However, these designs are based on air-bridge structures with air cladding on both sides, i.e. the PhC structures are freely suspended in air and hence are mechanically unstable from practical perspective as well as not

* Corresponding author. Tel.: +91 11 27871017; fax: +91 11 27871023.
E-mail addresses: swati.rawal@yahoo.com (S. Rawal), dr_rk_sinha@yahoo.com (R.K. Sinha).

0030-4018/$ - see front matter © 2009 Elsevier B.V. All rights reserved.
doi:10.1016/j.optcom.2009.06.046

suitable for large scale integration. Structures with solid support are more realistic. To overcome this instability, SOI based PhC DBWD are required to be designed and developed. In these structures, mechanical robustness is improved by existence of supporting dielectric material under the slab [21–24]. Further such *Y* type structures are also required to be optimized for high transmission from both output waveguides [25].

In this paper, we report a design of DBWD based on SOI substrates. The proposed device separates the TE like mode of two popularly used optical communication wavelengths, 1.31 μm and 1.55 μm. 3D plane wave expansion (PWE) method is used to calculate PBG and demultiplexing function is demonstrated using 3D finite difference time domain (FDTD) method. Numerical analysis indicates that the proposed structure demultiplexes TE like polarization of 1.31 μm and 1.55 μm effectively. Optimization of the structure is also carried out for increasing transmittance from two output waveguides with considerably high extinction ratio. We further carry out the tolerance of the device to fabrication by varying the radius of air holes, etch depth and refractive index of Si core. It is expected that such design and development will help in realizing devices and components for broad band optical communication systems and networks.

2. Structure design

The *Y* type DBWD was designed consisting of hexagonal arrangement of embedded air holes in Si ($n = 3.42$) PhC slab having thickness 0.35 μm on silica (SiO_2) cladding with thickness of 3 μm. Selection of radius of the holes of the entire structure is based upon the fact that bandgap exist for both the telecom wavelengths, 1.31 μm and 1.55 μm so that when line defect is created in the structure, they produce guided modes corresponding to both these wavelengths. Defect radius in the two arms of *Y* type structure is chosen so that bandgap exist for 1.55 μm in one arm and not for 1.31 μm in the same arm and vice versa for the other arm (Fig. 1). To obtain PBG for desired range of wavelength covering both 1.31 μm and 1.55 μm, we have chosen lattice constant, a to be 0.42 μm and hole radius, $r = 0.175$ μm. 3D PWE method is utilized for calculating guided modes below silica lightline. With these parameters, the structure supports a large photonic band gap for TE like modes in the range of normalized frequency ($\omega a/2\pi c$) varying from 0.2558 to 0.4367, i.e. wavelength λ ranging from 1.64 μm to 0.96 μm (Fig. 2). The input waveguide (Input Wg) is formed by removing a few holes in a row from the direction of propagation. Since the designed structure possess PBG for TE like modes of telecom wavelengths, 1.31 μm and 1.55 μm, the line defect created supports the guided modes for these wavelengths to exist within the Input Wg.

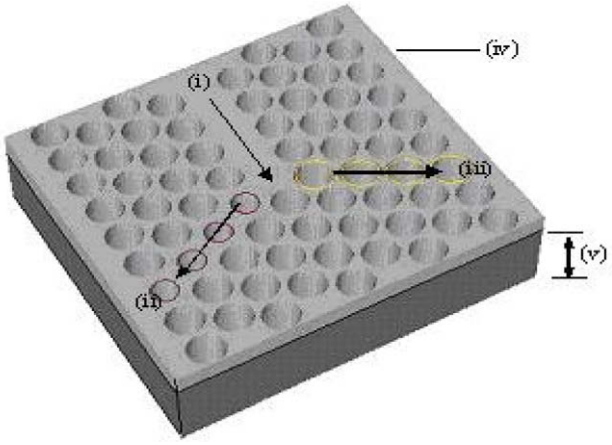

Fig. 1. Schematic view of proposed non optimized DBWD having embedded air holes in silicon material with (i) Input Wg. (ii) Output Wg1 with $r_1 = 0.129$ μm. (iii) Output Wg2 with $r_2 = 0.187$ μm. (iv) Silicon material. (v) Silica radius of holes in the bulk structure is chosen to be 0.175 μm.

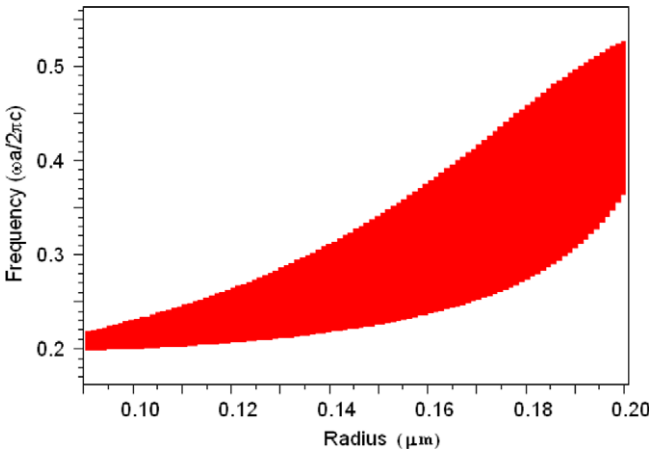

Fig. 2. Band structure for TE like modes for hexagonal lattice having hole radius, $r = 0.175$ μm, $r_1 = 0.129$ μm, $r_2 = 0.187$ μm and lattice constant $a = 0.42$ μm.

Fig. 3(a) shows the dispersion curve for Input Wg, which supports the light propagation for normalized frequency, 0.3206 and 0.2709, in the proposed design of PhC. The black solid line is the SiO_2 light line. The waveguide modes which lie below the light line are guided modes while those which lie above the light line become resonant, i.e. they are still guided in the plane along the line defect but they are lossy in the vertical direction. Thus wavelengths, 1.31 μm and 1.55 μm are guided in the input waveguide. The PBG based DBWD is then created by changing the geometrical parameters in two arms of *Y* type structure. The radii in the two arms of the structure are chosen such that signal for wavelength of 1.31 μm is obtained from output end of one arm and signal for wavelength of 1.55 μm is obtained from output end of other arm. For this we need to have bandgap for 1.55 μm in first arm and for 1.31 μm in second arm. Fig. 2 explains that for defect radius $r_1 = 0.129$ μm, PBG exist for normalized frequency 0.2709 ($\lambda = 1.55$ μm) and not for 0.3206 ($\lambda = 1.31$ μm). While for defect radius $r_2 = 0.187$ μm, PBG exist for normalized frequency of 0.3206 and not for 0.2709. Thus we change the radii of holes in one arm of the *Y* type structure to r_1 and named it as Output Wg1 and radii of holes in other arm of the *Y* type structure to r_2 and named it as Output Wg2. Thus Output Wg1 is a reduced index region because it is obtained by increasing the radii of embedded air holes in silicon slab while Output Wg2 is an increased index region because it is obtained by increasing the radii of air holes.

Dispersion curve in Fig. 3(b) shows that the guided modes exist for normalized frequency 0.3206 corresponding to optical wavelength of 1.31 μm while normalized frequency of 0.2709, i.e. wavelength of 1.55 μm is clearly not supported by Output Wg1. Hence if incident light is 1.31 μm, it will be well confined within the waveguide having defect radius r_1, i.e. Output Wg1. However if the incident light is 1.55 μm, it will be completely radiated out from Output Wg1. In the same way dispersion curve in Fig. 3(c) shows that guided mode exist for normalized frequency of 0.2709 corresponding to optical wavelength of 1.55 μm in Output Wg2 while no guided mode exist for 1.31 μm in the same waveguide having defect radius r_2. Thus the incident light of 1.55 μm is propagated in Output Wg2 and 1.31 μm is radiated out. Hence in the proposed design of DBWD, we obtain wavelength of 1.31 μm from Output Wg1 and 1.55 μm from Output Wg2.

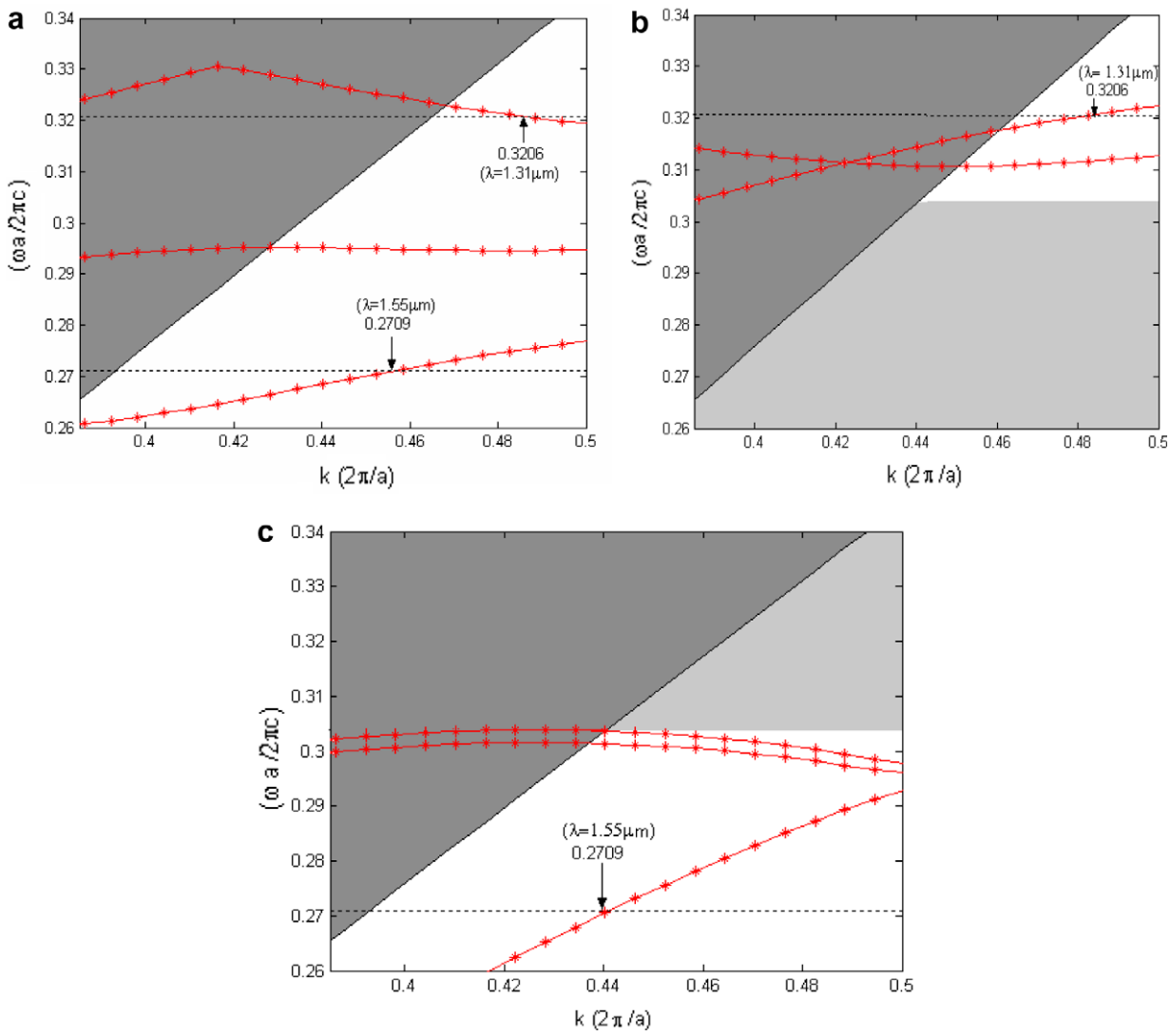

Fig. 3. Dispersion relations of the three involved PhC waveguides. The black (solid) line corresponds to SiO_2 light line and the red lines corresponds to the respective single guided modes in: (a) Input Wg. (b) Output Wg1. (c) Output Wg2.

3. FDTD simulation results and discussion

3D FDTD simulation was performed to determine the demultiplexing efficiency of the designed DBWD for separating two telecom wavelengths, 1.31 μm and 1.55 μm. 3D FDTD simulations are carried out by PhotonD (crystal wave) package where mesh size is taken to be Period/3 and device dimensions are taken to be 3.31 μm × 5.86 μm in *XZ* plane. Here transmittance (*T*) is defined as the ratio of output power obtained from either of the output waveguides to the input power, i.e. $T = P_{out}/P_{in}$. Fig. 4 shows the spectral response of proposed DBWD for TE like polarization of incident light. From figure, it is clear that the proposed structure successfully split the two telecom wavelengths but the maximum peaks obtained from two output waveguides is 50% of input signal for 1.55 μm and 58% of input signal for 1.31 μm. This weak transmission is due to backward scattering in the input waveguide from *Y* junction as well as excitation of higher order modes which cannot correctly propagate in the output waveguides. In order to improve transmission, junction region has to be modified by adding a smaller hole near the junction in input waveguide. This reduces multimode effect and backward scattering by varying the optical width of the waveguide.

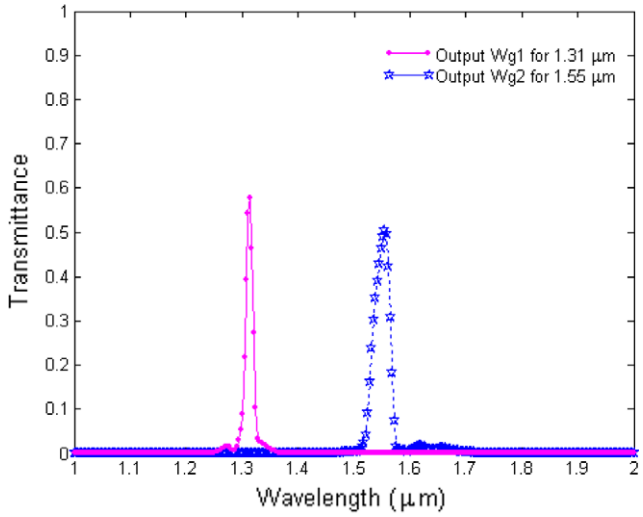

Fig. 4. Variation of transmittance with wavelength from two output waveguides for TE like polarization of incident light for non optimized SOI based DBWD.

4. Optimized structure

In order to enter proper optimization for increasing the transmission at two output ports, one has to define the position and radius of the hole which is inserted near the *Y* junction of proposed SOI based DBWD. This caused gentle perturbation of the incoming wave while changing its direction from input waveguide to either of the output waveguides. By tailoring the radius of induced air hole, transmittance peaks from two output waveguides can be increased. Fig. 5 shows the variation of radius (R) of the additional air hole placed at different positions (L as shown in Fig. 6) with transmittance from two output waveguides corresponding to two telecom wavelengths, 1.31 μm and 1.55 μm.

It is observed that for $R = 0.0245$ μm and $L = 0.625$ μm, transmittance from two output waveguides increases significantly which corresponds to decrease in backward scattering from the junction. The resulting optimized SOI based DBWD is shown in Fig. 6. Placing the additional air hole near the junction clearly increases the power transmission as observed in 3D FDTD simulation of optimized structure (Fig. 6).

Spectral response of transmittance for proposed optimized SOI based photonic crystal DBWD is shown in Fig. 7. It explains that the two wavelengths 1.31 μm and 1.55 μm separate out efficiently and are received from the two output waveguides. Power transmittance efficiency for 1.31 μm obtained from Output Wg1 is calculated to be 89% and transmission efficiency of 1.55 μm obtained from Output Wg2 is found to be 69%.

Efficiency of the device is further confirmed by calculating its extinction ratio which is defined as:

$$ER1 = 10\log_{10} \times \frac{\text{Transmittance for 1.31 μm obtained from Output Waveguide1}}{\text{Transmittance for 1.31 μm obtained from Output Waveguide2}}$$

and

$$ER2 = 10\log_{10} \times \frac{\text{Transmittance of 1.55 μm obtained from Output Waveguide2}}{\text{Transmittance of 1.55 μm obtained from Output Waveguide1}}$$

It is found to be ER1 = 26.10 dB for 1.31 μm and ER2 = 27.50 dB for 1.55 μm. It is mentioned here that these values of extinction ratio are sufficiently high for SOI based PhCs.

5. Tolerance analysis

In this section we study the effect of change in air hole radius, variation of angle from vertical of the optimizing air hole near *Y* junction and variation of refractive index of silicon core by 0.01–0.001 on the transmission characteristics of optimized SOI based DBWD in PhC. First we will show how the transmission changes for ±3% variation in r_1 and r_2 because for these variations, r_1 and r_2 lie well within the desired bandgap. Fig. 8 shows the variation of transmittance plotted on both left and right hand *y*-axis of graph with tolerance on *x*-axis. The solid curve corresponds to the toler-

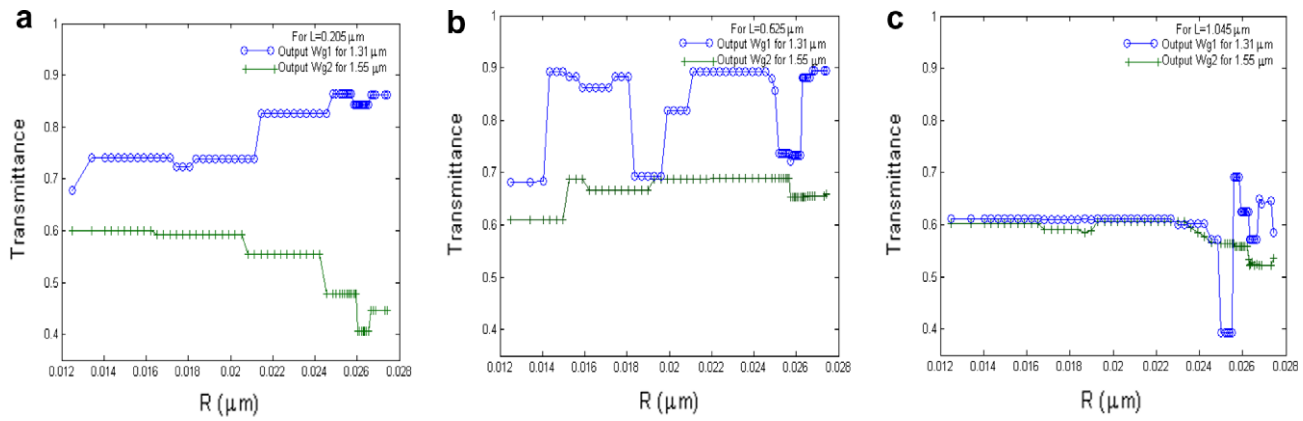

Fig. 5. Variation of Transmittance with radius R of additional air hole added at different positions: (a) $L = 0.205$ μm, (b) $L = 0.625$ μm and (c) $L = 1.045$ μm.

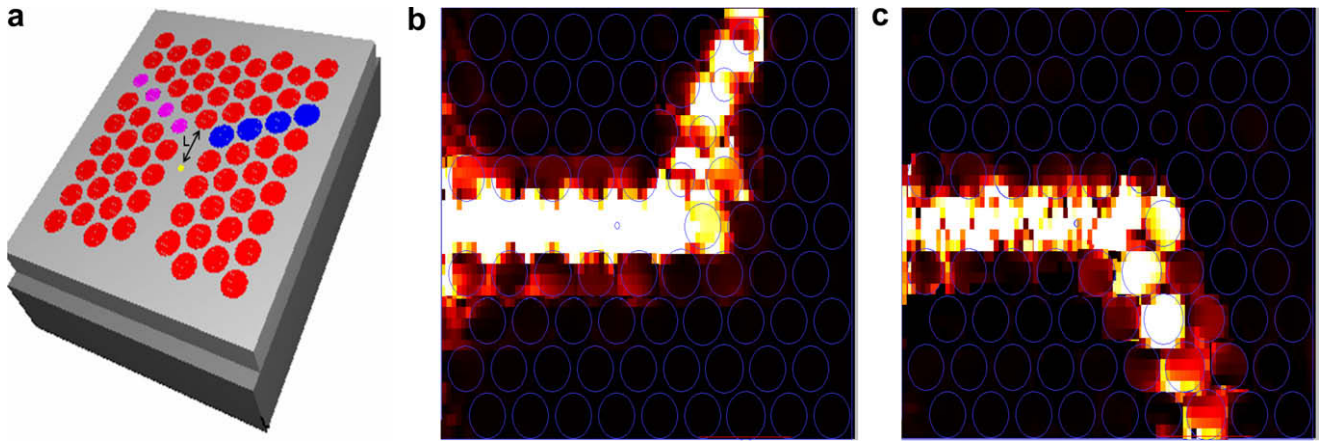

Fig. 6. (a) Optimized structure of SOI based DBWD with $R = 0.0245$ μm and $L = 0.625$ μm. Field pattern for TE like polarization at (b) $\lambda = 1.31$ μm and (c) $\lambda = 1.55$ μm for the proposed SOI based DBWD.

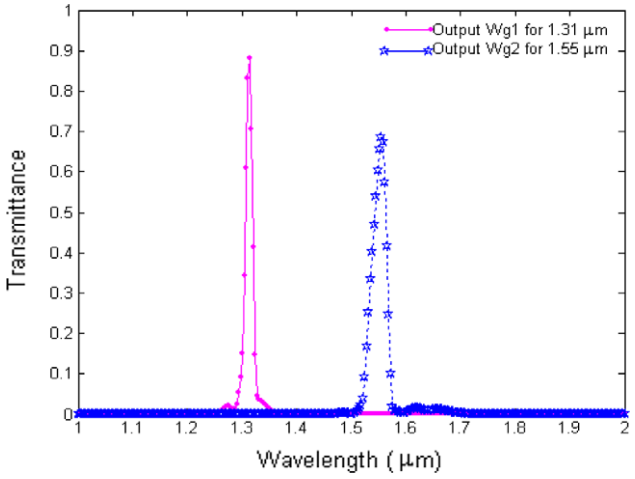

Fig. 7. Variation of transmittance with wavelength from two output waveguides for TE like polarization of incident light for optimized SOI based DBWD.

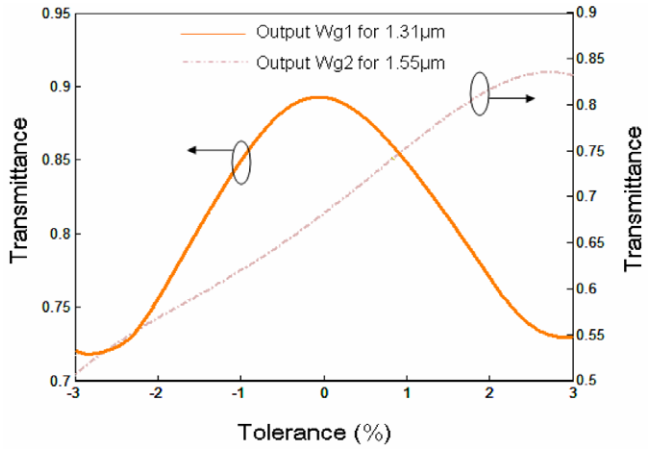

Fig. 8. Effect of tolerances in defect radius r_1 and r_2 on the transmission characteristics of proposed optimized DBWD.

ance in Output Wg1, i.e. in defect radius r_1 while the dash–dot curve corresponds to the tolerance in Output Wg2, i.e. in defect radius r_2. It can be seen from the tolerance analysis that although increase or decrease in defect radii by ±3% do not cause significant change in photonic band gap, and hence the wavelength region of the guided mode remains unaffected in the proposed DBWD. Simulation result in Fig. 8 explains (i) the change in intensity of the transmitted light of wavelength 1.55 μm falls to 52% from 69% with −3% change in defect radius r_2 in Output Wg2 while it rises to 83% when r_2 increases by 3% and (ii) the intensity of the transmitted light of wavelength 1.31 μm with ±3% change in defect radius r_1 in Output Wg1 varies approximately from 89% to 72%.

We further carry out the tolerance analysis of the device for variation in etch depth of optimizing air hole having radius $R = 24.5$ nm inserted near the Y junction of the structure. During fabrication, air holes with small radius usually etch at a slower rate and hence tend to be shallower. Also the shape of the hole would be conic since the defect is quiet small with regard to lattice holes. Therefore impact of conic angle from vertical, with a corresponding change in etch depth, on transmittance is shown in Fig. 9. We also study the variation in refractive index of silicon core and its impact on transmission characteristics of proposed SOI based DBWD (Fig. 9(b)). It is observed that transmittance changes by less than ±0.02% from either of the output waveguides.

Tolerance analysis of above factors leads us to conclude that the proposed DBWD on SOI based photonic crystal has a reasonable fabrication tolerance.

6. Conclusion

In the proposed paper, we have presented a design of SOI based DBWD to split the TE like polarization of two telecommunication wavelengths, 1.31 μm and 1.55 μm. The principle of the design of DBWD is based on the phenomenon of light wave guidance due to Photonic Bandgap in horizontal direction and refractive index contrast in vertical direction and thereby the existence of guided modes in defect waveguides. The filtering characteristics were computed using 3D FDTD method and it was found that the two telecom wavelengths can be demultiplexed efficiently. Transmission characteristics are enhanced by optimizing the structure by adding smaller air hole near the Y junction. Transmittance peaks obtained from two output waveguides is 89% for 1.31 μm and 69% for 1.55 μm. Extinction ratio of the optimized structure is calculated to be 26.10 dB for 1.31 μm and 27.50 dB for 1.55 μm. Tolerance analysis of the device is also carried out for ±3% change in

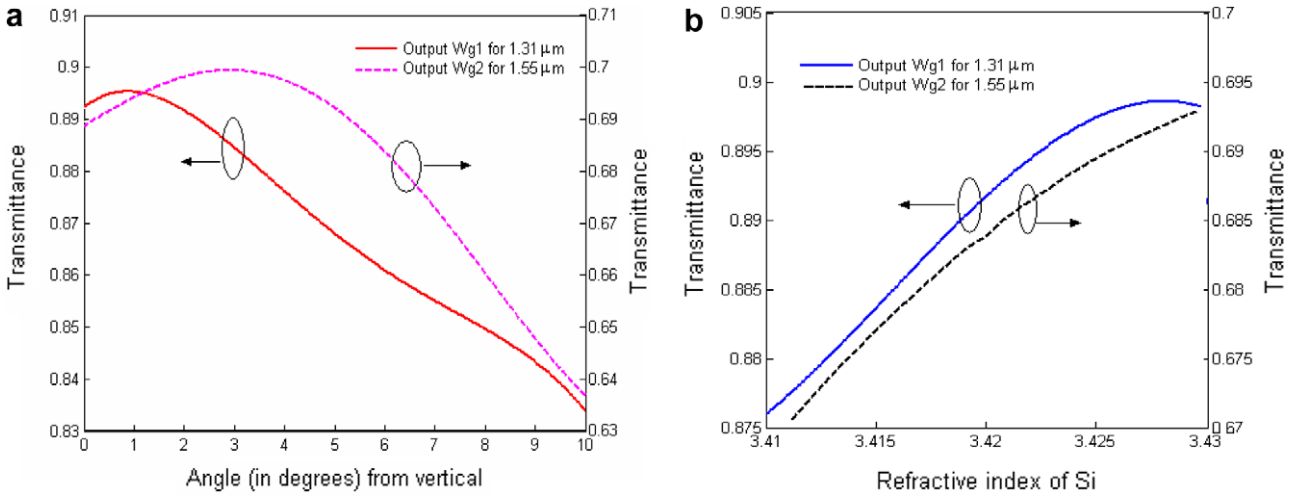

Fig. 9. Effect of tolerances in (a) angle from vertical of optimizing defect radius R having conic shape and (b) variation of refractive index of Si core on the transmission characteristics of proposed optimized DBWD.

defect radius in the two output waveguides. It is found that wavelength region of the guided mode remains unaffected in the proposed optimized SOI based DBWD with increase or decrease in defect radii by 3%. Effect of variation in etch depth of the optimizing air hole and variation of refractive index of slab on transmittance is also studied.

Acknowledgements

The authors gratefully acknowledge the initiatives and support towards establishment of "TIFAC Centre of Relevance and Excellence in Fiber Optics and Optical Communication at Delhi College of Engineering, Delhi" through "Mission REACH" program of Technology Vision-2020, Government of India. One of the authors (RKS) also acknowledges the useful discussion on the result and outcome of this paper with Prof Richard M. De La Rue, University of Glasgow, UK during his (RKS) short research assignment supported by Royal Academy of Engineering, UK in June 2008.

References

[1] E. Yablonovitch, J. Opt. Soc. Am. B 10 (1993) 283.
[2] S. John, Phys. Rev. Lett. 58 (1987) 2486.
[3] R.D. Meade, A.M. Rappe, K.D. Brommer, J.D. Joannopoulos, Phys. Rev. B 48 (1993) 8434.
[4] S.G. Johnson, S. Fan, P.R. Villeneuve, J.D. Joannopoulos, L.A. Kolodziejski, Phys. Rev. B 60 (1999) 5751.
[5] M. Notomi, A. Shinya, K. Yamada, J. Takahashi, C. Takahashi, I. Yokohama, Electr. Lett. 37 (2001) 293.
[6] A. Shinya, M. Notomi, I. Yokohama, C. Takahashi, J. Takahashi, Opt. Quant. Electron. 34 (2002) 113.
[7] N. Kawai, K. Inoue, N. Carlsson, N. Ikeda, Y. Sugimoto, K. Asakawa, T. Takemori, Phys. Rev. Lett. 86 (2001) 2289.
[8] R.K. Sinha, Y. Kalra, Opt. Express 14 (2006) 10790.
[9] M. Settle, M. Salib, A. Michaeli, T.F. Krauss, Opt. Express. 14 (2006) 2440.
[10] Y.J. Quan, P.D. Han, Q.J. Ran, F.P. Zeng, L.P. Gao, C.H. Zhao, Opt. Commun. 281 (2008) 3105.
[11] E. Schonbrun, Q. Wu, W. Park, T. Yamashita, C.J. Summers, Opt. Lett. 31 (2006) 3104.
[12] Y. Cui, Q. Wu, E. Schonbrun, M. Tinker, J.-B. Lee, W. Park, IEEE Phot. Tech. Lett. 20 (2008) 641.
[13] A. Camargo, H.M.H. Chong, R.M. De La Rue, Phot. Nanostruct. 2 (2004) 207.
[14] A. Camargo, R.M. De La Rue, Photonic crystal channel guide Y-junction beam splitter based on an AlGaAs/GaAs epitaxial structure, Integrated Photonics Research, San Francisco, CA, 2004 (IWB2).
[15] Fyberdyne Labs. <http://www.fiberdyne.com/products/pdf/cwdmintro.PDF>, 2007 (Cited 11.09.2007).
[16] L.W. Chung, S.L. Lee, Opt. Quant. Electr. 39 (2007) 677.
[17] F.S.-S. Chien, S.-C. Cheng, Y.-J. Hsu, W.-F. Hsieh, Opt. Commun. 266 (2006) 592.
[18] I.A. Sukhoivanov, I.V. Guryev, O.V. Shulika, A.V. Kublyk, O.V. Mashoshina, E. Alvarado-Mendez, J.A. Andrade-Lucio, J. Optoelectr. Adv. Mater. 8 (2006) 1622. ISSN 1454-4164.
[19] W. Huang, Y. Zhang, B. Li, Opt. Express 16 (2008) 1600.
[20] R.K. Sinha, S. Rawal, Opt. Quant. Elect. 40 (2008) 603.
[21] M. Notomi, A. Shinya, K. Yamda, J. Takahashi, C. Takahashi, I. Yokohama, IEEE J. Quant. Elect. 38 (2002) 736.
[22] M. Qiu, Phys. Rev. B 66 (2002) 033103.
[23] Y. Tanaka, T. Asano, R. Hatsuta, S. Noda, IEEE J. Lightwave Technol. 22 (2004) 2787.
[24] Y. Tanaka, Y. Sugimoto, N. Ikeda, H. Nakamura, Y. Watanabe, K. Asakawa, K. Inoue, IEEE J. Lightwave Technol. 23 (2005) 2749.
[25] L. Dekkiche, R. Naoum, Electr. Eng. 89 (2006) 71.

Slow light miniature devices with ultra-flattened dispersion in silicon-on-insulator photonic crystal

Swati Rawal[1], Ravindra K. Sinha[1] and Richard M. De La Rue[2]

[1]*TIFAC- Centre of Relevance and Excellence in Fiber Optics and Optical Communication, Department of Applied Physics, Delhi College of Engineering (Faculty of Technology, University of Delhi), Bawana Road, Delhi-110042, India.*

[2]*Optoelectronics Research Group, Department of Electronics and Electrical Engineering, University of Glasgow G 128LT, Scotland, U.K*

dr_rk_sinha@yahoo.com, swati.rawal@yahoo.com

Abstract: We propose a silicon-on-insulator (SOI) photonic crystal waveguide within a hexagonal lattice of elliptical air holes for slow light propagation with group velocity in the range 0.0028c to 0.044c and ultra-flattened group velocity dispersion (GVD). The proposed structure is also investigated for its application as an optical buffer with a large value of normalized delay bandwidth product (DBP), equal to 0.778. Furthermore it is shown that the proposed structure can also be used for time or wavelength-division demultiplexing to separate two telecom wavelengths, 1.31μm and 1.55μm, on a useful time-scale and with minimal distortion.

OCIS codes: (130.5296) Photonic crystal waveguides; (060.1810) Buffers; (130.2790) Guided waves.

References and links

1. T. F. Krauss, "Why do we need slow light?," Nat. Photon. **2**, 448-450 (2008).
2. Richard M. De La Rue, "Slower for longer," Nat. Photon. **2**(12), 715-716, December (2008).
3. Y. A. Vlasov, M. O'Boyle, H. F. Hamann, and S. J. McNab, "Active control of slow light on a chip with photonic crystal waveguides," Nature **438**, 65-69 (2005).
4. V. R. Almeida, C. A. Barrios, R. R. Panepucci, and M. Lipson, "All optical control of light on a silicon chip," Nature **481**, 1081-1084 (2004).
5. R. S. Jacobsen, k. Andersen, P. I. Borel, J. F. Pedersen, O. Hansen, M. Kristensen, A. Lavrinenko, G. Moulin, H. Ou, C. Peucheret, B. Zsigri, and A. Bjarklev, "Strained silicon as a new electro-optic material," Nature **441**, 199-202 (2006).
6. M. Soljacic, S. G. Jhonson, S. Fan, M. I. Baneseu, E. Ippen, and J. D. Joannopolous, "Photonic crystal slow light enhancement of non linear phase sensitivity," J. Opt. Soc. Am. B **19**, 2052-2059 (2002).
7. H. Gersen, T. J. Karle, R. J. P. Engelen, W. Bogaerts, J. P. Korterik, N. F. Van Hulst, T. F. Krauss, and L. Kuipers, " Real space observation of ultra slow light in photonic crystal waveguides," Phys. Rev. Lett. **94**, 073903 (2005).
8. T. Baba and D. Mori, "Slow light engineering in photonic crystals," J. Phys. D: Appl. Phys. **40**, 2659-2665 (2007)
9. L. H. Frandsen, A. V. Lavrinenko, J. Fage-Pedersen, and P. I. Borel, "Photonic crystal waveguides with semi-slow light and tailored dispersion properties," Opt. Express **14**, 9444-9450 (2006).
10. R. S. Tucker, P. C. Ku, and C. J. Chang-Hasnain, "Slow light optical buffers: Capabilities and fundamental limitations," J. Lightwave Technol. **23**, 4046-4066 (2005).
11. M. L. Povinelli, S. G. Johnson, and J. D. Joannopoulous, "Slow light, band edge waveguides for tunable time delays," Opt. Express **13**, 7145-7159 (2005).
12. T. Baba, D. Mori, K. Inoshita, and Y. Kuroki, "Light localization in line defect photonic waveguides," IEEE J. Quantum Electron. **10**, 484-491 (2004).
13. T. F. Krauss, "Slow light in photonic crystal waveguides," J. Phys. D: Appl. Phys. **40,** 2666-2670 (2007).
14. D. Mori and T. Baba, "Wideband and low dispersion slow light by chirped photonic crystal coupled waveguide," Opt. Express **13**, 9398-9408 (2005).
15. D. Mori and T. Baba, "Dispersion controlled optical group delay device by chirped photonic crystal waveguides," Appl. Phys. Lett. **85**, 1101-1103 (2004).

#111046 - $15.00 USD Received 6 May 2009; revised 18 Jun 2009; accepted 18 Jun 2009; published 20 Jul 2009

16. A. Shinya, M. Notomi, I. Yokohama, C. Takahashi, and J. Takahashi "Two-dimensional Si photonic crystals on oxide using SOI substrate," Opt. Quantum. Electron. **34** 113-121 (2002)
17. A. Di Falco, L. O'Faolain, and T. F. Krauss, "Dispersion control and slow light in slotted photonic crystal waveguides," Appl. Phys. Lett. **92**, 083501 (2008).
18. F. Wang, J. Ma, and C. Jiang, "Dispersionless slow wave in Novel 2-D photonic crystal line defect waveguides," J. Lightwave Technol. **26**, 1381-1386 (2008).
19. M. Plihal and A. A. Maradudin, "Photonic band structures of two dimensional systems- The Triangular lattice," Phy. Rev. B **44**, 1865-8571 (1991).
20. A. Taflove "Advances in Computational Electrodynamics- The Finite Difference Time Domain Method," Artech House (1998).
21. M. D. Settle, R. J. P.Engelen, M. Salib, A. Michaeli, L. Kuipers, and T. F. Krauss, "Flatband slow light in photonic crystals featuring spatial pulse compression and terahertz bandwidth," Opt. Express **15**, 219 (2007).
22. J. Ma and C. Jiang, "Demonstration of ultra slow modes in asymmetric line defect photonic crystal waveguides," IEEE Phot. Technol. Lett. **20**, 1237-1239 (2008).
23. G. P. Agarwal, Fiber Optic Communication systems, Hoboken, NJ: Wiley-Interscience (1997).
24. S. Assefa and Y. A. Vlasov, "High order dispersion in photonic crystal waveguides," Opt. Express **15**, 17562 (2007).
25. J. Ma and C. Jiang, "Flat band slow light in asymmetric line defect photonic crystal waveguide featuring low group velocity and dispersion," IEEE J. Quantum Electron. **44**, 763-769 (2008).

1. Introduction

Slow light refers to reduction of the group velocity of light - and is a promising technology for future all-optical communication networks. It can be used for the enhancement of light-matter interaction and for the miniaturization of optoelectronic integrated circuits (OEICs) [1-5]. Photonic crystal (PhC) line-defect waveguides that are created within the photonic bandgap (PBG) are extensively used for achieving slow light in the flat band regions of guided modes supported by these waveguides [6-9]. Therefore they have strong application possibilities in optical buffers and other optical storage devices [10]. The high refractive index contrast achievable in SOI structures provides strong confinement of light in the vertical direction, while the PBG of the PhC lattice provides confinement of light in the horizontal direction. Slow light in PhCs has already been observed by several authors [11-13] near the edge of the Brillouin zone. Recently Mori and Baba have experimentally demonstrated a slow light device based on a chirped PhC coupled waveguide [14, 15] and have achieved the low group velocity of 0.017c. However fabrication of such complex devices is challenging and may limit their practical utilization in large scale integration.

In this paper, we report the design of SOI based PhC structures having elliptical air holes within a silicon core. For symmetric structures in the vertical direction, like air-bridge structures, light can be strictly classified into Transverse Electric (TE)-and Transverse Magnetic (TM) modes – and as even and odd modes. In such structures the PBG for TE even modes can be used selectively. However for asymmetrical structures, such as SOI structures, the modes cannot be classified selectively- and each mode has even as well as odd components. Modes with H_y as the predominant component are referred to as TE-like modes - and those with E_y as the predominant component is referred to as TM-like modes. (See Fig.1) Thus in asymmetrical structures, TE-like modes have both TE and TM components. If the amount of the TM component is negligible for the TE-like mode, there is a quasi PBG in the PhC properties, where propagation of the TE-like mode is almost completely stopped. The thickness of the PhC waveguide core layer should then satisfy the single-mode condition, in order to exploit the quasi PBG effectively [16]. The SOI waveguide structure is made up of a silicon core layer sandwiched between a silica cladding layer below and an air cladding above. The major and minor axes of the elliptical air holes are tuned to obtain a flat section of dispersion curve below the silica lightline for slow light propagation.

#111046 - $15.00 USD Received 6 May 2009; revised 18 Jun 2009; accepted 18 Jun 2009; published 20 Jul 2009

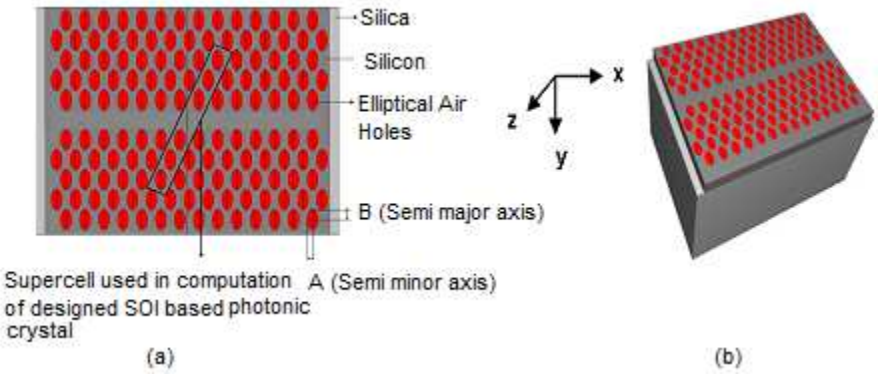

Fig. 1 (a) Schematic of the proposed design for the W1 line defect channel waveguide configuration with super-cell dimensions – and with length equal to 15*a*. (b) Diagram defining the coordinate system.

Figure 1 shows a schematic of the proposed design that has elliptical holes in a hexagonal arrangement - with a W1 line-defect channel waveguide configuration. The inset in Fig. 1 shows the super-cell used in computational modelling of the designed structure. For the device applications of such waveguides, the group velocity dispersion (GVD) and other higher-order dispersion parameters should be very low [17-,18] thereby enabling the optical signal to propagate with reduced distortion - as we have demonstrated using Finite-Difference Time-Domain (FDTD) simulation. The band structure was obtained using a 3D Plane Wave Expansion (PWE) method [19,20]. Using these simulation tools we have been able to design an SOI based PhC channel waveguide with slow light behaviour - having a group velocity in the range from 0.0028c to 0.044c – and with vanishing GVD, third order dispersion (TOD) and fourth order dispersion (FOD) parameters. The structure designed has also been investigated for its possible application in the design of (i) an optical buffer with a value of normalized DBP that is equal to 0.778 - a value that is higher than previously reported values [14, 21, 22] - and (ii) a time and wavelength division demultiplexing device. The proposed device is designed to de-multiplex the two telecommunication wavelengths, 1.31 μm and 1.55 μm as well as other wavelengths around 1.55 μm, using time discrimination and with minimal distortion, while exhibiting an ultra-flattened dispersion curve for both wavelengths.

2. Design aspects and device description

For the design, we have firstly assumed a hexagonal arrangement of air holes in an SOI based PhC structure. The refractive index of silicon has been taken to be 3.5 and its thickness has been taken to be 450 nm. Computed results for the band-structure of a W1 channel guide aligned along the Γ-K direction. They indicate that only a single guided mode exists below the silica light-line - and the calculated value of the effective index of the guided mode for the fundamental TE-like guided mode is calculated to be 3.25. This core guiding layer of silicon is typically bonded on to a silica (SiO_2) lower cladding layer that may be as much as 3 μm thick, in practice. The lattice constant for the air holes has been chosen to be a =0.42 μm, with a basic air hole radius of 0.33a.

As shown in Fig. 2(a), the bandgap of the designed structure lies in the frequency range 0.2130($2\pi c/a$) to 0.3058($2\pi c/a$), for the TE like polarization. A W1 PhC channel waveguide was then obtained by creating a single line defect in the photonic crystal. By examining the dispersion diagram in Fig. 2(b), it is possible to identify a flat section for the even-symmetry transverse mode of the W1 waveguide located at frequencies around 0.24($2\pi c/a$). The inset in the figure shows the super-cell used in the 3D PWE calculation. It is observed that the group velocity becomes very low because of the flat (i.e. near horizontal) dispersion curve, but the waveform of the optical signal is likely to be severely distorted by the large GVD parameter,

#111046 - $15.00 USD Received 6 May 2009; revised 18 Jun 2009; accepted 18 Jun 2009; published 20 Jul 2009

on the order of 10^8 ps^2/km for this situation, thus limiting the achievable bandwidth for slow light transmission.

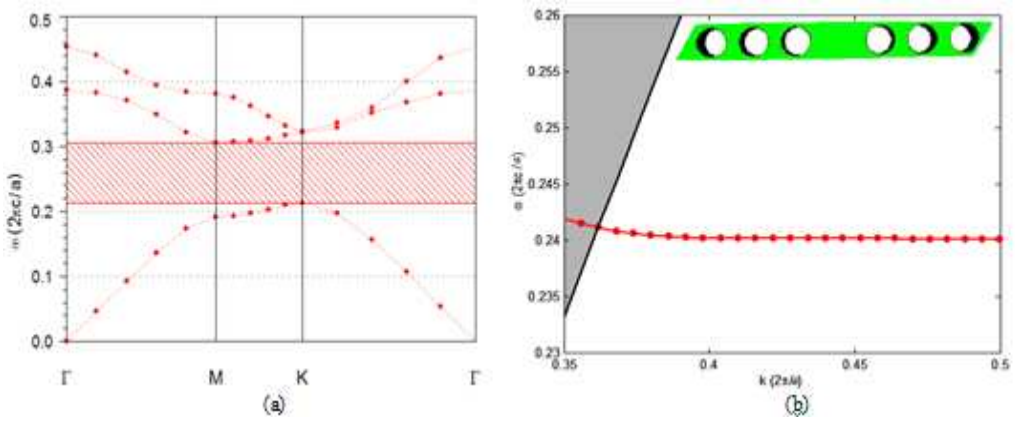

Fig. 2. (a) TE Bandgap map and (b) dispersion diagram having flat section of guided modes in the hexagonal lattice with lattice constant a = 0.35 μm and basic air hole radius r=0.33a. The inset in the figure shows the super-cell used in the 3D PWE method. The black solid line is the silica lightline, while the red line is the dispersion curve.

Our main goal in this work is to obtain slow guided-light modes that feature the combination of low group velocity and vanishing GVD parameter. The main requirements for such modes to be achieved are: (a) operation below the silica light-line, because the modes which lie above the light-line are intrinsically lossy (i.e. leaky) in the vertical direction - and (b) a flat section of dispersion curve should be obtained i.e. the slope of the dispersion curve should not only be small but it should also be close to constant for a given range. Otherwise the higher order derivatives of the dispersion curve will lead to GVD, third-order dispersion (TOD) and fourth-order dispersion (FOD).

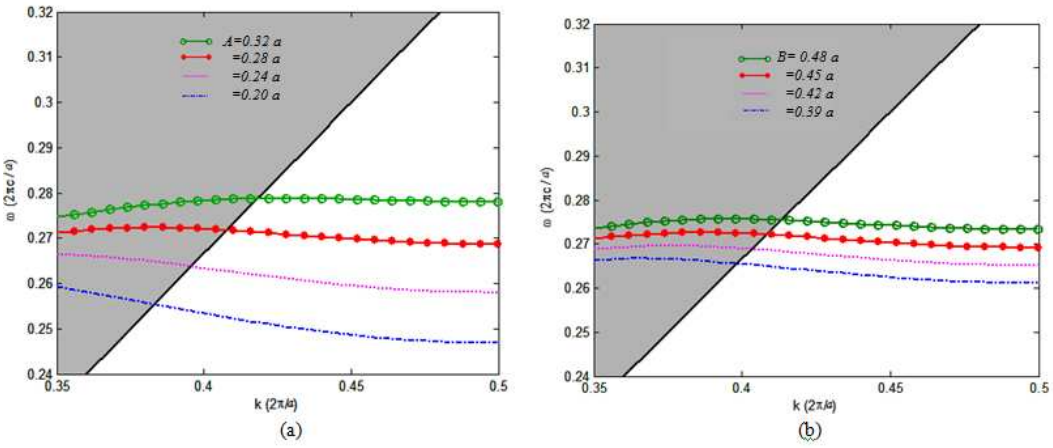

Fig. 3. Movement of the dispersion curves when (a) the semi-minor axis A and (b) the semi-major axis B changes gradually.

To satisfy the above requirements we change the embedded circular air holes into an array of identical elliptical air holes with semi minor axis (A) and semi major axis (B), while retaining a hexagonal lattice arrangement. The dependence of the dispersion diagram on the semi-minor axis (A) and semi-major axis (B) of the air holes is shown in Fig. 3(a) and 3(b). As indicated earlier, these are the normalized dispersion curves for propagation for a W1

#111046 - $15.00 USD Received 6 May 2009; revised 18 Jun 2009; accepted 18 Jun 2009; published 20 Jul 2009

channel guide oriented along the ΓK axis of the PhC lattice, for different values of A and B. Figure 3(a) shows that the dispersion curves move up in frequency in the slow light regime when the magnitude of the semi-minor axis A of the elliptical air holes is varied progressively from 0.20*a* to 0.32*a* -and the effective indices of the modes of the structure increase. In obtaining these curves, the value of the semi-major axis B has been fixed at 0.45*a*. In the same way, when the semi-major axis B is varied progressively from 0.39*a* to 0.48*a*, the dispersion curve again moves up in frequency, as shown in Fig. 3(b) - where A is fixed at 0.28*a*. The tuning of the two structural parameters, A and B has been performed in order to tailor the dispersion properties of the waveguide in the slow light regime below the silica light line and for the desired frequency range.

Finally we obtain an optimal waveguide with elliptical air holes that have a semi-minor axis A = 0.286*a* and semi-major axis B = 0.457*a*. Fig. 4(a) shows the band structure for TE-like modes of the designed structure with lattice constant *a* = 0.42 μm, semi-minor axis A = 0.286*a* and semi-major axis B = 0.457*a*. For these parameter values, the bandgap ranges from 0.2352(2πc/*a*) to 0.3277(2πc/*a*). The dispersion curve obtained for the fundamental mode of the W1 waveguide is shown in Fig. 4(b), together with the super-cell used in the 3D PWE method. The region 0.41< (2π/*a*) < 0.5 is chosen for slow light transmission - because in this region the flattest section of the dispersion curve is obtained that lies below silica light-line and is within the PBG region. i.e. the slow modes are confined vertically by total internal reflection and horizontally by the photonic bandgap of the PhC regions.

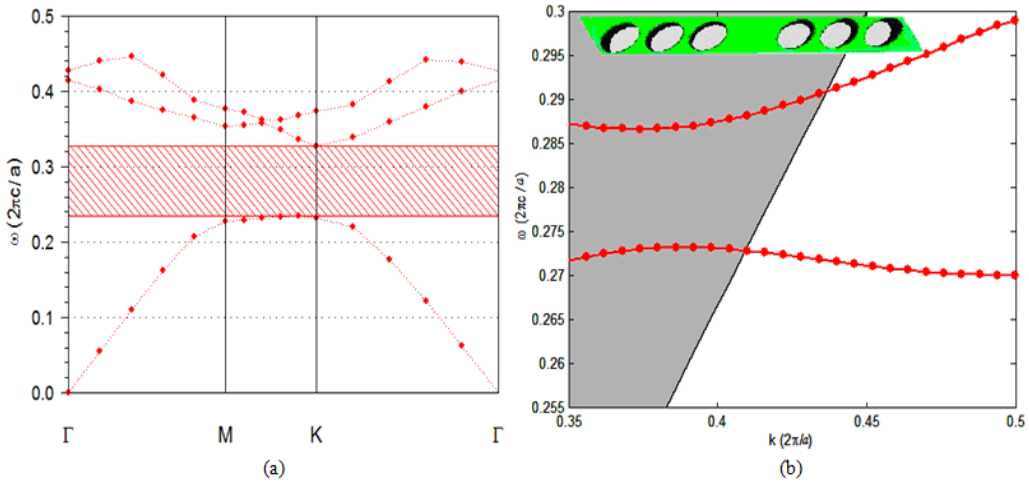

Fig. 4. (a) TE band diagram of finally designed structure. (b) Dispersion diagram for the proposed SOI based single line defect photonic crystal having elliptical air holes with semi-minor axis A=0.286*a* and semi-major axis B=0.457*a*. Flat section of dispersion curve corresponds to slow light region.

3. Numerical results and discussion

3.1. Group velocity and Group Velocity Dispersion (GVD):

In the previous section we have designed a W1 channel waveguide in an SOI based photonic crystal structure with a hexagonal lattice of elliptical air holes in silicon. The structure shows a flat dispersion curve below the silica light line. The key velocity of such modes is their group velocity, defined as the velocity with which the envelope of a short pulse propagates through space. The standard definition for group velocity is [23]:

$$v_g = \frac{d\omega}{dk} \qquad (1)$$

#111046 - $15.00 USD Received 6 May 2009; revised 18 Jun 2009; accepted 18 Jun 2009; published 20 Jul 2009

where ω is the angular frequency and *k* is the wave-vector along the waveguide.

3.2. Group Velocity Dispersion (GVD):

The GVD is defined as the derivative of the inverse group velocity w.r.t. angular frequency.

$$\beta = \frac{d^2 k}{d\omega^2}$$

$$= \frac{d}{d\omega}\left(\frac{1}{d\omega/dk}\right)$$

$$= -\frac{1}{\left(d\omega/dk\right)^3}\frac{d^2\omega}{dk^2}$$

$$\beta = -\frac{1}{v_g^3}\frac{d^2\omega}{dk^2} \qquad (2)$$

From Eq. (2), it can be observed that if the group velocity converges to zero, the GVD parameter goes to infinity - which causes the spreading of an optical pulse in time and as a result of different frequency components of the pulse travelling at different velocities may merge together. Keeping the above fact in view, we have designed our structure to obtain a flat-band situation that is characterized by small and nearly constant slope, with relatively low group velocity and GVD parameter.

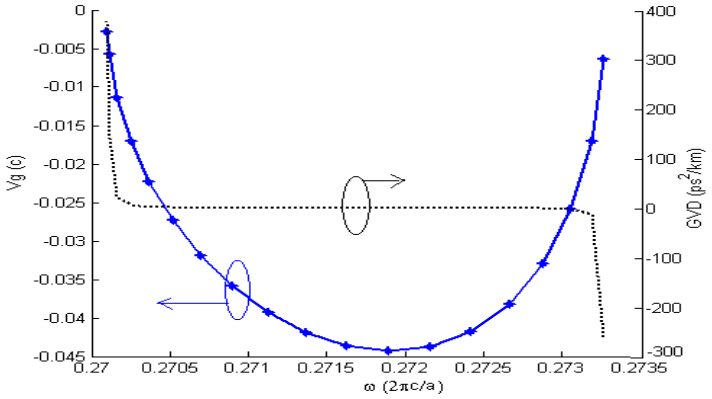

Fig. 5. Variation of group velocity and Group Velocity Dispersion (GVD) parameter for flat section of dispersion curve plotted in Fig. 4.

In Fig. 5 the frequency dependence of the group velocity - and the GVD parameter - on normalized frequency are plotted for the slow wave region shown in Fig. 4(b). We have considered the flat band of the dispersion curve lying below silica lightline i.e. the frequency range between 0.2700(2πc/*a*) and 0.2733(2πc/*a*). It can be observed that, for this range of frequencies, the group velocity remains in the range 0.0028c to 0.044c - and the GVD parameter lies in the range of 10^2 ps^2/km. The GVD has positive as well as negative values and, for a particular spectral region, it becomes flat - i.e., for a bandwidth of $\Delta\upsilon = \frac{\Delta\omega}{2\pi} = 2.1$ THz , the GVD parameter lies below 10 ps^2/km.The low group velocity obtained at the extreme points (~0.005c) is at the cost of large GVD, on the order of 10^2 ps^2/km - while near the mid point, around ω = 0.2718 (2πc/*a*), vg ~ 0.044c and the GVD parameter vanishes. Hence a very low GVD value is obtained over the wide spectral bandwidth of 2.1 THz.

#111046 - $15.00 USD Received 6 May 2009; revised 18 Jun 2009; accepted 18 Jun 2009; published 20 Jul 2009

3.3 Third Order Dispersion (TOD) and Fourth Order Dispersion (FOD):

The TOD parameter was deduced by calculating:

$$TOD = \frac{1}{v_g}\frac{\partial(GVD)}{\partial k} \quad (3)$$

i.e. the first derivative of the GVD.
and theFOD parameter was deduced by calculating:

$$FOD = \frac{1}{v_g}\frac{\partial(TOD)}{\partial k} \quad (4)$$

i.e. first derivative of the TOD.

Figure 6(a) shows that the upper limit of the TOD is on the order of 10^4 ps^3/km for the slow light regime below the silica light-line i.e. in the frequency range from 0.2700 ($2\pi c/a$) to 0.2733 ($2\pi c/a$) However we obtain a flat curve near the centre of frequency range, over a bandwidth of 2.1 THz, where TOD varies from 10^1 to 10^2 ps^3/km. Figure 6(b) shows that the upper limit of the FOD is on the order of 10^6 ps^4/km for the slow light regime, but again a flat curve is obtained for a bandwidth of 2.1 THz near the centre. These values of TOD and FOD are less than those reported in previous work [17, 24]. Thus both TOD and FOD vanish for a particular frequency range in the proposed SOI based structure having elliptical air holes PhC.

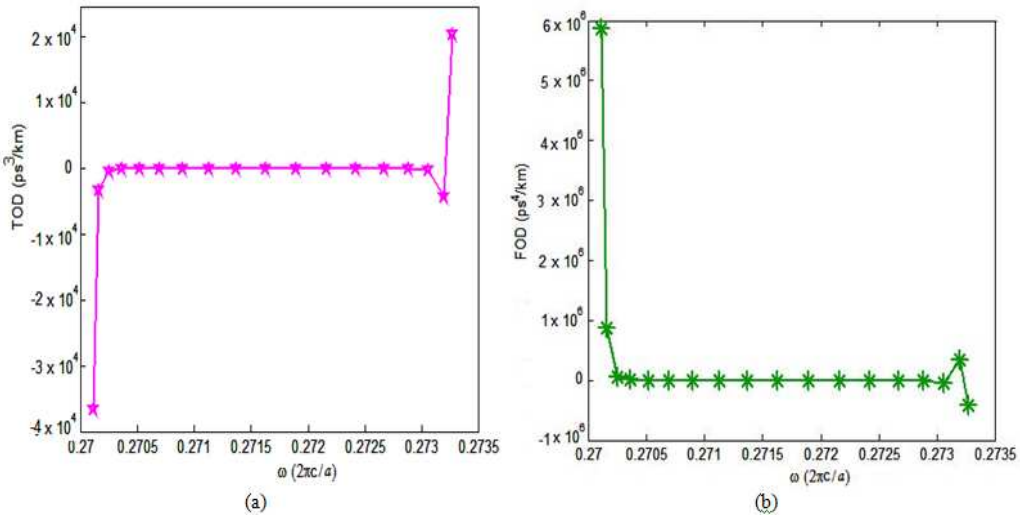

Fig. 6. Variation of higher order dispersion parameters (a) TOD and (b) FOD with frequency**.**

The results obtained for the TOD and FOD are important for evaluating the pulse broadening that is due to higher order dispersion, as well as for evaluating nonlinear effects that are dependent on high order dispersion in the slow light regime. Their low values, tending to zero in a bandwidth of 2.1 THz, show that the proposed waveguide can be used for device applications such as multiplexing and demultiplexing, as well as in realizing delay lines for optical buffers.

4. Photonic crystal waveguide as an optical buffer

The optical Buffer is a device that temporarily stores and adjusts the timing of optical packets. Application of PhC waveguides with slow light in optical buffers has recently been attracting wide attention [10]. We shall now investigate the properties of the SOI-based elliptical air hole W1 channel waveguide for use as an optical buffer - and determine the limitations of slow light propagation in the proposed structure. The number of bits that can be stored in a

#111046 - $15.00 USD Received 6 May 2009; revised 18 Jun 2009; accepted 18 Jun 2009; published 20 Jul 2009

slow light device is given by its Delay Bandwidth Product (DBP). The expression for the DBP is:

$$DBP = T_d \,.\, B \tag{5}$$

where T_d is the time of propagation of a pulse in the waveguide and B is the bandwidth. If L is the length of the structure and the pulse is propagating with minimum distortion, the upper limitation on the DBP is given by [25]

$$DBP = T_d \,.B \le \frac{L}{\tilde{v}_g}\left(\frac{1}{4\pi L\,|\beta|}\right)^{1/2}$$

$$\Rightarrow DBP \le \left(\frac{L}{4\pi}\right)^{1/2} \frac{1}{\tilde{v}_g\,|\beta|^{1/2}} \tag{6}$$

Thus the DBP depends upon the length of the structure, the average group velocity and the GVD parameter. If the length of the structure is fixed, the DBP is inversely proportional to $\tilde{v}_g\,|\beta|^{1/2}$. i.e., in order to increase the value of DBP, we need to decrease the value of the average group velocity $\tilde{v}_g$ and the GVD parameter, β. We shall next calculate the upper limit of the DBP in the proposed SOI-based PhC having a hexagonal arrangement of elliptical air holes, in the slow light regime below the silica light-line. At frequencies $\omega_0 = 0.2709$ ($2\pi c/a$), i.e. for an incoming wave at $\lambda_0 = 1.55$ μm, the average group velocity is calculated to be 0.035c - and the average GVD parameter is $\beta = 0.5$ ps^2/km (from Fig. 5). Therefore, $\tilde{v}_g|\beta|^{1/2} \simeq 0.0247c.\text{ps km}^{1/2}$. This value is highly reduced as compared to the value of 4.4c ps.km$^{1/2}$ in reference [25]. Even for the slowest velocity achieved at a frequency of $0.27009(2\pi c/a)$ i.e. $\lambda_0 = 1.555$ μm, the average group velocity is 0.0028c and $\beta = 376$ ps^2/km - and therefore, $\tilde{v}_g|\beta|^{1/2} \simeq 0.0543c.\text{ps km}^{1/2}$. Hence we observe that the upper limitation on the delay bandwidth product is strongly enhanced in our structure.

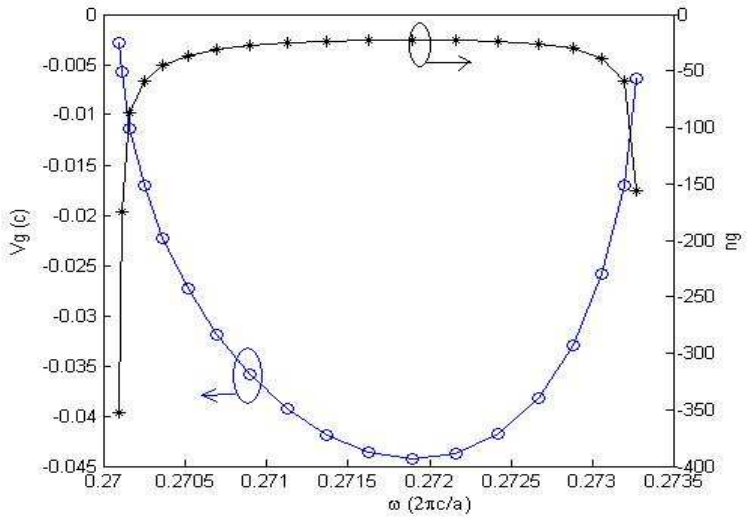

Fig. 7. Variation of group velocity and group index with frequency in the slow light region below the silica light-line.

#111046 - $15.00 USD Received 6 May 2009; revised 18 Jun 2009; accepted 18 Jun 2009; published 20 Jul 2009

The DBP, defined by T_d.B, provides a measure of the buffering capacity that a slow light device potentially provides. However its normalized form can become more useful if devices that have different lengths and different frequencies are compared. We shall now calculate the value of the normalized DBP for the proposed SOI based photonic-crystal channel-waveguide. Figure 7 shows the variation of the group index and group velocity with frequency. The average group index in the frequency range $\Delta\omega$ is calculated as:

$$\tilde{n}_g = \int_{\omega_0 - \Delta\omega/2}^{\omega_0 + \Delta\omega/2} n_g(\omega) \frac{d\omega}{\Delta\omega} \tag{7}$$

From Fig. 7, the average value of group index is- $\tilde{n}_g = 66.60$, in the normalized frequency bandwidth of $\frac{\Delta\omega}{\omega} = 0.0117$. The normalized DBP is calculated to be- $\tilde{n}_g \frac{\Delta\omega}{\omega} = 0.778$, which is substantially greater than that reported in references [14 and 22]. The normalized DBP calculated in [21] is equal to 0.359, which is also less than the value of 0.778 that we have calculated for the proposed structure. The proposed structure can therefore be used as an optical buffer with a high DBP value.

5. FDTD simulation

In this section an investigation is described for the broadening of pulses propagating through the waveguide of the proposed structure, using FDTD simulations. FDTD simulations are carried out using the RSOFT FULLWAVE package with the mesh size taken to be Period/3 and device dimensions- taken to be 6.72μm x 5.04μm in XZ plane. If we set the central frequency at $\omega_0 = 0.2709(2\pi c/a)$ i.e. at $\lambda_0 = 1.55$ μm, the group velocity and GVD parameter at this wavelength are 0.035c and 0.5 ps^2/km. As shown in Figure 8(a), for wavelength of 1.55 μm, time delay between the input peak and output peak is nearly 0.57 ps for a waveguide length of 15*a*. Hence the corresponding group velocity is 0.036c which is slightly larger than that observed using PWE method (i.e. 0.035c). The slowdown factor, which is defined as the ratio of the phase velocity to the group velocity ($S=v_p/v_g$) is calculated to be 17 at $\lambda_0 = 1.55$ μm. Thus the width of the Gaussian pulse at the output end is approximately equal to that of the pulse at the input end, with very little pulse expansion, as shown in Fig. 8(a). Here we have considered the length of waveguide to be 15*a*, as shown in Fig. 1. The incident pulse with a full width at half-maximum (FWHM) of 0.07 ps expands to 0.11 ps at the output. We observe the modal field distribution for an incident wave at a wavelength of 1.55 μm in Fig. 8(b) - which shows that the light spreads substantially into the first and second nearest rows of elliptical air holes of the PhC, due to the slow light propagation in the waveguide. Figure 8(c) shows the spreading of the wave for $\lambda_0 = 1.555$ μm - for which the slowest group velocity value of 0.0028c is achieved in the proposed SOI based photonic crystal waveguide.

#111046 - $15.00 USD Received 6 May 2009; revised 18 Jun 2009; accepted 18 Jun 2009; published 20 Jul 2009

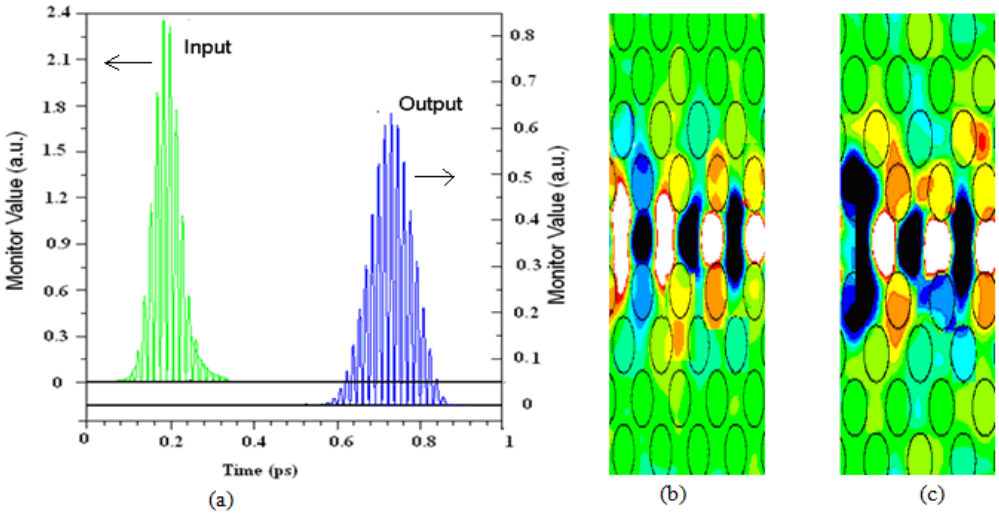

Fig. 8. (a) Field amplitude of the Gaussian pulse recorded at the input end and output end of the waveguide as a function of time for λ_0=1.55μm. Modal field distribution in the PhC waveguide for (b) 1.550 μm and (c) 1.555 μm.

6. Time and Wavelength Division Demultiplexing (TDM and WDM)

The proposed SOI based PhC, with elliptical air holes, is next investigated for use in time and wavelength division demultiplexing (TDM and WDM). It is found that the proposed structure has a bandgap in the frequency range of 0.2352 (2πc/*a*) to 0.3277 (2πc/*a*) as shown in Figure 4(a). Hence the bandgap exist for both the wavelengths, 1.31 μm, which corresponds to a frequency of 0.3206 (2πc/*a*) and 1.55μm, which corresponds to a frequency of 0.2709 (2πc/*a*).

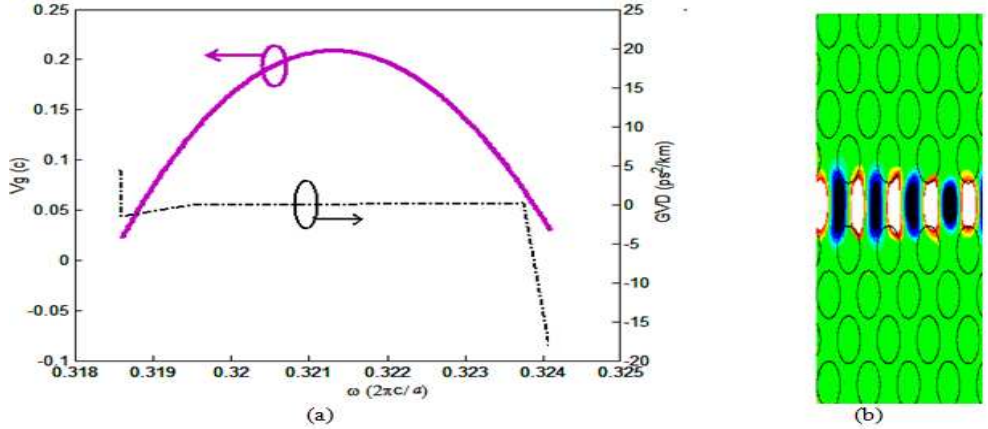

Fig. 9. (a)Variation of group velocity and Group Velocity Dispersion (GVD) parameter for region having central wavelength near 1.31μm (b) Modal field distribution in PhC channel waveguide for a wavelength of 1.31μm.

Figure 9(a) shows the frequency dependence of the group velocity and GVD parameter for a section of dispersion curve below the silica light-line. For an incoming pulse of light at a wavelength of 1.31 μm, the group velocity is calculated to be 0.178c and the GVD parameter is 0.0083 ps^2/km, which implies low signal distortion for a wavelength of 1.31 μm. Thus a signal at a wavelength of 1.31 μm is more than five times faster than one at 1.55 μm, where the velocity is equal to 0.035c. Therefore the channel guides a signal at a wavelength of 1.31μm at faster velocity -and hence it reaches the output end of the W1 waveguide earlier than a signal at the wavelength of 1.55 μm. The FDTD simulation for 1.31 μm is shown in

#111046 - $15.00 USD Received 6 May 2009; revised 18 Jun 2009; accepted 18 Jun 2009; published 20 Jul 2009

Fig. 9(b), indicating that the spread of light wave in theW1 waveguide at 1.31 µm is less than that for 1.55 µm, as observed in Fig. 8(b).

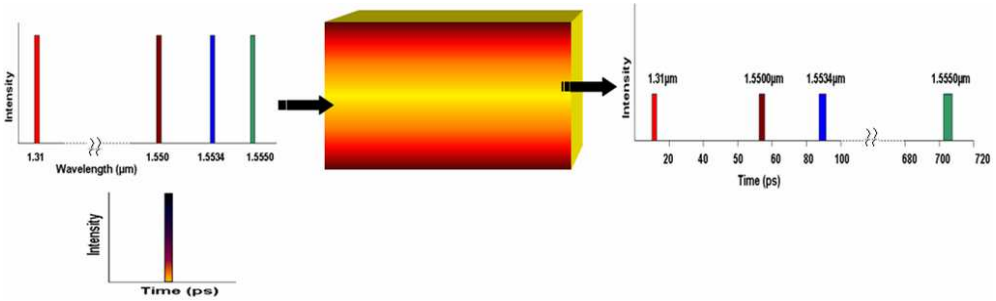

Fig. 10. Schematic for separation of pulses of light at telecom wavelength 1.31 µm, 1.5500 µm, 1.5534 µm and 1.5550 µm for time and wavelength division de-multiplexing.

If we now assume the device length to be 600 µm, the delay time for a wavelength of 1.55 µm is calculated to be 57 ps - and for a wavelength of 1.5534 µm it is calculated to be 89 ps. For a wavelength of 1.5550 µm, it is calculated to be 704 ps, while for a wavelength of 1.31 µm; it is calculated to be 11 ps (Fig. 10). Here we observe that even for the slowest velocity achieved i.e. 0.0028c, the GVD parameter is relatively small (on the order of 10^2 ps^2/km) and hence this waveguide PhC structure can be used in both time and wavelength division de-multiplexing.

7. Conclusions

In this paper, we have reported on the design of an SOI based PhC channel waveguide with elliptical air holes for use in slow light propagation with group velocities in the range from 0.0028c to 0.044c – and with extremely low GVD, TOD and FOD parameters. This combination of small values for key parameters causes an input signal to pass through the PhC waveguide with much less distortion. The proposed structure has considerable potential for use in photonic device applications such as optical buffers, TDM and WDM processing -as we have demonstrated.

Acknowledgements

The authors gratefully acknowledge the initiatives and support towards establishment of the "TIFAC Centre of Relevance and Excellence in Fiber Optics and Optical Communication at the Delhi College of Engineering, Delhi" through the "Mission REACH" program of Technology Vision-2020 of the Government of India. Two of the authors (R.K.Sinha and Richard M De La Rue) are also grateful to the Royal Academy of Engineering (UK) for providing financial support to carry out research and development work in the area of Photonic Crystal Devices.

#111046 - $15.00 USD Received 6 May 2009; revised 18 Jun 2009; accepted 18 Jun 2009; published 20 Jul 2009

Low-Loss Slow Light Transmission in Photonic Crystal Waveguides Comprising of Liquid Crystal Infiltration

Swati Rawal and R. K. Sinha

***Abstract*—A low loss photonic crystal (PhC) waveguide having rectangular air holes in Si core is proposed having an average group index of 55 in the bandwidth of 1.2 THz. The possible propagation losses due to inefficient coupling are also investigated for proposed structure. It is found that high transmission is obtained for a broad bandwidth from the output of the finally designed heterogeneous waveguide consisting of a slow liquid crystal infiltrated PhC waveguide surrounded by fast PhC waveguides on both sides.**

***Index Terms*—Liquid crystal, photonic crystal waveguide, slow light.**

doi: 10.3969/j.issn.1674-862X.2010.01.007

1. Introduction

Slow light which refers to reduction of group velocity, leads to increased light matter interaction thereby enabling time delay for optical signals which is a key component for processing, storing and buffering desired in future all optical communications and information processing systems[1]-[6]. However, tunability of photonic crystals (PhCs) can further be extended and controlled by filling its segments with certain liquid crystal material[7],[8]. They offer the possibility of shifting the frequency of the defect modes and tuning the dispersion curves for obtaining flat slow modes with low group velocity dispersion[9]. Propagation losses and their dependence on group velocity is another issue of concern which is tackled efficiently in the proposed paper to obtain a highly efficient slow light PhC waveguide with a simple design for easy fabrication.

2. Design Aspects

For the design, we consider the slow light system in silicon on Insulator (SOI) based rectangular air hole PhC waveguide consisting of 335 nm thick silicon layer followed by a 3000 nm thick silica layer.

Parameter scan was performed to achieve a flat section of dispersion curve below silica light line and for desired frequency range. The first neighboring row on either side of the waveguide created is filled with liquid crystal having ordinary refractive index as 1.6 and extra-ordinary refractive index as 2.2. Fig. 1 (b) allows us to trace a flat band slow light region for triangular lattice arrangement of rectangular air holes with X_1=223 nm and Y_1=335 nm and lattice constant a=420 nm along ΓK direction.

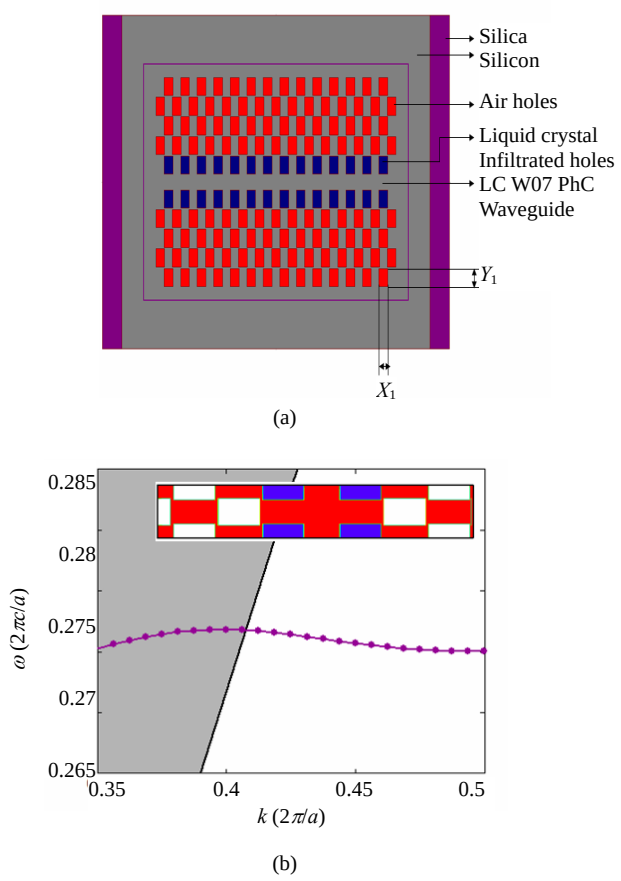

Fig. 1. Proposed SOI based liquid infiltrated photonic crystal waveguide: (a) schematic of the finally designed slow light PhC waveguide with rectangular air holes. First row closest to the waveguide on either side is infiltrated with liquid crystal, and (b) single guided dispersion curve with a flat section of dispersion curve for achieving slow light.

Manuscript revised December 29, 2009; presented at 2010 International Conference on Nanotechnology, Optoelectronics and Photonics Technologies (NOPT'2010), Singapore, February 26-28, 2010. This work was supported by the TIFAC Centre of Relevance and Excellence in Fiber Optics and Optical Communication at the Delhi College of Engineering, Delhi" through the "Mission REACH" Program of Technology Vision-2020 of the Government of India.

S. Rawal and R. K. Sinha are with TIFAC-Centre of Relevance and Excellence in Fiber Optics and Optical Communication, Department of Applied Physics, Delhi College of Engineering (Faculty of Technology, University of Delhi), Bawana Road, Delhi-110042, India. (email: swati.rawal@yahoo.com)

Color versions of one or more of the figures in this paper are available online at http://www.intl-jest.com.

3. Numerical Results

The structure designed in Section 2 shows a flat dispersion curve below the silica light line. The group velocity of such modes is defined as

$$v_g = \frac{d\omega}{dk}$$

where ω is the angular frequency and k is the wave vector along the waveguide whereas ground velocity dispersion (GVD) is defined as derivative of inverse group velocity w.r.t. angular frequency and is given as

$$\beta = \frac{dk}{d\omega} = -\frac{1}{v}\cdot\frac{d\omega}{dk}.$$

Here it is observed that if the group velocity converges to zero, the GVD parameter goes to infinity, which causes the spreading of an optical pulse in time. Keeping the above fact in view, we have designed our structure to obtain a flat-band situation that is characterized by small and nearly constant slope, with relatively low group index and GVD parameter.

In Fig. 2 the frequency dependence of the group index- and the GVD parameter on normalized frequency are plotted for the slow wave region shown in Fig. 1. High value of group index (~347) obtained at the extreme points is at the cost of high GVD on the order of 10^3 ps^2/km. Hence a very low GVD is obtained for a wide spectral width of 1.19 THz with an average group index of 54.7. We will now estimate the quantitative performance of the proposed SOI based LC W07 PhC waveguide. The upper limitation of DBP can be evaluated by reducing the value of $\tilde{v}|\beta|^{1/2}$ in

$$\mathrm{DBP} \le \left(\frac{L}{4\pi}\right)^{1/2} \frac{1}{\tilde{v}|\beta|^{1/2}}.$$

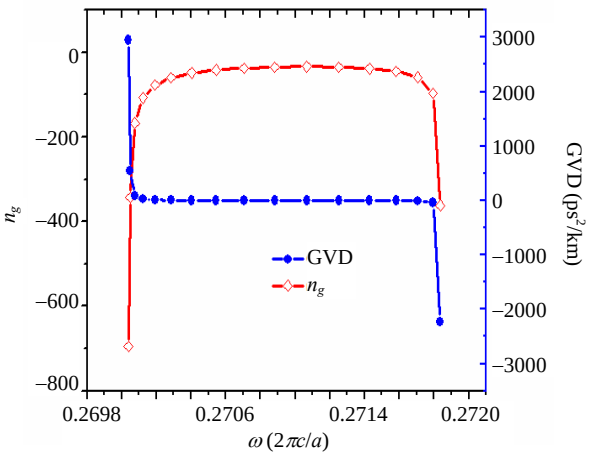

Fig. 2. Variation of group index and GVD parameter for flat section of dispersion curve plotted in Fig. 1(b).

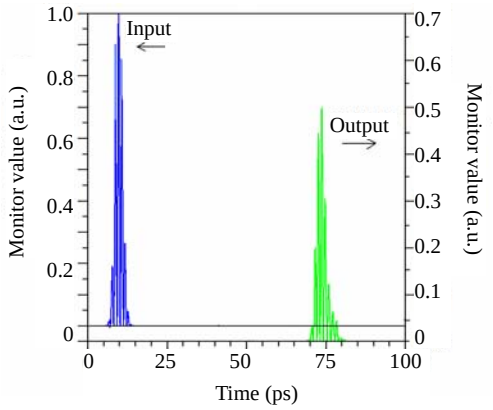

Fig. 3. Field amplitude of the pulse recorded at input and output ends of LC W07 PhC waveguide.

For the operating wavelength λ_2=1.55 μm i.e. for frequency of 0.2709 ($2\pi c/a$), the average group velocity is calculated to be 0.029c and GVD parameter β=0.0243 ps^2/km. Thus $\tilde{v}|\beta|^{1/2}$ =0.0007c ps·km$^{1/2}$. This value is highly reduced as compared to 4.4c ps·km$^{1/2}$ in [10].

We further calculated the slow down factor achieved in LC W07 PhC waveguide. It is defined as the ratio of phase velocity to group velocity ($S=V_p/V_g$) and is calculated to be 20.91 at λ=1.55 μm for designed rectangular hole infiltrated PhC waveguide. For a Gaussian pulse at central frequency ω_0=0.2709 ($2\pi c/a$) i.e. at λ_0=1.55 μm, v_g=0.029c and GVD=0.0243 ps^2/km. Due to this vanishing dispersion, the width of the pulse at input end is nearly equal to that at the output end as shown in Fig. 3.

4. Pulse Transmittance Measurements

An immediate problem arising from the designed slow light waveguide is its capability to couple slow mode efficiently into the slow light regime. This is because of the large impedance mismatch at the boundaries of PhC waveguide arising from large difference in group index. To solve this complex problem, we have added short intermediate fast PhC waveguides which act as coupler sections on both sides in addition to the slow light PhC waveguide obtained through liquid crystal infiltration. The calculated photonic band structures of the fast PhC waveguide with a stretched period (a'=450 nm) obtained using 3D PWE method is shown in Fig. 4. From the slope of dispersion curve of fast waveguide, it is observed that the velocity of a signal of 1.55 μm is 0.169c which is higher than that obtained in slow light LC W07 PhC waveguide (~0.029c) or homogeneous waveguide.

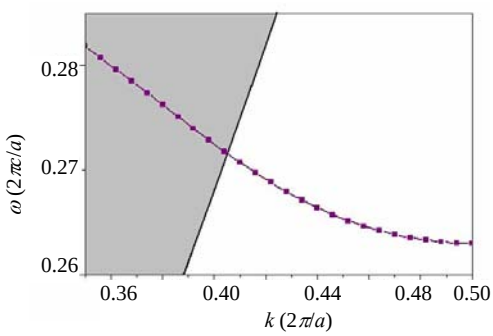

Fig. 4. Dispersion diagram for the fast photonic crystal waveguide having stretched period equal to a'=450 nm.

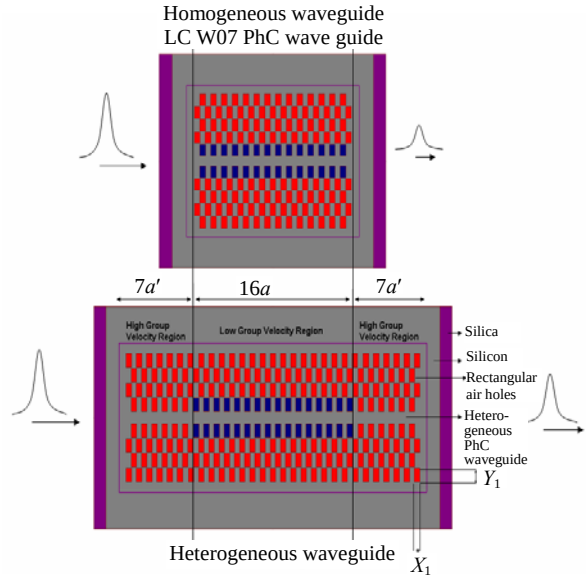

(a)

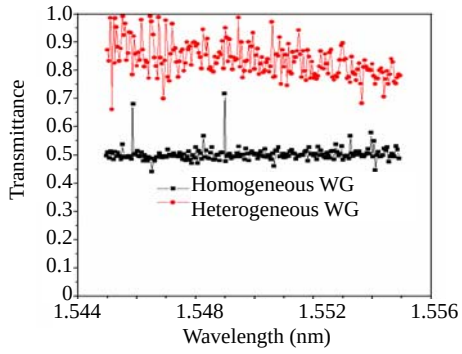

(b)

Fig. 5 Proposed heterogeneous LC infiltrated photonic crystal waveguide (WG): (a) schematic of the proposed heterogeneous PhC waveguide and (b) variation in transmittance from homogeneous and heterogeneous waveguide.

3D FDTD method is used for calculating the transmittance through the proposed heterogeneous PhC waveguide shown in Fig. 5 (a). Fig. 5 (b) summarizes the transmittance of the propagating pulse through heterogeneous PhC waveguide consisting of 16a long infiltrated LC W07 slow light waveguide surrounded by two coupler sections made up of high group velocity regions. As it is seen from Fig. 5 (b), transmittance of heterogeneous PhC waveguide for the described slow light flat band window ranging from 1.545 μm to 1.555 μm is higher than that obtained for homogeneous LC W07 PhC waveguide. This is because of the poor coupling obtained when light is directly inserted into the slow light infiltrated homogeneous LC W07 PhC waveguide due to larger impedance mismatch at the boundaries due to large group velocity difference. However, in case of heterogeneous waveguide, transmittance recovery is achieved in the slow light regime because of low impedance mismatch realized at the interface of fast and low velocity waveguides. Hence, the intensity reduction at this interface is not significant. Coupler based approach described in [11] and [12] can be used for efficient coupling into the slow light regimes.

5. Conclusions

We have proposed an SOI based liquid infiltrated photonic crystal W07 channel waveguide having rectangular air holes in Si core for achieving slow light propagation with an average group index of 55 in the bandwidth of 1.2 THz and vanishing group velocity dispersion. It was found that due to large impedance mismatch at the boundaries and large group velocity difference, the transmittance is very low. However, in case of heterogeneous waveguide, transmittance recovery is achieved in the slow light regime consisting of a slow liquid crystal infiltrated PhC waveguide surrounded by fast PhC waveguide on both sides.

Acknowledgment

The authors gratefully acknowledge the initiatives and support towards establishment of the “TIFAC Centre of Relevance and Excellence in Fiber Optics and Optical Communication at the Delhi College of Engineering, Delhi” through the “Mission REACH” program of Technology Vision-2020 of the Government of India.

References

[1] T. F. Krauss, “Why do we need slow light,” *Nature Photonics*, vol. 2, pp. 448-450, Aug. 2008.

[2] Richard M. De La Rue, “Slower for longer,” *Nature Photonics*, vol. 2, no. 12, pp. 715-716, 2008.

[3] Y. A. Vlasov, M. O’Boyle, H. F. Hamann, and S. J. McNab, “Active control of slow light on a chip with photonic crystal waveguides,” *Nature*, vol. 438, pp. 65-69, Nov. 2005.

[4] V. R. Almeida, C. A. Barrios, R. R. Panepucci, and M. Lipson, “All optical control of light on a silicon chip,” *Nature*, vol. 481, pp. 1081-1084, Oct. 2004.

[5] R. S. Jacobsen, K. Andersen, P. I. Borel, J. F. Pedersen, O. Hansen, M. Kristensen, A. Lavrinenko, G. Moulin, H. Ou, C. Peucheret, B. Zsigri, and A. Bjarklev, “Strained silicon as a new electro-optic material,” *Nature*, vol. 441, pp. 199-202, May 2006.

[6] R. S. Tucker, P. C. Ku, and C. J. Chang-Hasnain, "Slow light optical buffers: Capabilities and fundamental limitations," *J. Lightwave Technology*, vol. 23, no. 12, pp. 4046-4066, 2005.

[7] G. Alagappan, X. W. Sun, M.-B. Yu, P. Shum, and D. Den Engelsen, "Tunable dispersion properties of liquid crystal infiltrated into a two-dimensional photonic crystal," *IEEE J. Quant. Elect.*, vol. 42, no. 8, pp. 404-407, 2006.

[8] E. P. Kosmidou, E. E. Kriezis, and T. D. Tsiboukis, **"**Analysis of tunable photonic crystal devices comprising liquid crystal materials as defects," *IEEE J. Quant. Elect.*, vol. 41, no. 5, pp. 657-665, 2005.

[9] M. Ebnali-Heidari, C. Grillet, C. Monat, and B. J. Eggleton, "Dispersion engineering of slow light photonic crystal waveguides using microfluidic infiltration," *Optics Express*, vol. 17, no. 3, pp. 1628-1635, 2009.

[10] J. Ma and C. Jiang, "Flatband slow light in asymmetric line-defect photonic crystal waveguide featuring low group velocity and dispersion," *IEEE J. Quant. Elect.*, vol. 44, no. 8, pp. 763-769, 2008.

[11] N. Ozaki, Y. Kitagawa, Y. Takata, N. Ikeda, Y. Watanabe, A. Mizutani, Y. Sugimoto, and K.i Asakawa, "High transmission recovery of slow light in a photonic crystal waveguide using a hetero groupvelocity waveguide," *Optics Express*, vol. 15, no. 13, pp. 7974-7983, 2009.

[12] J. P. Hugonin, P. Lalanne, T. P. White, and T. F. Krauss, "Coupling into slow-mode photonic crystal waveguides," *Opt. Lett.*, vol. 32, no. 18, pp. 2638-2640, 2007.

Swati Rawal was born in Delhi, India, in 1983. She received the B.S. degree from Delhi University in 2004 and the M.S. degree from Chowdhary Charan Singh University, in 2006, both in physics with electronics as specialization. She is currently pursuing the Ph.D. degree with the Department of Applied Physics, Delhi College of Engineering (Faculty of Technology), University of Delhi, India. Her current research interests include photonic crystal waveguides, devices and slow light in Photonic crystals.

Ravindra K. Sinha received the M.S. degree in physics from the Indian Institute of Technology (IIT), Kharagpur, India, in 1984, and the Ph.D. degree in fiber optics and optical communication from the IIT, Delhi, India, in 1990. During 1989 to 1991, he was a postdoctoral research student at Osaka University for Foreign Studies, Osaka, Japan, and in the Electronics Engineering Department, Kobe University, Japan. He is currently a professor of applied physics and the chief coordinator of the technology information, Forecasting and Assessment Council (TIFAC)–Centre of Relevance and Excellence in Fiber Optics and Optical Communication, Delhi College of Engineering (Faculty of Technology, University of Delhi), Delhi. He is the author or coauthor of more than 100 publications in various national and international journals/conference proceedings/reports, etc. His current research interests include nanophotonics with special interests on photonic crystal fibers and photonic band gap devices. Prof. R. K. Sinha was awarded the Emerging Optoelectronics Technology Award (Conference on Emerging Optoelectronic Technologies–Institute of Electronics and Telecommunication Engineers (CEOT-IETE, India) for outstanding research work in the area of nanophotonics in 2006, S. K. Mitra Memorial Award for best research papers published in *IETE Technical Review* in 2002 on nanostructure electron waveguides and devices and Swarna Jayanti Puraskar (Gold Medal) from the National Academy of Science for best coauthored research papers in the area of nano scale optical devices for the year 2001. He has also been awarded the Japan Society for Promotion of Science (JSPS) Fellowship-2007 and the Royal Academy of Engineering (U.K.-India short-term exchange) Fellowship-2008 to carry out research work in the area of multi-core photonic crystal fiber and photonic crystal devices, respectively. He is a fellow of the IETE (India), a member of the SPIE, USA, and a member of the Optical Society of America (OSA, USA). He is also a Faculty Advisor to the SPIE-DCE Chapter.

Slow Light Propagation in Liquid-Crystal Infiltrated Silicon-On-Insulator Photonic Crystal Channel Waveguides

Swati Rawal, R. K. Sinha, and Richard M. De La Rue, *Fellow, IEEE*

***Abstract*—An SOI-based liquid-crystal (LC)-infiltrated photonic-crystal channel waveguide having rectangular air holes in a Silicon core is proposed—and has an average group index of 43 over a bandwidth of 1.02 THz, with vanishing group velocity dispersion, as well as reduced higher-order dispersion. The possible propagation losses due to coupling inefficiency are also investigated for the proposed structure. It is found that high transmission is obtained for a broad bandwidth from the output of the heterogeneous waveguide finally designed, which consists of an LC-infiltrated PhC slow waveguide surrounded by fast PhC regions on either side. The LC-infiltrated W0.7 PhC waveguide that has been designed for slow light propagation should be highly tolerant to fabrication errors—and has enhanced sensitivity in comparison with conventional PhC waveguides.**

***Index Terms*—Group velocity dispersion, liquid crystal infiltration, photonic crystal, slow wave structures.**

I. Introduction

SINCE their proposal by Yablonovitch and by John [1], [2] in 1987, photonic crystals (PhCs) with photonic bandgap (PBG) properties have attracted much attention as a possible platform for densely integrated photonic circuits and novel photonic functionality. By carefully engineering the photonic dispersion relationship, one may obtain unique opportunities for realization of devices that exploit slow light effects [3]–[6]. PhC channel waveguides can be used as defect-mode slow light structures. Slow light, which refers to reduction of the group velocity, leads to increased light-matter interaction strength, thereby enabling increased time-delay for optical signals, which is a key functionality for the processing, storing and buffering desired in future all-optical communications and information processing systems [7]–[12]. Slow light in PhC waveguide structures has already been investigated by a number of authors [13]–[16], near the edge of the Brillouin zone. It is typically accompanied by large amounts of dispersion, which can remove much of the advantage of operation in the slow light regime—because it limits the bandwidth that can be utilized [17]. This bandwidth-dispersion issue can be overcome by tuning the structure towards dispersion-free behaviour [18]. This approach has resulted in more complex devices, fabrication of which is challenging and hence potentially limits their practical utilization. Recently we have demonstrated the feasibility and benefits of using an elliptical air-hole based photonic crystal structure to obtain slow light behaviour [19]. However, it has been shown by a number of authors that square hole photonic crystal structures present better performance in comparison with circular hole PhC structures in terms of transmittivity, loss characteristics and maximization of the transmission bit rate of the signal in optical networks. Even the group index obtained in the low GVD regime of PhC channel waveguides is higher in square hole waveguides than in circular hole waveguides [20]–[22]. The tunability of PhC lattices can further be extended and controlled by filling their segments with certain types of liquid crystal (LC) material [23], [24]. This combination offers the possibility of shifting the frequency of the defect modes and tuning the dispersion curves, in order to obtain flat slow modes with low group velocity dispersion (GVD) [25]. Liquid Crystal (LC) material has been simulated using an anisotropic form of the finite-difference time-domain (FDTD) method [26]. Since dynamically tuned devices are essential components in optical systems, PhC waveguide configurations with microfluidic infiltration of *LC* material offer a strong potential for realizing integrated micro-photonic devices. C.L.C. Smith and co-workers [27] have described how the required *LC* infiltration in a PhC can be achieved by using a tapered glass micro-tip. The droplets that are attached to the length of capillary tube due to adhesive forces between glass and liquid are deposited on a device chip besides the PhC structure. A microscope objective is used—which resolves properly the air holes in the PhC and provides sufficient working distance for the tapered microtip to draw the chosen droplet along the airhole, perpendicular to the PhC waveguide, during infiltration. Propagation losses and their dependence on group velocity are another matter of concern. There is little justification in exploring the slow light regime if any advantage

Manuscript received February 11, 2010; revised May 03, 2010; accepted June 08, 2010. Date of publication June 28, 2010; date of current version August 20, 2010. This work is carried out at "TIFAC Centre of Relevance and Excellence in Fiber Optics and Optical Communication in Delhi Technological University (Formerly Delhi College of Engineering, Delhi University), Delhi" through the "Mission Reach" program of Technology Vision-2020, Government of India. The work of R. K. Sinha and Richard M De La Rue was supported in part by the Royal Academy of Engineering (U.K.) to carry out research and development work in the area of Photonic Crystal Devices.

S. Rawal and R. K. Sinha are with TIFAC—Centre of Relevance and Excellence in Fiber Optics and Optical Communication, Department of Applied Physics, Delhi Technological University (Formerly Delhi College of Engineering, Delhi University) Delhi-110042, India (e-mail: swati.rawal@yahoo.com; dr_rk_sinha@yahoo.com).

R. M. De La Rue is with Optoelectronics Research Group, Department of Electronics and Electrical Engineering, University of Glasgow, G12 8LT, Scotland, U.K. (e-mail: r.delarue@elec.gla.ac.uk).

Color versions of one or more of the figures in this paper are available online at http://ieeexplore.ieee.org.

Digital Object Identifier 10.1109/JLT.2010.2053915

obtained is immediately counteracted by excessive losses. These losses include losses due to backscattering (into the guided Bloch modes), with propagation in the opposite direction—and losses due to inefficient coupling. Backscattering is mainly disorder-induced and increases with the inverse group velocity squared [28]–[30]. Hence, it is dominant in the case of slow group velocities, while inefficient coupling occurs due to the large mismatch at the interface between the slow light PhC waveguide that results from large changes in group index. This mismatch can be considered, in a general sense, as a form of impedance mismatch that involves conservation of power flow and the possibility of energy storage in evanescent modes. One way of overcoming the problem of impedance mismatch is the use of adiabatic tapers [31], but these tend to be relatively long and the construction of systematic design procedures is challenging. An alternative way is to introduce a finite region that firstly couples the light from a ridge or stripe waveguide into a fast mode PhC waveguide and then into the slow mode PhC waveguide [32]–[35]. Such issues of concern are tackled directly in the present paper—in order to obtain a highly efficient slow light PhC waveguide with a simple design that is suitable for fabrication.

In this paper we report the design of an SOI based PhC structure that has a silicon core sandwiched between a silica cladding layer below the core and an air cladding region above. A hexagonal lattice arrangement of rectangular air holes is introduced into the silicon waveguide core. Since it is an asymmetric structure vertically, the Bloch modes of the waveguide cannot be strictly classified into purely transverse electric (TE) and transverse magnetic (TM) modes, since each Bloch mode has an even as well as an odd distribution component. For the even modal components, the magnetic field should lie in the direction perpendicular to the plane of the structure, i.e., along the y-direction—and, for odd components, the electric field should lie along the y-direction. In general a mixture of all six field components is obtained for the modal distributions when periodic structuring is added. This periodic structuring leads to Bloch modes having only quasi-TE or quasi-TM characteristics. Modes with $\mathrm{H_y}$ as the predominant component are referred to as TE-like modes and those with $\mathrm{E_y}$ as the predominant component are referred to as TM-like modes [36]. The PhC structure is designed to exhibit a full PBG for TE-like modes. Therefore, these modes are horizontally confined by PBG effects and vertically by total internal reflection. The rectangular holes are then filled with *LC* material, which provides an extra free parameter for achieving very small dispersion slow light waveguides. The infilling *LC* material is assumed to occupy only the exact depth of the holes in the silicon waveguide core—and only in one row of holes on either side of the waveguide. Fig. 1 gives a schematic of the proposed design, with the first neighbouring holes on either side of the W0.7 waveguide having liquid crystal infiltration. The minimum values for the losses and defect mode dispersion below the silica light-line are found for the W0.7 waveguide. For this reason, a typical structure employed in the experiments is a W0.7 PhC waveguide [29], [31], [37], [38]. For the device application of such waveguides, the group velocity dispersion (GVD) and other higher order dispersion parameters should be very low, thereby enabling the optical signal

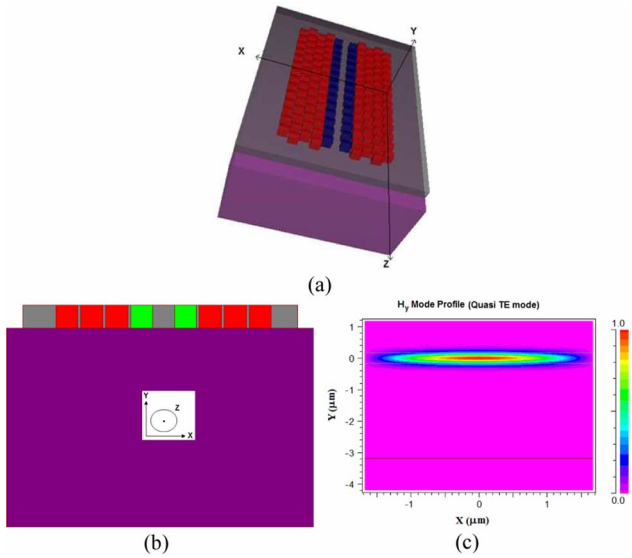

Fig. 1. (a) Schematic of the proposed design with the first neighboring holes on either sides of the W0.7 waveguide having Liquid Crystal infiltration. (b) XY view of slow light photonic crystal channel waveguide with (c) field component of the quasi-TE guided mode.

to propagate with least distortion, as we have demonstrated previously [19]—and will demonstrate again in the present paper. We shall also describe the tolerance analysis of the proposed structure with respect to variations in the waveguide geometry and variations in the refractive index of the liquid crystal and silicon core. The sensitivity of the proposed LC-infiltrated PhC channel waveguide is also compared with that of conventional waveguides. The structure designed has also been investigated for possible propagation losses, which include losses due to coupling inefficiency. It is found that high transmission is obtained over a broad bandwidth for the hetero-waveguide finally designed, which consists of a locally *LC* infiltrated slow PhC channel waveguide terminated at either end by fast PhC waveguide sections.

II. Slow Light in Photonic Crystal Waveguides

Line defect PhC waveguides can lead to guided mode bands that can either be index-guided or bandgap guided—or a combination of both. anticrossing between these two types of mode can determine the local shape of dispersion curves, the slope of which determines the group velocity of the mode [16], [37], [39] and [40]. These guided mode bands can be made as flat as desired by appropriate design for the achievement of slow group velocity, together with low group velocity dispersion (GVD), over a broad bandwidth. In order to obtain slow guided modes with low group velocity and a vanishing GVD parameter, two basic requirements have to be fulfilled. The first one is structure oriented, i.e., the geometrical properties (waveguide width, hole size or position) are modified to obtain a flat section of dispersion curve, with not only small but constant slope—over a given range of frequencies—because, otherwise, higher order derivatives of the dispersion curve will lead to GVD, third-order dispersion (TOD) and fourth-order dispersion (FOD). The second requirement is loss oriented, i.e., the possibility of operation

of the waveguide below the silica light-line is considered—because modes that lie above the light-line are intrinsically lossy (i.e., leaky) out-of-plane. The Finite Difference Time Domain (FDTD) method and the Plane Wave Expansion (PWE) method [41] are two powerful numerical tools that can be used to simulate Maxwell's Equations with minimal approximation. They are known to be able to reproduce experimental results very closely. RSOFT's version 8.1 is used for carrying out PWE and FDTD analysis. Some useful parameters for characterization of PhC waveguides are:

1) *Group Velocity*: which is defined as the velocity at which the envelope of a short pulse propagates through space—and is expressed as [42]

$$\mathrm{v_g} = \frac{\mathrm{d}\omega}{\mathrm{dk}} \tag{1}$$

$$\text{Group index } n_g = \frac{c}{v_g} \tag{2}$$

The average values of group velocity and group index in frequency range $\Delta\omega$ are given as

$$\widetilde{v}_g = \int_{\omega_0-\Delta\omega/2}^{\omega_0+\Delta\omega/2} v_g(\omega)\frac{d\omega}{\Delta\omega} \tag{3}$$

and

$$,\widetilde{n}_g = \int_{\omega_0-\Delta\omega/2}^{\omega_0+\Delta\omega/2} n_g(\omega)\frac{d\omega}{\Delta\omega} \tag{4}$$

2) *Group Velocity Dispersion (GVD):* is defined as the derivative of the inverse group velocity i.e.

$$\beta = \frac{d^2k}{d\omega^2} = \frac{d}{d\omega}\left(\frac{1}{d\omega/dk}\right) = -\frac{1}{(d\omega/dk)^3}\frac{d^2\omega}{dk^2}$$

$$\beta = -\frac{1}{v_g^3}\frac{d^2\omega}{dk^2} \tag{5}$$

It is observed that to obtain a distortion-less slow light pulse, i.e., low GVD parameter, the value of group velocity should be small—and with nearly constant slope.

3) *Third order Dispersion (TOD) and Fourth order Dispersion (FOD)*: TOD and FOD are expressed as

$$\mathrm{TOD} = \frac{1}{v_g}\frac{\partial(\mathrm{GVD})}{\partial k} \tag{6}$$

$$\text{and FOD} = \frac{1}{v_g}\frac{\partial(\mathrm{TOD})}{\partial k} \tag{7}$$

4) *Delay-Bandwidth-Product (DBP):* which defines the number of bits stored in a slow light device—and is expressed as

$$\mathrm{DBP} = \mathrm{T_d}\cdot\mathrm{B} \tag{8}$$

where $\mathrm{T_d}$ is the delay time of the propagating pulse and B is the bandwidth. For a given length L of the structure, the upper limit on the DBP is given by [43]

$$\mathrm{DBP} \le \left(\frac{L}{4\pi}\right)^{1/2}\frac{1}{\widetilde{v}_g|\beta|^{1/2}} \tag{9}$$

Therefore, in order to increase the value of the DBP, one has to decrease the value of the product $\widetilde{v}_g|\beta|^{1/2}$ for a fixed length L of the device. For comparison of devices having varying lengths, the normalized form of DBP can be useful—and is defined as $\mathrm{DBP} = \widetilde{n}_g\frac{\Delta\omega}{\omega}$.

A. Design Aspects

For the design, we first consider the possibilities for slow light propagation in an SOI based waveguide PhC structure realized in a 335 nm thick silicon layer supported by a 3000 nm thick silica $(\mathrm{n} = 1.45)$ layer, with air above the silicon waveguide core. The hexagonal periodic arrangement of square holes having $\mathrm{width} = 300$ nm and lattice constant $a = 420$ nm is embedded in silicon $(\mathrm{n} = 3.50)$.

Fig. 2(a) shows the plane view schematic of the square hole SOI structure designed to obtain a flat dispersion curve. The PhC structure that has been designed exhibits a bandgap for TE-like modes between $\omega_{\min} = 0.2573(2\pi c/a)$ and $\omega_{\max} = 0.4311(2\pi c/a)$, as shown in Fig. 2(b). In order to guide Bloch modes in the structure, a line defect W0.7 PhC waveguide is conceptually created by removing a row of square holes along the Γ K direction and shifting the two PhC regions closer to one another—resulting in a PhC waveguide width 0.7 times that of W1, i.e., a W0.7 PhC waveguide. The dispersion diagram shown in Fig. 2(c), which was obtained using the 3-D PWE method, indicates the existence of only a single guided mode below the silica light-line. By examining the dispersion diagram in Fig. 2(c), we have found that only a modestly enhanced group index (~ 15) with high GVD ($\sim 10^5$ ps^2/km) is achieved for this situation, limiting its possible use in slow light based PhC devices.

In order to satisfy the two requirements, (structure-oriented and loss-oriented) for achieving slow light systems, we have chosen to change the embedded square air holes into an array of rectangular air holes by varying the width of the X axis (X1) and Z axis (Z1) of each square, while retaining the hexagonal lattice arrangement. A parameter scan was performed in order to tailor the dispersion properties of the waveguide and is shown in Figs. 3(a) and (b). As mentioned earlier, these are dispersion curves for W0.7 PhC waveguides oriented along the Γ K direction, with different values of X1 and Z1 for the square air holes.

In Fig. 3(a), the value of Z1 is fixed at 330 nm, while in Fig. 3(b) the value of X1 is fixed at 220 nm. A parameter scan was then performed to achieve a flat section of dispersion curve below the silica light line and for the desired frequency range. Fig. 3 makes it possible to trace a flat-band slow-light region for $\mathrm{X1} = 223$ nm and $\mathrm{Z1} = 335$ nm. Hence, a slow light waveguide is achieved for triangular lattice rectangular air holes with $\mathrm{X1} = 223$ nm and $\mathrm{Y1} = 335$ nm together with a lattice constant of $a = 420$ nm, along the Γ K direction.

For these parameter values, the bandgap ranges from $\omega_{\min} = 0.2579(2\pi c/a)$ to $\omega_{\max} = 0.3217(2\pi c/a)$, as shown in Fig. 4(a). The dispersion diagram for this W0.7 waveguide design is shown in Fig. 4(b), together with the super-cell used in the 3-D PWE method.

However, an even slower group velocity, together with less GVD, can further be achieved by the use of liquid crystal (LC)

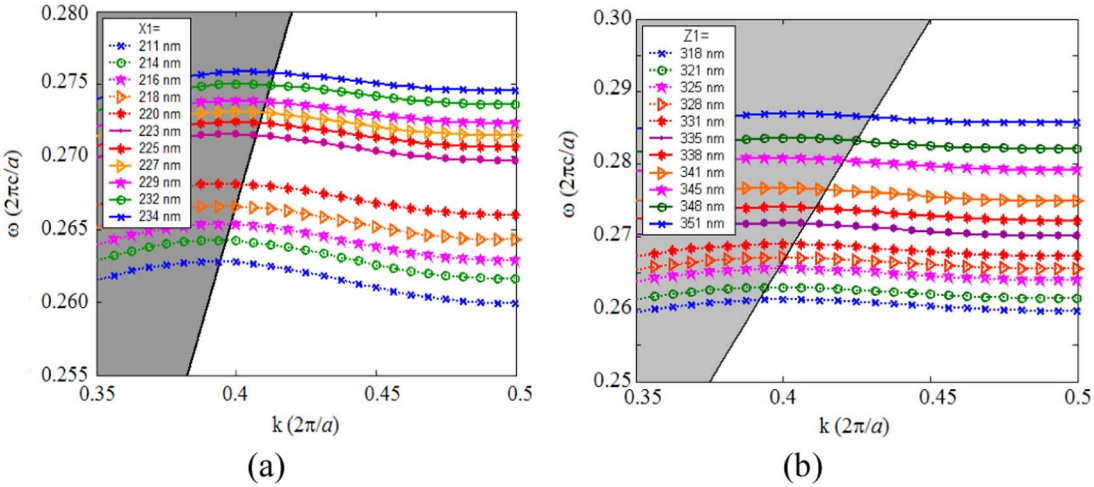

Fig. 3. Movement of the dispersion curves when (a) X1 and (b) Z1 vary gradually. The black solid line is the silica light-line.

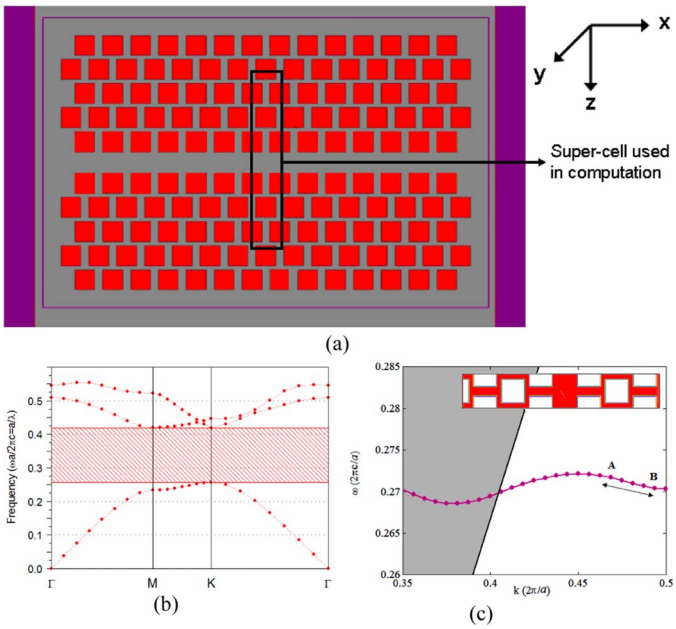

Fig. 2. (a) Plane view schematic of square hole SOI structure showing the supercell used in the computation, (b) TE bandgap map and (c) dispersion diagram having flat section AB of guided mode with lattice constant $a = 420$ nm and square hole width as 300 nm. The black solid line is the silica light-line, while the red line is the dispersion curve. The inset in the figure (c) shows the super-cell used in 3-D PWE calculation.

infiltration. The combination of the rectangular hole PhC structure with such micro-fluidic regions gives an extra free parameter in the waveguide design, which allows the fine tuning of its group velocity and dispersion.

B. Vanishing Dispersion Slow Light in Photonic Crystal Waveguides With Liquid Crystal Infiltration

Liquid crystals (LCs) offer a tuning mechanism for achieving slow light waveguides with highly reduced GVD, as their refractive index can be varied with temperature change—or by applying a local electric field [44]. Selective liquid crystal infiltration in the some of the rectangular air holes of the PhC channel waveguide offers the possibility of shifting the frequency of the defect mode in the desired range—and obtaining a flat section of dispersion curve with small but constant slope. In order to investigate the shape of the dispersion curve, calculations on the *LC* infiltrated photonic crystal were carried out using the PWE method. The refractive index of TE polarized light or TM polarized light depends upon the alignment of the optic axis of the liquid crystal inside the rectangular holes. If we now assume that the extraordinary axis lies along the y axis parallel to the main axis of the holes, then the TM-like polarization, with the electric field aligned along the y-axis, samples only the extraordinary index of refraction, and TE-like polarization, with the electric field lying in the x-z plane, samples only the ordinary index of refraction. Hence, the calculation for TE polarized light was carried out using the ordinary refractive index of liquid crystal [45]. The *LC* material that we have used to generate refractive index values for our calculations is a phenyl acetylene derivative (nematic LC), that has an ordinary refractive index $\mathrm{n_o}$ equal to 1.6 and an extraordinary refractive index $\mathrm{n_e}$ equal to 2.2. [23], [46].

The first row of rectangular air holes closest to the W0.7 waveguide on either side is infiltrated with the LC, in order to obtain a flat dispersion curve with vanishing GVD, as displayed in Fig. 5(b). The region chosen for slow light transmission varies over the range $0.4 < \mathrm{k}(2\pi/a) < 0.5$ because, in this region, the dispersion curve satisfies the single mode guidance condition below the silica light-line and has a flat section with small but constant slope. Fig. 5(a) shows a schematic of the SOI-based *LC* W0.7 PhC waveguide with liquid crystal infiltration.

We have then compared the group index $\mathrm{n_g}$ and the GVD for the flat band obtained from the W0.7 PhC waveguide shown in Fig. 4(b) and the one obtained from the *LC* W0.7 PhC waveguide shown in Fig. 5(b). The results obtained are shown in Fig. 6(a) and (b). As can be observed, the average group index $\widetilde{n}_g$ increases from 8 in the W0.7 PhC waveguide to 54.7 in the partially LC-infilled W0.7 PhC waveguide, because of the increased effective index of the waveguide produced by liquid crystal infiltration. However, the variation in β is comparatively small, since it reduces from 1 $\mathrm{ps^2/km}$ in the W0.7 PhC waveguide to 0.2 $\mathrm{ps^2/km}$ in the partially LC-infilled W0.7 PhC waveguide, for frequencies near the centre of the slow group velocity band. The high value of the group index ($\sim$ 347) obtained at

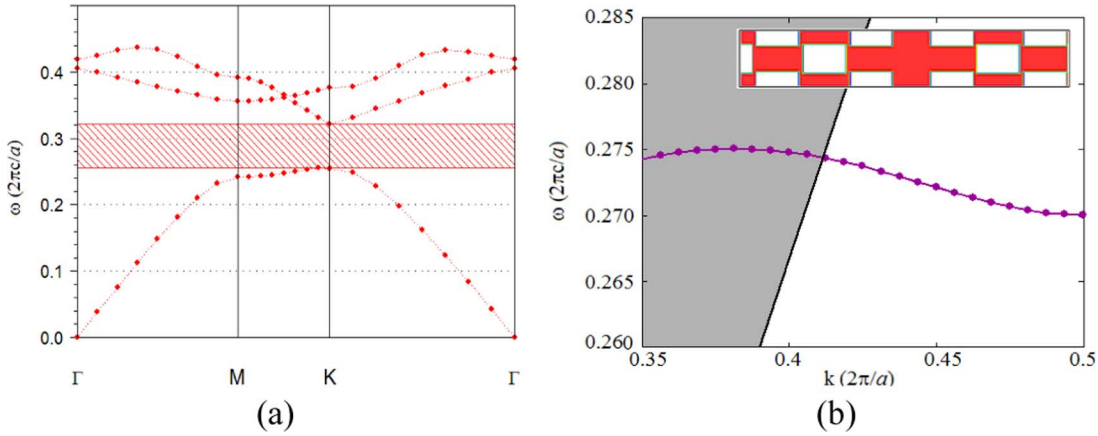

Fig. 4. (a) TE bandgap map for the PhC having rectangular air holes with parameters $\mathrm{X1} = 223$ nm and $\mathrm{Z1} = 335$ nm. (b) Dispersion curve with single mode guidance for the designed structure. Inset shows the supercell used in 3-D PWE method.

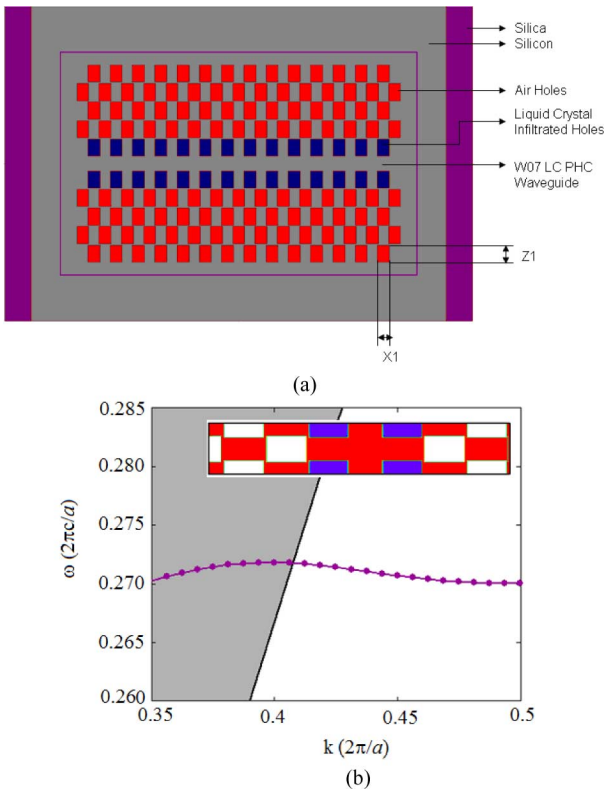

Fig. 5. (a) Schematic of the final design for the slow light PhC waveguide with rectangular air holes. The first row closest to the waveguide on either side is infiltrated with liquid crystal. (b) Single guided dispersion curve with a flat section of dispersion curve for achieving slow light.

the extreme points is at the cost of high GVD, on the order of 10^3 ps^2/km.

As a result, it is possible to identify a region of very low GVD over the wide spectral width of 1.02 THz, with an average group index of 43.05. Since the value of the GVD parameter β is nearly constant in a region near the centre of the range, the values of the TOD and FOD are also low, as observed in Fig. 6(c). The upper limit of the TOD is on the order of 10^4 ps^3/km, for the slow light regime, below the silica light-line. However near the centre it varies from 10^1 to 10^2 ps^3/km. Similarly the upper limit of the FOD is on the order of 10^6 ps^4/km, but near the centre it varies from 10^2 to 10^3 ps^4/km. These results indicate that the higher order dispersion is strongly suppressed in the proposed partially LC-in-filled W0.7 PhC waveguide for a bandwidth of 1.02 THz, with average group index of 43.05, which further suppresses the pulse broadening and non-linear effects that are dependent on the higher-order dispersion parameters. As a result, the proposed partially infiltrated PhC waveguide has considerable potential for device applications such as multiplexers and de-multiplexers, delay lines and optical buffers. We shall now estimate the quantitative performance of the proposed SOI based partially LC-infilled W0.7 PhC waveguide.

From (9), the high value for the upper limit of the delay-bandwidth product (DBP) can be evaluated by reducing the value of $\widetilde{v}_g|\beta|^{1/2}$. At the operating wavelength, $\lambda = 1.55$ μm, i.e., for a frequency of 0.2709 ($2\ \pi$ c/ a), the average group velocity is calculated to be 0.029c and the GVD parameter is $\beta = 0.0243$ ps^2/km.

Therefore $\widetilde{v}_g|\beta|^{1/2} = 0.0007c$ ps.km$^{1/2}$. This value is highly reduced as compared to the value of 4.4c ps.km$^{1/2}$ in [38]. We therefore observe that, for a given length of waveguide, the upper limitation on the DBP is greatly enhanced in our structure. The normalized DBP ($= \widetilde{n}_g(\Delta\omega)/(\omega)$) is calculated to be 0.226, which is sufficiently large for the possible use of tunable slow light PhC waveguides in optical buffers.

We have further calculated the slow-down factor achieved in the partially LC-infilled W0.7 PhC channel waveguide. It is defined as the ratio of phase-velocity to group-velocity ($\mathrm{S} = \mathrm{V_p/V_g}$)—and is calculated to be 20.91 at $\lambda = 1.55$ μm, for the designed rectangular-hole PhC-infiltrated channel waveguide. Assuming that the optical axis of the *LC* in-fill is perpendicular to the periodic plane, i.e., it lies parallel to the y-axis, then we obtain the dielectric tensor $\varepsilon = \mathrm{diag}(\mathrm{n_o}, \mathrm{n_e}, \mathrm{n_e})$ [47]. Applying 2-D FDTD method, TE polarized analysis of PhC waveguide along Γ K direction is obtained in Fig. 7. For a Gaussian pulse at a centre frequency of $\omega_0 = 0.2709(2\pi$ c/a), i.e., at $\lambda_0 = 1.55$ μm, $\mathrm{v_g} = 0.029$c and the GVD $= 0.0243$ ps^2/km. Due to this vanishing dispersion, the width of the pulse at the input end is nearly equal to that at the output end, as shown in Fig. 7(a). The length of waveguide is nearly 16 a, where a is

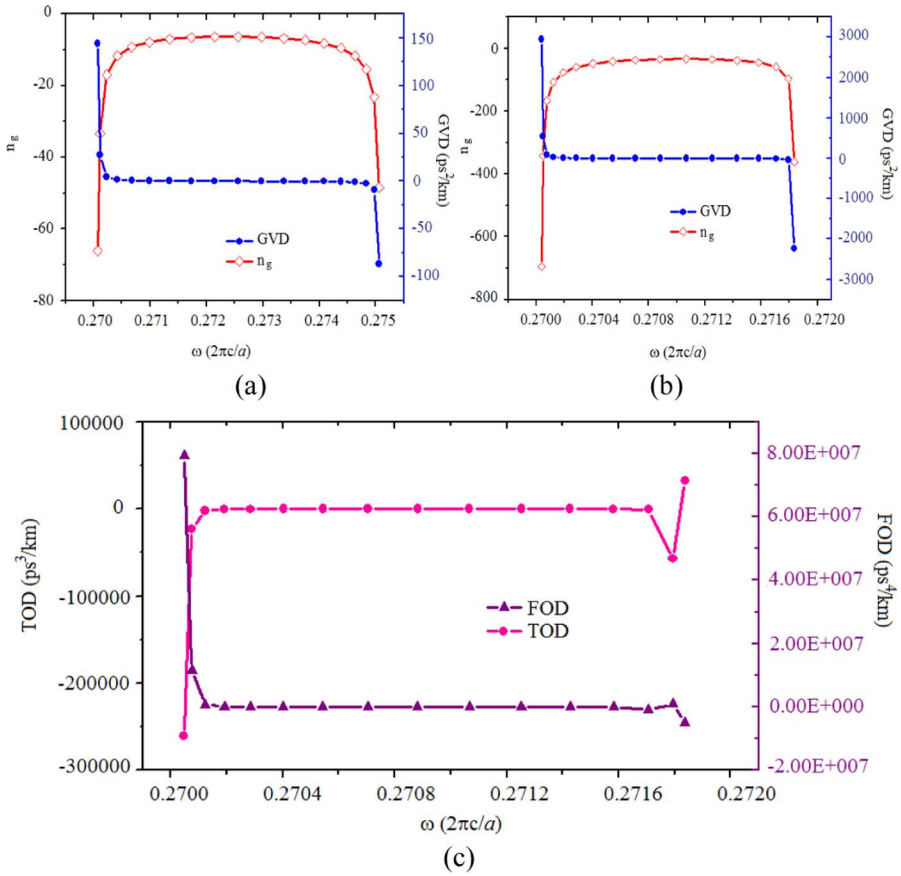

Fig. 6. Variation of group velocity and GVD parameter for the flat section of dispersion curve, for: (a) a W0.7 PhC waveguide and (b) the partially infilled *LC* W07 PhC waveguide. (c) Variation of higher order dispersion parameters TOD and FOD for *LC* W0.7 PhC waveguide with frequency in slow light region.

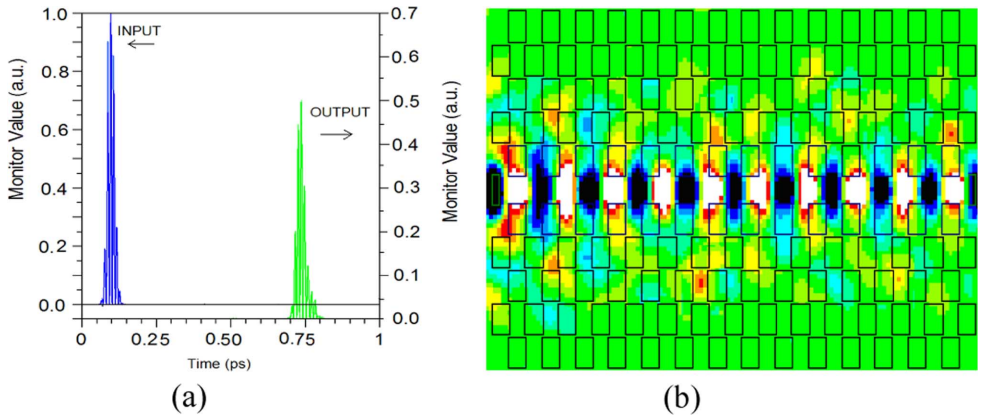

Fig. 7. (a) Field amplitude of the pulse recorded at the input and output ends of the partially LC-infiltrated W0.7 PhC waveguide. (b) Modal field distribution at $\lambda = 1.55\ \mu$m.

the lattice constant. The modal field distribution for the input wave is shown in Fig. 7(b). It can be seen that the incident pulse spreads substantially into the neighbouring rows of partially LC-infilled W0.7 PhC waveguide, due to the slow light propagation.

III. Tolerance Analysis

In this section we describe a study of the tolerances associated with the infiltration based approach for variations in the parameters of the rectangular air holes—and for variation in the refractive index of the Si core and infiltrated liquid crystal regions.

A. Parameter Tolerances for Rectangular Air Holes

Firstly we shall show how the group index of the designed, SOI-based, partially LC-infiltrated W0.7 PhC waveguide varies with a $\pm 4\%$ variation in either X1 or Z1—and Fig. 8(a) and (b) show this variation. Fig. 8(c) and (d) show the corresponding

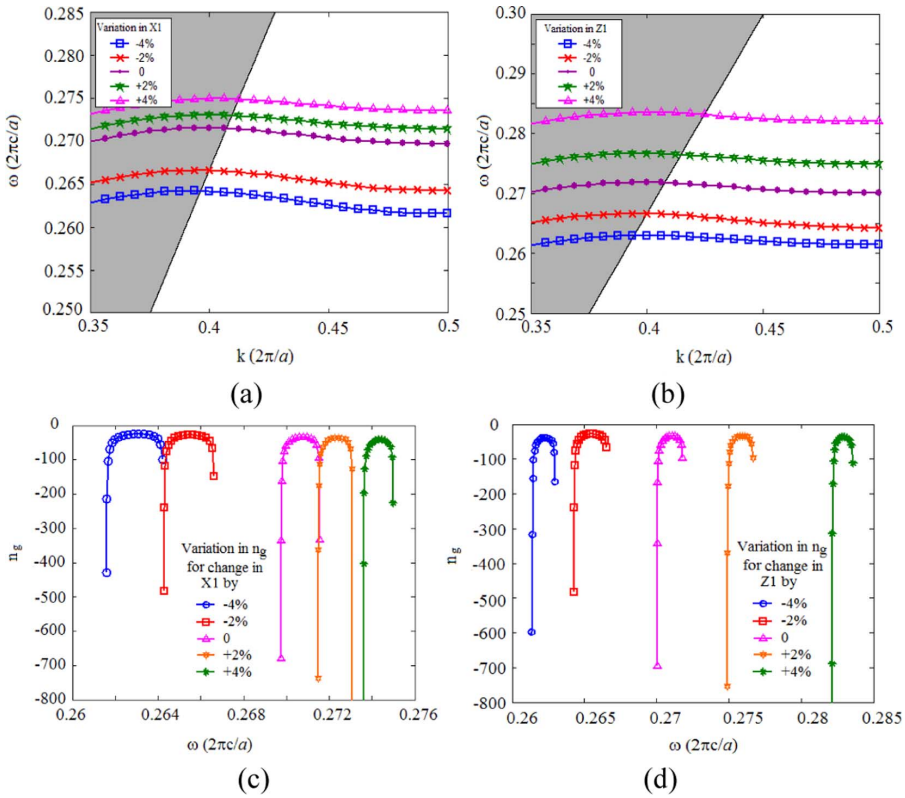

Fig. 8. (a) and (b) show the shift in the dispersion curve with $\pm 4\%$ variation in X1 or Z1. (c) and (d) show the corresponding change in the group index of the partially LC-infilled W07 PhC waveguide.

change in the group index of the partially LC-infiltrated W0.7 PhC waveguide.

It can be seen that changes in the parameters of the rectangular air holes, by $\pm 4\%$, shift the dispersion curve up in frequency—but that there is less than 2.5 dB change in the group index for this particular frequency range, i.e., it still remains constant near the centre—and hence much less variation can be seen in the DBP (Delay Bandwidth Product).

B. Tolerance in Refractive Index

Tolerance analysis of the device will be carried out for variations in the refractive index of the silicon core and of the liquid crystal used. Fig. 9(a) shows the shift in the dispersion curve when the refractive index of Si changes by ± 0.05. Corresponding variations in the group index are shown in Fig. 9(b). Similarly, Fig. 9(c) shows the shift in the dispersion curve for $\Delta \mathrm{n} = \pm 0.05$ variation in the ordinary refractive index of the liquid crystal in-fill—and the corresponding variation in the group index is shown in Fig. 9(d).

It can be seen that the small variations in refractive index (less than 20 %) incurred during PhC fabrication or changes in temperature still allow us to achieve the flat-band situation corresponding to the slow light regime with nearly constant group velocity—and near the centre. In the above, we have shown that the proposed SOI based partially LC-infilled W0.7 PhC waveguide is highly tolerant for small variations in refractive index—and there is no significant change in the group index of the partially LC-infilled W0.7 waveguide produced by such fabrication errors. The average group index in the respective ranges of frequency remains approximately the same—with a variation of less than 25 %.

C. Material Dispersion Considerations

Material dispersion, which corresponds to the dependence of refractive index on the optical frequency, is now considered in the PWE method. We first calculate the guided modes in LC-infilled PhC waveguides for different refractive indexes of Si, as shown in Fig. 9(a). Reference data of refractive index for material dispersion of Si is calculated by using the Sellmeier-type formula [48], [49]

$$n^2 - 1 = \frac{C_1\lambda^2}{(\lambda^2 - C_2^2)} + \frac{C_3\lambda^2}{(\lambda^2 - C_4^2)} + \frac{C_5\lambda^2}{(\lambda^2 - C_5^2)}$$

where

$$\mathrm{C_1} = 10.6684293, \mathrm{C_2} = 0.301516485, \mathrm{C_3} = 0.003043475,$$
$$\mathrm{C_4} = 1.13475115, \mathrm{C_5} = 1.54133408, \mathrm{C_6} = 1104.0$$

The intersection between the material dispersion curve and the line formed by different eigen frequencies taken at a specific k point, for different refractive index values, gives the eigen frequency of the structure with material dispersion taken into account, as shown in Fig. 10.

If we now consider all k-points of the guided mode, the intersection with the material dispersion curve takes the form of points that give rise to a new guided mode with material dispersion taken into account. We then calculated the variation in group index for the new guided mode in a partially LC-infilled PhC waveguide (Fig. 11). It shows that there is a slight decrease

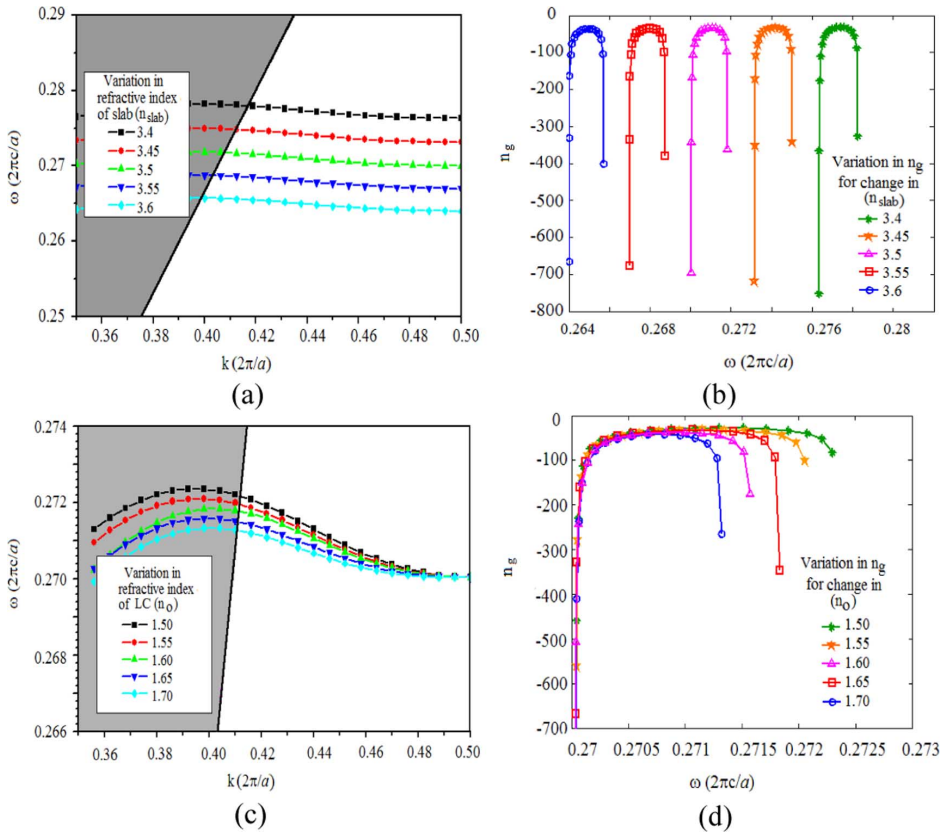

Fig. 9. Movement of dispersion curve with variation in (a) refractive index of slab, $\mathrm{n_{slab}}$ and (c) ordinary refractive index of liquid crystal, $\mathrm{n_{LC}}$. (b) and (d) represents the corresponding change in group index with variation in refractive index of slab and liquid crystal respectively.

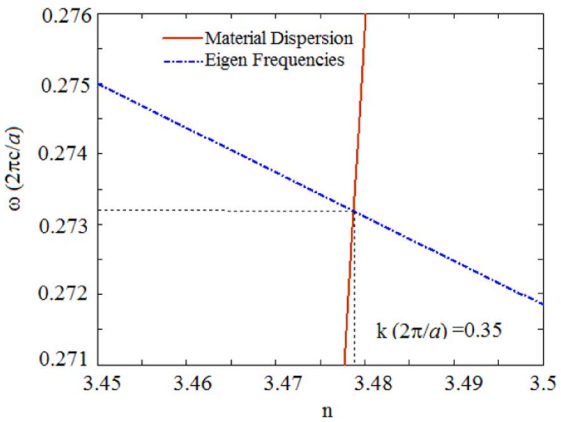

Fig. 10. Variation of eigen frequencies at k $(2\pi/\mathrm{a}) = 0.35$ (dash dot line) with refractive index and material dispersion of (solid line) silicon.

in average group index to ∼41.00 but also that the bandwidth increases, raising the normalized value of the DBP to 0.245.

IV. Sensitivity

Sensitivity can be evaluated by determining the magnitude of the change in the cut-off frequency of the even guided mode with variation in the refractive index of the medium. In this section we have compared the sensitivity of the cut-off frequency for a liquid-infiltrated photonic crystal waveguide (LC W0.7 PhC waveguide) with conventional PhC waveguide (W0.7 PhC waveguide), both composed of a hexagonal arrangement of rectangular air holes in an SOI-based PhC. Here we consider a situation where the volume above the conventional stripe waveguide, the W0.7 PhC waveguide—and inside the holes is filled with air of refractive index n_a. Fig. 12(a) shows the cut-off wavelength as a function of refractive index $\mathrm{n_o}$ (the ordinary refractive index of the liquid crystal) for *LC* infiltrated W0.7 PhC waveguide and $\mathrm{n_a}$ (refractive index of gas in-filled holes) for the 'conventional' W0.7 PhC waveguide. The change in wavelength is nearly linear with variation in refractive index. If we now define sensitivity as $(\Delta\lambda)/(\lambda_0)$ expressed as a percentage, then the sensitivity is 0.0012% for infiltrated *LC* W0.7 PhC waveguides and 0.0005% for the conventional waveguide. Therefore, a PhC waveguide infiltrated with *LC* that has its optical axis perpendicular to the x-z plane is more than twice as sensitive as a conventional W0.7 PhC waveguide to variations in the refractive index of the holes.

If we now consider that the photonic crystal is locally filled with a liquid crystal for which the optic axis orientation changes randomly and becomes parallel to the periodic plane, i.e., the x-z plane, then it acts as an isotropic material with refractive index given by $\mathrm{n_{LC}} = (\mathrm{n_e} + 2\mathrm{n_o})/3$ [46]. Here the liquid crystal used has extra-ordinary and ordinary refractive index values of 2.20 and 1.60, respectively. Therefore, $\mathrm{n_{LC}} = 1.8$. Fig. 12(b) shows the variation of cut-off wavelength as a function of $\mathrm{n_{LC}}$, since now the optic axis of the liquid crystal is parallel to the periodic plane. The sensitivity is calculated to be 0.00147%, which is nearly three times as sensitive as for conventional waveguides.

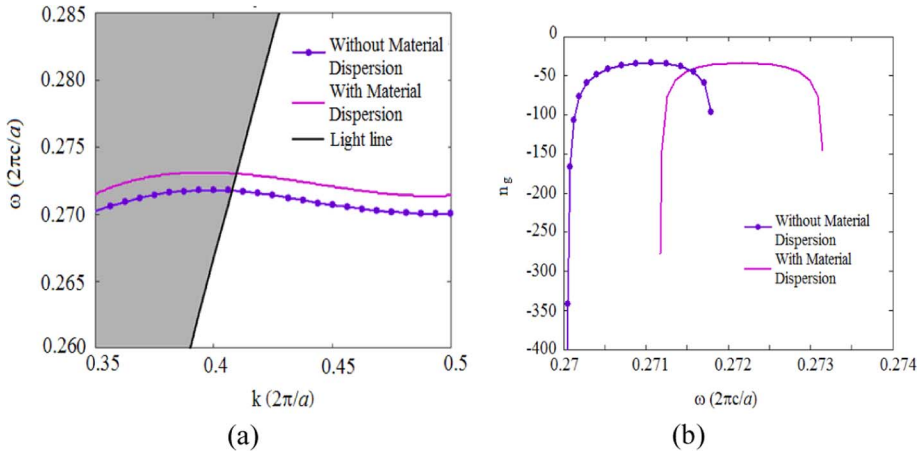

Fig. 11. (a) Band structure and (b) variation in group index with (solid line) and without (dotted marked line) material dispersion consideration.

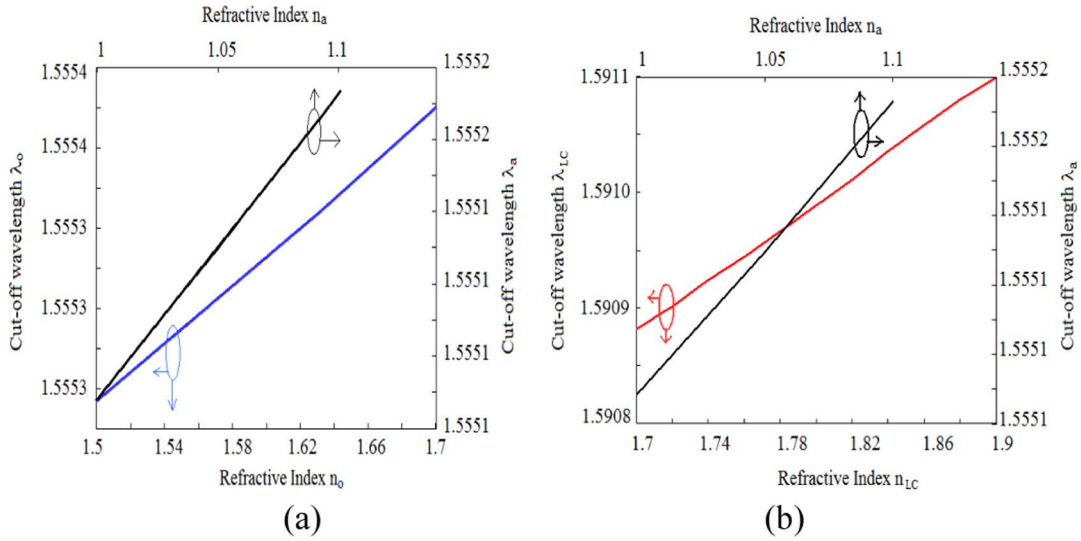

Fig. 12. Variation of cut-off wavelength as a function of refractive index of air n_a and (a) n_o and (b) n_{LC}.

These results show that the tunability of photonic crystal waveguides can be significantly increased by field enhancement and slow light effects.

V. Pulse Transmittance Measurements

An immediate problem arising from the design of the slow-light waveguide is its capability for input and output coupling of slow modes efficiently, in the slow light regime. This problem arises from the large mismatch at the boundaries of the PhC waveguide that arises from large differences in the group index. To solve this complex problem, we have added short intermediate sections of fast PhC channel waveguide that act as coupler sections at both ends, in addition to the slow light PhC waveguide obtained through partial liquid crystal infiltration. The model of the proposed heterogeneous waveguide is shown schematically in Fig. 13(a). The calculated photonic band structure of the fast PhC waveguide with a stretched period ($a' = 450$ nm) obtained using the 3-D PWE method is shown in Fig. 13(b). From the slope of the dispersion curve of the fast waveguide, it is observed that the velocity of a signal at 1.55 μm is 0.169c, which is much higher than that obtained in slow-light partially LC-infilled W0.7 PhC waveguide ($\sim$ 0.029c)—or homogeneous waveguide. The 3-D FDTD method was used for calculating the transmittance through the proposed heterogeneous PhC waveguide.

As observed in [35], efficient coupling of light is obtained between the fast and slow photonic crystal waveguides having large group index mismatch, (of the order of 20) at the interface. This optimization of injection efficiency is carried out by adding a taper between the two waveguides in a region which forms a transition zone. However in our case, the group index mismatch between the fast and the slow waveguides is only (35/6) 5.83, so we do not require such modification for efficient coupling. Fig. 13(d) shows the modal field distribution with a continuous wave at $\lambda_0 = 1.55$ μm going from a fast PhC waveguide into a slow PhC waveguide. It shows the existence of a transition zone at the interface where the field varies smoothly as it penetrates the slow waveguide. Fig. 13(c) summarizes the transmittance of the propagating pulse through a heterogeneous PhC waveguide consisting of a 16 a long partially LC-infiltrated W0.7 slow light waveguide surrounded by two sections of fast PhC channel waveguide made up of high group velocity regions. The coupler length is chosen so that maximum coupling efficiency is obtained along the coupler and through the transition zone

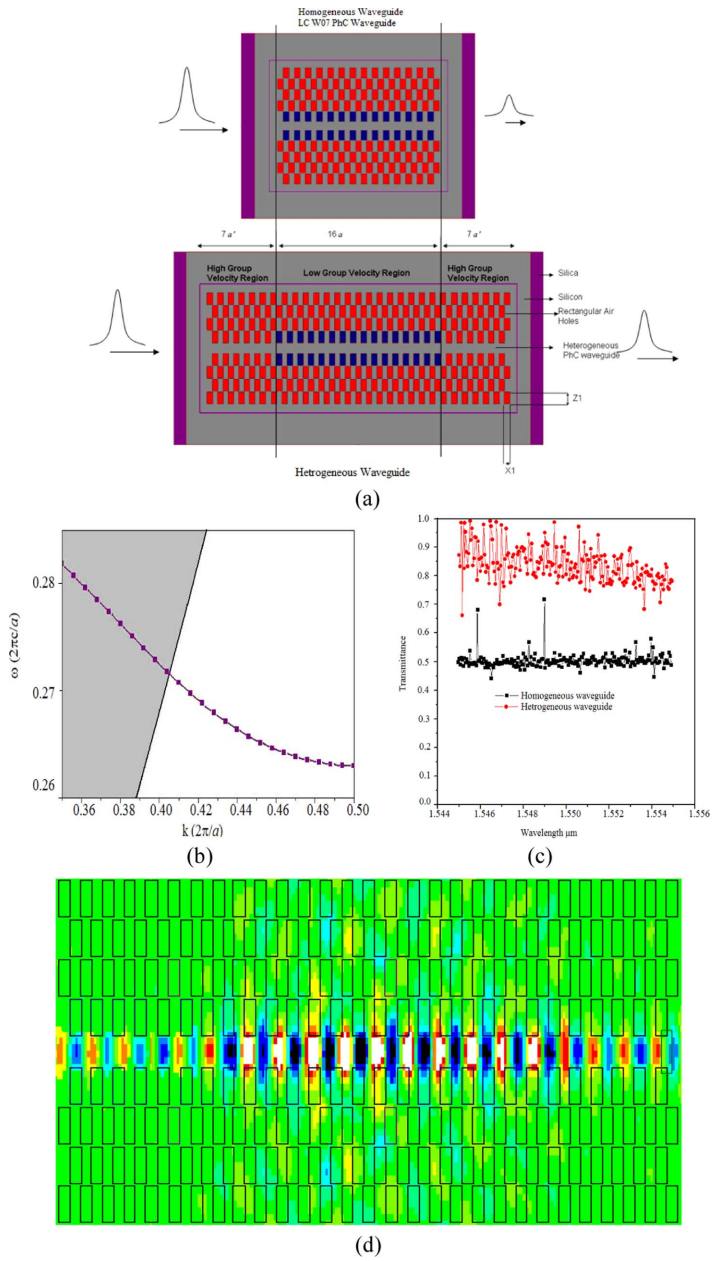

Fig. 13. (a) Schematic of the proposed heterogeneous PhC waveguide. (b) The dispersion curve of the fast PhC waveguide with a stretched period $a' = 450$ nm obtained using the 3-D PWE method. (c) Transmittance obtained from the homogeneous and heterogeneous liquid infilled PhC waveguide. (d) Modal distribution with a continuous wave at $\lambda_0 = 1.55\ \mu$m.

i.e., evanescent modes excited at each end of the coupler do not overlap and interfere destructively [50]. This results in maximum transmission. As shown in Fig. 13(c), the transmittance of the heterogeneous PhC waveguide for the slow-light flat-band window ranging from 1.545 μm to 1.555 μm is higher than 80% while the transmittance obtained for a homogeneously LC-infilled W0.7 PhC waveguide alone is nearly 50%. This higher (lower) transmittance in a heterogeneous (homogeneous) waveguide is due to better (poorer) coupling into the slow mode.

VI. Conclusion

We have proposed an SOI-based partially liquid-infiltrated photonic crystal W0.7 channel waveguide having rectangular air holes in a silicon core. It has been demonstrated that the proposed structure has an average group index of 43 over a bandwidth of 1.02 THz, with vanishing group velocity dispersion and likewise small values of the other higher-order dispersion terms. The designed partially LC-infiltrated W0.7 PhC waveguide for slow light propagation is highly tolerant of fabrication errors and has nearly twice higher sensitivity than conventional PhC waveguides. The structure designed has also been investigated for possible propagation losses, which include losses due to coupling inefficiency. It is found that high transmission can be obtained over a broad bandwidth in the heterogeneous waveguide that was finally designed—and consists of a partially LC-infiltrated PhC slow waveguide, surrounded by fast PhC waveguide on either side.

ACKNOWLEDGMENT

The authors gratefully acknowledge the initiatives and support towards establishment of the "TIFAC Centre of Relevance and Excellence in Fiber Optics and Optical Communication at the Delhi College of Engineering, Delhi" through the "Mission REACH" program of Technology Vision-2020 of the Government of India.

REFERENCES

[1] E. Yablonovitch, "Inhibited spontaneous emission in solid-state physics and electronics," *Phys. Rev. Lett.*, vol. 58, no. 20, pp. 2059–2062, 1987.

[2] S. John, "Strong localization of photon in certain disorder dielectric super-lattices," *Phys. Rev. Lett.*, vol. 58, pp. 2486–2489, 1987.

[3] M. Soljacic, S. G. Johnson, S. Fan, M. I. Baneseu, E. Ippen, and J. D. Joannopolous, "Photonic crystal slow light enhancement of non linear phase sensitivity," *J. Opt. Soc. Amer. B*, vol. 19, pp. 2052–2059, 2002.

[4] H. Gersen, T. J. Karle, R. J. P. Engelen, W. Bogaerts, J. P. Korterik, N. F. Van Hulst, T. F. Krauss, and L. Kuipers, "Real space observation of ultra slow light in photonic crystal waveguides," *Phys. Rev. Lett.*, vol. 94, pp. 073903–, 2005.

[5] T. Baba and D. Mori, "Slow light engineering in photonic crystals," *J. Phys. D: Appl. Phys.*, vol. 40, pp. 2659–2665, 2007.

[6] L. H. Frandsen, A. V. Lavrinenko, J. Fage-Pedersen, and P. I. Borel, "Photonic crystal waveguides with semi-slow light and tailored dispersion properties," *Opt. Exp.*, vol. 14, pp. 9444–9450, 2006.

[7] T. F. Krauss, "Why do we need slow light?," *Nature Photonics*, vol. 2, pp. 448–450, 2008.

[8] R. M. De and L. Rue, "Slower for longer," *Nature Photon.*, vol. 12, no. 2, pp. 715–716, Dec. 2008.

[9] Y. A. Vlasov, M. O'Boyle, H. F. Hamann, and S. J. McNab, "Active control of slow light on a chip with photonic crystal waveguides," *Nature*, vol. 438, pp. 65–69, 2005.

[10] V. R. Almeida, C. A. Barrios, R. R. Panepucci, and M. Lipson, "All optical control of light on a silicon chip," *Nature*, vol. 481, pp. 1081–1084, 2004.

[11] R. S. Jacobsen, K. Andersen, P. I. Borel, J. F. Pedersen, O. Hansen, M. Kristensen, A. Lavrinenko, G. Moulin, H. Ou, C. Peucheret, B. Zsigri, and A. Bjarklev, "Strained silicon as a new electro-optic material," *Nature*, vol. 441, pp. 199–202, 2006.

[12] R. S. Tucker, P. C. Ku, and C. J. Chang-Hasnain, "Slow light optical buffers: Capabilities and fundamental limitations," *J. Lightw. Technol.*, vol. 23, no. 12, pp. 4046–4066, Dec. 2005.

[13] M. L. Povinelli, S. G. Johnson, and J. D. Joannopoulous, "Slow light, band edge waveguides for tunable time delays," *Opt. Exp.*, vol. 13, p. 7145, 2005.

[14] T. Baba, D. Mori, K. Inoshita, and Y. Kuroki, "Light localization in line defect photonic waveguides," *IEEE J. Quant. Electron.*, vol. 10, no. 3, pp. 484–491, Jun. 2004.

[15] T. F. Krauss, "Slow light in photonic crystal waveguides," *J. Phys. D: Appl. Phys.*, vol. 40, pp. 2666–2670, 2007.

[16] O. Khayam and H. Benisty, "General recipe for flat bands in photonic crystal waveguides," *Opt. Exp.*, vol. 17, pp. 14634–48, 2009.

[17] R. J. P. Engelen, Y. Sugimoto, Y. Watanabe, J. P. Korterik, N. Ikeda, N. F. van Hulst, K. Asakawa, and L. Kuipers, "The effect of higher-order dispersion on slow light propagation in photonic crystal waveguides," *Opt. Exp.*, vol. 14, pp. 1658–1672, 2006.

[18] M. F. Yanik and S. Fan, "Stop Light on a Chip," *Phys. Rev. Lett.*, vol. 92, pp. 083901–, 2004.

[19] S. Rawal, R. K. Sinha, and R. M. De La Rue, "Slow light miniature devices with ultra-flattened dispersion in silicon-on-insulator photonic crystal," *Opt. Exp.*, vol. 17, pp. 13315–13325, 2009.

[20] K. Bayat, S. K. Chaudhuri, S. S. Naeini, and M. F. Baroughi, "Design and simulation of photonic crystal based polarization converter," *J. Lightw. Technol.*, vol. 27, no. 23, pp. 5483–5491, Dec. 2009.

[21] K. J. K. Koerkamp, S. Enoch, F. B. Segerink, N. F. van Hulst, and L. Kuipers, "Strong influence of hole shape on extraordinary transmission through periodic arrays of subwavelength holes," *Phys. Rev. Letts.*, vol. 92, pp. 183901–, 2004.

[22] X. Zhang, H. Tian, and Y. Ji, "Group index and dispersion properties of photonic crystal waveguides with circular and square air holes," *Opt. Comm.*, vol. 283, pp. 1768–1772, 2010.

[23] G. Alagappan, X. W. Sun, M. B. Yu, P. Shum, and D. D. Engelsen, "Tunable dispersion properties of liquid crystal infiltrated into a two-dimensional photonic crystal," *IEEE J. Quantum Electron.*, vol. 42, no. 4, pp. 404–407, Apr. 2006.

[24] E. P. Kosmidou, E. E. Kriezis, and T. D. Tsiboukis, "Analysis of tunable photonic crystal devices comprising liquid crystal materials as defects," *IEEE J. Quantum Electron.*, vol. 41, no. 5, pp. 657–665, May 2005.

[25] M. Ebnali-Heidari, C. Grillet, C. Monat, and B. J. Eggleton, "Dispersion engineering of slow light photonic crystal waveguides using microfluidic infiltration," *Opt. Exp.*, vol. 17, no. 3, pp. 1628–1635, 2009.

[26] E. E. Kriezis and S. J. Elston, "Light wave propagation in liquid crystal displays by the 2-D finite difference time domain method," *Opt. Commun.*, vol. 177, pp. 69–77, 2000.

[27] C. L. C. Smith, U. Bog, S. Tomljenovic-Hanic, M. W. Lee, D. K. C. Wu, L. O'Faolain, C. Monat, C. Grillet, T. F. Krauss, C. Karnutsch, R. C. McPhedran, and B. J. Eggleton, "Reconfigurable microfluidic photonic crystal slab cavities," *Opt. Exp.*, vol. 16, pp. 15887–15897, 2008.

[28] A. Petrov, M. Krause, and M. Eich, "Backscattering and disorder limits in slow light photonic crystal waveguides," *Opt. Exp.*, vol. 17, no. 10, pp. 8676–8684, 2009.

[29] E. Kuramochi, M. Notomi, S. Hughes, A. Shinya, T. Watanabe, and L. Ramunno, "Disorder-induced scattering loss of line-defect waveguides in photonic crystal slabs," *Phys. Rev. B*, vol. 72, pp. 161318–, 2005.

[30] D. Gerace and L. C. Andreani, "Light-matter interaction in photonic crystal slabs," *Phys. Status Solidi B*, vol. 244, pp. 3528–3539, 2007.

[31] P. Pottier, M. Gnan, Richard, and M. De La Rue, "Efficient coupling into slow-light photonic crystal channel guides using photonic crystal tapers," *Opt. Exp.*, vol. 15, no. 11, pp. 6569–6576, 2007.

[32] N. Ozaki, Y. Kitagawa, Y. Takata, N. Ikeda, Y. Watanabe, A. Mizutani, Y. Sugimoto, and K. Asakawa, "High transmission recovery of slow light in a photonic crystal waveguide using a hetero group velocity waveguide," *Opt. Exp.*, vol. 15, no. 13, pp. 7974–7983, 2007.

[33] P. Velha, J. P. Hugonin, and P. Lalanne, "Compact and efficient injection of light into band-edge slow-modes," *Opt. Exp.*, vol. 15, no. 10, pp. 6102–6112, 2007.

[34] C. Martijn de Sterke, J. Walker, K. B. Dossou, and L. C. Botten, "Efficient slow light coupling into photonic crystals," *Opt. Exp.*, vol. 15, no. 17, pp. 10984–10990, 2007.

[35] J. P. Hugonin, P. Lalanne, T. P. White, and T. F. Krauss, "Coupling into slow-mode photonic crystal waveguides," *Opt. Lett.*, vol. 32, no. 18, pp. 2638–2640, 2007.

[36] A. Shinya, M. Notomi, I. Yokohama, C. Takahashi, and J. Takahashi, "Two-dimensional Si photonic crystals on oxide using SOI substrate," *Opt. Quantum Electron.*, vol. 34, pp. 113–121, 2002.

[37] A. Yu, P. , and M. Eich, "Zero dispersion at small group velocities in photonic crystal waveguides," *Appl. Phys. Lett.*, vol. 85, pp. 4866–4868, 2004.

[38] M. Notomi, A. Shinya, K. Yamada, J. Takahashi, C. Takahashi, and I. Yokohama, "Singlemode transmission within photonic bandgap of width-varied single-line-defect photonic crystal waveguides on SOI substrates," *Electron. Lett.*, vol. 37, pp. 293–295, 2001.

[39] M. Notomi, K. Yamada, A. Shinya, J. Takahashi, C. Takahashi, and I. Yokohama, "Extremely large group velocity dispersion of line-defect waveguides in photonic crystal slabs," *Phys. Rev. Lett.*, vol. 87, pp. 253902–, 2001.

[40] J. Li, T. P. White, L. O'Faolain, A. Gomez-Iglesias, and T. F. Krauss, "Systematic design of flat band slow light in photonic crystal waveguides," *Opt. Exp.*, vol. 16, pp. 6227–6232, 2008.

[41] M. Plihal and A. A. Maradudin, "Photonic band structures of two dimensional systems—The Triangular lattice," *Phys. Rev. B*, vol. 44, pp. 1865–8571, 1991.

[42] G. P. Agarwal, *Fiber Optic Communication Systems*. Hoboken, NJ: Wiley-Interscience, 1997.

[43] J. Ma and C. Jiang, "Flat band slow light in asymmetric line defect photonic crystal waveguide featuring low group velocity and dispersion," *IEEE J. Quantum Electron.*, vol. 44, pp. 763–769, 2008.

[44] S. Chandrashekhar, *Liquid Crystals*. Cambridge, U.K.: Cambridge Univ. Press, 1995.

[45] S. W. Leonard, J. P. Mondia, H. M. van Driel, O. Toader, S. John, K. Busch, A. Birner, U. Gösele, and V. Lehmann, "Tunable two dimensional photonic crystals using liquid crystal infiltration," *Phys. Rev. B*, vol. 61, pp. R2389–, 2000.

[46] H. Takeda and K. Yoshino, "Tunable photonic band schemes of opals and inverse opals infiltrated with liquid crystals," *J. Appl. Phys.*, vol. 92, no. 10, pp. 5658–5662, 2002.

[47] C.-L. Kao and C.-P. Yu, "Band structure analysis of liquid-crystal photonic crystal fibers," in *Progress In Electromagnetics Research Symposium*, Beijing, China, Mar. 23–27, 2009.
[48] *Handbook of Optics*, 2nd ed. New York: McGraw-Hill, 1994, vol. 2.
[49] I. V. Guryev and I. A. Sukhoivanov, "Plane wave expansion method with considered material dispersion," CADSM'2007. Polyana, Ukraine, Feb. 20-24, 2007.
[50] A. Säynätjoki, K. Vynck, M. Mulot, D. Cassagne, J. Ahopelto, and H. Lipsanen, "Efficient light coupling into a photonic crystal waveguide with flatband slow mode," *Photon. Nanostruct.*, vol. 6, pp. 1127–133, 2008.

Swati Rawal received the B.Sc. (Hons). degree from Delhi University in 2004 and the M.Sc. degree from C.C.S. University, in 2006, both in Physics with electronics as specialization. She is currently pursuing the Ph.D. degree with the Department of Applied Physics, Delhi Technological University (Formerly Delhi College of Engineering, University of Delhi) India.

Her current research interests include Photonic crystal waveguides, devices and slow light in Photonic crystals.

Ms. Rawal is recipient of "SPIE Best Research Paper Award " for her research paper related to slow light in Photonic Crystal during Internal Conference on Optics and Photonics-2009 held at CSIO Chandigarh, India. She is also recipient of student leadership award from Optical Society of America for participating in international conference " Frontiers in Optics" held in San Jose, CA, USA during October 10–15, 2009.

R. K. Sinha received the M.Sc. degree in physics from the Indian Institute of Technology (IIT), Kharagpur, India, in 1984, and the Ph.D. degree in fiber optics and optical communication from the IIT, Delhi, India, in 1990.

During 1989–1991, he was a Postdoctoral Research Student at Osaka University for Foreign Studies, Osaka, Japan, and Electronics Engineering Department, Kobe University, Japan. Later he worked at Indian Institute of Science Bangalore during April 1991–December 1991, Birla Institute of Science and Technology, Pilani during January 1992–September 1994 and at Regional Engineering College (Now NIT) Hamirpur during October 1994–December 1998 in various research and academic positions. Since January 1999, he is associated with Delhi College of Engineering, Delhi. He is currently a Professor, Head of Applied Physics Department, Chief Coordinator of the Technology Information, Forecasting and Assessment Council (TIFAC)—Centre of Relevance and Excellence (CORE) in Fiber Optics and Optical Communication and Dean (Industrial Research & Development), Delhi Technological University (Formerly Delhi College of Engineering, University of Delhi), Delhi. He is the author or coauthor of more than 140 research publications in the leading national and international journals and conference proceedings. He has also held visiting scientist appointment at ICTP-Italy in 1991 and University of Campinass, Brazil in the year 1995.

Prof. Sinha was awarded the Emerging Optoelectronics Technology Award [(CEOT-IETE, India)]-2006 for outstanding research work in the area of Nanophotonics, S. K. Mitra Memorial Award for in Best Research Paper in IETE Technical Review 2002 on Nanostructure Electron Waveguides and Devices and Swarna Jayanti Puraskar (Gold Medal) from the National Academy of Science for best co-authored research paper in the area of Nano scale Optical Devices for the year 2001. Professor Sinha had been academic visitor of several universities of USA, U.K. and Japan. Later in the year 2006, he was awarded "Project Formulation Grant" from British Council of India to initiate collaborative research between leading university of U.K. and his organization, DCE (now DTU) Delhi. He has also been awarded the Japan Society for Promotion of Science (JSPS) Invited Fellowship-2007 at Hokkaido University, Sapporo, Japan and the Royal Academy of Engineering (U.K.-India short-term exchange) Fellowship-2008 to carry out research on Photonic Crystal Waveguides and Devices at Glasgow University, U.K., Indo Swiss Bilateral Research Fellowship-2009 to initiate collaborative research in the area of Nano photonic Devices with EPFL Switzerland and DTU, Delhi, India and National Science Council Taiwan Fellowship-2009 to pursue collaborative research and deliver invited talk on Photonic Crystal based Nano Photonic Devices. He is a Fellow of the IETE (India). Professor Sinha is also Faculty Adviser of SPIE-DCE Chapter and OSA-DCE Chapter at Delhi Technological University, Delhi. In addition to these, Prof. Sinha has been actively involved in supervising several innovative projects on the design and development of unmanned and autonomous vehicles and in the establishment of Knowledge and Innovation Park with focus on student led innovation and product development.

Richard M. De La Rue (F'03) was appointed as Lecturer at Glasgow University, Glasgow, U.K., in 1971, became a Senior Lecturer in 1982, a Reader in 1985 and Professor of Optoelectronics in 1986.

His research is particularly concerned with photonic crystal and photonic wire structures, waveguide micro-cavities and metamaterials. His research in the area of photonic crystals has evolved to cover compact lasers, planar micro-cavities, photonic-crystal LEDs, synthetic opal and inverse opal structures. His research on metamaterials has particularly emphasized the use of semiconductor substrates—and the impact of the choice of metallization. Other research interests include integrated optics technology more generally, photonic integrated circuits (PICs), DFB and DBR semiconductor lasers, quantum well intermixing—and phase masks for silica waveguide photorefractive grating devices. His historic interest in lithium niobate integrated optics is currently reviving in the context of photonic crystal structure fabrication. He has published more than 200 articles and papers in journals and as book chapters. He has also given several hundred conference, workshop and school presentations, many of which were invited—and several of which were plenary presentations. Current involvement in European Community funded collaborations is through the SPLASH and P3SENS projects. The recently completed PQLDI project, supported by the U.K. Technology Strategy Board, involved collaboration with three other groups—and was concerned with the application of photonic quasi-crystal (PQC) techniques for enhanced extraction of light from blue LEDs.

Dr. De La Rue has previously been involved in European-scale research activity through the ePIXnet, SMILED and PICCO projects, as well as being co-leader for working group 2 (WG2) in the COST 268 action on "Wavelength Scale Photonics." He was general co-chair for the CLEO-Europe/IQEC 2009 conference and has been leading co-chair for the 'Photonic Crystal Materials and Devices' conference at Photonics Europe in 2004, 2006 and 2008. He was also deputy leader for the COST P11 Action 'Linear, Nonlinear and Active Photonic Crystals'. For two years from mid–1999 he served as IEEE-LEOS Distinguished Lecturer. He is a Fellow of OSA, Fellow of the Royal Academy of Engineering, Fellow of the Royal Society of Edinburgh, and Fellow of the Institution of Engineering and Technology.

Photonic Crystal Waveguides and Devices

A thesis submitted to
Faculty of Technology, University of Delhi
for the award of the degree of

DOCTOR OF PHILOSOPHY
in
APPLIED PHYSICS

by

Swati Rawal

Under the supervision of

Dr. R. K. SINHA
Professor and Head, Department of Applied Physics
Delhi College of Engineering
Faculty of Technology
University of Delhi
Delhi-110 042, India

Summary & Future Scope

In this chapter, a recapitulation of the main results obtained has been presented, conclusions have been drawn and a perspective of the open problem and the further work has been selected. The research work in this thesis involves the design and characterization of various photonic crystal line defect waveguides for the realization of a new generation of photonic components with application in compact dual band wavelength demultiplexers, optical buffers, time and wavelength demultiplexers, optical switches, logic gates and as soliton propagator. The controlled propagation of light in PhC waveguides has also led to a variety of novel optical phenomenon including slow light generation and the enhancement of nonlinear effects because of the light matter interaction in photonic crystals. The present thesis discusses about various new interesting phenomenon and physical systems, achievable in photonic crystals. However, it also opened up the possibilities of exciting new research for future work.

As a first step towards the analysis of photonic crystals, design, modelling and optimization of dual band wavelength demultiplexers based on both air bridge photonic crystals as well as SOI photonic crystals were carried out in chapter 2 and 3. It would be interesting to design triple band and quad band wavelength demultiplexers based on the same phenomenon for separating different wavelengths in infra-red regions, desired in dense wavelength demultiplexing communication systems.

Chapter 4 focuses on hexagonal arrangement of elliptical hole architecture of photonic crystals for achieving slow light, which have strong application possibilities in optical buffers and other optical storage devices. Such devices can also be used in

time and wavelength demultiplexing. The tunability of PhC lattices can further be extended and controlled by filling its segments with certain liquid crystals as shown in Chapter 5. It would be interesting to utilize these tunable slow light photonic crystals for the design and development of various other optical components with high value of normalised delay bandwidth product. These tunable slow light structures can also be designed using nonlinear photonic crystals for second and third order generation.

As the optical pulses propagate through photonic crystals, their evolution in both time and frequency domain is further governed by the interplay of linear dispersion and nonlinearity. It is reported in Chapter 6, that in slow light regime, these nonlinear effects are enhanced and the resulting increase in the induced phase shift can be used to decrease the size and power requirements needed to operate devices such as optical switches, logic gates etc. Consequently, the study of these effects can also be carried out in GaAs photonic crystal waveguides. The larger total magnitude of nonlinearity, including two photon absorption and free carrier absorption, in GaAs can be used for the design and development of tunable photonic crystal demultiplexers. The effect of slow light on the propagation of dark and bright solitons can also be studied further.

Finally, the theory of designing various types of optical components in photonic crystals can be extended from 2D PhC to 3D PhCs, having periodicity in three dimensions. Since, these structures control light in all dimensions, the extra dimensionality would also add more richness to the various opto-electronic systems.